Linear Scaling High-spin Open-shell Local Correlation Methods

Von der Fakultät Chemie der Universität Stuttgart

zur Erlangung der Würde eines Doktors der

Naturwissenschaften (Dr. rer. nat.) genehmigte Abhandlung

vorgelegt von

Yu Liu

aus Dalian

Hauptberichter:	Prof. Dr. H.-J. Werner, Universität Stuttgart
Mitberichter:	Prof. Dr. G. Rauhut, Universität Stuttgart
Tag der mündlichen Prüfung:	15 March 2011

Institut für Theoretische Chemie der Universität Stuttgart

2011

Acknowledgments

First, I would like to thank my parents, and specially, I give my best thanks to my grandfather. In the 1940s, he was also a student who studied chemistry. He believed that the best place to learn chemistry in the word is Germany. He really dreamed about getting a PhD in Germany. Unfortunately, due to the second world war, it was impossible. Four years ago, he sent me to Germany to continue his dream. Unfortunately, he could not wait for me to bring the degree back. However, I really wish that my grandfather can finish this dream now. I believe that this PhD is also belonging to him. .....of course, I also thank my grandmother, who is lonely waiting for me to be back.

I give my thanks to all the friends from the Stuttgart group, especially Frau Rosenkranz who took care of all the complicated administration works. I give my thanks to Aron Bona and Judith Rommel for their works in the application part of this thesis. I give my thanks to Oliver Marchetti and Christoph Köppl for their translation of 'Zusammenfassung'. I give my thanks to Dr. Filipe Agapito for his great help in the modification of the manuscript.

I thank all my friends in Stuttgart and Tübingen, who I will never forget.

I give my thanks to Dr. Martin Albrecht for his help before I came to Germany, and also for his great help to correct the English in this thesis.

Finally, I thank Prof. Werner for the 18 emails and complicated discussions to bring me here, for his patient modification of my posters, and for his help of my programming.

Additionally, I want to thank my computer, my clothes, my chair, my mouse and my cat for their patience and endurance.

Abstract

Human beings use different methods to understand the world, religiously or scientifically, empirically or theoretically, synthetically or analytically. Quantum chemistry is one of the these methods. Starting from first principles of quantum mechanics, applying different mathematical and physical approximations, the behaviors of molecules are described. Before the discussion of the complex theories in quantum chemistry, it is better to answer two questions first. One is for which kind of system quantum chemistry is needed? The other is what is the accuracy needed for the results of quantum chemistry calculations?

Quantum chemistry is used to study the molecular world, but it is not true that quantum chemistry is needed for all molecules. It is not possible and also not necessary to apply quantum chemistry to huge molecules, for example, a DNA or a protease molecule. To study very large systems, there are bio-chemical databases, molecular dynamics based on molecular mechanics (MM), and semi-empirical methods. If the electron structure in the system changes smoothly and slowly, the above methods generally provide acceptable results. However, there are also rapid changes of electron structure, for example, in chemical reactions such as bonding breaking, bonding forming, charge transfer, etc. To describe chemical reactions, using quantum chemistry is necessary and important. Fortunately, even for a complex biological chemical reaction, the active region where the electron structure changes rapidly is rather local, i.e., the region has a size of maximum up to two or three hundred atoms, but usually less than 100 atoms. Using quantum chemistry to study the active region in combination with other methods which describe the remaining system is the basic methodology to study very large molecules. The quantum mechanics / molecular mechanics (QM/MM) approach is a good example of such methodologies.

The accuracy needed for the energies calculated by quantum chemistry depends on how far a calculation is from reality or experiment. A single energy calculated by quantum chemistry (for example, a Hartree-Fock (HF) or a density functional theory (DFT) calculation) can be applied to "bare" and "static" molecules. These are molecules in vacuum or in a gas field, at zero kelvin, without excited levels of vibrations and rotations, without relativistic effects, and under adiabatic and Born-Oppenheimer approximations. The aim of quantum chemistry research is to find different methods, based on first principle, or experience, to bring traditional quantum chemistry calculations back to reality. Basically, to perform a calculation to a

real system and obtain true results, it is needed to do a traditional quantum chemistry calculation together with zero point vibrational energy (ZPVE) correction, temperature correction, solution effect correction, relativistic correction, beyond Born-Oppenheimer correction, and so on. The accuracy depends on the system, but in the best cases the above approximation leads to a total error between 0.1 and 1 kcal/mol. It is clear now, that if quantum chemistry calculations have an accuracy of 1 kcal/mol or below, there is a chance to obtain results as meaningful as chemical experiments, for which 1 kcal/mol is also generally the limit in accuracy.

However, to do a calculation with this accuracy for a system with 100-300 atoms is not a trivial task. There are two major difficulties: one is that the accuracy of the method may not be good enough, the other is that the computational cost of the more accurate methods increases too fast with the molecular size.

There are two kinds of popular methods in quantum chemistry: those based on wave function theory, which are usually named *ab initio* methods, and density functional theory (DFT). DFT is applicable to systems with 100-300 atoms, but it is also well known that its accuracy can not be systematically improved. DFT can sometimes provide results with errors smaller than 1 kcal/mol, but it can also lead to errors of more than 10 kcal/mol. Consequently, DFT is a powerful method, but not always a reliable one. On the other hand, the accuracy of *ab initio* methods can be systematically improved by increasing the level of the treatment of electron correlation effects. Therefore, if enough calculation resources are available, *ab initio* methods can always provide reliable results for electronic structure calculations. However, it is well know that *ab initio* methods consume huge amounts of computational resources and their cost increases too fast with the system size.

One of the main reasons for the steep scaling of *ab initio* methods is caused by the use of canonical molecular orbitals (MOs), which are generally extended over the whole system. Delocalized MOs not only prevent the omission of small correlation effects of distant electrons, but also lead to the circumstance that for correlating each particular electron pair the number of virtual orbitals needed increases unphysically fast. By localizing molecular orbitals and using projected atomic orbitals as virtual orbitals, a set of local correlation methods have been developed in the last 15 years. Using these methods, high level correlated treatments can be performed for much larger systems. For example, using the local singles and doubles coupled cluster (LCCSD(T)) program in `Molpro` together with the density fitting technique, it is possible to treat the system with about 150 atoms with basis sets of triple-zeta plus polarization quality. However, so far most of the low scaling correlated methods were only implemented for closed shell cases, especially, the high accuracy

one, LCCSD(T). Given the importance of the open-shell systems in chemistry, it is fundamental to develop efficient high-level low scaling open-shell local correlation methods.

In this work, a set of newly developed open-shell linear scaling or low scaling correlation methods is presented. They are the local restricted second-order Møller-Plesset perturbation theory (LRMP2), local unrestricted singles and doubles coupled cluster (LUCCSD), and local unrestricted CCSD(T) with perturbative triples (LUCCSD(T)) methods. In all above methods, restricted open-shell Hartree-Fock (RHF) orbitals are used as the reference. Two different localization schemes are compared and discussed. In the first case localization is performed separately in the closed-shell and open-shell orbital spaces. In the second case localization is performed separately for the alpha and beta spin orbitals. The excitations are restricted to domains, and only strong pairs are treated at the highest level. Local density fitting approximations are used to compute integrals. Provided that the orbitals can be well localized, this leads to linear scaling of the computational effort with molecular size and extends the applicability of the local RMP2 and UCCSD methods to systems with 100-150 correlated orbitals and 2000-4000 basis functions. The scaling of the methods is demonstrated, and then the accuracy is tested. The methods are tested for computing radical stabilization energies, vertical ionization potentials, and molecular electron affinities. The accuracy is found to be comparable to the corresponding canonical methods. Finally, two applications using the new methods have been carried out and the results are discussed.

The structure of this thesis is as follows. In Chapter 1 the theoretical background is given. After a brief review of various electron correlation methods, the open-shell RMP2, UCCSD and UCCSD(T) methods which are related to this work are explained. After the introduction of electron correlation methods, the local correlation methods previously developed in our group are discussed. Localized molecular orbitals (LMOs), projected atomic orbitals (PAOs), and different approximations in local correlation methods are introduced. Finally a brief introduction of the density fitting approximation is given.

Chapter 2 describes the open-shell local correlation methods which are developed in this work. Starting from the localization of RHF orbitals, the LRMP2, LUCCSD and LUCCSD(T) theories are discussed. Two different kinds of localization schemes are presented. In the first, the singly occupied space and the doubly occupied space are localized separately. In the second, alpha orbitals and beta orbitals are localized separately. The working equations of these methods are presented and how to theoretically achieve linear scaling is discussed.

In Chapter 3 the scaling test results of open-shell local correlation methods are discussed. Using local fitting, LRMP2 shows a linear scaling behavior in the region of the presented tests. LUCCSD achieves a nearly linear scaling with the exception of one term. LUCCSD without this term achieves linear scaling. The local non-iterative triples (T0) calculation turns out to be quite cheap and comparable with the LCCSD part.

Chapter 4 discusses the accuracy of open-shell local correlation methods. Radical stabilization energies (RSE), ionization potentials (IP), and electron affinities (EA) are calculated for several sets of mid-sized molecules, for which UCCSD(T) calculations are still possible. The results obtained by local and canonical methods are compared. A systematical study of different settings for some parameters is done, and the effects of skipping the non-linear term in LUCCSD and LUCCSD(T) are discussed.

In Chapter 5 two applications of the new local methods for large systems are discussed. One is the calculation of formation energies of copper-oxygen complexes. The other is the the transition states and intermediates for the inter conversion from (S)-glutamate to (2S,3S)-3-methylaspartate.

The structures of the molecules needed in this work are given in Appendix A. All the calculated RSEs, IPs, and EAs, together with some absolute energies of corresponding radicals, molecules, cations, and anions are collected in Appendix B.

Zusammenfassung

Eine der großen Herauforderungen in der theoretischen Chemie ist die Berechnung großer Systeme von 100-200 Atomen mit einer Genauigkeit von 1 kcal / mol. Dabei sieht man sich zwei großen Herausforderungen gegenüber, zum einen ist die verwendete Methode nicht genau genug und zum anderen steigen die Kosten der genaueren Methoden zu schnell mit der Molekülgröße.

Konventionelle Methoden wie Coupled-cluster mit Ein- und Zweifachanregungen mit perturbtativen Dreifachanregungen (CCSD(T)) ist eine Methode, bei der man davon ausgeht, dass sie die Anforderung an die Genauigkeit von 1 kcal / mol für „singel reference“ Systeme übertrifft. Allerdings skaliert diese Methode mit $\mathscr{O}(\mathscr{N}^7)$ was Hauptspeicher, Festplattenplatz und Rechenzeit angeht. Der Hauptgrund für den steilen Anstieg der Kosten mit der Molekülgröße ist die Verwendung von kanonischen Molekülorbitalen, welche über das ganze System delokalisiert sind. Delokalisierte Orbitale führen nicht nur dazu, dass man kleine Korrelationseffekte weit entfernter Elektronen nicht vernachlässigen kann sondern auch dazu, dass für jedes Elektron die unphysikalisch große Zahl aller virtuellen Orbitale für die Korrelation verwendet werden. Diese Problems können durch Lokalisierung der Orbitale und Verwendung projizierter Atomorbitale für den virtuellen Raum vermieden werden. In den letzen 15 Jahren wurde eine Vielzahl von lokalen Methoden entwickelt. Bei lokaler Behandlung der Korrelation können auch genaue Methoden für die Beschreibung großer Systeme verwendet werden. Mit `Molpro` ist es bei Verwendung der lokalen Nährung möglich, Systeme mit ca. 150 Atomen auf CCSD(T) Niveau mit triple-zeta Basis mit zusätzlichen Polarisationsfunktionen zu behandeln (LCCSD(T)/VTZ+d). Bisher wurden lokalen Coupled-cluster Methoden nur für closed-shell-Systeme implementiert. Open-shell Systemen kommt eine große Bedeutung bei der Beschreibung chemischer Phänomene zu, deshalb ist die Entwicklung von effizienten Korrelationsmethoden mit niedriger Skalierung wichtig, die solche Systeme beschreiben können.

In dieser Arbeit werden neu entwickelte niedrig oder linear skalierende open-shell-Korrelationsmethoden präsentiert. Diese sind local restricted second-order Møller-Plesset perturbation theory (LRMP2), local unresticted coupled cluster (LCCSD(T)) Bei allen oben genannten Methoden werden die restricted open-shell Hartree-Fock (RHF) Orbitale als Referenz verwendet. Es werden zwei verschiedene Lokalisationsmethoden verglichen und bewertet. Im ersten Fall werden closed-shell und open-shell Orbitale separat lokalisiert. Im zweiten Fall werden alpha- und beta-Spinorbitale getrennt lokalisiert. Die Anregungen werden auf die jeweiligen Domänen eingeschränkt

und nur die starken Paare werden auf hohem Niveau behandelt. Lokale Dichtefitting-Näherungen wurden zur Berechnung der Integrale verwendet. Für den Fall, dass die Orbitale gut lokalisiert werden konnten führt das zu einer linearen Skalierung und macht die Beschreibung von Systemen mit 100-150 korrelierten Orbitalen und 2000-4000 Basisfunktionen mit lokalem RMP2 und UCCSD möglich. Die Skalierung und die Genauigkeit der oben genannten Methoden wurde überprüft. Um die Leistungsfähigkeit der Methoden zu überprüfen wurden Stabilisierungs-Energien von Radikalen und Ionisierungs-Potentiale bei starren Molekül-Geometrien berechnet. Die Rechnungen lieferten Ergebnisse, die mit den entsprechenden kanonischen Methoden vergleichbar waren.

Die Arbeit wurde in Sechs Kapitel unterteilt. Im Kapitel 1 wird die Theorie der einzelnen Methoden wie Hartree-Fock, coupled cluster und configuration interaction besprochen. Später wird dann genauer auf open-shell restricted second order Møller-Plesset perturbation theory, unrestricted singles and doubles coupled cluster (UCCSD) Theorie und die unrestricted singles and doubles coupled cluster mit störungstheoretischen Dreifachanregungen (UCCSD(T)) eingegangen, da sie einen starken Bezug zu dieser Arbeit haben.

Nach der Einführung der Elektronen-Korrelations-Methoden werden die in dieser Arbeitsgruppe entwickelten lokalen Methoden besprochen. Lokalisierte Molekülorbitale (LMOs), projizierte Atomorbitale (PAOs) und verschiedene Näherungen der lokalen Methoden werden eingeführt. Letztendlich wird eine Einführung in density-fitting (DF) und lokales density-fitting (LDF) gegeben.

In Kapitel 2 werden die lokalen open-shell Korrelationsmethoden beschrieben, die in dieser Arbeit entwickelt wurden. Die Lokalisierung der RHF Orbitale sowie LRMP2, LUCCSD und LCCSD(T) werden beschrieben. Es werden zwei verschiedene Lokalisations-Verfahren vorgestellt: die so genannte sd-Lokalisation, in der die open-shell und closed-shell Teile separat lokalisiert werden und die ab- Lokalisation, in der alpha- und beta- Spinorbitale separat lokalisiert werden. Die Gleichungen für diese Arbeit werden präsentiert und es wird besprochen wie eine lineare Skalierung erreicht werden kann.

In Kapitel 3 wird das Skalierungsverhalten der lokalen open-shell Korrelationsmethoden besprochen. Unter Verwendung von lokalem Fitting zeigt LRMP2 ein lineares Skalierungsverhalten in den verwendeten Testrechungen. LUCCSD zeigt beinahe ein lineares Skalierungsverhalten mit Ausnahme eines Terms. Bei Vernachlässigung dieses Terms kann lineare Skalierung erreicht werden. Die lokalen (nichtiterativen) Tripels (T0) erweisen sich als relativ wenig rechenintensiv und mit dem LCCSD-Teil vergleichbar.

Kapitel 4 befasst sich mit der Genauigkeit von lokalen open-shell Korrelationsmethoden. Dazu wurden die lokalen Fehler von DF-LRMP2, DF-LUCCSD und DF-LUCCSD(T) durch die Berechnung von 30 Radikalstabilisierungenergien (RSE), 30 vertikalen Ionisierungsenergien (IP) und 30 molekularen Elektronenaffinitäten (EA) bestimmt. Während die mittleren Fehler unter 1 kcal/mol betragen, finden sich maximale Fehler im Bereich von 2-4 kcal/mol. Der Fehler von DF-LRMP2 und DF-LUCCSD ist hierbei nicht bedeutend größer als der von RMP2 und entsprechendes gilt für UCCSD beim Vergleich zur UCCSD(T) Methode. Sowohl die sd- als auch die ab- Lokalisierung führen dabei zu vergleichbaren Fehlern; in Abhängigkeit vom jeweils untersuchten Fall sind hierbei die Fehler entweder mit der sd- oder mit der ab-Lokalisierung größer.

In Kapitel 5 werden zwei Anwendungen der neuen lokalen Methoden für große Systeme besprochen. Der lokale Fehler bei der Berechnung von Dissoziationsenergien von Kupfer-Sauerstoff (Triplett) Komplexen beträgt weniger als 1 kcal/mol wobei kleinere Fehler mit der sd-Lokalisierung auftreten. Bei der Berechnung des Reaktionspfades für die interne Umwandlung von (S)-Glutamat zu (2S,3S)-3-Methylaspartat beträgt der lokale Fehler von DF-LRMP2 etwa 2-3 kcal/mol für die Übergangszustände als auch die Zwischenstufen. Für die zweite Zwischenstufe (Acrylsäureester und Glycyl in GluM) und den Übergangzustand davor und danach sind die Energien die mit LUCCSD(T) berechnet wurden etwa 8 kcal/mol über denjenigen, die mit DFT/B3LYP berechnet wurden. Für die anderen Gebiete des Reaktionspfades hingegen stimmen die Ergebnisse von LUCCSD(T) und DFT bis auf etwa 1 kcal/mol überein. Daraus folgt, dass die Energie der zweiten Zwischenstufe durch DFT/B3LYP nicht hinreichend gut beschrieben wird. Der LUCCSD(T) Reaktionspfad entspricht demnach eher dem tatsächlichen Reaktionspfad.

Die in dieser Arbeit verwendeten Strukturen finden sich in Anhang A wieder. Alle berechneten RSE, IP und EA Werte, sowie einige Absolutenergien entsprechender Radikale, Moleküle, Ionen und Anionen befinden sich in Anhang B.

Schlussfolgernd kann man sagen, dass die neu entwickelte DF-LUCCSD(T) Methode die Anwendbarkeit von UCCSD(T) auf Systeme mit 100-150 korrelierten Orbitalen und 2000-4000 Basisfunktionen erweitert hat. Beim Vergleich zu UCCSD(T) ist der mittlere Fehler von DF-LUCCSD(T) unter 2 kcal/mol, der maximale Fehler beträgt 2-4 kcal/mol. Diese Fehlergrenzen sind jedoch noch immer nicht ausnahmslos zufriedenstellend. Die entsprechende F12 Methode sollte allerdings in der Lage sein diese Fehler zusammen mit dem Basissatzfehler unter 1 kcal/mol zu bringen. Die DF-LRMP2-F12, DF-LUCCSD(T)-F12 und DF-LUCCSD(T)-F12 Methoden werden von Dr. Filipe Agapito deshalb in unserer Arbeitsgruppe entwickelt.

Abbreviations

CC	Coupled cluster
CCSD	Singles and doubles coupled cluster
CCSD(T)	Singles and doubles coupled cluster with perturbative triples
CCSDT	Singles, doubles, and triples coupled cluster
CI	Configuration interaction
DF	Density fitting
LDF	Local density fitting
DFT	Density functional theory
EA	Electron affinity
FCI	Full configuration interaction
GluM	Glutamate mutase
HF	Hartree-Fock
IP	Ionization potential
LCCSD	Local CCSD
LCCSD(T)	Local CCSD(T)
LCCSD(T0)	Local CCSD with non-iterative triples
LMO	Localized molecular orbital
LMP2	Local MP2
LRMP2	Local spin restricted open-shell MP2
LUCCSD	Local UCCSD
LUCCSD(T)	Local UCCSD(T)
LUCCSD(T0)	Local UCCSD with non-iterative triples
MAE	Mean absolute error
MaxE	Maximum error
MM	Molecular mechanics
MO	Molecular orbital
MP	Møller-Plesset
MP2	Second-order Møller-Plesset perturbation theory
PAO	Projected atomic orbital
PM	Pipek-Mezey
QM	Quantum mechanics
QM/MM	Quantum mechanics / molecular mechanics
RHF	Restricted open-shell HF
RMP2	Restricted open-shell MP2
RMSE	Root mean square error

ROMP2	RMP2
RSE	Radical stabilization energy
RSPT	Rayleigh-Schrödinger perturbation theory
RSPT1	First-order RSPT
RSPT2	Second-order RSPT
SCF	Self-consistent field
UCCSD	Unrestricted open-shell CCSD
UCCSD(T)	Unrestricted open-shell CCSD(T)
UHF	Unrestricted open-shell HF
UMP	Unrestricted open-shell Møller-Plesset perturbation theory
ZPVE	Zero-point vibrational energy

Contents

Acknowledgments **3**

Abstract **5**

Zusammenfassung **9**

Abbreviations **12**

1 Theoretical Background **17**

1.1 Electron Correlation 17

1.1.1 Introduction to Wave Function Methods 17

1.1.2 Møller-Plesset Perturbation Theory 23

1.1.3 Coupled Cluster with Singles and Doubles 26

1.1.4 Perturbative Triple Excitations 29

1.2 Local Correlation 30

1.2.1 Localized Molecular Orbitals (LMOs) 31

1.2.2 Projected Atomic Orbitals (PAOs) 32

1.2.3 Pair Approximation 33

1.2.4 Domain Approximation 34

1.3 Density Fitting Approximation 35

2 Open-shell Local Correlation Methods **37**

2.1 Localization Schemes of Restricted Open-shell HF orbitals 37

2.2 LRMP2 Method 38

2.3 LUCCSD Method 44

2.4 Local (T0) Approximation 52

3 Scaling Tests of Open-shell Local Correlation Methods **55**

3.1 Scaling of LRMP2 55

3.2 Scaling of LUCCSD 64

3.2.1 Scaling Using Default Settings 64

3.2.2 Scaling with Setting ‘igskip=1’ and ‘igskip=2’ 68
3.3 Scaling of (T0) Calculation 71

4 Accuracy Tests of Open-shell Local Correlation Methods 75
4.1 Tested Systems 75
4.2 Accuracy of LRMP2 82
4.3 Accuracy of LUCCSD 88
4.3.1 Default Settings of LUCCSD 88
4.4 Accuracy of LUCCSD(T) 94

5 Applications 101
5.1 Formation Energy of Copper-Oxygen Complex 101
5.2 Inter Conversion of (S)-glutamate 103

6 Summary 109

Appendix A: Optimized Stationary Points Structures 111

Appendix B: Supplementary Data 153

1 Theoretical Background

1.1 Electron Correlation

1.1.1 Introduction to Wave Function Methods

In wave function theory, under adiabatic and Born-Oppenheimer approximations, a N-electron system is described by a N-body wave function. While some of the N-electron wave functions can be well approximated by a single Slater determinant, others cannot. Correspondingly, there are single reference and multi reference methods which deal with these two cases. In this thesis only the single reference methods will be discussed. In single reference wave function theory, the starting point is Hartree-Fock (HF) theory. HF theory is also called self-consistent field method (SCF). In this theory, each particle is subjected to a mean field created by all other particles. The HF wave function is an anti-symmetrized product of spin orbitals, which are optimized using the variational principle. There are two types of spin orbitals: restricted spin orbitals, which are constructed to have the same spatial function for different spin functions, and unrestricted spin orbitals, which have different spatial functions for different spins. Because of the well-known spin contamination problem of post HF methods using unrestricted spin orbitals [1–6], restricted HF spin orbitals are used in this work for the correlation treatment of open-shell species.

Although the HF approximation is remarkably successful in many cases, it is also well know to be quite limited. The HF energy represents about 99% of the total energy, but the missing 1% turns out to be very important in most cases. Because of the mean-field approximation in the HF method, the instantaneous correlation between electrons as they move, which is often essential for chemical phenomena, is missing. This energy term is generally called correlation energy. There is a variety of procedures for improving the HF approximation. To obtain the correlation energy, a linear combination of Slater determinants with different orbital occupations can be used to build better wave functions. The determinants are usually constructed

from the HF (occupied and virtual) orbitals, and their expansion coefficients are optimized. Therefore, these methods are still called single reference methods, in contrast with multi reference methods in which both the Slater determinants and the combination coefficients are optimized.

In order to describe HF method in more details, it is necessary to start with the definition of wave function and the equation of it, i.e., Schrödinger equation. A wave function Ψ defines the state of a system in quantum mechanics. The Schrödinger equation

$$\hat{H}\Psi = E\Psi \tag{1.1}$$

determines the states Ψ occurred in a system which is described by the Hamiltonian operator $\hat{H}$. For a N-electron-M-nuclei system, the Hamiltonian is written (in atomic units) as

$$\hat{H} = -\frac{1}{2}\sum_{i=1}^{N}\nabla_i^2 - \frac{1}{2}\sum_{m=1}^{M}\frac{1}{M_m}\nabla_m^2 - \sum_{m=1}^{M}\sum_{i=1}^{N}\frac{Z_m}{r_{im}} + \sum_{i<j}\frac{1}{r_{ij}} + \sum_{m<n}\frac{Z_m Z_n}{r_{mn}}, \tag{1.2}$$

where the indices i and j refer to the indices of electrons, m and n to the indices of nuclei. M_m denote the masses of the nuclei and Z_m denote their charges. r_{im}, r_{ij}, and r_{mn} denote the distances between an electron and a nucleus, the distances between two electrons, and the distances between two nuclei, respectively. Under Born-Oppenheimer and adiabatic approximations, for the energy of a given electronic state, the above Hamiltonian can be substituted by an electronic Hamiltonian of the form

$$\hat{H}_{electron} = -\frac{1}{2}\sum_{i=1}^{N}\nabla_i^2 - \sum_{m=1}^{M}\sum_{i=1}^{N}\frac{Z_m}{r_{im}} + \sum_{i<j}\frac{1}{r_{ij}}, \tag{1.3}$$

and adding the nuclear repulsion potentials a posteriori. In the following discussions, all Hamiltonian operators $\hat{H}$ will take the form of $\hat{H}_{electron}$ which is given in the above equation. Defining a single particle operator $\hat{h}(\mathbf{r}_i)$ as

$$\hat{h}(\mathbf{r}_i) = -\frac{1}{2}\nabla_i^2 - \sum_{m=1}^{M}\frac{Z_m}{r_{im}}, \tag{1.4}$$

the electronic Hamiltonian can be written in a shorter form

$$\hat{H}_{electron} = \sum_{i=1}^{N}\hat{h}(i) + \sum_{i<j}\frac{1}{r_{ij}}. \tag{1.5}$$

In the following discussion, indices $r, s, t, ...$ denote arbitrary spin-orbitals. Denoting the molecular spin-orbitals as $\{\psi_r\}$, the HF wave function is the single determinant formed by them and can be written as

$$|\Psi_0\rangle = |\psi_1\psi_2\psi_3...\psi_r\psi_s...\psi_N\rangle, \tag{1.6}$$

where N is the number of electrons. According to the variational principle, the spin orbitals can be optimized by minimizing the HF electronic energy

$$E_0 = \langle\Psi_0|\hat{H}|\Psi_0\rangle = \sum_r \langle r|\hat{h}|r\rangle + \frac{1}{2}\sum_{rs}\left\{[rr|ss] - [rs|sr]\right\}, \tag{1.7}$$

where use has been made of the following notations for one and two-electron integrals

$$\langle r|\hat{h}|s\rangle = \int d\mathbf{x_1}\psi_r^*(\mathbf{x_1})h(\mathbf{r_1})\psi_j(\mathbf{x_1}) \tag{1.8}$$

$$[rs|tu] = \int d\mathbf{x_1}\int d\mathbf{x_2}\psi_r^*(\mathbf{x_1})\psi_s(\mathbf{x_1})r_{12}^{-1}\psi_t^*(\mathbf{x_2})\psi_u(\mathbf{x_2}). \tag{1.9}$$

The electron coordinates are given as a vector $\mathbf{x}_r = \{\mathbf{r}_r, \mathbf{s}_r\}$, for spatial and spin coordinates respectively.

Minimizing the HF energy E_0, an equation known as integro-differential equation which defines the best spin orbitals is obtained as

$$\begin{aligned}\hat{h}(\mathbf{r_1})\psi_r(\mathbf{x_1}) &+ \sum_{s\neq r}\left[\int d\mathbf{x_2}|\psi_s(\mathbf{x_2})|^2 r_{12}^{-1}\right]\psi_r(\mathbf{x_1}) \\ &- \sum_{s\neq r}\left[\int d\mathbf{x_2}\psi_s^*(\mathbf{x_2})\psi_r(\mathbf{x_2})r_{12}^{-1}\right]\psi_s(\mathbf{x_1}) = \varepsilon_r\psi_r(\mathbf{x_1}).\end{aligned} \tag{1.10}$$

The orbital energy of the spin orbital ψ_r is denoted as ε_r. Defining a Coulomb operator $\hat{J}$ and an exchange operator $\hat{K}$ as

$$\hat{J}_s(\mathbf{r_1})\psi_r(\mathbf{x_1}) = \left[\int d\mathbf{x_2}|\psi_s(\mathbf{x_2})|^2 r_{12}^{-1}\right]\psi_r(\mathbf{x_1}) \tag{1.11}$$

$$\hat{K}_s(\mathbf{r_1})\psi_r(\mathbf{x_1}) = \left[\int d\mathbf{x_2}\psi_s^*(\mathbf{x_2})\psi_r(\mathbf{x_2})r_{12}^{-1}\right]\psi_s(\mathbf{x_1}), \tag{1.12}$$

the HF equation can be written as

$$\left[\hat{h}(\mathbf{r}_1) + \sum_{s\neq r}\hat{J}_s(\mathbf{r}_1) - \sum_{s\neq r}\hat{K}_s(\mathbf{r}_1)\right]\psi_r(\mathbf{x}_1) = \varepsilon_r\psi_r(\mathbf{x}_1). \tag{1.13}$$

Because of the restricted summation over $s \neq r$, the above equation is different for every spin orbital. From the definition of the Coulomb and exchange operators, it is obvious that

$$\left[\hat{J}_r(\mathbf{r}_1) - \hat{K}_r(\mathbf{r}_1)\right] \psi_r(\mathbf{x}_1) = 0. \tag{1.14}$$

By inserting this term to the above expression of the HF equation, eliminating the restriction on the summation, and defining a Fock operator $\hat{f}$ by

$$\hat{f} = \hat{h} + \sum_s \left[\hat{J}_s - \hat{K}_s\right], \tag{1.15}$$

the Hartree-Fock equations finally becomes

$$\hat{f}|\psi_r\rangle = \varepsilon_r|\psi_r\rangle. \tag{1.16}$$

Using the above definition, one can show that the general matrix element of the Fock operator has the form

$$\langle i|\hat{f}|j\rangle = \langle i|\hat{h}|j\rangle + \sum_s \{[ij|ss] - [is|sj]\}. \tag{1.17}$$

The full configuration interaction (FCI) method is the most accurate correlation method. If a complete basis set is used, FCI provides the exact numerical solution of the Schrödinger equation under the above mentioned approximations. The FCI wave function consists of using all possible Slater determinants with different occupations for HF molecular orbitals (MOs). Unfortunately, FCI is horribly expensive and only feasible for very small systems using small basis sets. Therefore, some more important Slater determinants must be selected out from all the possible ones. In the Slater determinant for the HF ground state, there are occupied HF orbitals with an occupation number of 1 or 2, and virtual HF orbitals with an occupation number of 0. In other determinants, the number of electrons in HF occupied orbitals is smaller than in the ground state, while the number of electrons in HF virtual orbitals is non-zero. These configurations can be imaged as formed by exciting electrons from the occupied HF orbitals to virtual HF orbitals. Therefore, these configurations are named excited configurations. The excited configurations are classified according to the above number n, i.e., singly excited configurations, doubly excited configurations,...,nth excited configurations. In the following parts, the notations will be used as: the indices $i, j, ...$ denote the occupied spin-orbitals, the indices $a, b, ...$ denote the unoccupied spin-orbitals. The indices with tilde above

denote alpha-orbitals and the indices with bar above denote beta-orbitals. Using the notation $\Psi^{\mathtt{HF}}$ for the HF ground state, Ψ_a^i for singly excited configurations in which an electron is excited from the $i^{\mathtt{th}}$ occupied HF orbital to the $a^{\mathtt{th}}$ virtual HF orbital, Ψ_{ab}^{ij} for doubly excited configurations, and correspondingly for higher order excitations, the correlated wave function Ψ can be described as follows,

$$|\Psi\rangle = |\Psi^{\mathtt{HF}}\rangle + \sum_{i,a} c_a^i |\Psi_a^i\rangle + \sum_{ij,ab} c_{ab}^{ij} |\Psi_{ab}^{ij}\rangle + \sum_{ijk,abc} c_{abc}^{ijk} |\Psi_{abc}^{ijk}\rangle + ... \tag{1.18}$$

$$|\Psi^{\mathtt{corr}}\rangle = \sum_{i,a} c_a^i |\Psi_a^i\rangle + \sum_{ij,ab} c_{ab}^{ij} |\Psi_{ab}^{ij}\rangle + \sum_{ijk,abc} c_{abc}^{ijk} |\Psi_{abc}^{ijk}\rangle + ... \tag{1.19}$$

Correspondingly, the electronic energies are expressed as

$$E^{\mathtt{HF}} = \langle \Psi^{\mathtt{HF}} | \hat{H} | \Psi^{\mathtt{HF}} \rangle, \tag{1.20}$$

$$E^{\mathtt{corr}} = \langle \Psi^{\mathtt{HF}} | \hat{H} | \Psi^{\mathtt{corr}} \rangle, \tag{1.21}$$

$$E = E^{\mathtt{HF}} + E^{\mathtt{corr}}. \tag{1.22}$$

If all the possible excitations are considered, the FCI expression is generated. To obtain more efficient expressions it is needed to truncate the excitations. For the discussion of truncations it is convenient to employ second quantization and spin-orbital excitation operators $\hat{e}_{ai}$, $\hat{e}_{bj}$, $\hat{e}_{ck}$...as given in the following,

$$|\Psi_a^i\rangle = \hat{e}_{ai} |\Psi^{\mathtt{HF}}\rangle, \tag{1.23}$$

$$|\Psi_{ab}^{ij}\rangle = \hat{e}_{ai}\hat{e}_{bj} |\Psi^{\mathtt{HF}}\rangle, \tag{1.24}$$

$$|\Psi_{abc}^{ijk}\rangle = \hat{e}_{ai}\hat{e}_{bj}\hat{e}_{ck} |\Psi^{\mathtt{HF}}\rangle, \tag{1.25}$$

$$... \quad .$$

If the unit operator is notated as $\hat{1}$ and the excitation operators are defined as

$$\hat{T}_1 = \sum_{i,a} \hat{e}_{ai} t_a^i, \tag{1.26}$$

$$\hat{T}_2 = \sum_{i>j,a>b} \hat{e}_{ai}\hat{e}_{bj} t_{ab}^{ij}, \tag{1.27}$$

$$\hat{T}_3 = \sum_{i>j>k,a>b>c} \hat{e}_{ai}\hat{e}_{bj}\hat{e}_{ck} t_{abc}^{ijk}, \tag{1.28}$$

$$... \quad ,$$

and

$$\hat{T} = \hat{1} + \hat{T}_1 + \hat{T}_2 + \hat{T}_3 + ... \ , \tag{1.29}$$

the configuration interaction (CI) wave function can be expressed as,

$$|\Psi^{\mathtt{CI}}\rangle = \hat{T}|\Psi^{\mathtt{HF}}\rangle = (\hat{1} + \hat{T}_1 + \hat{T}_2 + \hat{T}_3 + ...)|\Psi^{\mathtt{HF}}\rangle. \tag{1.30}$$

Truncating the CI wave function at the nth excitation yields the CIS, CISD, CISDT,... wave functions, defined as

$$\begin{aligned} |\Psi^{\mathtt{CIS}}\rangle &= (\hat{1} + \hat{T}_1)|\Psi^{\mathtt{HF}}\rangle, & (1.31)\\ |\Psi^{\mathtt{CISD}}\rangle &= (\hat{1} + \hat{T}_1 + \hat{T}_2)|\Psi^{\mathtt{HF}}\rangle, & (1.32)\\ |\Psi^{\mathtt{CISDT}}\rangle &= (\hat{1} + \hat{T}_1 + \hat{T}_2 + \hat{T}_3)|\Psi^{\mathtt{HF}}\rangle, & (1.33)\\ &\ldots \quad . & (1.34) \end{aligned}$$

If the Nth (N is the number of electrons in the system) excitation is included, then the FCI wave function is obtained.

Because the expansion coefficients of CISD are determined variationally, the resulting energy of it is always an upper bound to the exact energy. However, practically CISD usually yields poor results because it is neither size extensive nor size consistent. Size extensive means scale correctly with the number of electrons. Size consistent means scale correctly with the number of independent subsystems, i.e., dissociating correctly. Alternatively, an exponential ansatz

$$e^{\hat{T}} = \hat{1} + \hat{T} + \frac{\hat{T}^2}{2!} + \frac{\hat{T}^3}{3!} + ... \tag{1.35}$$

may be used and the coupled cluster (CC) [7–9] wave function is obtained as

$$|\Psi^{\mathtt{CC}}\rangle = e^{\hat{T}}|\Psi^{\mathtt{HF}}\rangle \ . \tag{1.36}$$

Truncating the CC wave function at the nth excitation yields the CCS, CCSD, CCSDT... wave functions, defined as

$$\begin{aligned} |\Psi^{\mathtt{CCS}}\rangle &= e^{\hat{T}_1}|\Psi^{\mathtt{HF}}\rangle, & (1.37)\\ |\Psi^{\mathtt{CCSD}}\rangle &= e^{(\hat{T}_1+\hat{T}_2)}|\Psi^{\mathtt{HF}}\rangle, & (1.38)\\ |\Psi^{\mathtt{CCSDT}}\rangle &= e^{(\hat{T}_1+\hat{T}_2+\hat{T}_3)}|\Psi^{\mathtt{HF}}\rangle, & (1.39)\\ &\ldots \quad . \end{aligned}$$

As in the CI case, if the Nth excitation in the CC expansion is included, the FCI wave function is again obtained. Comparing with CISD, CCSD method is both size extensive and size consistent. However, it is not a variational method. Instead of

expanding the wave function and optimizing the coefficients, it is also possible to use perturbation theory to get approximations for the coefficients of the determinants. In the following section perturbation theory will be first discussed, and then the CCSD and CCSD(T) methods will be introduced. These methods will be subsequently used to construct the local correlation methods in the next chapter.

1.1.2 Møller-Plesset Perturbation Theory

Møller-Plesset perturbation theory is one of the most traditional *ab initio* methods. Since the first publication of C. Møller and M. S. Plesset in 1934, [10] its applications for open-shell systems have been very well studied. [1, 2, 4, 6, 11–15]

For the perturbation theory, a zeroth order Hamiltonian and a perturbation are needed. Written in second quantization, the Møller-Plesset zeroth-order Hamiltonian is

$$\hat{H}^{(0)} = \sum_r \hat{f}(r) = \sum_{ij} f_{ij}\hat{e}_i^\dagger \hat{e}_j + \sum_{ia} f_{ia}\hat{e}_i^\dagger \hat{e}_a + \sum_{ab} f_{ab}\hat{e}_a^\dagger \hat{e}_b, \tag{1.40}$$

where $f_{rs} = \langle r|\hat{f}|s\rangle$ are the matrix elements of the Fock operator in the spin-orbital basis. For closed shell systems, due to the Brillouin theorem, f_{ia} must vanish for optimized orbitals. For open-shell systems, if α and β orbitals are varied independently to minimize the total energy, the unrestricted Hartree-Fock (UHF) optimized orbitals are generated. For UHF orbitals the Brillouin theorem still holds and the f_{ia} vanish. Therefore, based on UHF orbitals, it is straightforward to do an unrestricted Møller-Plesset perturbation (UMP) treatment. On the other hand, the UHF wavefunction is no longer an eigenfunction of the spin operator $\hat{S}^2$. This spin contamination problem is well known to be harmful, especially for molecules with stretched bonds and some unsaturated radicals [1–6], which are very important open-shell systems. To avoid spin contamination, during the orbital optimization, β orbitals can be restricted to be linear combinations of the α orbitals, from which the spin restricted open-shell (RHF) optimized orbitals are obtained. However, the Brillouin theorem does not hold for RHF orbitals and the elements f_{ia} are nonzero. The RHF reference function is then not even an eigenfunction of $\hat{H}^{(0)}$. Therefore, definition of the above zeroth-order Hamiltonian needs to be changed. Defining the projecting operator $\hat{o}$ as

$$\hat{o} = \sum_i |i\rangle\langle i|, \tag{1.41}$$

a projected Fock operator $\hat{g}$ can be used instead of $\hat{f}$, where

$$\hat{g} = \hat{o}\hat{f}\hat{o} + (1-\hat{o})\hat{f}(1-\hat{o}). \tag{1.42}$$

Now the zeroth-order Hamiltonian takes the simpler form

$$\hat{H}^{(0)} = \sum_{ij} f_{ij}\hat{e}_i^\dagger\hat{e}_j + \sum_{ab} f_{ab}\hat{e}_a^\dagger\hat{e}_b, \tag{1.43}$$

and the perturbation is defined as

$$\hat{V} = \hat{H} - \hat{H}^{(0)} \tag{1.44}$$

Therefore,

$$\begin{aligned} E^{(0)} &= \langle\Psi^{\mathtt{HF}}|\hat{H}^{(0)}|\Psi^{\mathtt{HF}}\rangle, && (1.45)\\ E^{(1)} &= \langle\Psi^{\mathtt{HF}}|\hat{V}|\Psi^{\mathtt{HF}}\rangle, && (1.46)\\ E^{(0)} + E^{(1)} &= \langle\Psi^{\mathtt{HF}}|(\hat{H}^{(0)} + \hat{V})|\Psi^{\mathtt{HF}}\rangle \\ &= \langle\Psi^{\mathtt{HF}}|\hat{H}|\Psi^{\mathtt{HF}}\rangle \\ &= E^{\mathtt{HF}}. && (1.47) \end{aligned}$$

The zero and first-order energy together give the HF energy. As a result, in this perturbation expression, the second-order of perturbation energy gives the first correction to the Hartree-Fock energy. The general expression of the second order energy is

$$E^{(2)} = \langle\Psi^{\mathtt{HF}}|\hat{H}|\Psi^{(1)}\rangle, \tag{1.48}$$

so a definition of first-order wave function is still needed. Notice that since $\hat{H}$ is a two-body operator, only singly and doubly excited configurations contribute to $\Psi^{(1)}$. Therefore, the first-order wave function can be written as

$$|\Psi^{(1)}\rangle = \sum_{i,a} t_a^i|\Psi_a^i\rangle + \frac{1}{4}\sum_{ij,ab} T_{ab}^{ij}|\Psi_{ab}^{ij}\rangle. \tag{1.49}$$

There are two ways to get the energy corrections for RMP2. The first is the non-iterative formula. If the projection $\hat{o}$ in operator $\hat{g}$ is on alpha or beta spin, block-diagonalized semi-Fock matrices for, respectively alpha or beta spin are obtained. The second is the iterative formula where an orbital invariant formulation is generated. [13–16] As discussed by G. Knizia and H.-J. Werner, [17] by inserting the

first-order wave function into the general Rayleigh-Schrödinger perturbation theory (RSPT) equation, the orbital invariant formulation is obtained. To generate the RSPT equation, the starting point is the perturbation expression of Schrödinger equation, i.e.,

$$(\hat{H}^{(0)} + \lambda\hat{V})|\Psi\rangle = E|\Psi\rangle. \tag{1.50}$$

Inserting the energy and wave function expansions as

$$E = \sum_k \lambda^k E^{(k)}, |\Psi\rangle = \sum_k \lambda^k |\Psi^{(k)}\rangle, \tag{1.51}$$

the RSPT equations are obtained, i.e.,

$$\begin{aligned}&(\hat{H}^{(0)} - E^{(0)})|\Psi^{(0)}\rangle \\ &+\lambda[(\hat{H}^{(0)} - E^{(0)})|\Psi^{(1)}\rangle + (\hat{V} - E^{(1)})|\Psi^{(0)}\rangle] + ... = 0,\end{aligned} \tag{1.52}$$

which hold for any value of λ. Therefore,

$$(\hat{H}^{(0)} - E^{(0)})|\Psi^{(0)}\rangle = 0 \quad , \tag{1.53}$$

$$(\hat{H}^{(0)} - E^{(0)})|\Psi^{(1)}\rangle + (\hat{V} - E^{(1)})|\Psi^{(0)}\rangle = 0 \quad . \tag{1.54}$$

The above equations are named RSPT0, RSPT1 equations. RSPT0 is simply the HF equation. To get the first order wave function, the solution of the RSPT1 equation is needed. Projecting the RSPT1 equation to single excitation determinants and double excitation determinants, and noticing that

$$\langle\Psi_a^i|\Psi^{(0)}\rangle = 0, \langle\Psi_{ab}^{ij}|\Psi^{(0)}\rangle = 0, \tag{1.55}$$

one obtains

$$\langle\Psi_a^i|(\hat{H}^{(0)} - E^{(0)})|\Psi^{(1)}\rangle + \langle\Psi_a^i|\hat{V}|\Psi^{(0)}\rangle = 0, \tag{1.56}$$

and

$$\langle\Psi_{ab}^{ij}|(\hat{H}^{(0)} - E^{(0)})|\Psi^{(1)}\rangle + \langle\Psi_{ab}^{ij}|\hat{V}|\Psi^{(0)}\rangle = 0, \tag{1.57}$$

which hold for any i, j, a, b. Inserting the above expression for $\hat{H}^{(0)}$, $\hat{H}^{(1)}$, $|\Psi^{(1)}\rangle$ in the RSPT1 equation, and carrying out the second quantization algebra, the equation

for excitation amplitudes t_a^i and T_{ab}^{ij} can be written as follows,

$$f_{ia} + \sum_b f_{ab} t_b^i - \sum_k f_{ki} t_a^k = 0, \tag{1.58}$$

$$\frac{1}{2}(K_{ab}^{ij} - K_{ab}^{ji}) + \sum_c (f_{cb} T_{ac}^{ij} + f_{ca} T_{bc}^{ji}) - \sum_k (f_{ki} T_{ab}^{kj} + f_{kj} T_{ab}^{ik}) = 0, \tag{1.59}$$

where $f_{rs} = \langle r|\hat{f}|s\rangle$ are the matrix elements of the Fock operator in the spin-orbital basis, and $K_{tu}^{rs} = [tr|su]$ are the matrix elements of the exchange operator in the spin-orbital basis. Solving the above equations iteratively provides the excitation amplitudes t_a^i and T_{ab}^{ij}, and therefore the expression of the first-order wave function is also obtained. The second-order energy can be calculated by Eq. 1.48; when carrying out second quantization algebra, the form

$$E^{(2)} = \sum_{i,a} f_{ia} t_a^i + \sum_{i>j,a>b} K_{ab}^{ij} T_{ab}^{ij} \tag{1.60}$$

is obtained. All of the above discussion is done using spin-orbitals. The equations can also be explicitly written out for different spins, which will be done later in the local expressions.

1.1.3 Coupled Cluster with Singles and Doubles

As discussed in the first section of this chapter, the CCSD wave function is written as

$$|\Psi^{\mathtt{CCSD}}\rangle = e^{(\hat{T}_1+\hat{T}_2)}|\Psi^{\mathtt{HF}}\rangle. \tag{1.61}$$

Because all HF orbitals are orthogonal, all the excited configurations are orthogonal to the ground state, $|\Psi^{\mathtt{HF}}\rangle$. Therefore,

$$\begin{aligned}\langle\Psi^{\mathtt{HF}}|\Psi^{\mathtt{CCSD}}\rangle &= \langle\Psi^{\mathtt{HF}}|\left[\hat{1} + (\hat{T}_1 + \hat{T}_2) + \frac{1}{2}(\hat{T}_1 + \hat{T}_2)^2 + ...\right]|\Psi^{\mathtt{HF}}\rangle \\ &= \langle\Psi^{\mathtt{HF}}|\Psi^{\mathtt{HF}}\rangle \\ &= 1. \end{aligned} \tag{1.62}$$

The CCSD energy can be written as

$$\begin{aligned} E^{\mathtt{CCSD}} &= E^{\mathtt{CCSD}}\langle\Psi^{\mathtt{HF}}|\Psi^{\mathtt{CCSD}}\rangle \\ &= \langle\Psi^{\mathtt{HF}}|\hat{H}|\Psi^{\mathtt{CCSD}}\rangle \end{aligned}$$

$$
\begin{aligned}
&= \langle \Psi^{\mathtt{HF}} | \hat{H} \left[\hat{1} + (\hat{T}_1 + \hat{T}_2) + \frac{1}{2}(\hat{T}_1 + \hat{T}_2)^2 + ... \right] | \Psi^{\mathtt{HF}} \rangle \\
&= E^{\mathtt{HF}} + \langle \Psi^{\mathtt{HF}} | \hat{H}(\hat{T}_1 + \frac{1}{2}\hat{T}_1^2 + \hat{T}_2) | \Psi^{\mathtt{HF}} \rangle. \qquad (1.63)
\end{aligned}
$$

Consequently, the correlation energy can be written as

$$
\begin{aligned}
E_{\mathtt{corr}}^{\mathtt{CCSD}} &= E^{\mathtt{CCSD}} - E^{\mathtt{HF}} \\
&= \langle \Psi^{\mathtt{HF}} | \hat{H}(\hat{T}_1 + \frac{1}{2}\hat{T}_1^2 + \hat{T}_2) | \Psi^{\mathtt{HF}} \rangle \\
&= \langle \Psi^{\mathtt{HF}} | \hat{H}(\hat{T}_1 + \frac{1}{2}\hat{T}_1^2 + \hat{T}_2) | \Psi^{\mathtt{HF}} \rangle \\
&= \langle \Psi^{\mathtt{HF}} | \hat{H}\hat{T}_1 | \Psi^{\mathtt{HF}} \rangle + \langle \Psi^{\mathtt{HF}} | \hat{H}(\frac{1}{2}\hat{T}_1^2 + \hat{T}_2) | \Psi^{\mathtt{HF}} \rangle \\
&= \sum_{ia} \langle \Psi^{\mathtt{HF}} | \hat{H} | \Psi_a^i \rangle t_a^i + \sum_{i>j,a>b} \langle \Psi^{\mathtt{HF}} | \hat{H} | \Psi_{ab}^{ij} \rangle \left(\frac{1}{2} t_a^i t_b^j + T_{ab}^{ij} \right). \qquad (1.64)
\end{aligned}
$$

Carrying out the second quantization algebra, the expression for the correlation energy is obtained,

$$
E_{\mathtt{corr}}^{\mathtt{CCSD}} = \sum_{ia} f_{ia} t_a^i + \sum_{i>j,a>b} K_{ab}^{ij} \left(\frac{1}{2} t_a^i t_b^j + T_{ab}^{ij} \right). \qquad (1.65)
$$

Notice that all the above indices run over spin orbitals.

In Eq. 1.65 the relationship between the excited amplitudes and the correlation energy is obtained. However, it is still needed to calculate the excitation amplitudes, i.e., it is needed to solve euqations

$$
\begin{aligned}
v_a^i &= \langle \Psi_a^i | (\hat{H} - E^{\mathtt{CCSD}}) | \Psi^{\mathtt{CCSD}} \rangle = 0, \qquad (1.66) \\
V_{ab}^{ij} &= \langle \Psi_{ab}^{ij} | (\hat{H} - E^{\mathtt{CCSD}}) | \Psi^{\mathtt{CCSD}} \rangle = 0, \qquad (1.67)
\end{aligned}
$$

which hold for any occupied spin orbital i, j and any virtual spin orbital a, b.

Insert the expression of CCSD wave function and take the zero terms, to obtain

$$
\begin{aligned}
v_a^i &= \langle \Psi^{\mathtt{HF}} | \hat{e}_{ia} (\hat{H} - E^{\mathtt{CCSD}}) (\hat{1} + \hat{T}_1 + \hat{T}_2 + \frac{1}{2}\hat{T}_1^2 + \hat{T}_1\hat{T}_2 + \frac{1}{6}\hat{T}_1^3) | \Psi^{\mathtt{HF}} \rangle, \qquad (1.68) \\
V_{ab}^{ij} &= \langle \Psi^{\mathtt{HF}} | \hat{e}_{ia}\hat{e}_{jb} (\hat{H} - E^{\mathtt{CCSD}}) (\hat{1} + \hat{T}_1 + \hat{T}_2 \\
&\quad + \frac{1}{2}\hat{T}_1^2 + \hat{T}_1\hat{T}_2 + \frac{1}{2}\hat{T}_2^2 + \frac{1}{6}\hat{T}_1^3 + \frac{1}{2}\hat{T}_1^2\hat{T}_2 + \frac{1}{24}\hat{T}_1^4) | \Psi^{\mathtt{HF}} \rangle. \qquad (1.69)
\end{aligned}
$$

Carrying out the second quantization algebra, the expression for the residuals is obtained. Because the residual equations of CCSD are quite complicated, it is necessary to introduce some intermediates first. These are the elements of Fock

matrices f_{ij}, f_{ia}, f_{ab}, the integrals

$$K_{kl}^{ij} = [ki|jl], \tag{1.70}$$
$$K_{ab}^{ij} = [ai|jb], \tag{1.71}$$
$$k_a^{ijk} = [ai|jk], \tag{1.72}$$
$$J_{ab}^{ij} = [ab|ij], \tag{1.73}$$

the combination of excitation amplitudes,

$$C_{ab}^{ij} = T_{ab}^{ij} + t_a^i t_b^j, \tag{1.74}$$

contractions of integrals and excitation amplitudes,

$$J(E^{ij})_{ab} = \sum_c [ab|ic] t_c^j, \tag{1.75}$$
$$K(E^{ij})_{ab} = \sum_c [ai|bc] t_c^j, \tag{1.76}$$
$$K(C^{ij})_a^k = \sum_{cd} [ac|dk] C_{cd}^{ij}, \tag{1.77}$$
$$K(C^{ij})_{ab} = \sum_{cd} [ac|db] C_{cd}^{ij}, \tag{1.78}$$

and the combinations

$$\alpha_{ij,kl} = K_{kl}^{ij} + \frac{1}{2} \sum_{ab} K_{ab}^{kl} C_{ab}^{ij}, \tag{1.79}$$
$$\beta_k^i = f_{ik} + \sum_a f_{ka} t_a^i + \sum_{l,ab} K_{ab}^{kl} C_{ab}^{il} + \sum_{l,a} t_a^l k_a^{lki}, \tag{1.80}$$
$$r_a^k = f_{ka} + \sum_{l,b} K_{ab}^{kl} t_b^l, \tag{1.81}$$
$$A_{ab} = \sum_{kl,c} K_{ac}^{kl} T_{cb}^{lk}, \tag{1.82}$$
$$\begin{aligned} s_a^i &= f_{ia} + \sum_b (f_{ab} - A_{ba}) t_b^i \\ &\quad - \sum_{kl,b} T_{ab}^{lk} k_b^{kli} + \sum_k K(C^{ik})_a^k + \sum_{k,b} (K_{ab}^{ik} - J_{ab}^{ik}) t_b^k, \end{aligned} \tag{1.83}$$
$$X_{ab} = f_{ab} - A_{ab} - \sum_k r_a^k t_b^k + \sum_k J(E_{ab}^{kk}) - \sum_k K(E_{ab}^{kk}), \tag{1.84}$$
$$Y_{ab}^{kj} = K_{ab}^{kj} - J_{ab}^{kj} + K(E^{kj})_{ab} - J(E^{kj})_{ab} + \frac{1}{2} \sum_{l,c} K_{ca}^{lk} T_{cb}^{lj} - \sum_l k_a^{klj} t_c^l, \tag{1.85}$$

$$Z_{ab}^{kj} = -J_{ab}^{kj} - J(E^{kj})_{ab} + \frac{1}{2}\sum_{l,c} K_{ca}^{kl} T_{cb}^{jl} + \sum_{l} k_a^{lkj} t_b^l, \tag{1.86}$$

$$\begin{aligned} G_{ab}^{ij} &= \sum_{c} T_{ac}^{ij} X_{cb} + \sum_{k,c} \left(T_{ac}^{ik} Y_{cb}^{kj} + T_{ac}^{kj} Z_{cb}^{ki} \right) \\ &\quad - \sum_{k} (t_a^k) \left[K(C^{ij})_b^k + k_b^{jik} \right] - \sum_{k,c} (t_a^k) \left(K_{bc}^{kj} t_c^i - J_{bc}^{kj} t_c^i \right). \end{aligned} \tag{1.87}$$

With the help of the above intermediates, the residuals can be written as

$$v_a^i = s_a^i + \sum_{k,b} T_{ab}^{ik} r_b^k - \sum_{k} \beta_k^i t_a^k \tag{1.88}$$

$$\begin{aligned} V_{ab}^{ij} &= K_{ab}^{ij} + K(C^{ij})_{ab} + K(E^{ij})_{ab} \\ &\quad + G_{ab}^{ij} + \sum_{kl} (\alpha_{kl}^{ij} - \delta_{ik}\beta_l^j - \delta_{jl}\beta_k^i) T_{ab}^{kl} \end{aligned} \tag{1.89}$$

Notice that all the above indices run over spin orbitals. If the equations are separated for different spins, some terms will vanish and some terms will be anti-symmetrized. The equations for different spins will be given later in the local CCSD discussion.

1.1.4 Perturbative Triple Excitations

To treat electron correlation properly, CCSD is known to be not enough for systems which can be described by a single determinant reference wave function, triple excitations are believed to be important for most cases. CCSDT and even CC methods with higher excitation have been implemented, unfortunately they are too expensive for most practical applications. Subsequent analysis of the terms of higher-order excitations provided by Rayleigh-Schrödinger perturbation theory (RSPT), leads to the conclusion that the two most important terms are those linear in triple excitations. [18–21] These are the fourth order term

$$\Delta E^{(4^{\mathrm{th}})} = \langle \Psi^{\mathrm{HF}} | \hat{T}_1^\dagger \hat{V} \hat{T}_3 | \Psi^{\mathrm{HF}} \rangle \tag{1.90}$$

and the most important fifth order term

$$\Delta E^{(5^{\mathrm{th}})} = \langle \Psi^{\mathrm{HF}} | \hat{T}_2^\dagger \hat{V} \hat{T}_3 | \Psi^{\mathrm{HF}} \rangle \tag{1.91}$$

where $\hat{V}$ denotes the perturbation operator in RSPT theory. This approximation is usually denoted as CCSD(T) and the perturbative triple correction is defined as

$$\Delta E^{(\mathrm{T})} = \langle \Psi^{\mathrm{HF}} | \left(\hat{T}_1 + \hat{T}_2 \right)^\dagger \hat{V} \hat{T}_3 | \Psi^{\mathrm{HF}} \rangle. \tag{1.92}$$

Working out the second quantization algebra, defining

$$\begin{aligned}\mathscr{W}_{abc}^{ijk} &= (i,j,k)(a,b,c) \\ &\times \left\{ \sum_e t_{ae}^{ij} \left[(kc|be) - (kb|ce)\right] + \sum_e t_{bc}^{kl} \left[(ai|jl) - (aj|il)\right] \right\} \end{aligned} \tag{1.93}$$

where (i,j,k) are permutation operators such that

$$(i,j,k)a_{ijk} \equiv a_{ijk} + a_{jki} + a_{kij}, \tag{1.94}$$

the (T) energy correction can be written as

$$\begin{aligned}\Delta E^{(T)} &= -\sum_{i>j>k} \sum_{a>b>c} \mathscr{W}_{abc}^{ijk} \times \\ &\left\{ \mathscr{W}_{abc}^{ijk} + (i,j,k)(a,b,c) \left\{ [(ia|bj) - (ib|aj)] t_c^k + t_{ab}^{ij} f_c^k \right\} \right\} / \epsilon_{abc}^{ijk}, \end{aligned} \tag{1.95}$$

where $\epsilon_{abc}^{ijk} \equiv \varepsilon_a + \varepsilon_b + \varepsilon_c - \varepsilon_i - \varepsilon_j - \varepsilon_k$ is the MP denominator. [22]

As in the above sections, all the orbitals here are RHF spin orbitals. Notice that the above expression does only hold exactly when the Fock matrix is diagonal, i.e., in the closed shell case or open-shell case with UHF orbitals. In the open-shell case with RHF orbitals, semi-cannonical orbitals need to be used [5,23]. With semi-canonical orbitals, the Fock matrix is diagonal within each of the occupied and virtual spaces, i.e. $\varepsilon_p \equiv f_{pp}$, but it is not diagonal in the occupied-virtual blocks. Using semi-canonical orbitals, all the above equations are exactly obeyed.

1.2 Local Correlation

Dynamical correlation, which describes the relationship between the movement of different electrons, is an important correction beyond mean field HF approximation where electrons do not know about each other's movements. Physically, dynamical correlation is a very short range effect, which decreases as fast as r^{-6}. Mathematically, the steep scaling of electron correlation methods is due to the fact that calculations are performed using a basis of canonical molecular orbitals, which are generally delocalized over the whole system. A localized description of electron correlation should be applied to avoid the steep scaling of electron correlation methods. In this section, the history of localization methods as well as the most popular localization methods are discussed.

The first local correlation methods are proposed in 1964 by Sinanoglu [24] and

Nesbet [25], and many other variants were developed later [26–57]. The success of the above methods are quite limited because of the use of orthogonal virtual orbitals which cannot be localized very satisfactorily. Pulay and Saebø avoided this problem by using nonorthogonal atomic orbitals as correlation space. [58–63] This ansatz has been applied to the whole hierarchy of closed shell single-reference electron correlation methods. [64–72]

There are also many other implementations in which the locality of electron correlation has been exploited. In the first class of these methods the whole molecule is treated as an entirety. There are AO-based methods developed by Maslen and Head-Gordon [73], Scuseria and Ayala [74], and Auer and Nooijen [75], the di- and tri- atomic in molecule schemes of Maslen and Head-Gordon *et al.* [76–78], the local coupled cluster doubles algorithms of Subotnik, Head-Gordon *et al.* [79–83], linear-scaling multi-reference singles and doubles configuration interaction approach based on local truncation schemes coupled with integral pre-screening of Chwee *et al.* [84], local CEPA using pair natural orbitals combined with the density fitting technique for evaluating the integrals by Neese *et al.* [85, 86]. The second class of methods divides the molecule into smaller subsystems for which CCSD (or others like CCSD, CCSD(T), and CC(2,3)) equations are solved separately. This was first described by Förner *et al.* [41], refined and generalized by Li *et al.* [87, 88]. In this class, there are the divide-and-conquer implementation of the CCSD(T) based on natural localized hybrid orbitals by Flocke and Bartlett [89, 90], and methods using the incremental scheme originally proposed by Stoll [91] and further developed by Friedrich and Dolg *et al.* [92–96].

1.2.1 Localized Molecular Orbitals (LMOs)

The localization of molecular orbitals is mathematically a unitary transformation of the canonical HF molecular orbitals. Because a unitary transformation maintains the orthonormality, in most localization methods the orthonormality of the orbitals is maintained which greatly simplifies the formalism. Many different localization schemes are available, the most popular being the Pipek-Mezey [49], Boys [97], and Edmiston-Ruedenberg [98] localizations. In Pipek-Mezey localization, the number of atoms at which the orbitals are located are minimized. The advantage of this scheme is the preservation of the $\sigma - \pi$ symmetry in planar molecules. Boys localization, which maximize distances between orbital centroids, is very inexpensive but has difficulty with radial localization. Furthermore, multiple bonds are usually localized as banana bonds. In the Edmiston-Ruedenberg scheme the maximization of intraorbital Coulomb repulsion is performed. It has the same advantage as the

Pipek-Mezey localization, but because a transformation of two-electron integrals is required it is rather expensive. Alternatively, local correlation methods with a natural localized molecular orbital (NLMO) basis have been developed as a new choice of the localization scheme. [99]

Choosing a localization method, a set of orthonormal localized molecular orbitals (LMOs) can be generated. The Pipek-Mezey localization procedure is chosen to generate LMOs in this application. LMOs $\{\breve{\phi}_i\}$ can be written as linear combinations of N basis functions or a unitary transformation of M MOs $\{\phi_i\}$, i.e.,

$$|\breve{\phi}_i\rangle = \sum_{\mu=1}^{N} |\chi_\mu\rangle L_{\mu i} = \sum_{j=1}^{M} |\phi_j\rangle U_{ji}. \tag{1.96}$$

If MOs are written as linear combinations of basis functions, i.e.,

$$|\phi_j\rangle = \sum_{\mu=1}^{N} |\chi_\mu\rangle C_{\mu j}, \tag{1.97}$$

one obtains $\mathbf{L} = \mathbf{CU}$.

1.2.2 Projected Atomic Orbitals (PAOs)

Atomic orbitals are localized on each atom naturally. If the LMOs are projected out from the AOs, a space consisting of atomic orbitals which are orthogonalized on the occupied space is generated. [58–63] These orbitals are named projected atomic orbitals (PAOs) and are localized by construction. Writing PAOs as $|\breve{\chi}_r\rangle$, the expression of PAOs is written as

$$|\breve{\chi}_r\rangle = \left(1 - \sum_i |\breve{\phi}_i\rangle\langle\breve{\phi}_i|\right) |\chi_r\rangle = \sum_\mu |\chi_\mu\rangle P_{\mu r}. \tag{1.98}$$

Therefore, the expression of projection matrix $\mathbf{P}$ can be written as

$$\mathbf{P} = \mathbf{1} - \mathbf{L}\mathbf{L}^\dagger\mathbf{S}, \tag{1.99}$$

where $\mathbf{S}$ is the overlap matrix in the AO basis.

Selecting LMOs as occupied space and PAOs as virtual space, a local correlation expression can be generated. This particular choice has the following properties. (1) All the space is covered with local orbitals. This is the important point for the saving of computing time in the following treatment. (2) Occupied orbitals are orthogonal among themselves and also orthogonal to the virtual space. This leads to

simpler expressions and easier convergence in the CCSD iteration. (3) The virtual orbitals are no longer orthogonal, with an overlap matrix as

$$\langle \breve{\chi}_r | \breve{\chi}_s \rangle = (\mathbf{P}^\dagger \mathbf{S} \mathbf{P})_{rs} = \breve{\mathbf{S}}_{rs}. \tag{1.100}$$

Notice that $\mathbf{S}$ represents the overlap matrix in AO basis while $\breve{\mathbf{S}}$ represents the overlap matrix in PAO basis. (4) There are linear dependencies in PAOs which should be eliminated out. This will be further discussed in section 2.2.4.

1.2.3 Pair Approximation

To each LMO, a subset of atoms is assigned using the Boughton-Pulay (BP) method [100]. Then the distance between LMOs can be defined as the closest distance of any pair of atoms assigned to the corresponding LMO. According to the distance of LMOs, the orbital pairs can be classified and approximations can be made on it, i.e., treat different pairs differently, neglect certain pairs. These approximations are called pair approximations.

In detail, orbital pairs are divided into strong pairs, close pairs, weak pairs, distant pairs, and very distant pairs. If the distance between i and j is written as R_{ij}, one has $R_c > R_{ij}$ for strong pairs, $R_w > R_{ij} \geq R_c$ for close pairs, $R_d > R_{ij} \geq R_w$ for weak pairs, $R_{vd} > R_{ij} \geq R_d$ for distant pairs, and $R_{ij} \geq R_{vd}$ for very distant pairs. R_c, R_w, R_d, R_{vd} are distance criteria with the default values 1, 3, 8, and 15 Bohr respectively. Mathematically, except very distant pairs, the number of all the other pairs scales linearly with the molecular size.

In the `Molpro` closed shell local CCSD(T) implementation, strong pairs are included in the CCSD iteration. For (T) treatment, a triple list is generated according to the pair classification. For three LMOs ijk, the pairs ij, ik, jk need to be strong pairs or close pairs, and at least one of them must be a strong pair. Except for the pairs included in CCSD, the other pairs are treated with MP2 except the very distant pairs, which are completely neglected. In open-shell local methods, the same classification and approximations will be used. Alternatively, setting 'nomp2=1', all pairs except very distant pairs can be treated by LUCCSD. With this option most errors caused by the pair approximation can be removed but it is rather expensive. To remove some of the errors of pair approximation with less cost, one can include MP2 close pair amplitudes in the LUCCSD strong pairs residuals calculations. This option can be used by setting 'keepcls=1'. The effects of 'nomp2=1' and 'keepcls=1' in LUCCSD and LUCCSD(T) will be tested and discussed in Chapter 4.

To be mentioned, the default values are a compromise between computational

cost and accuracy. For particular cases, a recheck of the values may be necessary.

1.2.4 Domain Approximation

Pair approximation reduces the number of excitation amplitudes in correlation treatment to linear scaling with molecular size. Furthermore, the size of matrices to constant independent of the molecular size needs to be reduced. In notations of this thesis, the size of vectors or matrices depend on the size of the virtual space. In order to reduce the scaling, it is necessary to restrict the size of the virtual space for excitation amplitudes. Notice that LMOs and PAOs are both localized. Therefore, the excitation from every LMO can be restricted to nearby PAOs. The subset of PAOs nearby LMO i is called the domain of i, and denoted as $[i]$. In order to select PAOs, different procedures can be applied. In the Boughton-Pulay (BP) procedure [100], a domain selection criterion is used, which is noted as 'domsel' in `Molpro` and has a default value 0.98 for double zeta basis sets, 0.985 for triple zeta basis sets, and 0.99 for quadruple zeta basis sets. One computes the overlap of the LMO with a trial function built as linear combination of AOs belonging to the domain centers only. The coefficients in the trial function are determined by a simple least squares fitting procedure. By adding centers to the list till this value exceeds the BP criterion 'domsel', the orbital domains $[i]$ can be determined. To generate a better domain, it is also possible to discard contributions of diffuse functions in Pipek-Mezey localization. In `Molpro` this function can be used by setting the parameter 'cpldel=1'. The selection of parameters 'domsel' and 'cpldel' will be tested for LRMP2 and discussed in Chapter 4.

Defining an orbital domain, single excitations from orbital i are restricted to the orbital domain $[i]$ which is independent of the molecular size. For double excitations from LMOs i and j, a pair domain $[ij]$ is defined as the union of orbital domains $[i]$ and $[j]$. Pair excitations from ij are restricted to pair domains $[ij]$, which are also independent of the molecular size. Furthermore, a triple domain $[ijk]$ can be defined as the union of orbital domains $[i]$, $[j]$ and $[k]$. Triple excitations from LMO ijk are restricted to the domain $[ijk]$.

Having defined the domains, the residuals $\mathbf{v}^i$, $\mathbf{V}^{ij}$, excitation amplitudes $\mathbf{t}^i$, $\mathbf{T}^{ij}$, as well as the overlap matrix $\check{\mathbf{S}}$ can be written in the basis of the PAOs of different domains. In the basis of the PAOs of domain $[ij]$, the overlap matrix can be denoted as $\check{\mathbf{S}}^{(ij)}$. Because of the redundancy of the PAO basis, in some domains the overlap matrix $\check{\mathbf{S}}^{(ij)}$ may have zero or very small eigenvalues. These are removed using singular value decomposition [65, 101]. Finally, the linear dependencies in the PAO set are removed for individual domains.

1.3 Density Fitting Approximation

The density fitting (DF) approximation is a powerful technology with a long history [97, 102, 103]. It is widely used for HF and DFT [104–109], as well as MP2 [71, 110–112], CC2 [113], MP2-F12 [114–117], CCSD [72, 118], DFT-SAPT [119, 120], and SAPT(CC) [121, 122].

To give a brief introduction of density fitting and local density fitting technique, 2-external exchange integrals will be discussed as an example. Defining one-electron orbital product densities ρ as

$$\rho_{ri}(\mathbf{r_1}) = \phi_r(\mathbf{r_1})\phi_i(\mathbf{r_1}), \tag{1.101}$$

2-external exchange integrals can be written as

$$K_{rs}^{ij} = (ri|sj) = \int d\mathbf{r_1} \int d\mathbf{r_2} \phi_r(\mathbf{r_1})\phi_i(\mathbf{r_1}) r_{12}^{-1} \phi_s(\mathbf{r_2})\phi_j(\mathbf{r_2}), \tag{1.102}$$

$$= \int d\mathbf{r_1} \int d\mathbf{r_2} \rho_{ri}(\mathbf{r_1}) r_{12}^{-1} \rho_{sj}(\mathbf{r_2}). \tag{1.103}$$

Expending the one-particle orbital product densities in an auxiliary fitting basis,

$$\rho_{ri}(\mathbf{r}) = \phi_r(\mathbf{r})\phi_i(\mathbf{r}) \approx \sum_A d_A^{ri} \chi_A(\mathbf{r}) = \bar{\rho}_{ri}(\mathbf{r}), \tag{1.104}$$

the integrals can be evaluated if the fitting coefficients d^{ri} are obtained. Here capital letters A, B, C, D denote the auxiliary basis functions. Minimizing

$$\Delta_{ri} = \int d\mathbf{r_1} \int d\mathbf{r_2} \frac{[\rho_{ri}(\mathbf{r_1}) - \bar{\rho}_{ri}(\mathbf{r_1})][\rho_{ri}(\mathbf{r_2}) - \bar{\rho}_{ri}(\mathbf{r_2})]}{r_{12}} \tag{1.105}$$

the fitting coefficients can be obtained [103, 104], which lead to

$$\sum_B J_{AB} d_B^{ri} = J_A^{ri}, \tag{1.106}$$

$$K_{rs}^{ij} = \sum_B d_B^{ri} (B|sj), \tag{1.107}$$

where

$$J_{AB} = \int d\mathbf{r_1} \int d\mathbf{r_2} \frac{\chi_A(\mathbf{r_1})\chi_B(\mathbf{r_2})}{r_{12}}, \tag{1.108}$$

$$J_A^{ri} \equiv (ri|A) = \int d\mathbf{r_1} \int d\mathbf{r_2} \frac{\phi_r(\mathbf{r_1})\phi_i(\mathbf{r_1})\chi_A(\mathbf{r_2})}{r_{12}}. \tag{1.109}$$

Assuming that the MOs are expanded in a basis of functions χ_μ, the 3-index integrals $(ri|A)$ in the MOs basis can be transformed from the 3-index integrals $(\mu\nu|A)$ into the AO basis by two steps, i.e.,

$$(\mu i|A) = \sum_\nu L_{\nu i}(\mu\nu|A), \tag{1.110}$$

$$(ri|A) = \sum_\mu P_{\mu r}(\mu i|A). \tag{1.111}$$

All the steps above only require simple matrix multiplications, and can be performed very efficiently on modern computers. This leads to a low prefactor for the algorithm, which makes the evaluation of integrals much faster. In local implementations, the scaling for evaluating the above step can also be reduced. First, because r, s is restricted in the pair domain of i, j, the number of them is independent of the molecular size. Neglecting very distant pairs, the number of pairs (ij) scales linearly. The number of the fitting basis also scales linearly, therefore, the assemble step of K_{rs}^{ij} scales as $\mathscr{O}(\mathscr{N}^2)$. Defining the domain which comprises all PAOs that belong to any pair domain $[ij]$ in which orbital i occurs as a united pair domain, PAOs r in the 3-index integrals $(ri|A)$ are restricted to this domain. For large molecules, the size of a united pair domain is independent of the molecular size. As i and A both scale linearly, the number of $(ri|A)$ scales as $\mathscr{O}(\mathscr{N}^2)$. Therefore, solving the linear equations of d_B^{ri} scales as $\mathscr{O}(\mathscr{N}^3)$. Because i is local, using prescreening techniques, the number of the terms in the summation is independent of the molecular size. Because the number of 3-index integrals scales as $\mathscr{O}(\mathscr{N}^2)$, the two transformation steps scale as $\mathscr{O}(\mathscr{N}^2)$.

In local density fitting, domains are also used for the fitting basis. For each LMO i, different fitting functions in fitting domain $[i]_{\texttt{fit}}$ are used. In order to minimize the error of this approximation, a robust fitting formula which is accurate to second-order in the fitting coefficients d_A^{ri} must be used [72, 123, 124], i.e.,

$$(ri|sj) \approx \sum_{A\in[i]_{\texttt{fit}}} (ri|A)d_A^{sj} + \sum_{B\in[j]_{\texttt{fit}}} (sj|B)d_B^{ri} - \sum_{A\in[i]_{\texttt{fit}}} \sum_{B\in[j]_{\texttt{fit}}} d_A^{ri} J_{AB} d_B^{sj}, \tag{1.112}$$

and the linear equations of fitting coefficients become

$$\sum_{B\in[i]_{\texttt{fit}}} J_{AB} d_B^{ri} = (ri|A). \tag{1.113}$$

The numbers of r, A, B, μ, ν are all independent of the molecular size for each K_{rs}^{ij}, so it is clear that every step of local density fitting transformation scales linearly.

2 Open-shell Local Correlation Methods

In this chapter the open-shell local correlation methods will be discussed. Starting from the different localization schemes of restricted open-shell HF orbitals, the local restricted MP2 (LRMP2), local unrestricted CCSD (LUCCSD), and local unrestricted CCSD(T) (LUCCSD(T)) method will be presented. The expressions of the working equations and the discussion about how linear scaling is achieved for different terms will be given.

2.1 Localization Schemes of Restricted Open-shell HF orbitals

The occupied RHF orbital space can be divided into two subspaces, i.e., the space spanned by singly occupied orbitals and the space spanned by doubly occupied orbitals. If a localization is done in the occupied RHF orbital space, the two subspaces would be mixed. In order to avoid this problem, the localization can be done in the singly occupied orbital space and the doubly occupied orbital space separately. This localization scheme is denoted as sd-localization, and the corresponding local methods are denoted as sd-LRMP2, sd-LUCCSD, and sd-LUCCSD(T). In sd-localization, if one of the two occupied subspaces is small, the localization in this subspace can not be well done. In particular, for doublet molecules such as radicals which have only one singly occupied orbital, the localization of this orbital is not possible. The only singly occupied orbital will remain delocalized, which can tremendously slow down the overall speed.

Instead of doing localization in the two subspaces of the occupied space, it is also possible to carry out the localization separately for alpha-spin orbitals and for beta-spin orbitals. Note that the localization is essentially a unitary transformation which keeps the RHF wave-function unchanged. Even though two sets of different local or-

bitals for alpha and beta spin are generated as in the UHF case, spin-contamination is still not introduced by the localization procedures. This localization scheme is denoted as ab-localization, and the corresponding methods are denoted as ab-LRMP2, ab-LUCCSD, and ab-LUCCSD(T). In ab-localization, both the alpha orbitals and the beta orbitals can be well localized. But because of the use of different orbitals for different spins, more integrals are needed. This will definitely take more time compared to generating one set of integrals.

2.2 LRMP2 Method

In local correlation methods, LMOs and PAOs are employed. Since LMOs are orthogonal to each other and orthogonal to PAOs, while PAOs are nonorthogonal with each other, the difference between LRMP2 and RMP2 will be the overlap matrices multiplied to excitation vectors and matrices in LRMP2. In the following sections, the tile above the letter of LMOs denotes α spin while the bar above the letter of LMOs denotes β spin.

The LMOs can be written as linear combinations of N basis functions $|\chi_\mu\rangle$ as

$$|\breve{\phi}_i\rangle = \sum_{\mu=1}^{N} |\chi_\mu\rangle L_{\mu i}. \tag{2.1}$$

The PAOs can be written as

$$|\breve{\chi}_r\rangle = \left(1 - \sum_{i=1}^{M} |\breve{\phi}_i\rangle\langle\breve{\phi}_i|\right) |\chi_r\rangle, \tag{2.2}$$

where M is the total number of LMOs. Defining

$$(\mathbf{D})_{rs} = \sum_i L_{ri} L_{si}, \tag{2.3}$$

expansion coefficients of the projected function can be written as

$$|\breve{\chi}_r\rangle = \sum_{\mu=1}^{N} |\chi_\mu\rangle \left(\mathbf{1} - \mathbf{DS}\right)_{\mu r}, \tag{2.4}$$

where $\mathbf{S}$ is the overlap matrix in the AO basis. By construction, the PAOs are automatically localized at individual atoms and nonorthogonal with matrix

$$\left(\breve{\mathbf{S}}\right)_{rs} = \left((\mathbf{1} - \mathbf{DS})^\dagger \mathbf{S} (\mathbf{1} - \mathbf{DS})\right)_{rs}. \tag{2.5}$$

In the following equations all the vectors and matrices are defined in the virtual spaces. The indices $\tilde{i}$, $\tilde{j}$, ... run over alpha-spin orbitals in occupied space and the indices $\bar{i}$, $\bar{j}$, ... run over beta-spin orbitals in occupied space. The numbering of elements for vectors and matrices, are denoted as $\tilde{r}$, $\tilde{s}$, ..., and $\bar{r}$, $\bar{s}$, which run over orbitals in virtual spaces for alpha and beta spins, respectively. Actually, in the current implementation, $\tilde{r}$ and $\bar{r}$ are always the same, no mater if sd-localization or ab-localization is considered.

Because there are singly occupied orbitals in open-shell cases, it is not straightforward to define the occupied and virtual spaces as in close-shell case. Practically, singly occupied orbitals are included in the virtual and the occupied space at the same time. For alpha-spin quantities, the excitations from doubly occupied orbitals to singly occupied orbitals, i.e., elements for singly occupied orbitals in the alpha-spin amplitude vectors and matrices, are manually set to zero. For beta-spin quantities, the excitations from singly occupied orbitals to virtual orbitals, i.e., the beta-spin amplitude vectors and matrices with the indices of singly occupied orbitals, are manually set to zero.

All the following equations are valid for both sd-localization and ab-localization, but with different definition of indices and elements of vectors and matrices, i.e., different definition of occupied and virtual spaces. For sd-localization, because of the usage of the same orbitals for alpha and beta spins, the occupied space is spanned by all doubly occupied LMOs and singly occupied LMOs together. In the following equations, $\tilde{i}$ and $\bar{i}$ run over all LMOs for sd-localization. However, for beta spin, all the quantities with index $\bar{i}$ are set to zero when $\bar{i}$ is a singly occupied LMO. For ab-localization, the occupied space is spanned by all alpha-spin LMOs for alpha-spin orbitals, and spanned by all beta-spin LMOs for beta-spin orbitals. The virtual space is spanned by all PAOs together with the singly occupied orbitals for sd-localization and singly occupied canonical orbitals for ab-localization.

The residuals and excitation amplitudes, which occur in the following equations, are local quantities, i.e., only have elements in the certain domains of virtual space. For example, $\mathbf{v}^{\tilde{i}}$ only have elements in domain $[\tilde{i}]$, and $\mathbf{V}^{\tilde{i}\tilde{j}}$ only have elements in domain $[\tilde{i}\tilde{j}]$. For sd-localization, domains $[\tilde{i}]$ and $[\bar{i}]$ are identical, because $\tilde{i}$ and $\bar{i}$ are using the same LMO. Therefore, the singly occupied orbitals are included in $[\tilde{i}]$ and $[\bar{i}]$, as discussed above. As a result, for quantities with indices $\tilde{i}$, the elements corresponding to singly occupied orbitals need to be set to zero, as they have been included in domain $[\tilde{i}]$. For ab-localization, domains $[\tilde{i}]$ and $[\bar{i}]$ are different. Therefore, the domain $[\tilde{i}]$ is constructed without singly occupied orbitals, and the corresponding elements will not appear in the quantities with index $\tilde{i}$. This

construction slightly saves computing efforts for ab-localization.

For different spins, the notations for internal-internal elements of the Fock matrix are defined as

$$f_{\tilde{i}\tilde{j}} = h_{\tilde{i}\tilde{j}} + \sum_{\tilde{k}} \left(\tilde{i}\tilde{j}|\tilde{k}\tilde{k}\right) + \sum_{\bar{k}} \left(\tilde{i}\tilde{j}|\bar{k}\bar{k}\right) - \sum_{\tilde{k}} \left(\tilde{i}\tilde{k}|\tilde{k}\tilde{j}\right), \tag{2.6}$$

$$f_{\bar{i}\bar{j}} = h_{\bar{i}\bar{j}} + \sum_{\bar{k}} \left(\bar{i}\bar{j}|\bar{k}\bar{k}\right) + \sum_{\tilde{k}} \left(\bar{i}\bar{j}|\tilde{k}\tilde{k}\right) - \sum_{\bar{k}} \left(\bar{i}\bar{k}|\bar{k}\bar{j}\right), \tag{2.7}$$

internal-external elements of the Fock matrix are defined as

$$\left(\mathbf{f}^{\tilde{i}}\right)_{\tilde{r}} = f_{\tilde{i}\tilde{r}} = h_{\tilde{i}\tilde{r}} + \sum_{\tilde{k}} \left(\tilde{i}\tilde{r}|\tilde{k}\tilde{k}\right) + \sum_{\bar{k}} \left(\tilde{i}\tilde{r}|\bar{k}\bar{k}\right) - \sum_{\tilde{k}} \left(\tilde{i}\tilde{k}|\tilde{k}\tilde{r}\right), \tag{2.8}$$

$$\left(\mathbf{f}^{\bar{i}}\right)_{\bar{r}} = f_{\bar{i}\bar{r}} = h_{\bar{i}\bar{r}} + \sum_{\bar{k}} \left(\bar{i}\bar{r}|\bar{k}\bar{k}\right) + \sum_{\tilde{k}} \left(\bar{i}\bar{r}|\tilde{k}\tilde{k}\right) - \sum_{\bar{k}} \left(\bar{i}\bar{k}|\bar{k}\bar{r}\right), \tag{2.9}$$

external-external elements of the Fock matrix are defined as

$$(\tilde{\mathbf{F}})_{\tilde{r}\tilde{s}} = f_{\tilde{r}\tilde{s}} = h_{\tilde{r}\tilde{s}} + \sum_{\tilde{k}} \left(\tilde{r}\tilde{s}|\tilde{k}\tilde{k}\right) + \sum_{\bar{k}} \left(\tilde{r}\tilde{s}|\bar{k}\bar{k}\right) - \sum_{\tilde{k}} \left(\tilde{r}\tilde{k}|\tilde{k}\tilde{s}\right), \tag{2.10}$$

$$(\bar{\mathbf{F}})_{\bar{r}\bar{s}} = f_{\bar{r}\bar{s}} = h_{\bar{r}\bar{s}} + \sum_{\bar{k}} \left(\bar{r}\bar{s}|\bar{k}\bar{k}\right) + \sum_{\tilde{k}} \left(\bar{r}\bar{s}|\tilde{k}\tilde{k}\right) - \sum_{\bar{k}} \left(\bar{r}\bar{k}|\bar{k}\bar{s}\right), \tag{2.11}$$

and exchange terms in four internal integrals are defined as

$$K^{\tilde{i}\tilde{j}}_{\tilde{k}\tilde{l}} = \left(\tilde{k}\tilde{i}|\tilde{j}\tilde{l}\right), \tag{2.12}$$

$$K^{\bar{i}\bar{j}}_{\bar{k}\bar{l}} = \left(\bar{k}\bar{i}|\bar{j}\bar{l}\right), \tag{2.13}$$

$$K^{\tilde{i}\bar{j}}_{\tilde{k}\bar{l}} = \left(\tilde{k}\tilde{i}|\bar{j}\bar{l}\right). \tag{2.14}$$

The residual vectors and matrices, which must vanish at convergence, are given by

$$\mathbf{v}^{\tilde{i}} = \mathbf{f}^{\tilde{i}} + \tilde{\mathbf{F}}\mathbf{t}^{\tilde{i}} - \sum_{\tilde{k}} \breve{\mathbf{S}} f_{\tilde{i}\tilde{k}} \mathbf{t}^{\tilde{k}}, \tag{2.15}$$

$$\mathbf{v}^{\bar{i}} = \mathbf{f}^{\bar{i}} + \bar{\mathbf{F}}\mathbf{t}^{\bar{i}} - \sum_{\bar{k}} \breve{\mathbf{S}} f_{\bar{i}\bar{k}} \mathbf{t}^{\bar{k}}, \tag{2.16}$$

$$\mathbf{V}^{\tilde{i}\tilde{j}} = \mathbf{K}^{\tilde{i}\tilde{j}} - \mathbf{K}^{\tilde{j}\tilde{i}} + \breve{\mathbf{S}}\mathbf{T}^{\tilde{i}\tilde{j}}\tilde{\mathbf{F}} + \tilde{\mathbf{F}}^{\dagger}\mathbf{T}^{\tilde{j}\tilde{i}\dagger}\breve{\mathbf{S}} - \sum_{\tilde{k}} \left(f_{\tilde{i}\tilde{k}}\breve{\mathbf{S}}\mathbf{T}^{\tilde{k}\tilde{j}}\breve{\mathbf{S}} + \breve{\mathbf{S}}\mathbf{T}^{\tilde{i}\tilde{k}}\breve{\mathbf{S}} f_{\tilde{j}\tilde{k}}\right), \tag{2.17}$$

$$\mathbf{V}^{\bar{i}\bar{j}} = \mathbf{K}^{\bar{i}\bar{j}} - \mathbf{K}^{\bar{j}\bar{i}} + \breve{\mathbf{S}}\mathbf{T}^{\bar{i}\bar{j}}\bar{\mathbf{F}} + \bar{\mathbf{F}}^{\dagger}\mathbf{T}^{\bar{j}\bar{i}\dagger}\breve{\mathbf{S}} - \sum_{\bar{k}} \left(f_{\bar{i}\bar{k}}\breve{\mathbf{S}}\mathbf{T}^{\bar{k}\bar{j}}\breve{\mathbf{S}} + \breve{\mathbf{S}}\mathbf{T}^{\bar{i}\bar{k}}\breve{\mathbf{S}} f_{\bar{j}\bar{k}}\right), \tag{2.18}$$

$$\mathbf{V}^{\tilde{i}\bar{j}} = \mathbf{K}^{\tilde{i}\bar{j}} + \breve{\mathbf{S}}\mathbf{T}^{\tilde{i}\bar{j}}\bar{\mathbf{F}} + \tilde{\mathbf{F}}^{\dagger}\mathbf{T}^{\tilde{i}\bar{j}}\breve{\mathbf{S}} - \left(\sum_{\tilde{k}} f_{\tilde{i}\tilde{k}}\breve{\mathbf{S}}\mathbf{T}^{\tilde{k}\bar{j}}\breve{\mathbf{S}} + \sum_{\bar{k}} \breve{\mathbf{S}}\mathbf{T}^{\tilde{i}\bar{k}}\breve{\mathbf{S}} f_{\bar{j}\bar{k}}\right). \quad (2.19)$$

Using a non-orthogonal basis, the Fock matrixes in PAOs are no longer diagonal. The equations of LRMP2 are solved iteratively. Convergence is reached when the change of energy and all elements of the residual vectors $\mathbf{v}$ and matrices $\mathbf{V}$ are smaller than certain thresholds. Notice that here all elements of the residual vectors and matrices means all the considered elements, which are limited in different domains of virtual space. Not the whole vectors or matrices on the full virtual space become zero.

To update the residuals, it is needed to transform them to an orthogonal basis. As the elements of the residuals are limited in different domains, the solution of Fock equations projected to each domain are performed. Notice that the following discussion holds for different spin combinations, i.e., $\tilde{i}\tilde{j}$, $\bar{i}\bar{j}$, $\tilde{i}\bar{j}$, therefore the tilde and bar will be omitted in the discussion of residuals update. In pair domain $[ij]$, the projected Fock equation is

$$\breve{\mathbf{F}}^{(ij)}\mathbf{W}^{(ij)} = \breve{\mathbf{S}}^{(ij)}\mathbf{W}^{(ij)}\mathbf{\Lambda}^{(ij)}, \quad (2.20)$$

where $\breve{\mathbf{F}}^{(ij)}$ and $\breve{\mathbf{S}}^{(ij)}$ are the Fock and overlap matrices in domain $[ij]$ of PAOs, $\mathbf{W}^{(ij)}$ are the solutions of above equations, and $\mathbf{\Lambda}^{(ij)}$ is a diagonal matrix of orbital energies. As discussed before, the PAOs in domain $[ij]$ may be linearly dependent. This redundancy is eliminated by the diagonalization of the overlap matrix $\breve{\mathbf{S}}^{(ij)}$ as

$$\left[\mathbf{X}^{(ij)\dagger}\breve{\mathbf{S}}^{(ij)}\mathbf{X}^{(ij)}\right]_{ab} = \delta_{ab}s_a, \quad (2.21)$$

and the renormalization of the eigenvectors $\mathbf{X}^{(ij)}$ according to

$$\breve{X}^{(ij)}_{ab} = \begin{cases} X^{(ij)}_{rs}/\sqrt{s_b} & \texttt{if } s_b > 10^{-6}, \\ 0 & \texttt{if } s_b < 10^{-6}. \end{cases} \quad (2.22)$$

The $\breve{\mathbf{X}}^{(ij)}$ transform $\breve{\mathbf{F}}^{(ij)}$ into an orthonormal basis, i.e.,

$$\ddot{\mathbf{F}}^{(ij)} = \breve{\mathbf{X}}^{(ij\dagger)}\breve{\mathbf{F}}^{(ij)}\breve{\mathbf{X}}^{(ij)}. \quad (2.23)$$

Digitalization of $\ddot{\mathbf{F}}^{(ij)}$, yields

$$\mathbf{U}^{(ij)\dagger}\ddot{\mathbf{F}}^{(ij)}\mathbf{U}^{(ij)} = \mathbf{\Lambda}^{(ij)}, \quad (2.24)$$

where $\mathbf{U}^{(ij)}$ is a unitary transformation and $\mathbf{\Lambda}_{ab}^{(ij)} = \delta_{ab}\varepsilon_a^{(ij)}$ are the orbital energies. Finally, the solution of Fock equations $\mathbf{W}^{(ij)}$ are obtained as

$$\mathbf{W}^{(ij)} = \breve{\mathbf{X}}^{(ij)}\mathbf{U}^{(ij)}, \tag{2.25}$$

which transform residuals into an orthogonal basis as

$$\ddot{\mathbf{v}}^i = \mathbf{W}^{(ii)\dagger}\mathbf{v}^i, \tag{2.26}$$

$$\ddot{\mathbf{V}}^{ij} = \mathbf{W}^{(ij)\dagger}\mathbf{V}^{ij}\mathbf{W}^{(ij)}. \tag{2.27}$$

All the transformation matrixes $\mathbf{W}^{(ij)}$ for different domains are computed once and stored. In the orthogonal basis the updates are obtained by first-order perturbation theory

$$\Delta\ddot{t}_a^i = \frac{-\ddot{v}_a^i}{\varepsilon_a^{ii} - f_{ii}}, \tag{2.28}$$

$$\Delta\ddot{T}_{ab}^{ij} = \frac{-\ddot{V}_{ab}^{ij}}{\varepsilon_a^{ij} + \varepsilon_b^{ij} - f_{ii} - f_{jj}}, \tag{2.29}$$

in which f_{ii} are the diagonal internal-internal elements of the Fock matrix which had been defined above. Finally, the updates are transformed back to the basis of non-orthogonal PAOs,

$$\Delta\mathbf{t}^i = \mathbf{W}^{(ii)}\Delta\ddot{\mathbf{t}}^i, \tag{2.30}$$

$$\Delta\mathbf{T}^{ij} = \mathbf{W}^{(ij)}\Delta\ddot{\mathbf{T}}^{ij}\mathbf{W}^{(ij)\dagger}. \tag{2.31}$$

Notice that

$$\mathbf{W}^{(ij)}\mathbf{W}^{(ij)\dagger} = (\breve{\mathbf{X}}^{(ij)}\mathbf{U}^{(ij)})(\breve{\mathbf{X}}^{(ij)}\mathbf{U}^{(ij)})^\dagger = \breve{\mathbf{X}}^{(ij)}\breve{\mathbf{X}}^{(ij)\dagger} = \breve{\mathbf{S}}^{(ij)*}, \tag{2.32}$$

where $\breve{\mathbf{S}}^{(ij)*}$ is the redundancy eliminated $\breve{\mathbf{S}}^{(ij)}$ by the definition of $\breve{\mathbf{X}}^{(ij)}$, it is clear now that the $\breve{\mathbf{S}}$ matrixes in the residuals are needed for taking care of the effect of two transformations.

With the excitation amplitudes, the correlation energy can be calculated by

$$\begin{aligned} E - E_0 &= \sum_{\tilde{i}} \mathbf{f}^{\tilde{i}\dagger}\mathbf{t}^{\tilde{i}} + \sum_{\bar{i}} \mathbf{f}^{\bar{i}\dagger}\mathbf{t}^{\bar{i}} \\ &\quad + \mathrm{Tr}\left[\frac{1}{2}\sum_{\tilde{i}\tilde{j}} \mathbf{T}^{\tilde{i}\tilde{j}}\mathbf{K}^{\tilde{j}\tilde{i}} + \frac{1}{2}\sum_{\bar{i}\bar{j}} \mathbf{T}^{\bar{i}\bar{j}}\mathbf{K}^{\bar{j}\bar{i}} + \sum_{\tilde{i}\bar{j}} \mathbf{T}^{\tilde{i}\bar{j}}\mathbf{K}^{\bar{j}\tilde{i}}\right]. \end{aligned} \tag{2.33}$$

Notice that for alpha-alpha spin and beta-beta spin, the matrices $\mathbf{T}^{\tilde{i}\tilde{j}}$ and $\mathbf{T}^{\bar{i}\bar{j}}$ are antisymmetric, but the matrices $\mathbf{T}^{\tilde{i}\bar{j}}$ are not. Correspondingly, the matrices $\mathbf{V}^{\tilde{i}\tilde{j}}$ and $\mathbf{V}^{\bar{i}\bar{j}}$ are antisymmetric but the matrices $\mathbf{T}^{\tilde{i}\bar{j}}$ are not.

Through the above expression, it can be shown how linear scaling is achieved in the calculation of residuals. In the section of pair approximation, the number of all the residuals scales linearly with molecular size. Therefore, in order to achieve linear scaling, every term in the residual calculation must become independent of the molecular size.

Term $\mathbf{f}^{\tilde{i}}$ in $\mathbf{v}^{\tilde{i}}$: The length of this vector is the same as the length of domain $[\tilde{i}]$ which is independent of the molecular size. So the computational effort of adding this term is independent of the molecular size.

Term $\tilde{\mathbf{F}}\mathbf{t}^{\tilde{i}}$ in $\mathbf{v}^{\tilde{i}}$: By the same token as first term, the size of this vector is independent of the molecular size. Writing out the expression of the matrix-vector multiplication, we have

$$\left(\mathbf{F}\mathbf{t}^{\tilde{i}}\right)_{\tilde{r}} = \sum_{\tilde{s}\in[\tilde{i}]} f_{\tilde{r}\tilde{s}}\mathbf{t}^{\tilde{i}}_{\tilde{s}} \qquad \forall \tilde{r} \in [\tilde{i}]. \tag{2.34}$$

As $\tilde{s}$ is restricted in the domain $[\tilde{i}]$, the number of the multiplications is the same as the number of PAOs in domain $[\tilde{i}]$. Therefore, the calculation amount needed for each term is independent of the molecular size as well.

Term $\sum_{\tilde{k}} \breve{\mathbf{S}} f_{\tilde{i}\tilde{k}}\mathbf{t}^{\tilde{k}}$: As above, the length of this term is the length of domain $[\tilde{i}]$. The expression of this term can be written as

$$\left(\sum_{\tilde{k}} \breve{\mathbf{S}} f_{\tilde{i}\tilde{k}}\mathbf{t}^{\tilde{k}}\right)_{\tilde{r}} = \sum_{\tilde{k}}\sum_{\tilde{s}\in[\tilde{k}]} \breve{S}_{\tilde{r}\tilde{s}} f_{\tilde{i}\tilde{k}} t^{\tilde{k}}_{\tilde{s}} \qquad \forall \tilde{r} \in [\tilde{i}]. \tag{2.35}$$

The summation over $\tilde{s}$ is limited in domain $[\tilde{k}]$, but the summation over $\tilde{k}$ is not limited. Therefore, the total number of multiplication times is equal to the summation of the size of all domain $[\tilde{k}]$, which scales linearly. Because the number of terms also scales linearly, the total scaling of these terms is quadratic. However, comparing to the number of pairs, the number of single is much smaller. Therefore, the pre-factor of this term is rather small, the quadratic scaling of this term has never been noticed in the later test. It may be more time consuming in very large cases, but not for systems with 100-200 atoms.

Term $\mathbf{K}^{\tilde{i}\tilde{j}}$ in $\mathbf{V}^{\tilde{i}\tilde{j}}$: The size of this term is equal to the size of domain $[\tilde{i}\tilde{j}]$ which is not related to molecular size.

Term $\breve{\mathbf{S}}\mathbf{T}^{\tilde{i}\tilde{j}}\tilde{\mathbf{F}}$ in $\mathbf{V}^{\tilde{i}\tilde{j}}$: The size of this term is the same as the above term. The

expression of this term can be written as

$$\left(\breve{\mathbf{S}}\mathbf{T}^{\tilde{i}\tilde{j}}\tilde{\mathbf{F}}\right)_{\tilde{r}\tilde{s}} = \sum_{\tilde{t}\tilde{u}\in[\tilde{i}\tilde{j}]} \breve{S}_{\tilde{r}\tilde{t}} T^{\tilde{i}\tilde{j}}_{\tilde{t}\tilde{u}} \tilde{F}_{\tilde{u}\tilde{s}} \qquad \forall \tilde{r}\tilde{s} \in [\tilde{i}\tilde{j}]. \tag{2.36}$$

The index $\tilde{t}\tilde{u}$, occurring in excitation amplitude $\mathbf{T}^{\tilde{i}\tilde{j}}_{\tilde{t}\tilde{u}}$, is restricted in domain $[\tilde{i}\tilde{j}]$. By the same token, index $\tilde{r}\tilde{s}$ occurring in residual $\mathbf{V}^{\tilde{i}\tilde{j}}_{\tilde{r}\tilde{s}}$, is also restricted in domain $[\tilde{i}\tilde{j}]$. Therefore, if L is the size of domain $[\tilde{i}\tilde{j}]$, the total number of multiplications for this term is equal to $2L^3$. As L is independent of the molecular size, $2L^3$ is also independent of the molecular size. Therefore, the total amount of calculation needed for this term is not related to the molecular size.

Term $\sum_{\tilde{k}} f_{\tilde{i}\tilde{k}}\breve{\mathbf{S}}\mathbf{T}^{\tilde{k}\tilde{j}}\breve{\mathbf{S}}$ in $\mathbf{V}^{\tilde{i}\tilde{j}}$: This is the most complex term in LRMP2 calculation and is also the most expensive term. This term can be explicitly written as

$$\left(\sum_{\tilde{k}} f_{\tilde{i}\tilde{k}}\breve{\mathbf{S}}\mathbf{T}^{\tilde{k}\tilde{j}}\breve{\mathbf{S}}\right)_{\tilde{r}\tilde{s}} = \sum_{\tilde{t}\tilde{u}\in[\tilde{j}]_{\mathtt{united}}} \breve{S}_{\tilde{r}\tilde{t}} \left(\sum_{\tilde{k}} f_{\tilde{i}\tilde{k}} T^{\tilde{k}\tilde{j}}_{\tilde{t}\tilde{u}}\right) \breve{S}_{\tilde{u}\tilde{s}} \qquad \forall \tilde{r}\tilde{s} \in [\tilde{i}\tilde{j}], \tag{2.37}$$

where $[\tilde{j}]_{\mathtt{united}}$ is the united pair domain of orbital $\tilde{j}$ which is defined as the domain comprising all PAOs that belong to any pair domain $[\tilde{j}\tilde{k}]$ in which orbital $\tilde{k}$ is not very far away from $\tilde{j}$, i.e., pair $\tilde{j}\tilde{k}$ is not very distant pair. In this term, $\tilde{r}\tilde{s}$ is restricted to the domain $[\tilde{i}\tilde{j}]$ and $\tilde{t}\tilde{u}$ is restricted to the domain $[\tilde{j}\tilde{k}]$. $\tilde{k}$ is summed for all the pairs $\tilde{k}\tilde{j}$ except very distant pairs, therefore the number of the summation of $\tilde{k}$ is independent of the molecular size. Although the united pair domain can be quite large, it is still not related to the size of the molecule. Therefore, the numbers of summations of $\tilde{t}$ and $\tilde{u}$ are also independent of the molecular size. Finally, the time consuming of this rather expensive term is also not related to molecular size.

The new sd-LRMP2 and ab-LRMP2 codes are developed in the framework of local methods in `Molpro`. The programs for localization and domain construction are modified and augmented from the closed-shell program [64, 65]. The density fitting integral transformations are using the same program as in closed-shell case [123] with some small modifications. The programs for updating amplitudes and calculating residues are newly written for sd-localization and ab-localization separately in this work.

2.3 LUCCSD Method

Similarly to LRMP2, the LUCCSD equations can be generated by inserting the PAO overlap matrix $\breve{\mathbf{S}}$ by the side of the corresponding excitation amplitudes in the

UCCSD expressions. In order to perform both ab-localization and sd-localization schemes, it is necessary to write the equations for different spins. For giving the expression of the LUCCSD working equations, it is necessary to define some notations and intermediates.

For different spins, the notations for the Fock matrix, exchange terms in four internal integrals have already been defined in the last section. Furthermore, Coulomb terms in two external integrals are defined as

$$(\mathbf{J}^{\tilde{i}\tilde{j}})_{\tilde{r}\tilde{s}} = \left(\tilde{r}\tilde{s}|\tilde{i}\tilde{j}\right), \tag{2.38}$$

$$(\mathbf{J}^{\bar{i}\bar{j}})_{rs} = (\bar{r}\bar{s}|\bar{i}\bar{j}), \tag{2.39}$$

exchange terms in one internal three external integrals are defined as

$$(\mathbf{k}^{\tilde{i}\tilde{j}\tilde{k}})_{\tilde{r}} = \left(\tilde{r}\tilde{i}|\tilde{j}\tilde{k}\right), \tag{2.40}$$

$$(\mathbf{k}^{\bar{i}\bar{j}\bar{k}})_{\bar{r}} = \left(\bar{r}\bar{i}|\bar{j}\bar{k}\right), \tag{2.41}$$

$$(\mathbf{k}^{\tilde{i}\bar{j}\bar{k}})_{\tilde{r}} = \left(\tilde{r}\tilde{i}|\bar{j}\bar{k}\right), \tag{2.42}$$

$$(\mathbf{k}^{\bar{i}\tilde{j}\tilde{k}})_{\bar{r}} = \left(\bar{r}\bar{i}|\tilde{j}\tilde{k}\right), \tag{2.43}$$

exchange terms in two internal two external integrals are defined as

$$(\mathbf{K}^{\tilde{i}\tilde{j}})_{\tilde{r}\tilde{s}} = \left(\tilde{r}\tilde{i}|\tilde{j}\tilde{s}\right), \tag{2.44}$$

$$(\mathbf{K}^{\bar{i}\bar{j}})_{\bar{r}\bar{s}} = (\bar{r}\bar{i}|\bar{j}\bar{s}), \tag{2.45}$$

$$(\mathbf{K}^{\tilde{i}\bar{j}})_{\tilde{r}\bar{s}} = \left(\tilde{r}\tilde{i}|\bar{j}\bar{s}\right), \tag{2.46}$$

Coulomb-like contractions between three external integrals and single excitation amplitudes are defined as

$$\mathbf{J}\left(\mathbf{E}^{\tilde{i}\tilde{j}}\right)_{\tilde{r}\tilde{s}} = \sum_{\tilde{t}} \left(\tilde{r}\tilde{s}|\tilde{i}\tilde{t}\right) t_{\tilde{t}}^{\tilde{j}}, \tag{2.47}$$

$$\mathbf{J}\left(\mathbf{E}^{\bar{i}\bar{j}}\right)_{\bar{r}\bar{s}} = \sum_{\bar{t}} \left(\bar{r}\bar{s}|\bar{i}\bar{t}\right) t_{\bar{t}}^{\bar{j}}, \tag{2.48}$$

exchange-like contractions between three external integrals and single excitation amplitudes are defined as

$$\mathbf{K}\left(\mathbf{E}^{\tilde{i}\tilde{j}}\right)_{\tilde{r}\tilde{s}} = \sum_{\tilde{t}} \left(\tilde{r}\tilde{i}|\tilde{s}\tilde{t}\right) t_{\tilde{t}}^{\tilde{j}}, \tag{2.49}$$

$$\mathbf{K}\left(\mathbf{E}^{\bar{i}\bar{j}}\right)_{\bar{r}\bar{s}} = \sum_{\bar{t}} \left(\bar{r}\bar{i}|\bar{s}\bar{t}\right) t_{\bar{t}}^{\bar{j}}, \tag{2.50}$$

$$\mathbf{K}\left(\mathbf{E}^{\tilde{i}\bar{j}}\right)_{\tilde{r}\bar{s}} = \sum_{\bar{t}} \left(\tilde{r}\tilde{i}|\bar{s}\bar{t}\right) t^{\bar{j}}_{\bar{t}}, \tag{2.51}$$

$$\mathbf{K}\left(\mathbf{E}^{\bar{i}\tilde{j}}\right)_{\bar{r}\tilde{s}} = \sum_{\tilde{t}} \left(\bar{r}\bar{i}|\tilde{s}\tilde{t}\right) t^{\tilde{j}}_{\tilde{t}}. \tag{2.52}$$

The combination of single and double excitation amplitudes are defined as

$$\mathbf{C}^{\tilde{i}\tilde{k}} = \mathbf{T}^{\tilde{i}\tilde{k}} + \mathbf{t}^{\tilde{i}}\mathbf{t}^{\tilde{k}\dagger} - \mathbf{t}^{\tilde{k}}\mathbf{t}^{\tilde{i}\dagger}, \tag{2.53}$$

$$\mathbf{C}^{\bar{i}\bar{k}} = \mathbf{T}^{\bar{i}\bar{k}} + \mathbf{t}^{\bar{i}}\mathbf{t}^{\bar{k}\dagger} - \mathbf{t}^{\bar{k}}\mathbf{t}^{\bar{i}\dagger}, \tag{2.54}$$

$$\mathbf{C}^{\tilde{i}\bar{k}} = \mathbf{T}^{\tilde{i}\bar{k}} + \mathbf{t}^{\tilde{i}}\mathbf{t}^{\bar{k}\dagger}, \tag{2.55}$$

$$\mathbf{B}^{\tilde{i}\tilde{k}} = \frac{1}{2}\mathbf{T}^{\tilde{i}\tilde{k}} + \mathbf{t}^{\tilde{i}}\mathbf{t}^{\tilde{k}\dagger} - \mathbf{t}^{\tilde{k}}\mathbf{t}^{\tilde{i}\dagger}, \tag{2.56}$$

$$\mathbf{B}^{\bar{i}\bar{k}} = \frac{1}{2}\mathbf{T}^{\bar{i}\bar{k}} + \mathbf{t}^{\bar{i}}\mathbf{t}^{\bar{k}\dagger} - \mathbf{t}^{\bar{k}}\mathbf{t}^{\bar{i}\dagger}, \tag{2.57}$$

$$\mathbf{B}^{\tilde{i}\bar{k}} = \frac{1}{2}\mathbf{T}^{\tilde{i}\bar{k}} + \mathbf{t}^{\tilde{i}}\mathbf{t}^{\bar{k}\dagger}. \tag{2.58}$$

For different spins, the exchange-like contractions between three external integrals and $\mathbf{C}$ matrices are defined as

$$\mathbf{K}\left(\mathbf{C}^{\tilde{i}\tilde{j}}\right)^{\tilde{k}}_{\tilde{r}} = \sum_{\tilde{s}\tilde{t}} \left(\tilde{r}\tilde{s}|\tilde{t}\tilde{k}\right) \mathbf{C}^{\tilde{i}\tilde{j}}_{\tilde{s}\tilde{t}}, \tag{2.59}$$

$$\mathbf{K}\left(\mathbf{C}^{\bar{i}\bar{j}}\right)^{\bar{k}}_{\bar{r}} = \sum_{\bar{s}\bar{t}} \left(\bar{r}\bar{s}|\bar{t}\bar{k}\right) \mathbf{C}^{\bar{i}\bar{j}}_{\bar{s}\bar{t}}, \tag{2.60}$$

$$\mathbf{K}\left(\mathbf{C}^{\tilde{i}\bar{j}}\right)^{\bar{k}}_{\tilde{r}} = \sum_{\bar{s}\bar{t}} \left(\tilde{r}\tilde{s}|\bar{t}\bar{k}\right) \mathbf{C}^{\tilde{i}\bar{j}}_{\tilde{s}\bar{t}}, \tag{2.61}$$

$$\mathbf{K}\left(\mathbf{C}^{\tilde{i}\bar{j}\dagger}\right)^{\tilde{k}}_{\bar{r}} = \sum_{\bar{s}\tilde{t}} \left(\bar{r}\bar{s}|\tilde{t}\tilde{k}\right) \left(\mathbf{C}^{\tilde{i}\bar{j}\dagger}\right)_{\bar{s}\tilde{t}} = \sum_{\bar{s}\tilde{t}} \left(\bar{r}\bar{s}|\tilde{t}\tilde{k}\right) \mathbf{C}^{\tilde{i}\bar{j}}_{\tilde{t}\bar{s}}, \tag{2.62}$$

and contractions between four external integrals and $\mathbf{C}$ matrices are defined as

$$\mathbf{K}\left(\mathbf{C}^{\tilde{i}\tilde{j}}\right)_{\tilde{r}\tilde{s}} = \sum_{\tilde{t}\tilde{u}} \left(\tilde{r}\tilde{t}|\tilde{u}\tilde{s}\right) \mathbf{C}^{\tilde{i}\tilde{j}}_{\tilde{t}\tilde{u}}, \tag{2.63}$$

$$\mathbf{K}\left(\mathbf{C}^{\bar{i}\bar{j}}\right)_{\bar{r}\bar{s}} = \sum_{\bar{t}\bar{u}} \left(\bar{r}\bar{t}|\bar{u}\bar{s}\right) \mathbf{C}^{\bar{i}\bar{j}}_{\bar{t}\bar{u}}, \tag{2.64}$$

$$\mathbf{K}\left(\mathbf{C}^{\tilde{i}\bar{j}}\right)_{\tilde{r}\bar{s}} = \sum_{\tilde{t}\bar{u}} \left(\tilde{r}\tilde{t}|\bar{u}\bar{s}\right) \mathbf{C}^{\tilde{i}\bar{j}}_{\tilde{t}\bar{u}}. \tag{2.65}$$

Using above notations, the intermediates can be defined. They are scalers

$$\alpha^{\tilde{i}\tilde{j}}_{\tilde{k}\tilde{l}} = K^{\tilde{i}\tilde{j}}_{\tilde{k}\tilde{l}} + \frac{1}{2}\mathrm{tr}\left(\mathbf{K}^{\tilde{k}\tilde{l}\dagger}\mathbf{C}^{\tilde{i}\tilde{j}}\right) + \mathbf{t}^{\tilde{i}\dagger}\mathbf{k}^{\tilde{k}\tilde{l}\tilde{j}} + \mathbf{t}^{\tilde{j}\dagger}\mathbf{k}^{\tilde{l}\tilde{k}\tilde{i}}, \tag{2.66}$$

$$\alpha_{\bar{k}\bar{l}}^{\bar{i}\bar{j}} = K_{\bar{k}\bar{l}}^{\bar{i}\bar{j}} + \frac{1}{2}\mathrm{tr}\left(\mathbf{K}^{\bar{k}\bar{l}\dagger}\mathbf{C}^{\bar{i}\bar{j}}\right) + \mathbf{t}^{\bar{i}\dagger}\mathbf{k}^{\bar{k}\bar{l}\bar{j}} + \mathbf{t}^{\bar{j}\dagger}\mathbf{k}^{\bar{l}\bar{k}\bar{i}}, \tag{2.67}$$

$$\alpha_{\tilde{k}\tilde{l}}^{\tilde{i}\tilde{j}} = K_{\tilde{k}\tilde{l}}^{\tilde{i}\tilde{j}} + \frac{1}{2}\mathrm{tr}\left(\mathbf{K}^{\tilde{k}\tilde{l}\dagger}\mathbf{C}^{\tilde{i}\tilde{j}}\right) + \mathbf{t}^{\tilde{i}\dagger}\mathbf{k}^{\tilde{k}\tilde{l}\tilde{j}} + \mathbf{t}^{\tilde{j}\dagger}\mathbf{k}^{\tilde{l}\tilde{k}\tilde{i}}, \tag{2.68}$$

$$\begin{aligned}\beta_{\tilde{i}\tilde{k}} &= f_{\tilde{i}\tilde{k}} + \mathbf{f}^{\tilde{k}\dagger}\mathbf{t}^{\tilde{i}} + \sum_{\tilde{l}}\left(\mathbf{t}^{\tilde{l}\dagger}\mathbf{k}^{\tilde{l}\tilde{k}\tilde{i}} - \mathbf{t}^{\tilde{l}\dagger}\mathbf{k}^{\tilde{k}\tilde{l}\tilde{i}}\right) + \sum_{\bar{l}}\mathbf{t}^{\bar{l}\dagger}\mathbf{k}^{\bar{l}\tilde{k}\tilde{i}} \\ &\quad + \sum_{\tilde{l}}\mathrm{tr}\left(\mathbf{K}^{\tilde{k}\tilde{l}\dagger}\mathbf{C}^{\tilde{i}\tilde{l}}\right) + \sum_{\bar{l}}\mathrm{tr}\left(\mathbf{K}^{\tilde{k}\bar{l}\dagger}\mathbf{C}^{\tilde{i}\bar{l}}\right),\end{aligned} \tag{2.69}$$

$$\begin{aligned}\beta_{\bar{i}\bar{k}} &= f_{\bar{k}\bar{i}} + \mathbf{f}^{\bar{k}\dagger}\mathbf{t}^{\bar{i}} + \sum_{\bar{l}}\left(\mathbf{t}^{\bar{l}\dagger}\mathbf{k}^{\bar{l}\bar{k}\bar{i}} - \mathbf{t}^{\bar{l}\dagger}\mathbf{k}^{\bar{k}\bar{l}\bar{i}}\right) + \sum_{\tilde{l}}\mathbf{t}^{\tilde{l}\dagger}\mathbf{k}^{\tilde{l}\tilde{k}\bar{i}} \\ &\quad + \sum_{\bar{l}}\mathrm{tr}\left(\mathbf{K}^{\bar{k}\bar{l}\dagger}\mathbf{C}^{\bar{i}\bar{l}}\right) + \sum_{\tilde{l}}\mathrm{tr}\left(\mathbf{K}^{\tilde{l}\tilde{k}\dagger}\mathbf{C}^{\tilde{l}\bar{i}}\right),\end{aligned} \tag{2.70}$$

s vectors

$$\begin{aligned}\mathbf{s}^{\tilde{i}} &= \mathbf{f}^{\tilde{i}} + \sum_{\tilde{k}}\mathbf{K}^{\tilde{i}\tilde{k}}\mathbf{t}^{\tilde{k}} + \sum_{\bar{k}}\mathbf{K}^{\tilde{i}\bar{k}}\mathbf{t}^{\bar{k}} - \sum_{\tilde{k}}\mathbf{J}^{\tilde{i}\tilde{k}}\mathbf{t}^{\tilde{k}} + \sum_{\tilde{k}}\mathbf{K}\Big(\mathbf{C}^{\tilde{i}\tilde{k}}\Big)^{\tilde{k}} + \sum_{\bar{k}}\mathbf{K}\Big(\mathbf{C}^{\tilde{i}\bar{k}}\Big)^{\bar{k}} \\ &\quad + \left(\mathbf{F} - \mathbf{A}^{\dagger}\right)^{\dagger}\mathbf{t}^{\tilde{i}} - \breve{\mathbf{S}}\left(\sum_{\tilde{k}\tilde{l}}\mathbf{T}^{\tilde{l}\tilde{k}}\mathbf{k}^{\tilde{k}\tilde{l}\tilde{i}} + \sum_{\bar{k}\tilde{l}}\mathbf{T}^{\tilde{l}\bar{k}}\mathbf{k}^{\bar{k}\tilde{l}\tilde{i}}\right),\end{aligned} \tag{2.71}$$

$$\begin{aligned}\mathbf{s}^{\bar{i}} &= \mathbf{f}^{\bar{i}} + \sum_{\bar{k}}\mathbf{K}^{\bar{i}\bar{k}}\mathbf{t}^{\bar{k}} + \sum_{\tilde{k}}\mathbf{K}^{\tilde{k}\bar{i}\dagger}\mathbf{t}^{\tilde{k}} - \sum_{\bar{k}}\mathbf{J}^{\bar{i}\bar{k}}\mathbf{t}^{\bar{k}} + \sum_{\bar{k}}\mathbf{K}\Big(\mathbf{C}^{\bar{i}\bar{k}}\Big)^{\bar{k}} + \sum_{\tilde{k}}\mathbf{K}\Big(\mathbf{C}^{\tilde{k}\bar{i}\dagger}\Big)^{\tilde{k}} \\ &\quad + \left(\mathbf{F} - \mathbf{A}^{\dagger}\right)^{\dagger}\mathbf{t}^{\bar{i}} - \breve{\mathbf{S}}\left(\sum_{\bar{k}\bar{l}}\mathbf{T}^{\bar{l}\bar{k}}\mathbf{k}^{\bar{k}\bar{l}\bar{i}} + \sum_{\tilde{k}\bar{l}}\mathbf{T}^{\tilde{k}\bar{l}\dagger}\mathbf{k}^{\tilde{k}\bar{l}\bar{i}}\right),\end{aligned} \tag{2.72}$$

r vectors

$$\mathbf{r}^{\tilde{k}} = \mathbf{f}^{\tilde{k}} + \sum_{\tilde{l}}\left(\mathbf{K}^{\tilde{k}\tilde{l}}\mathbf{t}^{\tilde{l}} - \mathbf{K}^{\tilde{k}\tilde{l}\dagger}\mathbf{t}^{\tilde{l}}\right) + \sum_{\bar{l}}\mathbf{K}^{\tilde{k}\bar{l}}\mathbf{t}^{\bar{l}}, \tag{2.73}$$

$$\mathbf{r}^{\bar{k}} = \mathbf{f}^{\bar{k}} + \sum_{\bar{l}}\left(\mathbf{K}^{\bar{k}\bar{l}}\mathbf{t}^{\bar{l}} - \mathbf{K}^{\bar{k}\bar{l}\dagger}\mathbf{t}^{\bar{l}}\right) + \sum_{\tilde{l}}\mathbf{K}^{\tilde{l}\bar{k}\dagger}\mathbf{t}^{\tilde{l}}, \tag{2.74}$$

and **A** matrices

$$\tilde{\mathbf{A}} = \left(\sum_{\tilde{k}\tilde{l}}\mathbf{K}^{\tilde{k}\tilde{l}}\mathbf{T}^{\tilde{l}\tilde{k}} + \sum_{\tilde{k}\bar{l}}\mathbf{K}^{\tilde{k}\bar{l}}\mathbf{T}^{\tilde{k}\bar{l}\dagger}\right)\breve{\mathbf{S}}, \tag{2.75}$$

$$\bar{\mathbf{A}} = \left(\sum_{\bar{k}\bar{l}}\mathbf{K}^{\bar{k}\bar{l}}\mathbf{T}^{\bar{l}\bar{k}} + \sum_{\bar{k}\tilde{l}}\mathbf{K}^{\tilde{l}\bar{k}\dagger}\mathbf{T}^{\tilde{l}\bar{k}}\right)\breve{\mathbf{S}}, \tag{2.76}$$

$\mathbf{G}(\mathbf{E})$ matrices

$$\mathbf{G}(\tilde{\mathbf{E}}) = \sum_{\tilde{k}} \mathbf{J}\Big(\mathbf{E}^{\tilde{k}\tilde{k}}\Big) + \sum_{\bar{k}} \mathbf{J}\Big(\mathbf{E}^{\bar{k}\bar{k}}\Big) - \sum_{\tilde{k}} \mathbf{K}\Big(\mathbf{E}^{\tilde{k}\tilde{k}}\Big), \tag{2.77}$$

$$\mathbf{G}(\bar{\mathbf{E}}) = \sum_{\tilde{k}} \mathbf{J}\Big(\mathbf{E}^{\tilde{k}\tilde{k}}\Big) + \sum_{\bar{k}} \mathbf{J}\Big(\mathbf{E}^{\bar{k}\bar{k}}\Big) - \sum_{\bar{k}} \mathbf{K}\Big(\mathbf{E}^{\bar{k}\bar{k}}\Big), \tag{2.78}$$

$\mathbf{X}$ matrices

$$\tilde{\mathbf{X}} = \tilde{\mathbf{F}} - \tilde{\mathbf{A}} - \left(\sum_{\tilde{k}} \mathbf{r}^{\tilde{k}}\mathbf{t}^{\tilde{k}}\right) \breve{\mathbf{S}} + \mathbf{G}(\tilde{\mathbf{E}}), \tag{2.79}$$

$$\bar{\mathbf{X}} = \bar{\mathbf{F}} - \bar{\mathbf{A}} - \left(\sum_{\bar{k}} \mathbf{r}^{\bar{k}}\mathbf{t}^{\bar{k}}\right) \breve{\mathbf{S}} + \mathbf{G}(\bar{\mathbf{E}}), \tag{2.80}$$

$\mathbf{Y}$ matrices

$$\begin{aligned}\mathbf{Y}^{\tilde{k}\tilde{j}} = & \left[\sum_{\tilde{l}} \left(\mathbf{K}^{\tilde{k}\tilde{l}}\mathbf{B}^{\tilde{l}\tilde{j}} - \mathbf{K}^{\tilde{k}\tilde{l}\dagger}\mathbf{B}^{\tilde{l}\tilde{j}}\right) + \sum_{\bar{l}} \mathbf{K}^{\tilde{k}\bar{l}}\mathbf{B}^{\tilde{j}\bar{l}\dagger} + \sum_{\tilde{l}} \left(\mathbf{k}^{\tilde{l}\tilde{k}\tilde{j}} - \mathbf{k}^{\tilde{k}\tilde{l}\tilde{j}}\right)\mathbf{t}^{\tilde{l}}\right] \breve{\mathbf{S}} \\ & + \mathbf{K}^{\tilde{k}\tilde{j}} - \mathbf{J}^{\tilde{k}\tilde{j}} + \mathbf{K}\Big(\mathbf{E}^{\tilde{k}\tilde{j}}\Big) - \mathbf{J}\Big(\mathbf{E}^{\tilde{k}\tilde{j}}\Big),\end{aligned} \tag{2.81}$$

$$\begin{aligned}\mathbf{Y}^{\bar{k}\bar{j}} = & \left[\sum_{\bar{l}} \left(\mathbf{K}^{\bar{k}\bar{l}}\mathbf{B}^{\bar{l}\bar{j}} - \mathbf{K}^{\bar{k}\bar{l}\dagger}\mathbf{B}^{\bar{l}\bar{j}}\right) + \sum_{\tilde{l}} \mathbf{K}^{\tilde{l}\bar{k}\dagger}\mathbf{B}^{\tilde{l}\bar{j}} + \sum_{\bar{l}} \left(\mathbf{k}^{\bar{l}\bar{k}\bar{j}} - \mathbf{k}^{\bar{k}\bar{l}\bar{j}}\right)\mathbf{t}^{\bar{l}}\right] \breve{\mathbf{S}} \\ & + \mathbf{K}^{\bar{k}\bar{j}} - \mathbf{J}^{\bar{k}\bar{j}} + \mathbf{K}\Big(\mathbf{E}^{\bar{k}\bar{j}}\Big) - \mathbf{J}\Big(\mathbf{E}^{\bar{k}\bar{j}}\Big),\end{aligned} \tag{2.82}$$

$$\begin{aligned}\mathbf{Y}^{\tilde{k}\bar{j}} = & \left[\sum_{\tilde{l}} \left(\mathbf{K}^{\tilde{k}\tilde{l}}\mathbf{B}^{\tilde{l}\bar{j}} - \mathbf{K}^{\tilde{k}\tilde{l}\dagger}\mathbf{B}^{\tilde{l}\bar{j}}\right) + \sum_{\bar{l}} \mathbf{K}^{\tilde{k}\bar{l}}\mathbf{B}^{\bar{l}\bar{j}} - \sum_{\bar{l}} \mathbf{k}^{\tilde{k}\bar{l}\bar{j}}\mathbf{t}^{\bar{l}}\right] \breve{\mathbf{S}} \\ & + \mathbf{K}^{\tilde{k}\bar{j}} + \mathbf{K}\Big(\mathbf{E}^{\tilde{k}\bar{j}}\Big),\end{aligned} \tag{2.83}$$

$$\begin{aligned}\mathbf{Y}^{\bar{k}\tilde{j}} = & \left[\sum_{\tilde{l}} \mathbf{K}^{\tilde{l}\bar{k}\dagger}\mathbf{B}^{\tilde{l}\tilde{j}} + \sum_{\bar{l}} \left(\mathbf{K}^{\bar{k}\bar{l}}\mathbf{B}^{\tilde{j}\bar{l}\dagger} - \mathbf{K}^{\bar{l}\bar{k}}\mathbf{B}^{\tilde{j}\bar{l}\dagger}\right) - \sum_{\tilde{l}} \mathbf{k}^{\bar{k}\tilde{l}\tilde{j}}\mathbf{t}^{\tilde{l}}\right] \breve{\mathbf{S}} \\ & + \mathbf{K}^{\bar{k}\tilde{j}} + \mathbf{K}\Big(\mathbf{E}^{\bar{k}\tilde{j}}\Big),\end{aligned} \tag{2.84}$$

$\mathbf{Z}$ matrices

$$\mathbf{Z}^{\tilde{k}\tilde{j}} = -\mathbf{J}^{\tilde{k}\tilde{j}} - \mathbf{J}\Big(\mathbf{E}^{\tilde{k}\tilde{j}}\Big) + \left[\sum_{\bar{l}} \left(\mathbf{K}^{\tilde{k}\bar{l}}\mathbf{B}^{\tilde{j}\bar{l}} + \mathbf{k}^{\tilde{l}\tilde{k}\tilde{j}}\mathbf{t}^{\bar{l}}\right)\right] \breve{\mathbf{S}}, \tag{2.85}$$

$$\mathbf{Z}^{\bar{k}\bar{j}} = -\mathbf{J}^{\bar{k}\bar{j}} - \mathbf{J}\Big(\mathbf{E}^{\bar{k}\bar{j}}\Big) + \left[\sum_{\tilde{l}} \left(\mathbf{K}^{\bar{k}\bar{l}}\mathbf{B}^{\bar{j}\tilde{l}} + \mathbf{k}^{\tilde{l}\bar{k}\bar{j}}\mathbf{t}^{\tilde{l}}\right)\right] \breve{\mathbf{S}} \tag{2.86}$$

and finally $\mathbf{G}$ matrices

$$\mathbf{G}^{\tilde{i}\tilde{j}} = \breve{\mathbf{S}}\Bigg\{\mathbf{T}^{\tilde{i}\tilde{j}}\mathbf{X} - \sum_{\tilde{k}}\mathbf{t}^{\tilde{k}}\left[\mathbf{K}\Big(\mathbf{C}^{\tilde{i}\tilde{j}}\Big)^{\tilde{k}} + \mathbf{k}^{\tilde{j}\tilde{i}\tilde{k}} - \mathbf{k}^{\tilde{i}\tilde{j}\tilde{k}} + \mathbf{K}^{\tilde{j}\tilde{k}}\mathbf{t}^{\tilde{i}} - \mathbf{K}^{\tilde{i}\tilde{k}}\mathbf{t}^{\tilde{j}} + \mathbf{J}^{\tilde{i}\tilde{k}}\mathbf{t}^{\tilde{j}} - \mathbf{J}^{\tilde{j}\tilde{k}}\mathbf{t}^{\tilde{i}}\right]$$
$$+\sum_{\tilde{k}}\Big(\mathbf{T}^{\tilde{i}\tilde{k}}\mathbf{Y}^{\tilde{k}\tilde{j}} - \mathbf{T}^{\tilde{j}\tilde{k}}\mathbf{Y}^{\tilde{k}\tilde{i}}\Big) + \sum_{\bar{k}}\Big(\mathbf{T}^{\tilde{i}\bar{k}}\mathbf{Y}^{\bar{k}\tilde{j}} - \mathbf{T}^{\tilde{j}\bar{k}}\mathbf{Y}^{\bar{k}\tilde{i}}\Big)\Bigg\}, \tag{2.87}$$

$$\mathbf{G}^{\bar{i}\bar{j}} = \breve{\mathbf{S}}\Bigg\{\mathbf{T}^{\bar{i}\bar{j}}\mathbf{X} - \sum_{\bar{k}}\mathbf{t}^{\bar{k}}\left[\mathbf{K}\Big(\mathbf{C}^{\bar{i}\bar{j}}\Big)^{\bar{k}} + \mathbf{k}^{\bar{j}\bar{i}\bar{k}} - \mathbf{k}^{\bar{i}\bar{j}\bar{k}} + \mathbf{K}^{\bar{j}\bar{k}}\mathbf{t}^{\bar{i}} - \mathbf{K}^{\bar{i}\bar{k}}\mathbf{t}^{\bar{j}} + \mathbf{J}^{\bar{i}\bar{k}}\mathbf{t}^{\bar{j}} - \mathbf{J}^{\bar{j}\bar{k}}\mathbf{t}^{\bar{i}}\right]$$
$$+\sum_{\bar{k}}\Big(\mathbf{T}^{\bar{i}\bar{k}}\mathbf{Y}^{\bar{k}\bar{j}} - \mathbf{T}^{\bar{j}\bar{k}}\mathbf{Y}^{\bar{k}\bar{i}}\Big) + \sum_{\tilde{k}}\Big(\mathbf{T}^{\tilde{k}\bar{i}\dagger}\mathbf{Y}^{\tilde{k}\bar{j}} - \mathbf{T}^{\tilde{k}\bar{j}\dagger}\mathbf{Y}^{\tilde{k}\bar{i}}\Big)\Bigg\}, \tag{2.88}$$

$$\mathbf{G}^{\tilde{i}\bar{j}} = \breve{\mathbf{S}}\Bigg\{\mathbf{T}^{\tilde{i}\bar{j}}\mathbf{X} - \sum_{\tilde{k}}\mathbf{t}^{\tilde{k}}\left[\mathbf{K}\Big(\mathbf{C}^{\tilde{i}\bar{j}\dagger}\Big)^{\tilde{k}} + \mathbf{k}^{\bar{j}\tilde{i}\tilde{k}} + \mathbf{K}^{\tilde{k}\bar{j}\dagger}\mathbf{t}^{\tilde{i}} - \mathbf{J}^{\tilde{k}\bar{j}\dagger}\mathbf{t}^{\tilde{i}}\right]$$
$$+\sum_{\tilde{k}}\mathbf{T}^{\tilde{i}\tilde{k}}\mathbf{Y}^{\tilde{k}\bar{j}} + \sum_{\bar{k}}\mathbf{T}^{\tilde{i}\bar{k}}\mathbf{Y}^{\bar{k}\bar{j}} + \sum_{\tilde{k}}\mathbf{T}^{\tilde{k}\bar{j}}\mathbf{Z}^{\tilde{k}\tilde{i}}\Bigg\}, \tag{2.89}$$

$$\mathbf{G}^{\bar{j}\tilde{i}} = \breve{\mathbf{S}}\Bigg\{\mathbf{T}^{\tilde{i}\bar{j}\dagger}\mathbf{X} - \sum_{\bar{k}}\mathbf{t}^{\bar{k}}\left[\mathbf{K}\Big(\mathbf{C}^{\tilde{i}\bar{j}}\Big)^{\bar{k}} + \mathbf{k}^{\tilde{i}\bar{j}\bar{k}} + \mathbf{K}^{\tilde{i}\bar{k}}\mathbf{t}^{\bar{j}} - \mathbf{J}^{\tilde{i}\bar{k}}\mathbf{t}^{\bar{j}}\right]$$
$$+\sum_{\bar{k}}\mathbf{T}^{\bar{j}\bar{k}}\mathbf{Y}^{\bar{k}\tilde{i}} + \sum_{\tilde{k}}\mathbf{T}^{\tilde{k}\bar{j}\dagger}\mathbf{Y}^{\tilde{k}\tilde{i}} + \sum_{\bar{k}}\mathbf{T}^{\bar{k}\tilde{i}}\mathbf{Z}^{\bar{k}\bar{j}}\Bigg\}. \tag{2.90}$$

Using the above notations and intermediates, it is possible to write the residual vectors and matrices in the compact form. They are one-excitation residual vectors

$$\mathbf{v}^{\tilde{i}} = \mathbf{s}^{\tilde{i}} + \breve{\mathbf{S}}\left(\sum_{\tilde{k}}\mathbf{T}^{\tilde{i}\tilde{k}}\mathbf{r}^{\tilde{k}} + \sum_{\bar{k}}\mathbf{T}^{\tilde{i}\bar{k}}\mathbf{r}^{\bar{k}} - \sum_{\tilde{k}}\beta_{\tilde{i}\tilde{k}}\mathbf{t}^{\tilde{k}}\right), \tag{2.91}$$

$$\mathbf{v}^{\bar{i}} = \mathbf{s}^{\bar{i}} + \breve{\mathbf{S}}\left(\sum_{\bar{k}}\mathbf{T}^{\bar{i}\bar{k}}\mathbf{r}^{\bar{k}} + \sum_{\tilde{k}}\mathbf{T}^{\tilde{k}\bar{i}\dagger}\mathbf{r}^{\tilde{k}} - \sum_{\bar{k}}\beta_{\bar{i}\bar{k}}\mathbf{t}^{\bar{k}}\right), \tag{2.92}$$

and two-excitation residual matrices

$$\mathbf{V}^{\tilde{i}\tilde{j}} = \mathbf{K}^{\tilde{i}\tilde{j}} - \mathbf{K}^{\tilde{i}\tilde{j}\dagger} + \mathbf{K}\Big(\mathbf{C}^{\tilde{i}\tilde{j}}\Big) + \mathbf{K}\Big(\mathbf{E}^{\tilde{i}\tilde{j}}\Big) - \mathbf{K}\Big(\mathbf{E}^{\tilde{i}\tilde{j}}\Big)^{\dagger} - \mathbf{K}\Big(\mathbf{E}^{\tilde{j}\tilde{i}}\Big) + \mathbf{K}\Big(\mathbf{E}^{\tilde{j}\tilde{i}}\Big)^{\dagger}$$
$$+\mathbf{G}^{\tilde{i}\tilde{j}} + \mathbf{G}^{\tilde{j}\tilde{i}\dagger} + \breve{\mathbf{S}}\left[\sum_{\tilde{k}\tilde{l}}\left(\alpha^{\tilde{i}\tilde{j}}_{\tilde{k}\tilde{l}} - \delta^{\tilde{i}}_{\tilde{k}}\beta_{\tilde{j}\tilde{l}} - \delta^{\tilde{j}}_{\tilde{l}}\beta_{\tilde{i}\tilde{k}}\right)\mathbf{T}^{\tilde{k}\tilde{l}}\right]\breve{\mathbf{S}}, \tag{2.93}$$

$$\begin{aligned}
\mathbf{V}^{\bar{i}\bar{j}} &= \mathbf{K}^{\bar{i}\bar{j}} - \mathbf{K}^{\bar{i}\bar{j}\dagger} + \mathbf{K}\Big(\mathbf{C}^{\bar{i}\bar{j}}\Big) + \mathbf{K}\Big(\mathbf{E}^{\bar{i}\bar{j}}\Big) - \mathbf{K}\Big(\mathbf{E}^{\bar{i}\bar{j}}\Big)^{\dagger} - \mathbf{K}\Big(\mathbf{E}^{\bar{j}\bar{i}}\Big) + \mathbf{K}\Big(\mathbf{E}^{\bar{j}\bar{i}}\Big)^{\dagger} \\
&\quad + \mathbf{G}^{\bar{i}\bar{j}} + \mathbf{G}^{\bar{j}\bar{i}\dagger} + \breve{\mathbf{S}}\left[\sum_{\bar{k}\bar{l}}\left(\alpha^{\bar{i}\bar{j}}_{\bar{k}\bar{l}} - \delta^{\bar{i}}_{\bar{k}}\beta_{\bar{j}\bar{l}} - \delta^{\bar{j}}_{\bar{l}}\beta_{\bar{i}\bar{k}}\right)\mathbf{T}^{\bar{k}\bar{l}}\right]\breve{\mathbf{S}}, \qquad (2.94)\\
\mathbf{V}^{\tilde{i}\tilde{j}} &= \mathbf{K}^{\tilde{i}\tilde{j}} + \mathbf{K}\Big(\mathbf{C}^{\tilde{i}\tilde{j}}\Big) + \mathbf{K}\Big(\mathbf{E}^{\tilde{i}\tilde{j}}\Big) + \mathbf{K}\Big(\mathbf{E}^{\tilde{j}\tilde{i}}\Big)^{\dagger} \\
&\quad + \mathbf{G}^{\tilde{i}\tilde{j}} + \mathbf{G}^{\tilde{j}\tilde{i}\dagger} + \breve{\mathbf{S}}\left[\sum_{\tilde{k}\tilde{l}}\left(\alpha^{\tilde{i}\tilde{j}}_{\tilde{k}\tilde{l}} - \delta^{\tilde{i}}_{\tilde{k}}\beta_{\tilde{j}\tilde{l}} - \delta^{\tilde{j}}_{\tilde{l}}\beta_{\tilde{i}\tilde{k}}\right)\mathbf{T}^{\tilde{k}\tilde{l}}\right]\breve{\mathbf{S}}. \qquad (2.95)
\end{aligned}$$

The energy expression of LUCCSD has a similar form as in the LRMP2 case

$$\begin{aligned}
E - E_0 &= \sum_{\tilde{i}} \mathrm{f}^{\tilde{i}} \cdot \mathrm{t}^{\tilde{i}} + \sum_{\bar{i}} \mathrm{f}^{\bar{i}} \cdot \mathrm{t}^{\bar{i}} \\
&\quad + \mathrm{Tr}\left[\frac{1}{2}\sum_{\tilde{i}\tilde{j}} \mathbf{C}^{\tilde{i}\tilde{j}}\mathbf{K}^{\tilde{j}\tilde{i}} + \frac{1}{2}\sum_{\bar{i}\bar{j}} \mathbf{C}^{\bar{i}\bar{j}}\mathbf{K}^{\bar{j}\bar{i}} + \sum_{\tilde{i}\bar{j}} \mathbf{C}^{\tilde{i}\bar{j}}\mathbf{K}^{\bar{j}\tilde{i}}\right], \qquad (2.96)
\end{aligned}$$

in which matrixes $\mathbf{T}^{\tilde{i}\tilde{j}}$, $\mathbf{T}^{\bar{i}\bar{j}}$, and $\mathbf{T}^{\tilde{i}\bar{j}}$ have been replaced by matrixes $\mathbf{C}^{\tilde{i}\tilde{j}}$, $\mathbf{C}^{\bar{i}\bar{j}}$, and $\mathbf{C}^{\tilde{i}\bar{j}}$, respectively.

The updating of residuals in the LUCCSD case is exactly the same as in the LRMP2 case, which has already been discussed. Actually, in the implementation, the same programs have been used for updating LRMP2 residuals and LUCCSD residuals. The same program has also been used for calculating the energy, except that matrices $\mathbf{T}^{\tilde{i}\tilde{j}}$, $\mathbf{T}^{\bar{i}\bar{j}}$, and $\mathbf{T}^{\tilde{i}\bar{j}}$ are replaced by matrices $\mathbf{C}^{\tilde{i}\tilde{j}}$, $\mathbf{C}^{\bar{i}\bar{j}}$, and $\mathbf{C}^{\tilde{i}\bar{j}}$, respectively, in LUCCSD case.

The LUCCSD equations are much more complicated than the LRMP2 equations. However, similar to the LRMP2 case, most terms in the LUCCSD equations can also be shown to be linearly scaling.

For example, term

$$\frac{1}{2}\breve{\mathbf{S}}\sum_{\tilde{k}}\mathbf{T}^{\tilde{i}\tilde{k}}\sum_{\tilde{l}}\mathbf{K}^{\tilde{k}\tilde{l}}\mathbf{T}^{\tilde{l}\tilde{j}}\breve{\mathbf{S}} \qquad (2.97)$$

in $\mathbf{V}^{\tilde{i}\tilde{j}}$, which occurs through intermediates $\mathbf{G}^{\tilde{i}\tilde{j}}$, $\mathbf{Y}^{\tilde{k}\tilde{j}}$, and $\mathbf{B}^{\tilde{l}\tilde{j}}$, can be written in more details as

$$\frac{1}{2}\sum_{\tilde{t}\in[\tilde{i}]_{\mathtt{united}}}\sum_{\tilde{w}\in[\tilde{i}]_{\mathtt{united}}}\breve{S}_{\tilde{r}\tilde{t}}\left(\sum_{\tilde{k}}\sum_{\tilde{u}\in[\tilde{i}\tilde{k}]}T^{\tilde{i}\tilde{k}}_{\tilde{t}\tilde{u}}\sum_{\tilde{l}}\sum_{\tilde{v}\in[\tilde{l}\tilde{j}]}K^{\tilde{k}\tilde{l}}_{\tilde{u}\tilde{v}}T^{\tilde{l}\tilde{j}}_{\tilde{v}\tilde{w}}\right)\breve{S}_{\tilde{w}\tilde{s}} \qquad \forall \tilde{r}\tilde{s}\in[\tilde{i}\tilde{j}], \quad (2.98)$$

where $[\tilde{i}\tilde{j}]_{\mathsf{op}}$ is the so called operator domain of $\tilde{i}\tilde{j}$. The operator domain for pair $\tilde{i}\tilde{j}$

is defined as the domain comprising all orbitals that belong to any pair domain $[\tilde{i}\tilde{k}]$ or $[\tilde{l}\tilde{j}]$ in which orbital $\tilde{k}$ is close to $\tilde{i}$ or orbital $\tilde{l}$ is close to $\tilde{j}$, respectively. 'Close to' means the pairs are in a certain pair list, for example, if only strong pairs are considered in LUCCSD, '$\tilde{i}$ is close to $\tilde{j}$' means pair $\tilde{i}\tilde{j}$ is a strong pair. Although the operator domain is rather large, it is still independent of the molecular size by construction. Therefore, from the above expression, it is obvious that all the calculations in these terms are independent of the molecular size, and the number of terms scales linearly as the number of pair $\tilde{i}\tilde{j}$ scales linearly. Therefore, the calculation of these terms scales linearly.

The only non-linear scaling terms in LUCCSD are those terms which involve the matrices $\mathbf{G}(\mathbf{E})$. To achieve linear scaling in LUCCSD, it is possible to neglect these terms together with some other terms. The alpha-spin $\mathbf{G}(\tilde{\mathbf{E}})$ terms contribute in the double residual $\mathbf{V}^{\tilde{i}\tilde{j}}$ as

$$\breve{\mathbf{S}}\mathbf{T}^{\tilde{i}\tilde{j}}\left[\sum_{\tilde{k}}\mathbf{J}\Big(\mathbf{E}^{\tilde{k}\tilde{k}}\Big)+\sum_{\bar{k}}\mathbf{J}\Big(\mathbf{E}^{\bar{k}\bar{k}}\Big)-\sum_{\tilde{k}}\mathbf{K}\Big(\mathbf{E}^{\tilde{k}\tilde{k}}\Big)\right], \tag{2.99}$$

the elements of the above term can be expressed as

$$\sum_{\tilde{t}\tilde{u}\in[\tilde{i}\tilde{j}]}\breve{S}_{\tilde{r}\tilde{t}}T^{\tilde{i}\tilde{j}}_{\tilde{t}\tilde{u}}\left[\sum_{\tilde{k}}\sum_{\tilde{v}\in[\tilde{k}]}\left(\tilde{u}\tilde{s}|\tilde{k}\tilde{v}\right)t^{\tilde{k}}_{\tilde{v}}+\sum_{\bar{k}}\sum_{\bar{v}\in[\bar{k}]}\left(\tilde{u}\tilde{s}|\bar{k}\bar{v}\right)t^{\bar{k}}_{\bar{v}}-\sum_{\tilde{k}}\sum_{\tilde{v}\in[\tilde{k}]}\left(\tilde{u}\tilde{k}|\tilde{s}\tilde{v}\right)t^{\tilde{k}}_{\tilde{v}}\right]. \tag{2.100}$$

In the above term, the quantities in the square bracket are calculated once for all pairs $\tilde{i}\tilde{j}$, and the multiply with $\mathbf{T}^{\tilde{i}\tilde{j}}$ later. Therefore, the indices $\tilde{u}\tilde{s}$ need to run over the whole molecule. There is no restriction for the summation over $\tilde{k}$, as a result, the summation over $\tilde{k}$ scales linearly. The summation of $\tilde{u}$ is limited in the domain $[k]$, which is independent of the molecular size. Altogether, the scaling of calculating the quantities in the square bracket should scale as $\mathscr{O}(\mathscr{N}^3)$. However, in the integral $\left(\tilde{u}\tilde{s}|\bar{k}\bar{v}\right)$, $\tilde{u}\tilde{s}$ should be close to each other. Using pre-screening techniques, the quadratic scaling of $\tilde{u}\tilde{s}$ can be reduced to linearly scaling. Therefore, the calculation of $\mathbf{G}(\tilde{\mathbf{E}})$ scales as $\mathscr{O}(\mathscr{N}^2)$ in the implementation, which will be proved in the next chapter by tests. As there are no explicit physical reasons of neglecting these terms, these terms are maintained in the implementation of LUCCSD in `Molpro`. Practically, it is also found that simply neglecting these terms or restricting them to some region of the molecule leads to unacceptably large errors. [66] An analysis of the expression of LUCCSD equations shows that there are the

following similar terms

$$\sum_{\tilde{t}\tilde{u}} \breve{S}_{\tilde{r}\tilde{t}} \sum_{\tilde{l}} T^{\tilde{i}\tilde{l}}_{\tilde{t}\tilde{u}} \left[\sum_{\tilde{k}\tilde{v}} \left(\tilde{l}\tilde{j}|\tilde{k}\tilde{v} \right) t^{\tilde{k}}_{\tilde{v}} + \sum_{\bar{k}\bar{v}} \left(\tilde{l}\tilde{j}|\bar{k}\bar{v} \right) t^{\bar{k}}_{\bar{v}} - \sum_{\tilde{k}\tilde{v}} \left(\tilde{l}\tilde{k}|\tilde{j}\tilde{v} \right) t^{\tilde{k}}_{\tilde{v}} \right] \breve{S}_{\tilde{u}\tilde{s}}, \quad (2.101)$$

which come from the third and fourth terms in the scalar intermediate $\beta_{\tilde{i}\tilde{k}}$. Because the above terms have exactly the same structure as the terms arising from $\mathbf{G}(\mathbf{E})$ and because they cancel them to a large extent, it is reasonable to neglect them together with the non-linear scaling term. In the `Molpro` implementation, the option 'igskip=1' can be used to neglect these terms together. The local error under this option is a little bit larger but still acceptable. This will be discussed in Chapter 4 and will be compared with the default option. Skipping these two kinds of terms using 'igskip=1', linear scaling is theoretically achieved for LUCCSD except for the integral transformation and some initializations. In the next chapter the scaling of LUCCSD will be tested and shown by figures.

In the same way as sd-LRMP2 and ab-LRMP2, the new sd-LUCCSD and ab-LUCCSD codes are also developed in the framework of local methods in `Molpro`. The programs for localization and domain construction are the same as for the LRMP2 case. The density fitting integral transformation for 1-2 external integrals are using the same program as LRMP2, and the 3- and 4- external density fitting integral transformations are using Martin Schütz's programs [72] together with some changes and the rewriting of the contraction part for different spin cases. As discussed above, for updating the amplitudes the same programs have been used as in the LRMP2 case. The programs for calculating residues are newly written for sd-localization and ab-localization separately in this work.

2.4 Local (T0) Approximation

As discussed earlier, triple excitations are often important for the accurate calculation of correlation energies. For the closed-shell local coupled cluster implementation, different kinds of triple approximations such as LCCSD(T), LCCSD(T0), and LCCSD(T1b) have been implemented and compared. [67–69] The difference of accuracy between different triple implementations are found to be quite small. As the (T0) approximation is cheap and shows very good linearity, it is implemented for our LUCCSD methods. Taking the zeroth iteration of the calculation of triple excitation amplitudes, it is possible to insert the expression of amplitudes into the expression of the (T) energy expression. Therefore, using spin orbitals, the expression of local

(T0) energy can be written as

$$\Delta E^{(T)} = -\sum_{ijk}\sum_{abc}\left(\sum_{rst}\mathscr{W}^{ijk}_{rst}W^{(ijk)}_{ra}W^{(ijk)}_{sb}W^{(ijk)}_{tc}\right)\times\left\{\left(\sum_{rst}\mathscr{W}^{ijk}_{rst}W^{(ijk)}_{ra}W^{(ijk)}_{sb}W^{(ijk)}_{tc}\right)\right.$$
$$\left.+\left\{[(ir|sj)-(is|rj)]t^k_t+T^{ij}_{rs}f^k_t\right\}W^{(ijk)}_{ra}W^{(ijk)}_{sb}W^{(ijk)}_{tc}\right\}/\epsilon^{ijk}_{abc}, \tag{2.102}$$

where $\mathbf{W}^{(ijk)}$ are the solution of the Fock equations projected to each triple domain $[ijk]$, which transform tensors in triple domains of PAOs to tensors in an orthonormal basis spanning the small domain. The calculation of $\mathbf{W}^{(ijk)}$ is exactly the same as the calculation of $\mathbf{W}^{(ij)}$ in LRMP2 and LUCCSD part. $\mathscr{W}$ are intermediates which will be given later for different spins. The denominators $\epsilon^{ijk}_{abc}=\varepsilon^{ijk}_a+\varepsilon^{ijk}_b+\varepsilon^{ijk}_c-f_{ii}-f_{jj}-f_{kk}$, where ε^{ijk}_a are the orbital energies in the orthogonal basis of domain $[ijk]$, which is calculated in the same manner as the calculation for ε^{ij}_a in the LRMP2 part. f_{ii}, f_{jj}, f_{kk} are the diagonal elements of the internal-internal Fock matrices. From the denominators, it is clear that taking the above expression of triples energy, only the diagonal elements of the internal-internal Fock matrices have been taken into account, i.e., the internal-internal coupling in Fock matrices has been neglected.

For different spin, the $\mathscr{W}$ are intermediates given by:

$$\mathscr{W}^{\tilde{i}\tilde{j}\tilde{k}}_{\tilde{r}\tilde{s}\tilde{t}} = \sum_{\tilde{m}}\left[\left(\tilde{t}\tilde{k}|\tilde{j}\tilde{m}\right)T^{\tilde{i}\tilde{m}}_{\tilde{s}\tilde{r}}+\left(\tilde{r}\tilde{i}|\tilde{k}\tilde{m}\right)T^{\tilde{j}\tilde{m}}_{\tilde{t}\tilde{s}}+\left(\tilde{s}\tilde{j}|\tilde{i}\tilde{m}\right)T^{\tilde{k}\tilde{m}}_{\tilde{r}\tilde{t}}-\left(\tilde{s}\tilde{j}|\tilde{k}\tilde{m}\right)T^{\tilde{i}\tilde{m}}_{\tilde{r}\tilde{t}}\right.$$
$$\left.-\left(\tilde{t}\tilde{k}|\tilde{i}\tilde{m}\right)T^{\tilde{j}\tilde{m}}_{\tilde{s}\tilde{r}}-\left(\tilde{r}\tilde{i}|\tilde{j}\tilde{m}\right)T^{\tilde{k}\tilde{m}}_{\tilde{t}\tilde{s}}\right]+\sum_{\tilde{u}}\left[\left(\tilde{i}\tilde{r}|\tilde{s}\tilde{u}\right)T^{\tilde{j}\tilde{k}}_{\tilde{u}\tilde{t}}+\left(\tilde{j}\tilde{s}|\tilde{t}\tilde{u}\right)T^{\tilde{k}\tilde{i}}_{\tilde{u}\tilde{r}}\right.$$
$$\left.+\left(\tilde{k}\tilde{t}|\tilde{r}\tilde{u}\right)T^{\tilde{i}\tilde{j}}_{\tilde{u}\tilde{s}}-\left(\tilde{i}\tilde{r}|\tilde{t}\tilde{u}\right)T^{\tilde{k}\tilde{j}}_{\tilde{s}\tilde{u}}-\left(\tilde{j}\tilde{s}|\tilde{r}\tilde{u}\right)T^{\tilde{i}\tilde{k}}_{\tilde{t}\tilde{u}}-\left(\tilde{k}\tilde{t}|\tilde{s}\tilde{u}\right)T^{\tilde{j}\tilde{i}}_{\tilde{r}\tilde{u}}\right], \tag{2.103}$$

$$\mathscr{W}^{\bar{i}\bar{j}\bar{k}}_{\bar{r}\bar{s}\bar{t}} = \sum_{\bar{m}}\left[\left(\bar{t}\bar{k}|\bar{j}\bar{m}\right)T^{\bar{i}\bar{m}}_{\bar{s}\bar{r}}+\left(\bar{r}\bar{i}|\bar{k}\bar{m}\right)T^{\bar{j}\bar{m}}_{fs}+\left(\bar{s}\bar{j}|\bar{i}\bar{m}\right)T^{\bar{k}\bar{m}}_{\bar{r}\bar{t}}-\left(\bar{s}\bar{j}|\bar{k}\bar{m}\right)T^{\bar{i}\bar{m}}_{rt}\right.$$
$$\left.-\left(\bar{t}\bar{k}|\bar{i}\bar{m}\right)T^{\bar{j}\bar{m}}_{\bar{s}\bar{r}}-\left(\bar{r}\bar{i}|\bar{j}\bar{m}\right)T^{\bar{k}\bar{m}}_{\bar{t}\bar{s}}\right]+\sum_{\bar{u}}\left[\left(\bar{i}\bar{r}|\bar{s}\bar{u}\right)T^{\bar{j}\bar{k}}_{\bar{u}\bar{t}}+\left(\bar{j}\bar{s}|\bar{t}\bar{u}\right)T^{\bar{k}\bar{i}}_{\bar{u}\bar{r}}\right.$$
$$\left.+\left(\bar{k}\bar{t}|\bar{r}\bar{u}\right)T^{\bar{i}\bar{j}}_{\bar{u}\bar{s}}-\left(\bar{i}\bar{r}|\bar{t}\bar{u}\right)T^{\bar{k}\bar{j}}_{\bar{s}\bar{u}}-\left(\bar{j}\bar{s}|\bar{r}\bar{u}\right)T^{\bar{i}\bar{k}}_{\bar{t}\bar{u}}-\left(\bar{k}\bar{t}|\bar{s}\bar{u}\right)T^{\bar{j}\bar{i}}_{\bar{r}\bar{u}}\right], \tag{2.104}$$

$$\mathscr{W}^{\tilde{i}\tilde{j}\tilde{k}}_{\bar{r}\tilde{s}\tilde{t}} = \sum_{\tilde{m}}\left[\left(\tilde{s}\tilde{k}|\tilde{j}\tilde{m}\right)T^{\bar{i}\tilde{m}}_{\bar{r}\tilde{t}}+\left(\bar{r}\tilde{i}|\tilde{k}\tilde{m}\right)T^{\tilde{j}\tilde{m}}_{\tilde{t}\tilde{s}}\right]+\sum_{\bar{m}}\left(\tilde{t}\tilde{j}|\bar{i}\bar{m}\right)T^{\tilde{k}\bar{m}}_{\tilde{s}\bar{r}}$$
$$-\sum_{\tilde{m}}\left[\left(\tilde{s}\tilde{j}|\tilde{k}\tilde{m}\right)T^{\bar{i}\tilde{m}}_{\bar{r}\tilde{t}}+\left(\bar{r}\tilde{i}|\tilde{j}\tilde{m}\right)T^{\tilde{k}\tilde{m}}_{\tilde{t}\tilde{s}}\right]-\sum_{\bar{m}}\left(\tilde{t}\tilde{k}|\bar{i}\bar{m}\right)T^{\tilde{j}\bar{m}}_{\tilde{s}\bar{r}}$$
$$+\sum_{\tilde{u}}\left[\left(\bar{i}\bar{r}|\tilde{s}\tilde{u}\right)T^{\tilde{j}\tilde{k}}_{\tilde{u}\tilde{t}}+\left(\tilde{j}\tilde{s}|\tilde{t}\tilde{u}\right)T^{\tilde{k}\bar{i}}_{\tilde{u}\bar{r}}\right]+\sum_{\bar{u}}\left(\tilde{k}\tilde{t}|\bar{r}\bar{u}\right)T^{\bar{i}\tilde{j}}_{\bar{u}\tilde{s}}$$
$$-\sum_{\tilde{u}}\left[\left(\bar{i}\bar{r}|\tilde{t}\tilde{u}\right)T^{\tilde{k}\tilde{j}}_{\tilde{s}\tilde{u}}+\left(\tilde{j}\tilde{t}|\tilde{s}\tilde{u}\right)T^{\bar{i}\tilde{k}}_{\bar{r}\tilde{u}}\right]-\sum_{\bar{u}}\left(\tilde{k}\tilde{s}|\bar{r}\bar{u}\right)T^{\tilde{j}\bar{i}}_{\tilde{t}\bar{u}}, \tag{2.105}$$

$$
\begin{aligned}
\mathscr{W}_{\bar{r}\bar{s}\tilde{t}}^{\bar{i}\bar{j}\tilde{k}} = \quad & \sum_{\tilde{m}} \left[\left(\tilde{t}\tilde{k}|\bar{j}\tilde{m} \right) T_{\bar{s}\bar{r}}^{\bar{i}\tilde{m}} + \left(\bar{r}\bar{j}|\bar{i}\tilde{m} \right) T_{\tilde{t}\bar{s}}^{\tilde{k}\tilde{m}} \right] + \sum_{\tilde{m}} \left(\bar{s}\bar{i}|\tilde{k}\tilde{m} \right) T_{\bar{r}\tilde{t}}^{\bar{j}\tilde{m}} \\
& - \sum_{\tilde{m}} \left[\left(\tilde{t}\tilde{k}|\bar{i}\tilde{m} \right) T_{\bar{s}\bar{r}}^{\bar{j}\tilde{m}} + \left(\bar{r}\bar{i}|\bar{j}\tilde{m} \right) T_{\tilde{t}\bar{s}}^{\tilde{k}\tilde{m}} \right] - \sum_{\tilde{m}} \left(\bar{s}\bar{j}|\tilde{k}\tilde{m} \right) T_{\bar{r}\tilde{t}}^{\bar{i}\tilde{m}} \\
& + \sum_{\tilde{u}} \left[\left(\bar{i}\bar{r}|\bar{s}\tilde{u} \right) T_{\tilde{u}\tilde{t}}^{\bar{j}\tilde{k}} + \left(\tilde{k}\tilde{t}|\bar{r}\tilde{u} \right) T_{\tilde{u}\bar{s}}^{\bar{i}\bar{j}} \right] + \sum_{\tilde{u}} \left(\bar{j}\bar{s}|\tilde{t}\tilde{u} \right) T_{\tilde{u}\bar{r}}^{\tilde{k}\bar{i}} \\
& - \sum_{\tilde{u}} \left[\left(\bar{i}\bar{s}|\bar{r}\tilde{u} \right) T_{\tilde{t}\tilde{u}}^{\tilde{k}\bar{j}} + \left(\tilde{k}\tilde{t}|\bar{s}\tilde{u} \right) T_{\bar{r}\tilde{u}}^{\bar{j}\bar{i}} \right] - \sum_{\tilde{u}} \left(\bar{j}\bar{r}|\tilde{t}\tilde{u} \right) T_{\bar{s}\tilde{u}}^{\bar{i}\tilde{k}}. \qquad (2.106)
\end{aligned}
$$

Restricting the triple excitations to the triple domains $[ijk]$, the calculation cost of every term in the above equations is constant and is not related to the molecular size. The triple excitations which are included in the above excitations are restricted with the condition that for each triple ijk, every two of them, i.e., ij, jk, ik must be strong or close pairs and at least one of the three pairs must be a strong pair. Under the above restrictions, it is obvious that the total number of triples scales linearly with the molecular size. Therefore, the calculation of the above (T0) approximation is theoretically linear scaling. Compared to the fact that (T) calculation is the most expensive and highest scaling part in canonical UCCSD(T) methods, the (T0) approximation in LUCCSD(T) method is rather cheap and mostly even cheaper than the LUCCSD iteration part, which will be shown in detail in the next chapter.

In this work, for sd-localization and ab-localization, different programs have been written for the (T0) approximation part. Because only (T0) is implemented, in the following discussions all (T) for LUCCSD will mean (T0) approximation. As there is no coupling between triples and doubles as well as triples and singles in this approximation, the (T) program is designed to be a post-processing after the LUCCSD program. All the integrals and amplitudes have been passed from the LUCCSD part to the (T) part. Notice that because some close pairs have been included in triple lists, there are more 3-external integrals needed compared to the LUCCSD part. In the program, if LUCCSD(T) is needed, the triple list is constructed before the integral transformation. The 3-external domains needed for the (T) part are pre-computed and merged with the ones for LUCCSD. Therefore, the 3-external integral transformation is done once but for more terms. This structure is the same as the one in close-shell case [68, 69]. As the triples are not coupled between themselves, all the intermediates are calculated for one triple ijk at a time and dropped after the calculation of this triple. The energies of triples are calculated directly from the intermediates and accumulated. No triple excitation amplitudes are actually calculated and stored. All of this leads to a linearly structured program and very small memory is needed. As a result, the (T0) programs turn out to be very efficient.

3 Scaling Tests of Open-shell Local Correlation Methods

During the last four years, the whole set of open-shell local correlation methods has been developed for this thesis. Theoretically, linear scaling of the most terms has been achieved. As discussed in the first chapter, it is important to make the quantum chemistry work for 100-200 atoms. To show the real efficiency of our local methods, LRMP2, LUCCSD, and LUCCSD(T) are used to calculate an open shell model system, i.e., linear polyvinyl fluoride chains with a radical position at one end. The molecular formula of it is $\cdot CHFCH_2-(CHFCH_2)_{(n-1)}-H$. The localizations of these molecules are always quite good. There are only one-center and two-center LMOs by PM localization, except in sd-localization, the domain of singly occupied orbital contains AOs of three atoms, i.e., C and F atom at one end and the first connected C atom. All the calculations have been done on a single Opteron 2380 2.5 GHz processor and the cc-pVDZ basis set has been used.

3.1 Scaling of LRMP2

In this section, the LRMP2 using sd-localization and ab-localization will be tested and compared. The density fitting approximation or the local density fitting approximation is applied to the different LRMP2 methods. In the following discussions and figures they will be denoted as DF-sd-LRMP2, DF-ab-LRMP2, LDF-sd-LRMP2, and LDF-ab-LRMP2, respectively.

Before the open-shell correlation treatment, a RHF calculation must be done. As in the closed shell case, the traditional HF calculation is much more expensive compared to DF-MP2 calculations. Alternatively, the density fitting approximation can also be used to improve the performance of the HF calculation. If local domains for fitting functions are assigned, the efficiency of HF can be further improved. [109] Similarly, density fitting (DF) and local density fitting (LDF) techniques are also used for RHF calculations. Therefore, as a starting point, the CPU time needed for

DF-RHF and LDF-RHF calculations are compared in Figure 3.1.

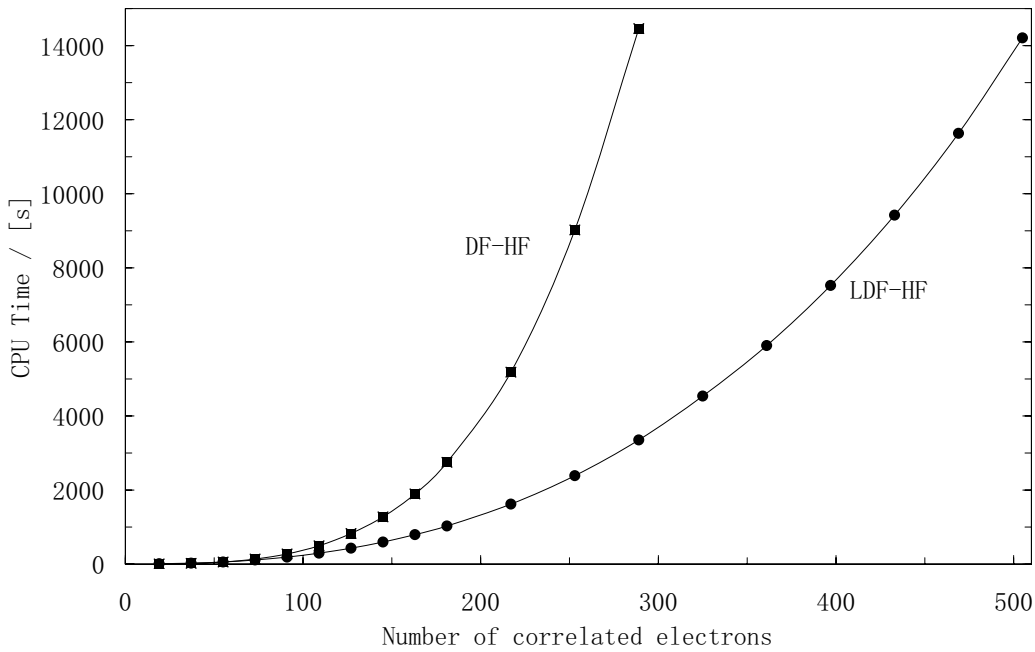

Figure 3.1: Total CPU times for DF-RHF and LDF-RHF calculations. The cc-pVDZ basis set has been used.

For DF-RHF, the calculations have been shown up to the molecule containing 289 correlated electrons, 97 atoms, and 917 basis functions. For LDF-RHF, the calculations have been further shown up to the molecule containing 505 correlated electrons, 169 atoms, and 1601 basis functions, for which the pre-allocated memory is 36 GB. In the figure, LDF-RHF is cheaper than DF-RHF, as expected. For the largest case, the LDF-RHF calculation takes 14208 seconds which is less than 4 hours. The DF-RHF calculation for the molecule containing 169 atoms takes about one day which has not been shown on this figure. Note that calculations are performed using a cc-pVDZ basis set, for a really accurate calculation cc-pVTZ basis set will be needed and it is approximately 10 times more expensive. Anyway, DF-RHF and LDF-RHF are both applicable to this size of system and can be completed in several days. Because the final iteration in LDF-RHF is done without local fitting, the largest error caused by local density fitting in these molecules is 0.25 micro-Hartree, which is really small.

In Figure 3.2 and Figure 3.3 DF-RHF is compared with DF-sd-LRMP2 and DF-

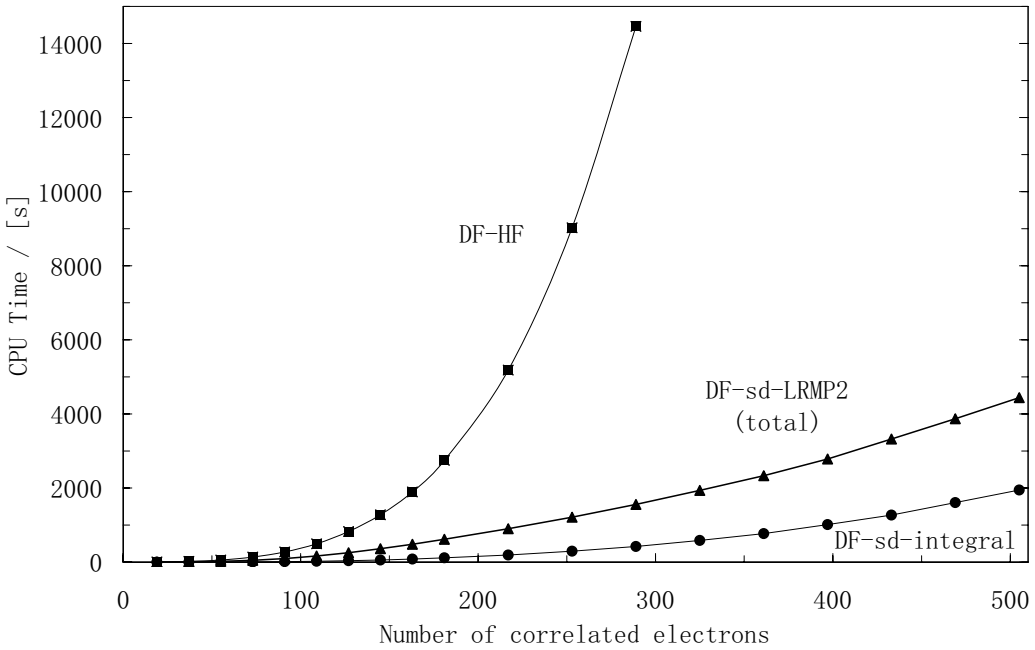

Figure 3.2: Total CPU times for DF-HF and DF-sd-LRMP2 calculations. The cc-pVDZ basis set has been used.

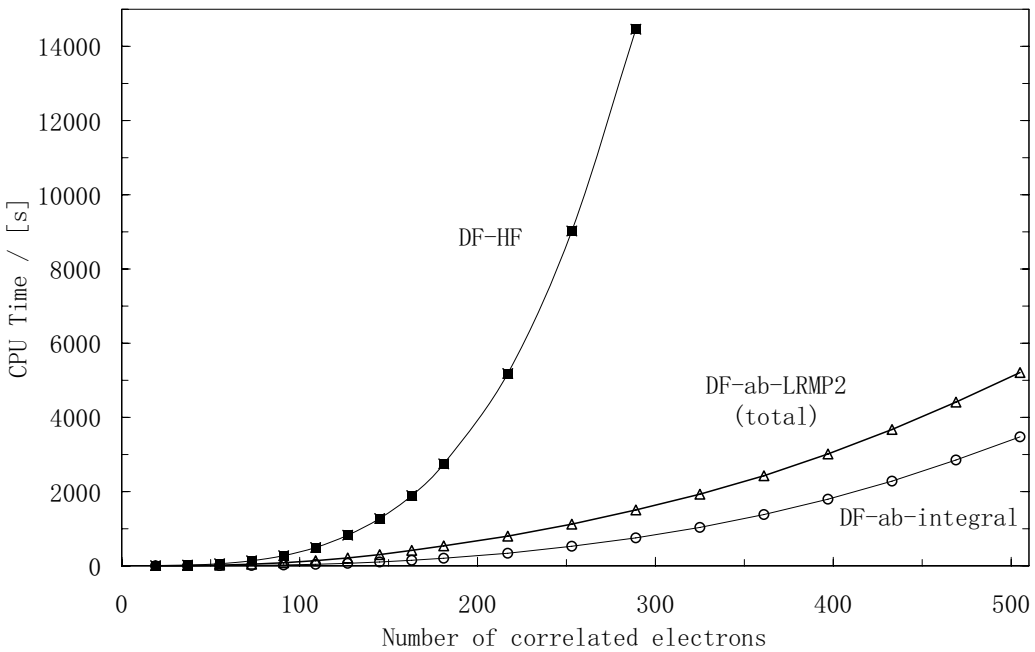

Figure 3.3: Total CPU times for DF-HF and DF-ab-LRMP2 calculations. The cc-pVDZ basis set has been used.

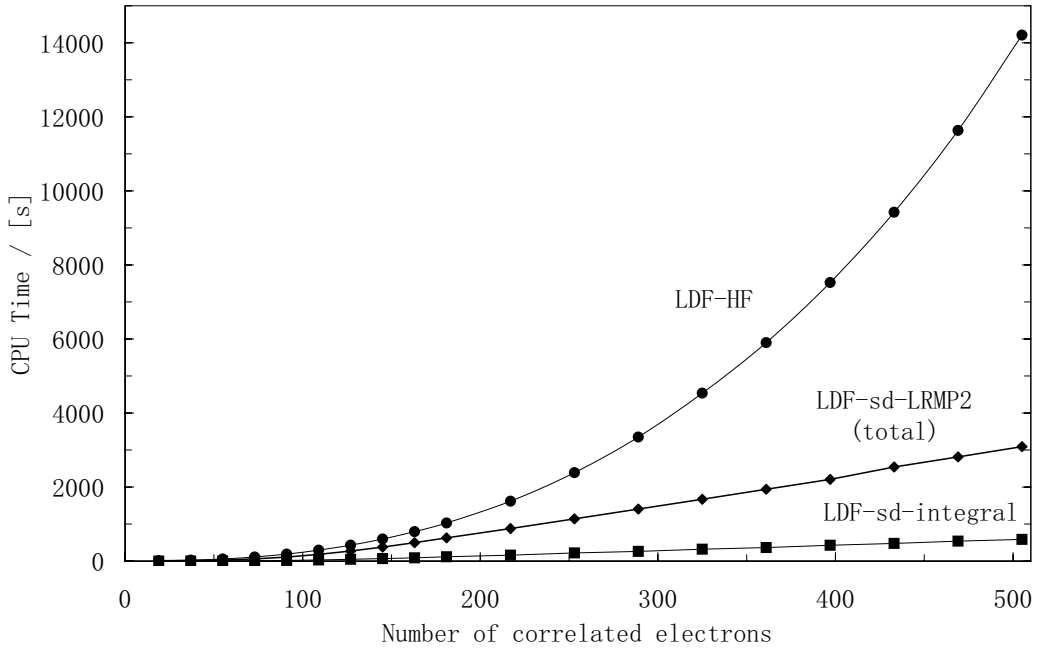

Figure 3.4: Total CPU times for LDF-HF and LDF-sd-LRMP2 calculations. The cc-pVDZ basis set has been used.

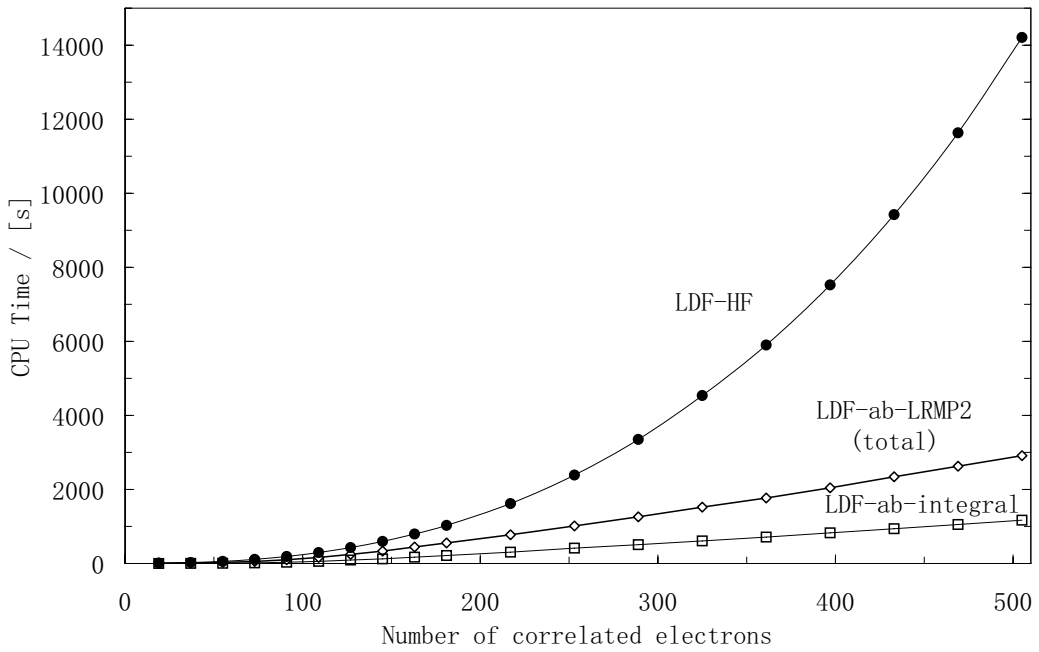

Figure 3.5: Total CPU times for LDF-HF and LDF-ab-LRMP2 calculations. The cc-pVDZ basis set has been used.

ab-LRMP2, respectively. In Figure 3.4 and Figure 3.5 LDF-RHF is compared with LDF-sd-LRMP2 and LDF-ab-LRMP2, respectively. It is clear that local RMP2 is more efficient than the RHF calculation. It is to be emphasized that even for the largest molecule with 505 electrons, the DF-sd-LRMP2 only takes about 1 hour while LDF-sd-LRMP2 takes less than 1 hour. Under cc-pVTZ basis, the above molecule, which containing 505 correlated electrons, 169 atoms, and 2918 basis functions, took only 4.74 hours for LDF-sd-LRMP2 and 6.17 hours for DF-sd-LRMP2. Therefore, it can be expected that a calculation with DF-LRMP2 for a system with about 200 atoms with a cc-pVTZ basis set takes one or two days. In Figure 3.4 and Figure 3.5, LDF-sd-LRMP2 and LDF-ab-LRMP2 show linear scaling in the tested region. Even for DF-sd-LRMP2 and DF-ab-LRMP2, near linear scaling is also displayed in the tested region while the final part of the curve starts to grow quadratically. For DF-sd-LRMP2, the last two points in Figure 3.2 scale as $\mathscr{O}(\mathscr{N}^{1.9})$. For DF-ab-LRMP2, the last two points in Figure 3.3 scale as $\mathscr{O}(\mathscr{N}^{2.2})$.

Comparing Figure 3.2 and Figure 3.3, it is found that the percentage for the integral transformation is higher for DF-ab-LRMP2. Similar conclusion can also be made by comparing Figure 3.4 and Figure 3.5. This is easy to understand because the disadvantage of ad-localization is that more integrals are needed, while the advantage of it are the smaller domains which save iteration time.

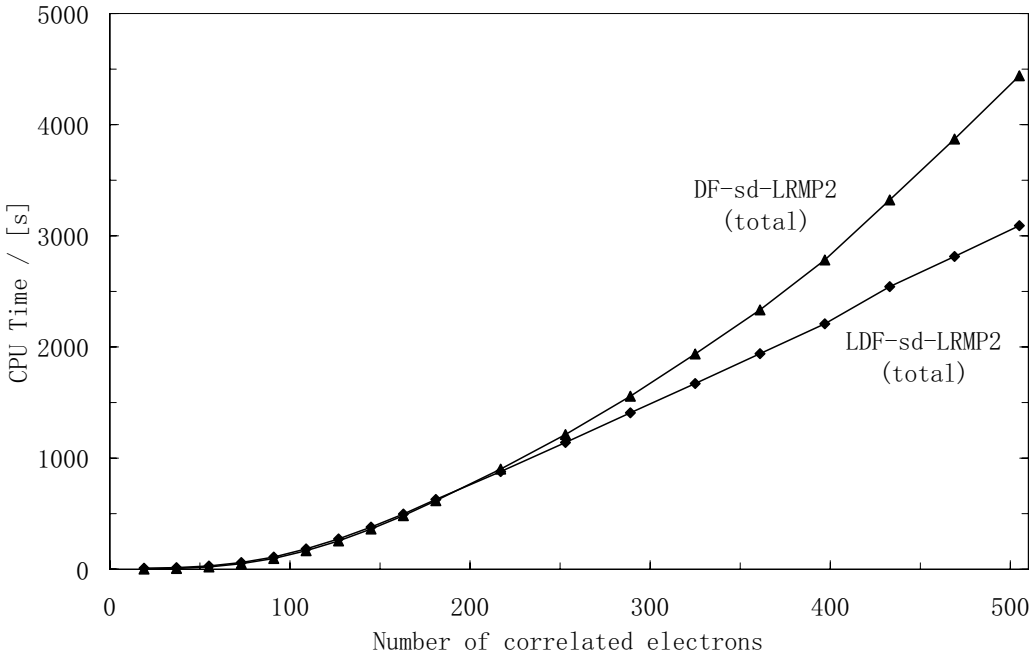

Figure 3.6: Total CPU times for DF-sd-LRMP2 and LDF-sd-LRMP2 calculations. The cc-pVDZ basis set has been used.

In Figure 3.6 DF-sd-LRMP2 and LDF-sd-LRMP2 are put together to compare the performance. Local density fitting improves the scaling behavior of DF-sd-LRMP2 especially at the final region. However, the difference of the total CPU time between DF-sd-LRMP2 and LDF-sd-LRMP2 is not large. In the largest molecule with 505 electrons, the above difference is only about 30 percent. With both DF-sd-LRMP2 and LDF-sd-LRMP2 being much more cheaper than the DF-RHF or LDF-RHF calculation, it is not really necessary to use local fitting for LRMP2 calculation which introduces another error by local density fitting.

Similarly, DF-ab-LRMP2 and LDF-ab-LRMP2 are put together in Figure 3.7. Linear scaling is clearly shown for the LDF-ab-LRMP2 method. The difference between DF-ab-LRMP2 and LDF-ab-LRMP2 is again not very pronounced, the largest case differs by about 40 percent. Therefore, for the same reason as before, the DF-ab-LRMP2 is preferred and it will be applied to different systems in the following chapters.

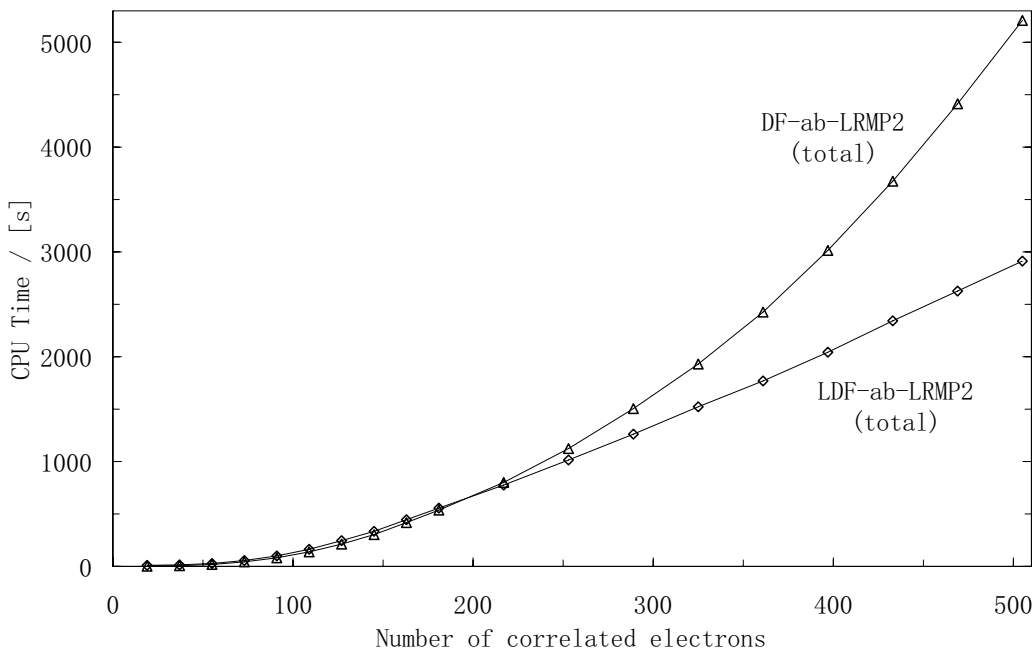

Figure 3.7: Total CPU times for DF-ab-LRMP2 and LDF-ab-LRMP2 calculations. The cc-pVDZ basis set has been used.

In Figure 3.8 DF-sd-LRMP2 is compared with DF-ab-LRMP2 while in Figure 3.9 LDF-sd-LRMP2 is compared with LDF-ab-LRMP2. In Figure 3.8, in the first half,

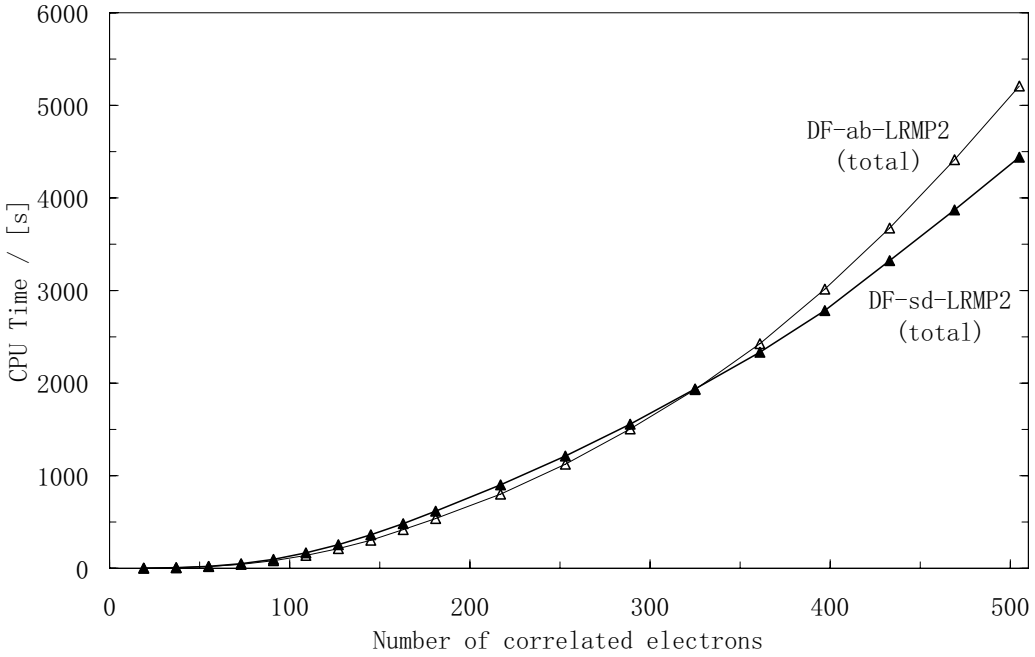

Figure 3.8: Total CPU times for DF-sd-LRMP2 and DF-ab-LRMP2 calculations. The cc-pVDZ basis set has been used.

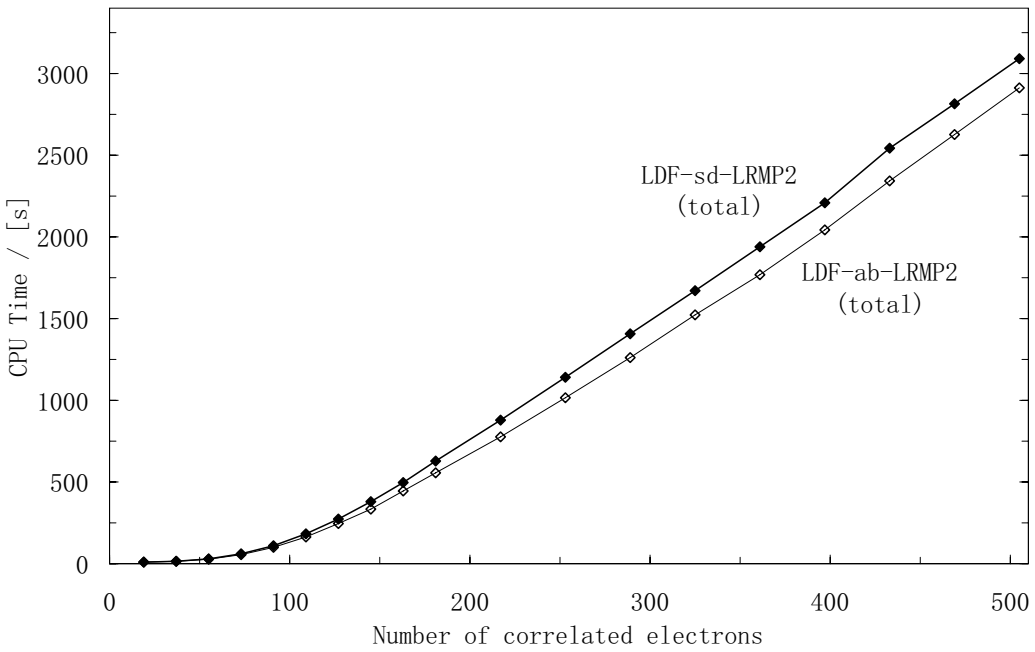

Figure 3.9: Total CPU times for LDF-sd-LRMP2 and LDF-ab-LRMP2 calculations. The cc-pVDZ basis set has been used.

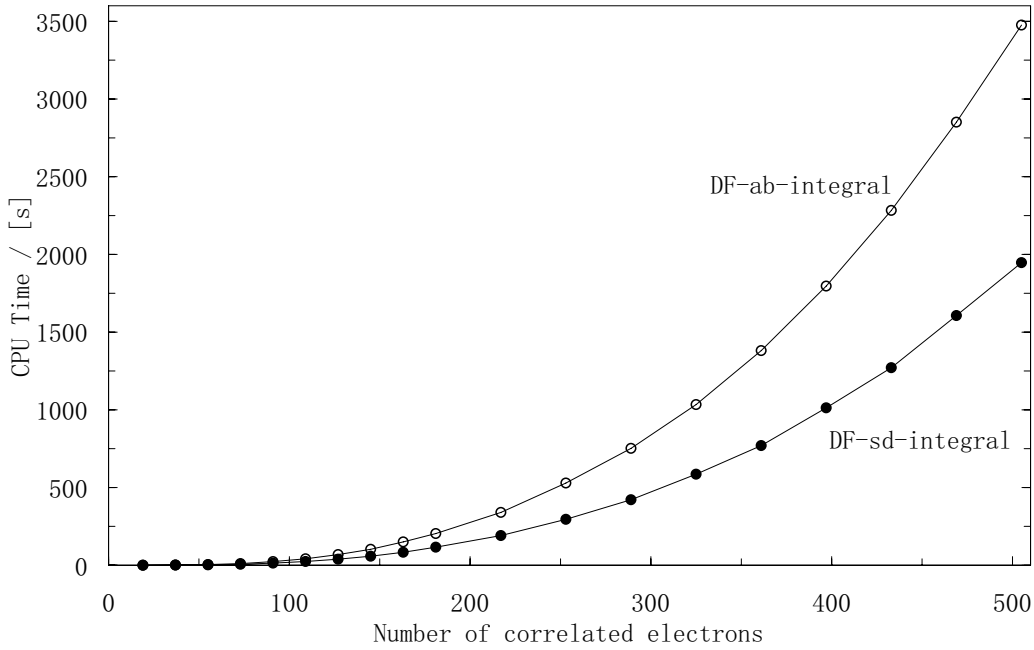

Figure 3.10: CPU times for the integral transformation in DF-sd-LRMP2 and DF-ab-LRMP2 calculations. The cc-pVDZ basis set has been used.

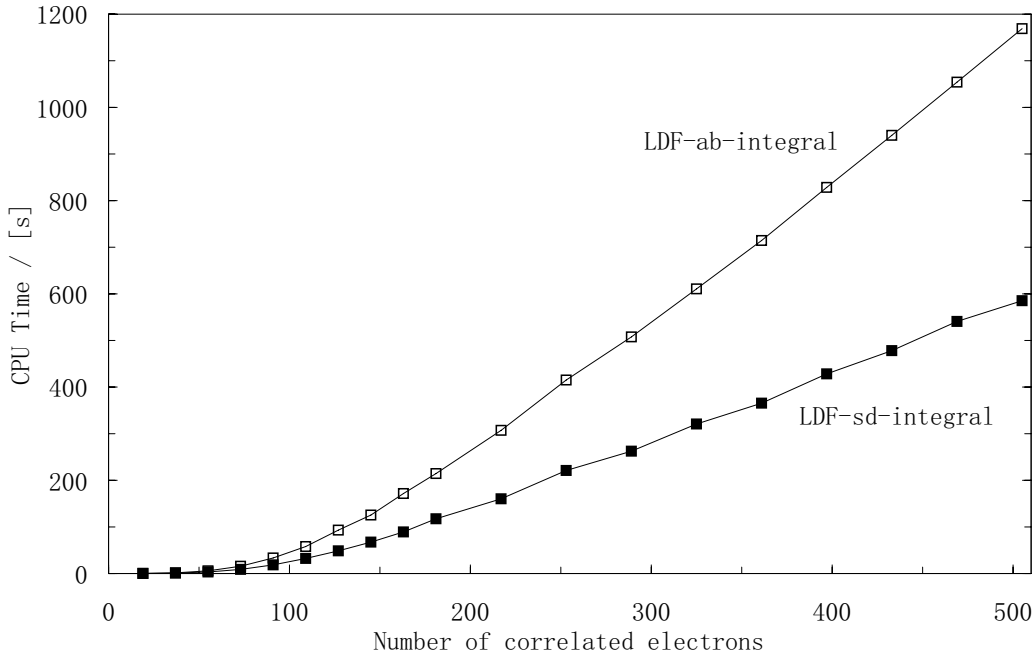

Figure 3.11: CPU times for the integral transformation in LDF-sd-LRMP2 and LDF-ab-LRMP2 calculations. The cc-pVDZ basis set has been used.

the curves show that DF-ab-LRMP2 is cheaper than DF-sd-LRMP2. This is due to the better localization in DF-ab-LRMP2. A larger domain is found for the DF-sd-LRMP2 method which is the singly occupied one and this has been removed in the DF-ab-LRMP2. For radical $\cdot CHFCH_2-(CHFCH_2)_2-H$, Figure 3.12 shows the singly occupied orbital, which is not localized by sd-localization. In ab-localization, this orbital is better localized for alpha spin orbitals, which is shown in Figure 3.13.

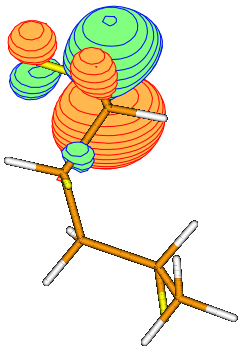

Figure 3.12: Singly occupied orbital in radical $\cdot CHFCH_2-(CHFCH_2)_2-H$ in sd-localization. The surface value is equal to 0.050. The figure is drawn by program 'MOLDEN'.

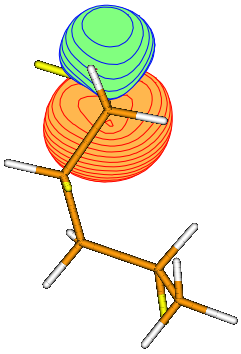

Figure 3.13: Localized alpha spin orbital corresponding singly occupied orbital in radical $\cdot CHFCH_2-(CHFCH_2)_2-H$ in ab-localization. The surface value is equal to 0.050. The figure is drawn by program 'MOLDEN'.

In the later part of the curves in Figure 3.8 DF-ab-LRMP2 becomes more expensive than DF-sd-LRMP2 due to the expense of the integral transformation. For DF-ab-LRMP2 different integrals are needed for alpha and beta orbitals, therefore the number of integrals has been doubled compared to DF-sd-LRMP2. As a result, the time consumed by the integral transformation in DF-ab-LRMP2 is also doubled.

Since the integral transformation is the only non-linear scaling part, it is not surprising that the time consumed by DF-ab-LRMP2 grows faster and becomes more expensive than DF-sd-LRMP2 for the larger molecules. A comparison of the integral transformation time for DF-sd-LRMP2 and DF-ab-LRMP2 is shown in Figure 3.10, and the one for LDF-sd-LRMP2 and LDF-ab-LRMP2 is shown in Figure 3.11. The local density fitting brings the time consumed by the integral transformation of LRMP2 into linear scaling and renders it quite cheap.

3.2 Scaling of LUCCSD

3.2.1 Scaling Using Default Settings

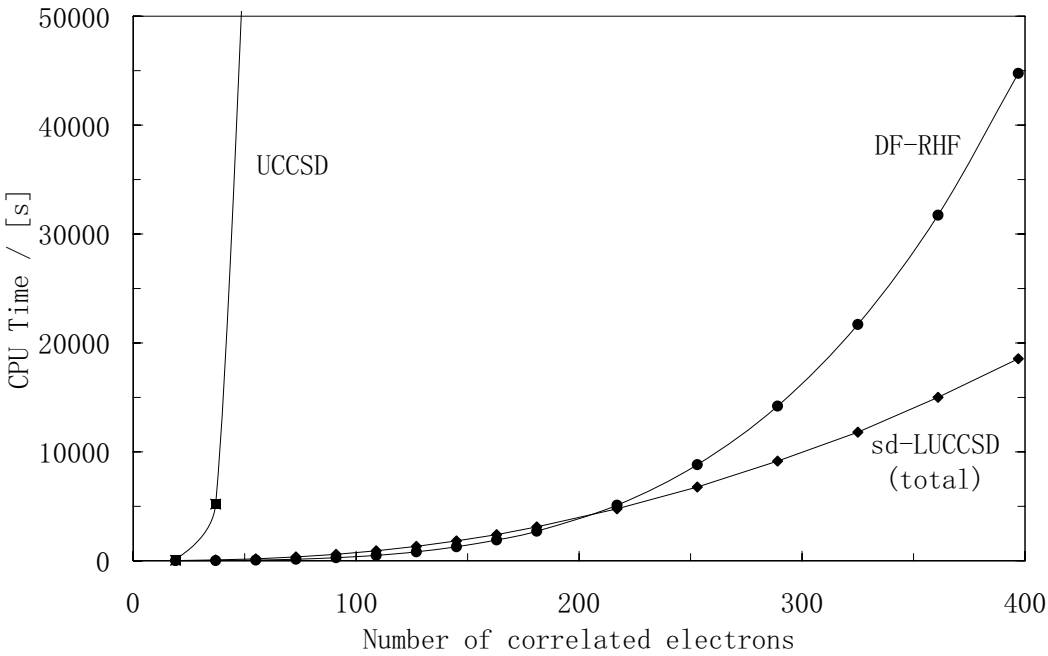

Figure 3.14: Total CPU times for UCCSD, DF-RHF, and sd-LUCCSD calculations. The cc-pVDZ basis set has been used.

Having discussed the time consumption of different LRMP2 methods, the LUCCSD methods will be discussed in this section. In Figure 3.14 the time consumption of UCCSD, DF-RHF, and sd-LUCCSD has been compared. The UCCSD time consumption grows so fast, as expected, that already after a molecule of 19 atoms it takes 80000 seconds and is out of the manageable range and could not be shown in the figure. Amazingly, the sd-LUCCSD time consumption is shown to be much cheaper than for the DF-RHF calculation. Notice that cc-pVDZ basis set are used.

If cc-pVTZ basis set is used, the time consumption of LUCCSD increases and becomes more expensive than the DF-RHF case, but still comparable. For example, for the largest molecule in Figure 3.14, DF-RHF takes 42.31 hours and sd-LUCCSD takes 42.68 hours with the cc-pVTZ basis. No matter whether LUCCSD is cheaper than DF-RHF or whether it is a little bit more expensive as compared to DF-RHF, after a DF-RHF calculation it will be possible to perform a LUCCSD calculation. For ab-LUCCSD, the total time is compared to the time of UCCSD and DF-RHF in 3.15.

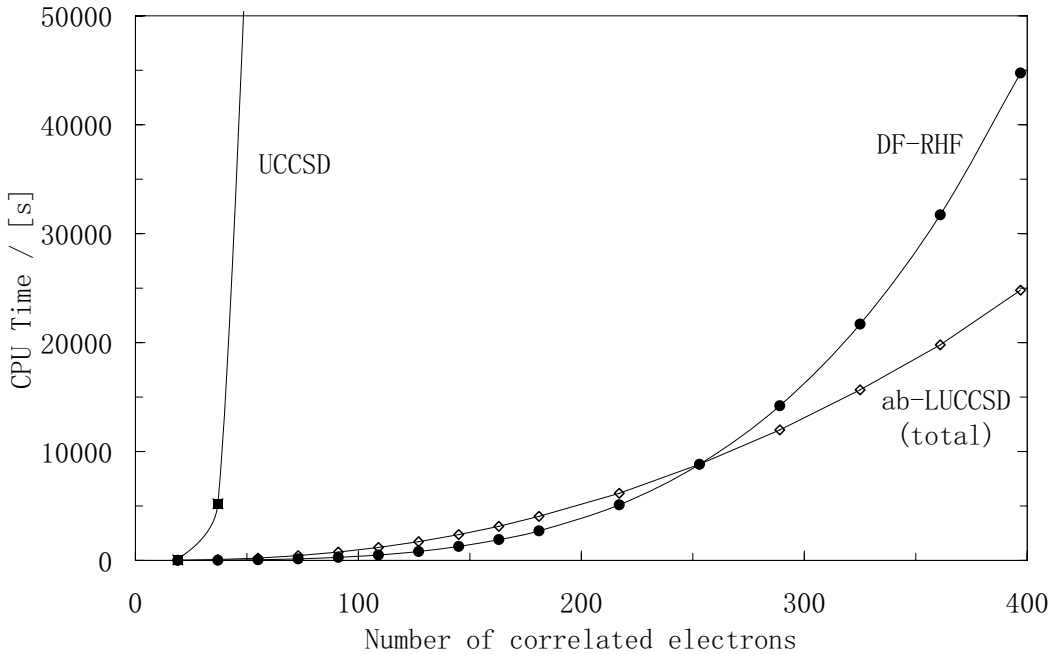

Figure 3.15: Total CPU times for UCCSD, DF-RHF, and ab-LUCCSD calculations. The cc-pVDZ basis set has been used.

The comparisons of time consumptions for the iteration part and the integral transformation part of sd-LUCCSD and ab-LUCCSD are shown in Figures 3.16 and 3.17, respectively. In Figure 3.16 it is shown that the integral transformation of sd-LUCCSD is a little cheaper than the iterative part of it. If cc-pVTZ is used, for the largest molecule in the figure, the iteration part of sd-LUCCSD takes 15.82 hours and the integral transformation part of sd-LUCCSD takes 26.76 hours. Although the integral transformation becomes more expensive for cc-pVTZ, it is still in the same range as compared to the iteration part. For ab-LUCCSD the curves of the two parts in Figure 3.17 are close to each other and cross. It is not surprising

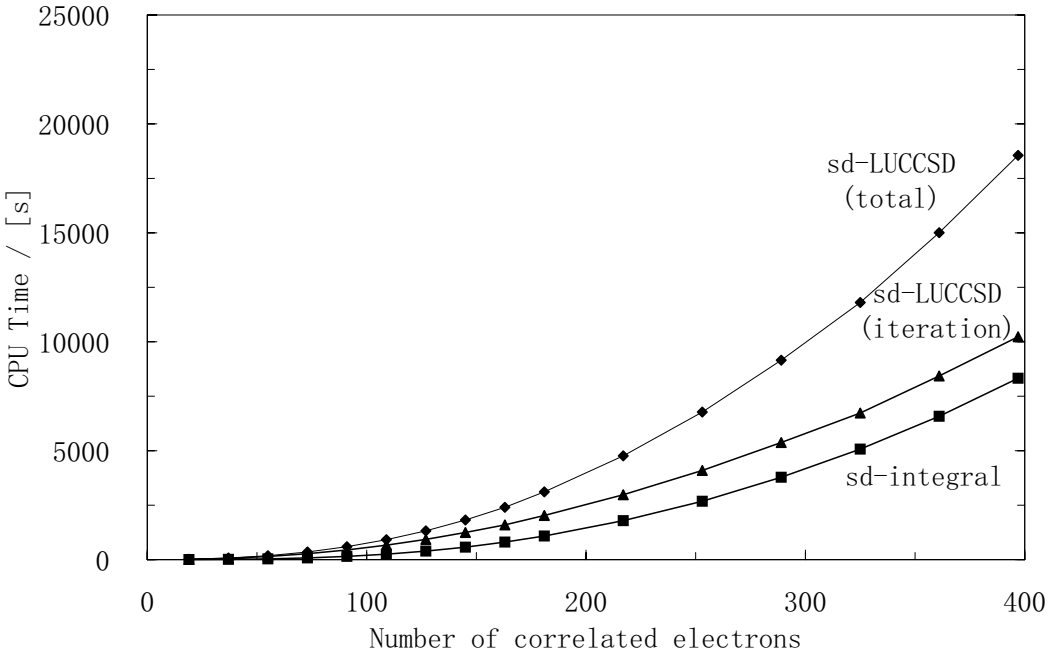

Figure 3.16: CPU times for the integral transformation, iteration and all together in sd-LUCCSD calculations. The cc-pVDZ basis set has been used.

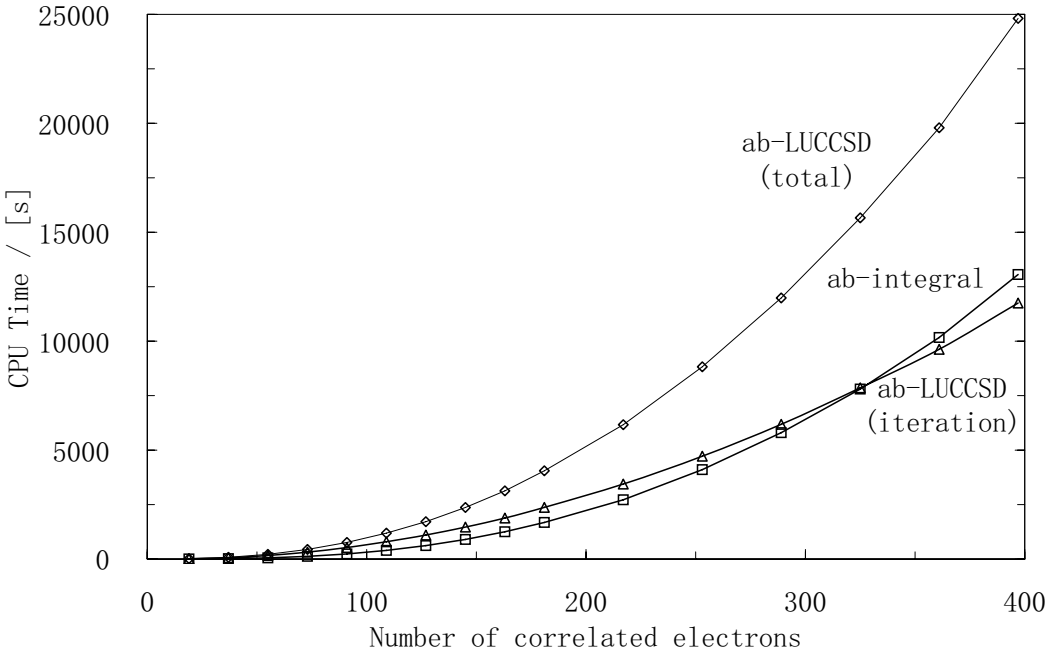

Figure 3.17: CPU times for the integral transformation, iteration and all together in ab-LUCCSD calculations. The cc-pVDZ basis set has been used.

that the integral transformation part is relatively larger for ab-LUCCSD due to the same reason as discussed in the LRMP2 section. If cc-pVTZ is used, for the largest molecule in the figure, the iteration part of ab-LUCCSD takes 18.45 hours and the integral transformation part of ab-LUCCSD takes 39.35 hours.

In Figure 3.18 sd-LUCCSD and ab-LUCCSD are compared for the integral transformation time. As supposed the integral transformation for ab-LUCCSD is more expensive than the integral transformation for sd-LUCCSD. The integral transformation scales as $\mathscr{O}(\mathscr{N}^{2.5})$ for sd-LUCCSD and as $\mathscr{O}(\mathscr{N}^{2.63})$ for ab-LUCCSD in Figure 3.18. If the local density fitting is applied for LUCCSD, this scaling can be further brought down. For 4-external integrals local density fitting will be helpful [72] and it can achieve linear scaling. However, 3-external integrals often dominate since large domains are always needed for triple calculations. It is more difficult to achieve linear scaling for 3-external integrals. Local density fitting is not yet implemented for LUCCSD in this work and will be done later. However, in the discussed region the local density fitting will not save much time. As the time consumed by LUCCSD is already comparable with DF-RHF, the local density fitting will not be essential for the discussed molecules.

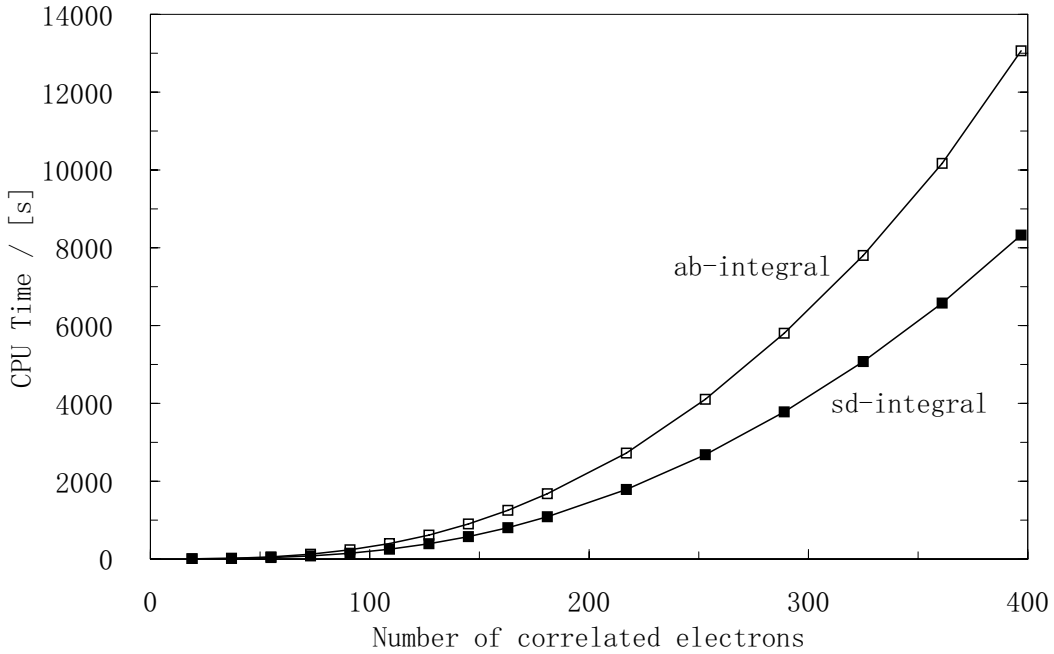

Figure 3.18: Total CPU times for integral transformation part in sd-LUCCSD and ab-LUCCSD calculations. The cc-pVDZ basis set has been used.

The time consumed by the iteration part of sd-LUCCSD and ab-LUCCSD are compared in Figure 3.19. The scaling in the figure is $\mathscr{O}(\mathscr{N}^{2.0})$ for sd-LUCCSD and

$\mathscr{O}(\mathscr{N}^{2.1})$ for ab-LUCCSD. Theoretically, this scaling should be $\mathscr{O}(\mathscr{N}^2)$ due to the scaling of calculating terms $\mathbf{G}(\mathbf{E})$, which agrees with the figures. In this figure, ab-LUCCSD is not cheaper than sd-LUCCSD, as expected. The only non-linear scaling term $\mathbf{G}(\mathbf{E})$ in LUCCSD needs to be transformed and contracted in every LUCCSD iteration. This term in ab-LUCCSD method is twice as frequent as in sd-LUCCSD. Therefore, it is easy to understand that sd-LUCCSD is cheaper than ab-LUCCSD. In the next subsection, the behavior of LUCCSD with the option of neglecting $\mathbf{G}(\mathbf{E})$ terms will be discussed.

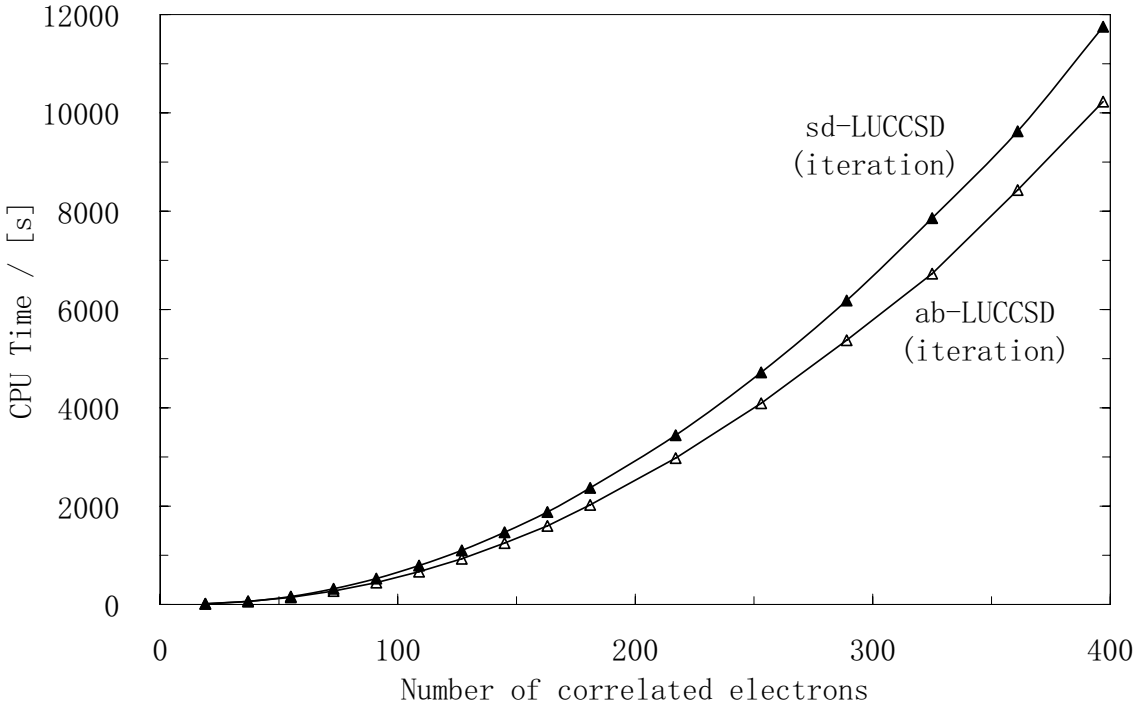

Figure 3.19: Total CPU times for iteration part in sd-LUCCSD and ab-LUCCSD calculations. The cc-pVDZ basis set has been used.

3.2.2 Scaling with Setting 'igskip=1' and 'igskip=2'

As discussed in the last chapter, using option 'igskip=1', the non-linear scaling terms $\mathbf{G}(\mathbf{E})$ can be neglected together with other similar terms with the same structure. In Figure 3.20 and Figure 3.21, respectively, sd-LUCCSD and ab-LUCCSD with different options of 'igskip' have been put together.

'igskip=0' is the default one, in which terms $\mathbf{G}(\mathbf{E})$ are included. With option 'igskip=1' terms $\mathbf{G}(\mathbf{E})$ are neglected together with other terms as discussed in the

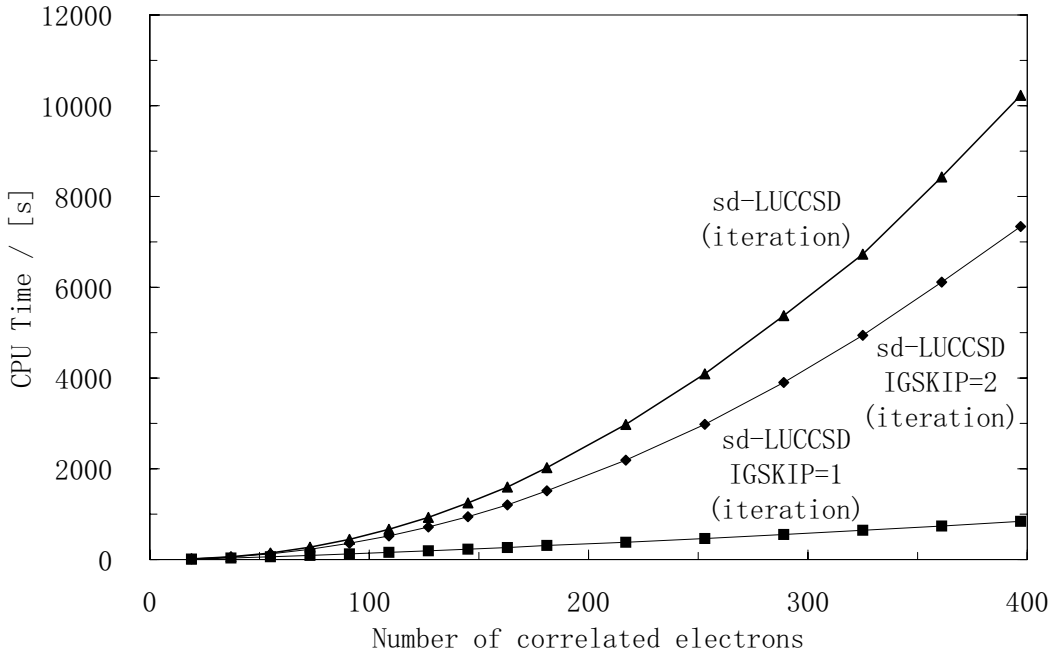

Figure 3.20: CPU times for iteration part of sd-LUCCSD calculations with 'igskip=0', 'igskip=1', and 'igskip=2'. The cc-pVDZ basis set has been used.

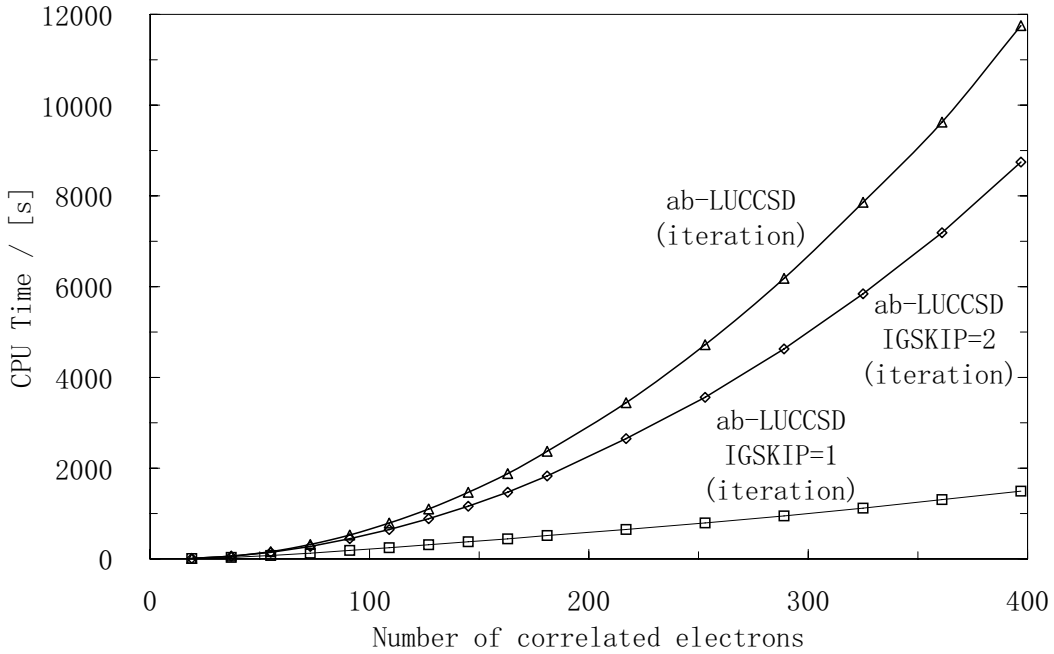

Figure 3.21: CPU times for iteration part of ab-LUCCSD calculations with 'igskip=0', 'igskip=1', and 'igskip=2'. The cc-pVDZ basis set has been used.

last chapter. The sd-LUCCSD and ab-LUCCSD without $\mathbf{G}(\mathbf{E})$ terms is really cheap and becomes a straight line which lies at the bottom of the figure. In this figure it is clearly shown that the $\mathbf{G}(\mathbf{E})$ terms are the most expensive part in sd-LUCCSD and ab-LUCCSD iterations. In the largest molecule these terms took more than 85 percent of the total time. Alternatively, it is possible to neglect $\mathbf{G}(\mathbf{E})$ and corresponding terms in the first several iterations and include them in the later ones. This treatment will give the same results compared to the case in which $\mathbf{G}(\mathbf{E})$ is always taken into account. This kind of option is set to be 'igskip=2'. Without loss of accuracy, about 25 percent of computing time can be saved using 'igskip=2' for the large molecules. Therefore 'igskip=2' is recommended for a LUCCSD calculation.

Without $\mathbf{G}(\mathbf{E})$ terms, both ab-LUCCSD and sd-LUCCSD scale nearly linearly which is clearly shown in Figure 3.22. Of course absolute linear scaling is not possible and there are still non-linearities in the curves. However, the computational time of this part is already as cheap as several minutes up to half an hour.

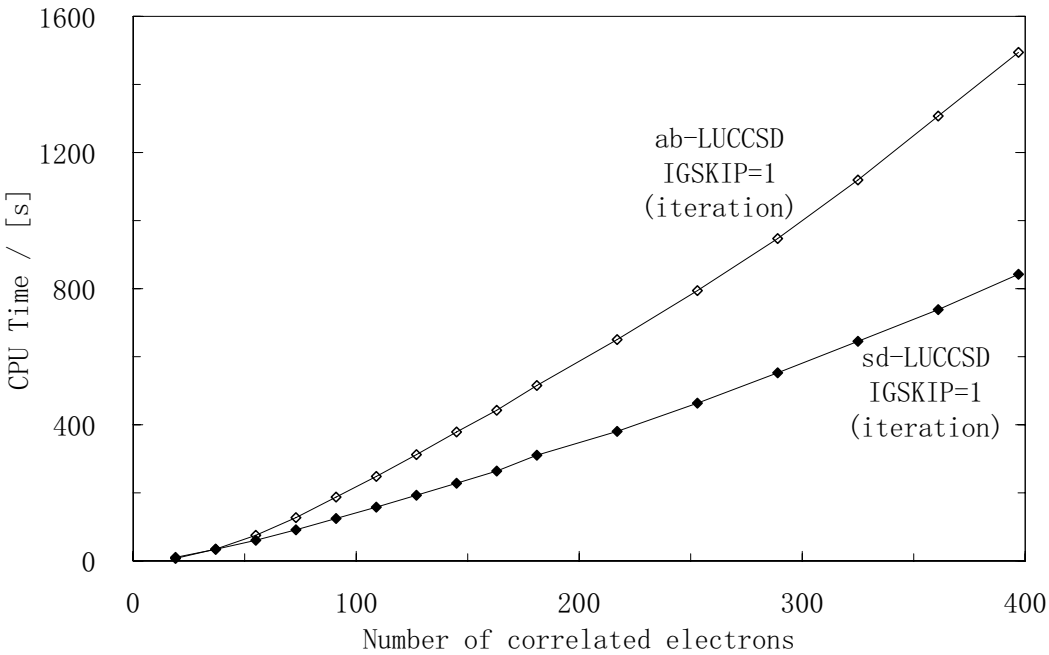

Figure 3.22: CPU times for iteration part sd-LUCCSD and ab-LUCCSD calculations with 'igskip=1'. The cc-pVDZ basis set has been used.

In Figure 3.22 the behaviors with the option 'igskip=1' of sd-LUCCSD and ab-LUCCSD are compared. Without $\mathbf{G}(\mathbf{E})$ terms the ab-LUCCSD is about twice as expensive as sd-LUCCSD for the tested molecules due to the double sets of integrals. Removing the delocalized single occupied orbital in ab-localization shows smaller

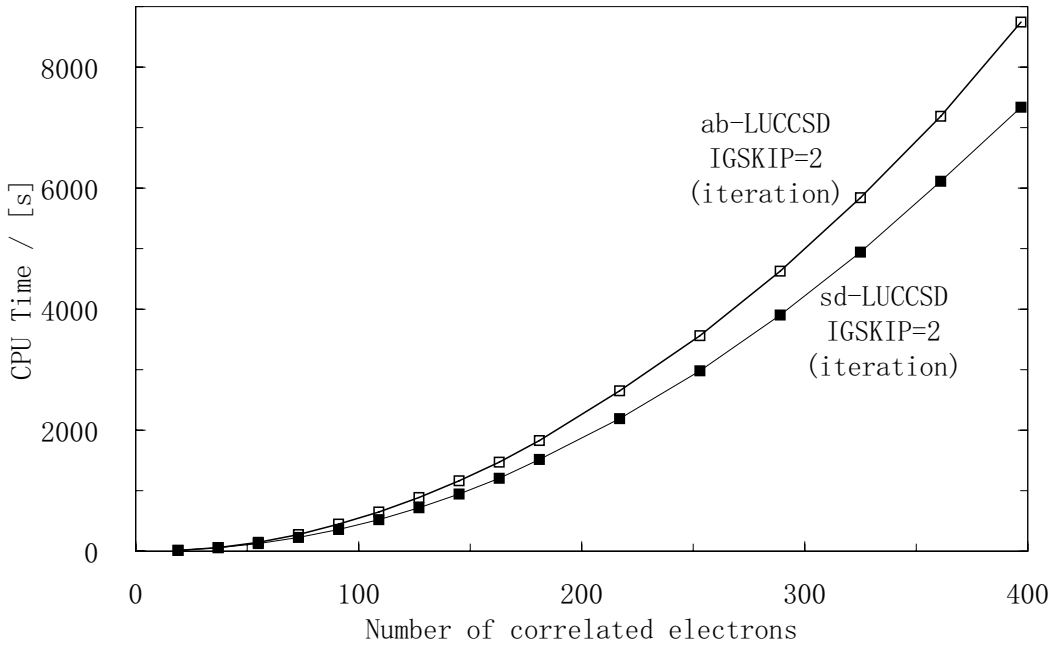

Figure 3.23: CPU times for iteration part sd-LUCCSD and ab-LUCCSD calculations with 'igskip=2'. The cc-pVDZ basis set has been used.

effects for LUCCSD calculations compared to LRMP2 calculations.

The behaviors with option 'igskip=2' of sd-LUCCSD and ab-LUCCSD are compared in 3.23. sd-LUCCSD is again found to be cheaper than ab-LUCCSD. The difference between the two different localizations are not large in this case.

So far the sd-localization and ab-localization show a very similar behavior. The ab-localization is a little more expensive than sd-localization for the tested molecules. Due to the fact that the singly occupied orbitals in these cases are not very diffuse, as shown in Figure 3.12, this behavior is not surprising. From the time consumption, it is hard to say which is better. Anyway, sd-localization can be used first and the domain size of the singly occupied orbital can be checked. If this domain is too large choosing the ab-localization method may be able to reduce it.

3.3 Scaling of (T0) Calculation

Finally the time consumption of the (T0) approximation is studied. In Figure 3.24 the time of sd-(T) part is compared with total time of DF-RHF and sd-LUCCSD(T). It is shown that the time consumption of the (T0) approximation is much smaller than of the other parts. Remembering that (T) is the most expensive and highest

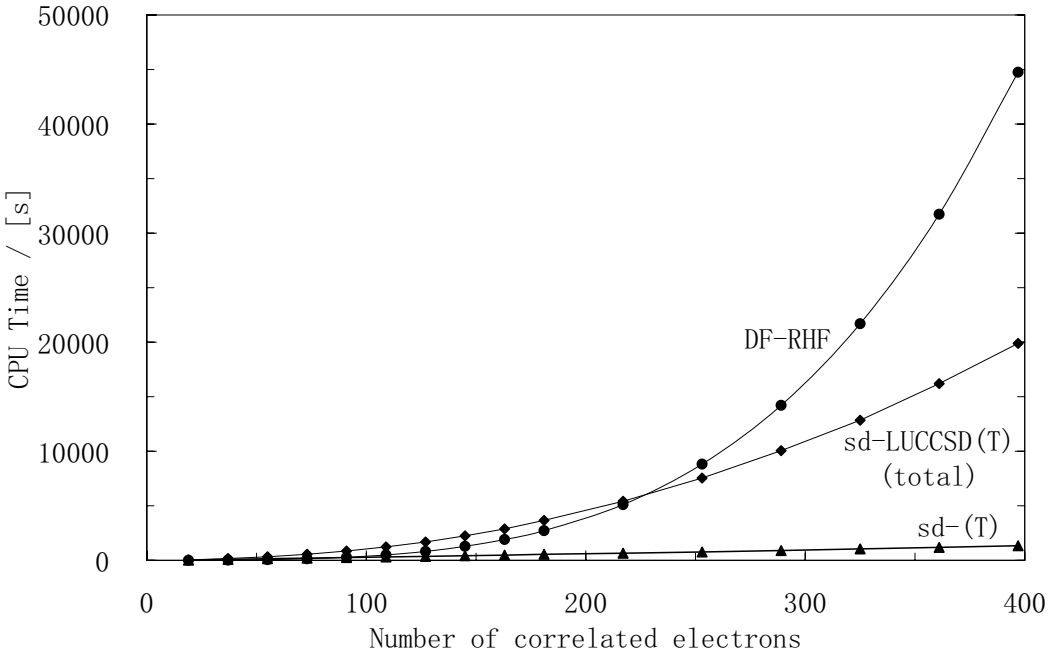

Figure 3.24: Total CPU times for DF-RHF, sd-LUCCSD(T), and (T) part in sd-LUCCSD(T) calculations. The cc-pVDZ basis set has been used.

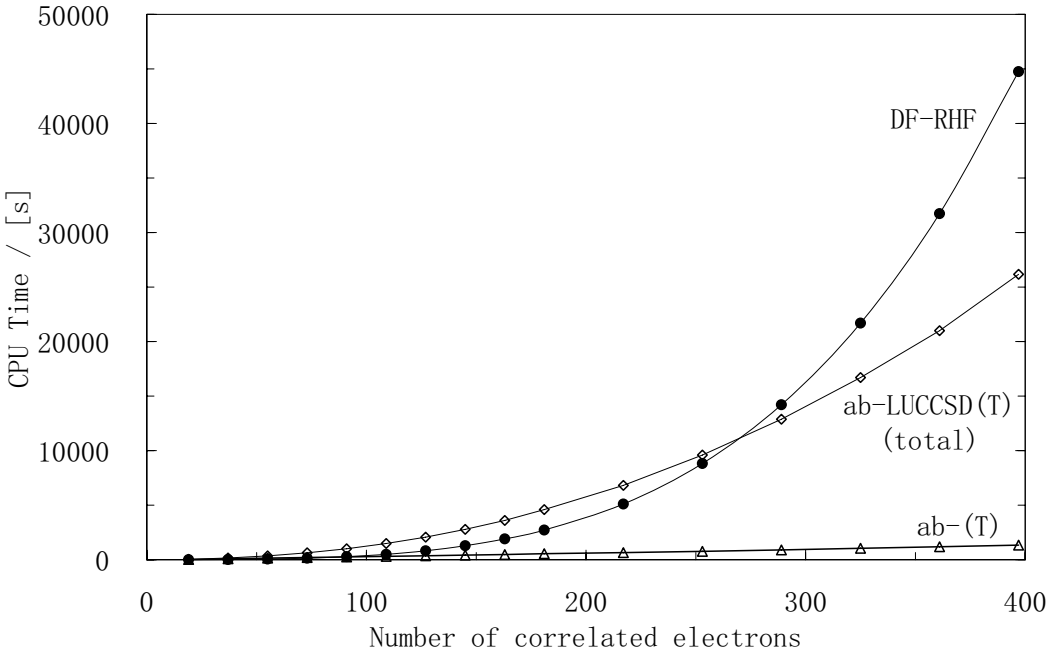

Figure 3.25: Total CPU times for DF-RHF, ab-LUCCSD(T), and (T) part in ab-LUCCSD(T) calculations. The cc-pVDZ basis set has been used.

scaling part in UCCSD(T), the (T0) approximation for LUCCSD is really cheap. Furthermore, the scaling of (T0) is very close to linear.

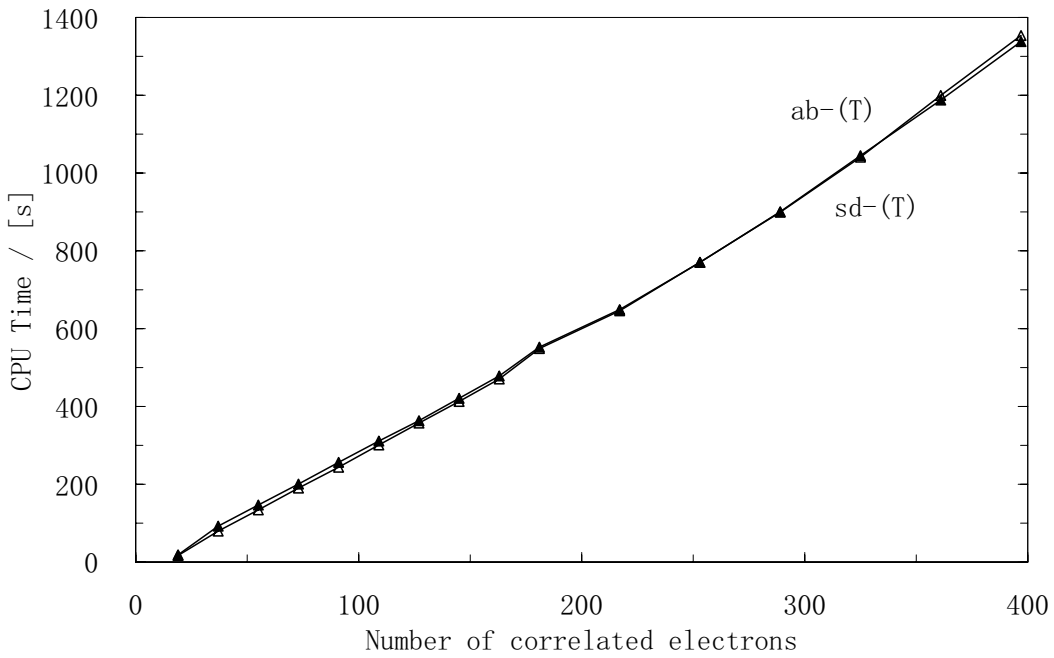

Figure 3.26: CPU times for (T) part in sd-LUCCSD and (T) part in ab-LUCCSD calculations. The cc-pVDZ basis set has been used.

In Figure 3.26, the (T0) calculations for sd-LUCCSD and ab-LUCCSD are compared. The two curves completely blend with each other, which means the (T0) approximation for sd-LUCCSD consumes nearly as much time as the ab-LUCCSD. The scaling of the (T0) calculation is close to linear and the linearity sets in rather early. Using cc-pVTZ, for the largest molecule in the figure, sd-LUCCSD(T) takes 48.54 hours totally and takes only 5.86 hours for (T) part. In (T) calculation, more 3-external integrals are needed, which should make the integral transformation more expensive. However, it is not much for the testing system. Using cc-pVTZ, for the largest molecule in the figure, integral transformation for sd-LUCCSD takes 26.47 hours while integral transformation for sd-LUCCSD(T) takes 26.76 hours.

4 Accuracy Tests of Open-shell Local Correlation Methods

4.1 Tested Systems

The accuracy of the newly developed open-shell local correlation methods is tested and discussed systematically in this chapter. Using different methods, radical stabilization energies, vertical ionization potentials, and molecular electron affinities are calculated and compared.

The radical stabilization energy is defined as the reaction energy of

$$\mathtt{R\text{-}H} + \mathtt{CH_3}\cdot \rightarrow \mathtt{R}\cdot + \mathtt{CH_4}. \tag{4.1}$$

A set of 30 different R groups are chosen and listed in Table 4.1. The symbol (from R01 to R30), the formulas of the radicals, the numbers of correlated electrons in the radicals, and the numbers of contractions in the aug-cc-pV(T+d)Z basis sets of the radicals are collected and listed in Table 4.1. The average domain sizes and the numbers of strong/close/weak pairs, are also given in Table 4.1 for sd-localization and ab-localization. In most cases, the average domain size is slightly smaller for ab-localization, and the number of strong pairs is also slightly smaller. But in a few cases, for example, R18, the average domain size of ab-localization is larger. Therefore, generally, ab-localization provides better domains, but not for every case.

For comparison, traditional canonical methods, i.e., HF, RMP2, UCCSD, and UCCSD(T), are used to obtain the 30 radical stabilization energies (RSE). The 30 RSEs are also obtained with sd-LRMP2 and ab-LRMP2 methods. In the default option of the above methods, the parameter 'domsel' was chosen to be 0.985 and the parameter 'cpldel' to be 0. To test the effect of them, the option 'domsel=0.990' together with 'cpldel=0' and the option 'domsel=0.985' together with 'cpldel=1' are tested for sd-LRMP2 and ab-LRMP2. All the results obtained with LRMP2 methods are compared with RMP2 and UCCSD(T) methods. Afterwards,

sd-LUCCSD, ab-LUCCSD, sd-LUCCSD(T), and ab-LUCCSD(T) are used to calculate the 30 RSEs. To check the effect of pair approximation, option 'nomp2=1' and option 'keepcls=1' are tested. The additional linear scaling approximation by setting 'igskip=1' is also tested. All the LUCCSD results are compared with UCCSD and UCCSD(T) results while all the LUCCSD(T) results are compared with UCCSD(T) results. The basis sets aug-cc-pV(T+d)Z are employed in all RSE calculations.

Table 4.1: Structures and other information of 30 radicals.

				average domain size		number of pairs strong/close/weak	
	Radical Formula	$N_e^{(a)}$	$N_b^{(b)}$	sd-	ab-	sd-	ab-
R01	$\cdot CH_2CF_3$	31	276	114	104	141/144/180	129/138/198
R02	$\cdot CH_2CH_2Cl$	19	239	121	110	87/ 24/ 60	81/ 24/ 66
R03	$\cdot CH_2CH_2F$	19	230	105	104	81/ 66/ 24	75/ 66/ 30
R04	$\cdot CH_2CH_2OH$	19	253	109	108	81/ 66/ 24	75/ 66/ 30
R05	$\cdot CH_2CH{=}CH_2$	17	253	123	124	86/ 34/ 16	80/ 40/ 16
R06	$\cdot CH_2CHO$	17	207	118	115	88/ 40/ 8	86/ 42/ 8
R07	$\cdot CH_2CN$	15	184	118	115	69/ 28/ 8	67/ 30/ 8
R08	$\cdot CH_2CONH_2$	23	276	134	125	133/ 88/ 32	131/ 90/ 32
R09	$\cdot CH_2CONH{-}CH_3$	29	368	139	132	160/124/122	158/126/122
R10	$\cdot CH_2COO{-}CH_3$	29	345	136	129	160/124/122	158/126/122
R11	$\cdot CH_2COOH$	23	253	131	122	133/ 88/ 32	131/ 90/ 32
R12	$\cdot CH_2CH(CH_2)_2$	23	345	137	129	113/100/ 40	107/106/ 40
R13	$\cdot CH_2F$	13	138	97	86	54/ 24/ 0	48/ 30/ 0
R14	$\cdot CH_2NH_2$	13	184	103	101	62/ 16/ 0	53/ 25/ 0
R15	$\cdot CH_2NH_3^+$	13	207	104	105	54/ 24/ 0	48/ 30/ 0
R16	$\cdot CH_2NHCH_3$	19	276	118	120	89/ 58/ 24	85/ 56/ 30
R17	$\cdot CH_2NHCHO$	23	276	139	132	143/ 62/ 48	131/ 72/ 50
R18	$\cdot CH_2N(CH_3)_2$	25	368	126	131	116/100/ 84	124/ 80/ 96
R19	$\cdot CH_2NO_2$	23	230	135	121	153/ 80/ 20	149/ 84/ 20
R20	$\cdot CH_2OCF_3$	37	322	111	110	170/166/330	167/181/318
R21	$\cdot CH_2OCH_3$	19	253	114	114	89/ 58/ 24	85/ 56/ 30
R22	$\cdot CH_2OCHO$	23	253	121	121	119/ 80/ 54	118/ 75/ 60
R23	$\cdot CH_2COOCH_3$	29	345	128	127	146/128/132	145/129/132
R24	$\cdot CH_2OH$	13	161	93	92	54/ 24/ 0	48/ 30/ 0
R25	$\cdot CH_2PH_3^+$	13	216	109	112	54/ 24/ 0	54/ 24/ 0
R26	$\cdot CH_2SH_2^+$	13	193	103	105	54/ 24/ 0	54/ 24/ 0
R27	$\cdot CH_2SH$	13	170	102	99	62/ 16/ 0	53/ 25/ 0
R28	$\cdot CH_2SOOCH_3$	31	354	139	130	209/ 42/214	193/ 40/232
R29	$\cdot CH_2SOCH_3$	25	308	123	125	136/ 14/150	126/ 12/162
R30	$\cdot CH_2C{\equiv}CH$	15	207	123	121	69/ 28/ 8	67/ 30/ 8

(a) Number of correlated electrons. (b) Number of contractions in aVTZ basis sets.

The vertical ionization potential (IP) is defined as the energy difference between the cation and neutral molecule with the same geometry. The molecular electron affinity (EA) is defined as the energy difference between the molecule and the molecule with one more charge but the same geometry. 30 different molecules are chosen for the IP and EA calculations. The structures of the 30 molecules are given in Table 4.2. These are molecules with different types of structures, i.e., linear ones, cyclic ones, aromatic molecules, acids, and others.

Table 4.2: Structures of 30 test molecules.

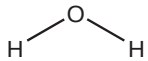				
M01 water	M02 formaldehyde	M03 methane	M04 hydrazine	M05 methylamine
		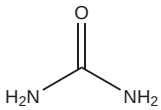	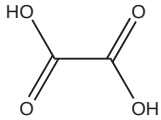	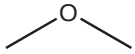
M06 oxirane	M07 ethane	M08 urea	M09 oxalic acid	M10 dimethylether
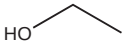				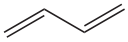
M11 ethanol	M12 furan	M13 imidazole	M14 thiophene	M15 butadiene
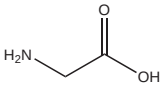	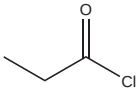	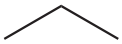	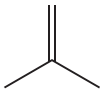	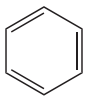
M16 glycine	M17 propionyl chloride	M18 propane	M19 isobutene	M20 benzene
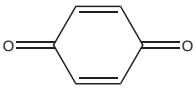	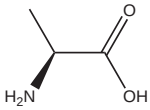	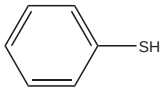		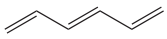
M21 benzoquinone	M22 alanine	M23 thiophenol	M24 butane	M25 hexatriene
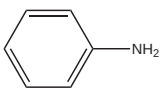	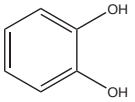			
M26 aniline	M27 catechol	M28 pentane	M29 cyclohexane	M30 hexane

More information about the 30 cations and 30 anions corresponding to 30 molecules

in the above table is given in Table 4.3 and Table 4.4, respectively. In Table 4.3, symbols (from M01 to M30), formulas, the numbers of correlated electrons (denoted as N_{electron}), the numbers of contractions in the cc-pV(T+d)Z basis (denoted as VTZ+d) sets, average domain sizes, and numbers of strong/close/weak pairs are given. For cations, the ab-localization always provides better localization, which is shown in Table 4.3.

Table 4.3: Information of 30 cations corresponding to 30 test molecules.

				average domain size		number of pairs strong/close/weak+distant	
	Formula	$N_{\mathrm{e}}^{(a)}$	$N_{\mathrm{b}}^{(b)}$	sd-	ab-	sd-	ab-
M01	H_2O^+	7	58	40	42	21/ 0/ 0	21/ 0/ 0
M02	CH_2O^+	11	88	60	62	47/ 8/ 0	47/ 8/ 0
M03	$CH_4{}^+$	7	86	60	56	21/ 0/ 0	21/ 0/ 0
M04	$N_2H_4{}^+$	13	116	66	64	62/ 16/ 0	53/ 25/ 0
M05	CH_5N^+	13	130	66	66	54/ 24/ 0	48/ 30/ 0
M06	$C_2H_4O^+$	17	146	84	81	104/ 32/ 0	95/ 41/ 0
M07	$C_2H_6{}^+$	13	144	84	72	62/ 16/ 0	53/ 25/ 0
M08	$CH_4ON_2{}^+$	23	176	98	88	149/ 72/ 32	137/ 84/ 32
M09	$C_2H_2O_4{}^+$	33	208	102	89	236/144/148	203/165/160
M10	$C_2H_6O^+$	19	174	75	75	87/ 48/ 36	87/ 48/ 36
M11	$C_2H_6O^+$	19	174	78	75	97/ 50/ 24	85/ 56/ 30
M12	$C_4H_4O^+$	25	206	98	100	162/ 98/ 40	168/ 92/ 40
M13	$C_3H_4N_2{}^+$	25	206	98	99	168/100/ 32	174/ 94/ 32
M14	$C_4H_4S^+$	25	215	105	105	174/ 48/ 78	174/ 48/ 78
M15	$C_4H_6{}^+$	21	204	93	89	114/ 48/ 48	106/ 56/ 48
M16	$C_2H_5O_2N^+$	29	220	85	81	154/138/114	148/134/124
M17	$C_3H_5OCl^+$	29	229	92	85	160/ 94/152	146/ 98/162
M18	$C_3H_8{}^+$	19	202	95	84	135/ 32/ 4	99/ 56/ 16
M19	$C_4H_8{}^+$	23	232	86	81	105/ 64/ 84	93/ 76/ 84
M20	$C_6H_6{}^+$	29	264	110	104	190/120/ 96	190/120/ 96
M21	$C_6H_4O_2{}^+$	39	296	117	113	301/188/252	293/200/248
M22	$C_3H_7O_2N^+$	35	278	97	91	191/176/228	175/170/250
M23	$C_6H_6S^+$	35	303	89	84	281/114/200	263/128/204
M24	$C_4H_{10}{}^+$	25	260	124	114	124/ 96/ 80	106/ 99/ 95
M25	$C_6H_8{}^+$	31	292	90	83	193/ 96/176	176/105/184
M26	$C_6H_7N^+$	35	308	107	99	265/162/168	249/168/178
M27	$C_6H_6O_2{}^+$	41	324	119	110	328/208/284	313/213/294
M28	$C_5H_{12}{}^+$	31	318	118	113	197/120/148	152/132/181
M29	$C_6H_{12}{}^+$	35	348	101	90	375/128/ 92	255/182/158
M30	$C_6H_{14}{}^+$	37	376	106	92	242/156/268	185/168/313

(a) Number of correlated electrons. (b) Number of contractions in VTZ basis sets.

In Table 4.4, symbols (from M01 to M30), formulas, the numbers of correlated electrons (denoted as N_{electron}), the numbers of contractions in the aug-cc-pV(T+d)Z basis (denoted as aVTZ+d) sets, average domain sizes, and numbers of strong/close/weak pairs are given. For anions, the ab-localization is worse than sd-localization, except for M21, for which the EA is negative. This is because of the instability of the additional charge. The orbital of this additional electron is too high, and could not mix with other orbitals well.

Table 4.4: Information of 30 anions corresponding to 30 test molecules.

				average domain size		number of pairs strong/close/weak+distant	
	Formula	$N_{\text{e}}^{(a)}$	$N_{\text{b}}^{(b)}$	sd-	ab-	sd-	ab-
M01	H_2O^-	9	92	73	76	36/ 0/ 0	36/ 0/ 0
M02	CH_2O^-	13	138	100	105	68/ 10/ 0	68/ 10/ 0
M03	CH_4^-	9	138	100	101	36/ 0/ 0	36/ 0/ 0
M04	$N_2H_4^-$	15	184	113	116	69/ 36/ 0	69/ 36/ 0
M05	CH_5N^-	15	207	118	122	67/ 38/ 0	71/ 34/ 0
M06	$C_2H_4O^-$	19	230	140	144	133/ 38/ 0	134/ 37/ 0
M07	$C_2H_6^-$	15	230	133	133	69/ 36/ 0	69/ 36/ 0
M08	$CH_4ON_2^-$	25	276	137	142	164/102/ 34	178/ 90/ 32
M09	$C_2H_2O_4^-$	35	322	137	131	231/192/172	225/198/172
M10	$C_2H_6O^-$	21	276	139	152	124/ 50/ 36	143/ 42/ 25
M11	$C_2H_6O^-$	21	276	119	131	94/ 80/ 36	107/ 73/ 30
M12	$C_4H_4O^-$	27	322	156	179	187/122/ 42	235/ 97/ 19
M13	$C_3H_4N_2^-$	27	322	161	170	197/114/ 40	225/ 99/ 27
M14	$C_4H_4S^-$	27	331	165	185	201/ 68/ 82	236/ 50/ 65
M15	$C_4H_6^-$	23	322	147	152	119/ 70/ 64	130/ 78/ 45
M16	$C_2H_5O_2N^-$	31	345	141	141	181/144/140	197/134/134
M17	$C_3H_5OCl^-$	31	354	136	136	153/100/212	159/102/204
M18	$C_3H_8^-$	21	322	146	149	102/ 72/ 36	116/ 69/ 25
M19	$C_4H_8^-$	25	368	150	169	124/ 92/ 84	165/ 80/ 55
M20	$C_6H_6^-$	31	414	216	225	261/108/ 96	315/ 99/ 51
M21	$C_6H_4O_2^-$	41	460	174	169	320/216/284	328/225/267
M22	$C_3H_7O_2N^-$	37	437	146	148	210/184/272	232/184/250
M23	$C_6H_6S^-$	37	469	190	198	282/118/266	309/108/249
M24	$C_4H_{10}^-$	27	414	153	156	133/110/108	148/118/ 85
M25	$C_6H_8^-$	33	460	164	185	196/120/212	242/126/160
M26	$C_6H_7N^-$	37	483	188	216	284/184/198	360/167/139
M27	$C_6H_6O_2^-$	43	506	187	200	347/230/326	397/235/271
M28	$C_5H_{12}^-$	33	506	158	160	164/148/216	183/152/193
M29	$C_6H_{12}^-$	37	552	175	185	198/216/252	270/213/183
M30	$C_6H_{14}^-$	39	598	162	185	195/186/360	265/190/286

(a) Number of correlated electrons. (b) Number of contractions in aVTZ basis sets.

Similarly as for RSEs, IPs and EAs are obtained with the HF, RMP2, UCCSD, UCCSD(T), sd-LRMP2, ab-LRMP2, sd-LUCCSD, ab-LUCCSD, sd-LUCCSD(T), and ab-LUCCSD(T) methods. In all the IP calculations the cc-pV(T+d)Z basis set is used. In all the EA calculations the aug-cc-pV(T+d)Z basis set is employed. In LRMP2 calculations, the default option is 'domsel=0.985', 'cpldel=0'. Option 'domsel=0.990', 'cpldel=0' and option 'domsel=0.985', 'cpldel=1' are tested as well. In the LUCCSD and LUCCSD(T) calculations, the default options, option 'nomp2=1', option 'keepcls=1', and option 'igskip=1' are tested. To discuss the local errors, LRMP2 results are compared with RMP2, LUCCSD results are compared with UCCSD, and LUCCSD(T) results are compared with UCCSD(T). To discuss the error of methods, RMP2, LRMP2, UCCSD, and LUCCSD results are compared with UCCSD(T) results.

Ten larger molecules are also employed to test the accuracy of the LRMP2 methods. The structure of these molecules are shown in Table 4.5 and more information is given in Table 4.6. The geometries of these molecules are provided by Thomas Adler [125, 126]. The numbers of atoms are from 37 (glutathione) to 78 (borrelidin), the numbers of correlated electrons range from 113 (glutathione and androstenedione) to 225 (glutathione disulfide), and the numbers of contractions in cc-pV(T+d)Z basis sets are from 847 (glutathione) to 1666 (glutathione disulfide). These 10 molecules are quite large, therefore the UCCSD(T) calculations under vtz basis sets are far away from possible. Although the LUCCSD(T) calculations are possible, they can not be used to investigate the accuracy. IPs of the 10 molecules are obtained with the RMP2 and LRMP2 methods. From these calculations it can be seen how the local errors increase when the molecular size increases.

The information of localization for 10 larger molecules is also shown in Table 4.6. The ab-localization provides better domains and less pairs. The average sizes of domains range from 98 to 110. In Table 4.3, the average domain sizes of smaller molecules range from 40 to 124. As the molecules in Table 4.6 are much larger than the ones in Table 4.3, it can be seen that the domain sizes are independent of the molecular size. In Table 4.6, the number of weak and distant pairs are added together, since the treatments of them are same in LRMP2, LUCCSD and LUCCSD(T). Comparing L01 with L08, the number of correlated electrons increases from 113 to 225, which is nearly an increase by a factor of two. The number of strong pairs increases from 652 to 1324, which is also nearly an increase by a factor of two. Therefore, the scaling of the number of pairs is shown to scale linearly.

Except for the 10 larger molecules, the geometries of all molecules involved in

Table 4.5: Structures of 10 larger molecules.

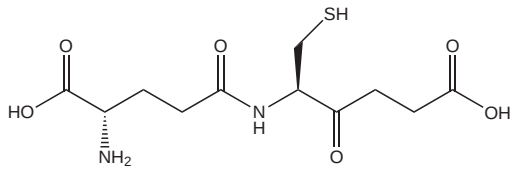

L01
glutathione

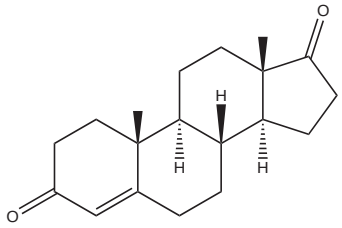

L02
androstenedione

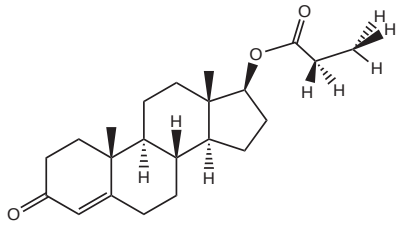

L03
testosterone

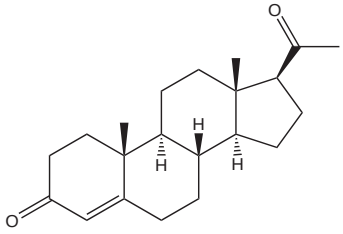

L04
progesterone

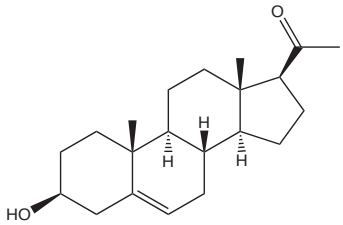

L05
pregnenolone

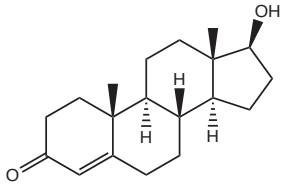

L06
testosterone propionate

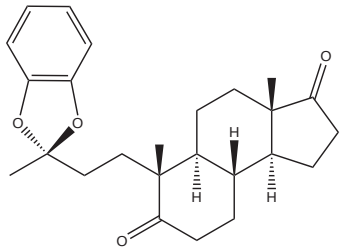

L07
androstenedione precursor

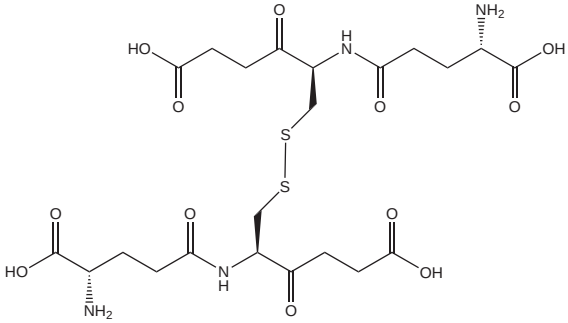

L08
glutathione disulfide

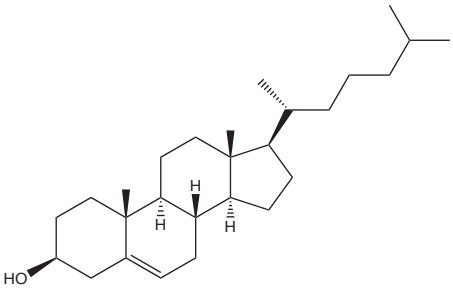

L09
cholesterol

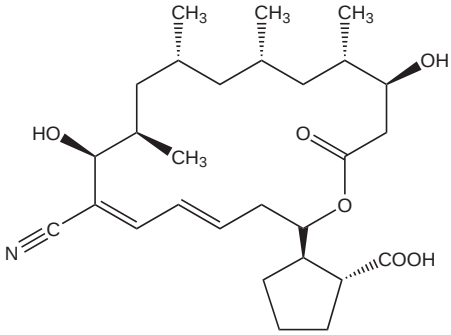

L10
borrelidin

Table 4.6: More information of cations corresponding to 10 larger molecules.

				average domain size		number of pairs strong/close/weak+distant	
	Formula	$N_e^{(a)}$	$N_b^{(b)}$	sd-	ab-	sd-	ab-
L01	$C_{10}H_{17}O_6N_3S^+$	113	847	98	98	652/ 688/4376	646/ 680/4384
L02	$C_{19}H_{26}O_2{}^+$	113	994	105	100	622/ 846/4648	597/ 830/4677
L03	$C_{19}H_{28}O_2{}^+$	115	1022	104	99	615/ 862/4818	590/ 846/4849
L04	$C_{21}H_{30}O_2{}^+$	125	1110	106	101	688/ 934/5604	663/ 918/5629
L05	$C_{21}H_{32}O_2{}^+$	127	1138	105	100	687/ 950/5548	664/ 931/5590
L06	$C_{22}H_{32}O_3{}^+$	137	1198	104	99	615/ 862/4818	590/ 846/4849
L07	$C_{25}H_{32}O_4{}^+$	155	1318	110	107	961/1132/7970	945/1124/7996
L08	$C_{20}H_{32}O_{12}N_6S_2{}^+$	225	1666	103	101	1324/1376/11790	1312/1360/11786
L09	$C_{27}H_{46}O^+$	159	1484	104	100	827/1126/8298	804/1107/8332
L10	$C_{28}H_{43}O_6N^+$	195	1652	104	101	1053/1256/13050	1037/1250/13052

(a) Number of correlated electrons. (b) Number of contractions in aVTZ basis sets.

calculations of RSEs, IPs, and EAs are optimized using density function theory with a B3LYP functional and cc-pV(T+d)Z basis set. The optimizations are done with program `Molpro` in this work. All optimized geometries are given in Appendix A.

Employing the systems discussed, a systematical study of the accuracy of open-shell local methods is performed. All the energies of radicals, molecules, cations, anions and all the RSEs, IPs, EAs are calculated and given in Appendix B. In this chapter, only the statistical results will be listed.

4.2 Accuracy of LRMP2

In Table 4.7, Table 4.9, and Table 4.11, the RSEs, IPs, and EAs obtained with RMP2, sd-LRMP2 and ab-LRMP2 methods with 'domsel=0.985' and 'cpldel=1' are given. More results are given in Appendix B. In Table 4.8, Table 4.10, and Table 4.12, the statistics of local errors for sd-LRMP2 and ab-LRMP2 with respect to RMP2 are listed and compared for different options. In column 'default', 'domsel=0.985' and 'cpldel=0'. In column 'domsel', 'domsel=0.990' and 'cpldel=0'. In column 'cpldel', 'domsel=0.985' and 'cpldel=1'. The mean absolute error (MAE), root mean square error (RMSE), and maximum error (MaxE) are shown. The RMSE is defined as the root of the mean square error (MSE), which is defined as

Table 4.7: RSEs (in kcal/mol) obtained with RMP2, sd-LRMP2 and ab-LRMP2 methods. The deviations from the canonical values are given in parenthesis. Parameters are set as 'domsel=0.985' and 'cpldel=1'.

	RMP2	sd-LRMP2	ab-LRMP2
R01	1.87	1.35 (-0.51)	1.83 (-0.03)
R02	-2.13	-2.61 (-0.48)	-2.36 (-0.23)
R03	-1.08	-1.23 (-0.15)	-1.10 (-0.02)
R04	-1.36	-1.45 (-0.08)	-1.31 (0.06)
R05	-19.38	-19.74 (-0.36)	-19.65 (-0.26)
R06	-9.09	-9.30 (-0.21)	-9.21 (-0.12)
R07	-7.84	-8.00 (-0.17)	-7.92 (-0.08)
R08	-5.71	-6.07 (-0.36)	-5.83 (-0.13)
R09	-5.68	-6.01 (-0.33)	-5.77 (-0.09)
R10	-5.92	-6.27 (-0.35)	-6.03 (-0.11)
R11	-5.77	-6.15 (-0.37)	-5.91 (-0.13)
R12	-5.56	-5.87 (-0.31)	-5.64 (-0.08)
R13	-3.41	-3.54 (-0.13)	-3.31 (0.10)
R14	-11.87	-12.18 (-0.31)	-11.94 (-0.07)
R15	4.79	4.81 (0.03)	4.91 (0.12)
R16	-12.27	-12.65 (-0.38)	-12.74 (-0.47)
R17	-10.51	-11.08 (-0.57)	-10.93 (-0.42)
R18	-12.11	-11.61 (0.50)	-11.87 (0.23)
R19	-3.16	-3.46 (-0.30)	-3.19 (-0.03)
R20	-3.32	-3.30 (0.02)	-3.28 (0.04)
R21	-8.28	-8.16 (0.11)	-8.05 (0.23)
R22	-3.99	-4.04 (-0.05)	-3.98 (0.01)
R23	-4.43	-4.44 (-0.01)	-4.39 (0.05)
R24	-8.51	-8.46 (0.05)	-8.41 (0.11)
R25	1.51	1.36 (-0.15)	1.36 (-0.16)
R26	3.25	3.10 (-0.15)	3.10 (-0.15)
R27	-8.88	-9.45 (-0.57)	-9.19 (-0.31)
R28	1.19	0.74 (-0.45)	1.14 (-0.06)
R29	-1.12	-1.16 (-0.05)	-1.24 (-0.12)
R30	-12.33	-12.27 (0.06)	-12.20 (0.12)

Table 4.8: MAE, RMSE, and MaxE of RSEs (in kcal/mol) obtained with sd-LRMP2 and ab-LRMP2 with respect to the ones obtained with RMP2.

	sd-LRMP2			ab-LRMP2		
	default	domsel	cpldel	default	domsel	cpldel
MAE	0.26	0.34	0.25	0.17	0.26	0.14
RMSE	0.31	0.39	0.31	0.24	0.34	0.18
MaxE	-0.57	-0.76	-0.57	0.68	-0.75	-0.47

Table 4.9: IPs (in eV) obtained with RMP2, sd-LRMP2 and ab-LRMP2 methods. The deviations from the canonical values are given in parenthesis. Parameters are set as 'domsel=0.985' and 'cpldel=1'.

	RMP2	sd-LRMP2	ab-LRMP2
M01	12.645	12.626 (-0.020)	12.626 (-0.020)
M02	11.232	11.232 (0.000)	11.230 (-0.002)
M03	14.339	14.325 (-0.013)	14.331 (-0.008)
M04	8.763	8.727 (-0.036)	8.743 (-0.019)
M05	9.790	9.763 (-0.027)	9.764 (-0.027)
M06	11.745	11.716 (-0.029)	11.726 (-0.018)
M07	12.596	12.720 (0.124)	12.612 (0.016)
M08	10.553	10.484 (-0.069)	10.509 (-0.044)
M09	10.749	10.697 (-0.052)	10.725 (-0.024)
M10	10.414	10.421 (0.007)	10.414 (0.000)
M11	11.089	11.040 (-0.049)	11.050 (-0.039)
M12	9.023	9.026 (0.003)	9.021 (-0.003)
M13	9.183	9.190 (0.007)	9.178 (-0.006)
M14	9.079	9.075 (-0.004)	9.074 (-0.005)
M15	9.054	9.035 (-0.018)	9.040 (-0.013)
M16	10.204	10.157 (-0.046)	10.167 (-0.036)
M17	11.446	11.408 (-0.038)	11.420 (-0.026)
M18	12.164	12.135 (-0.029)	12.146 (-0.018)
M19	9.586	9.568 (-0.018)	9.571 (-0.015)
M20	9.418	9.417 (-0.001)	9.427 (0.008)
M21	11.006	10.985 (-0.021)	10.991 (-0.014)
M22	10.049	9.993 (-0.056)	10.008 (-0.042)
M23	8.348	8.278 (-0.070)	8.301 (-0.047)
M24	11.744	11.733 (-0.011)	11.734 (-0.010)
M25	8.308	8.282 (-0.026)	8.291 (-0.016)
M26	7.976	7.903 (-0.072)	7.927 (-0.049)
M27	8.323	8.267 (-0.056)	8.274 (-0.049)
M28	11.194	11.143 (-0.051)	11.163 (-0.031)
M29	10.397	10.283 (-0.114)	10.318 (-0.079)
M30	10.912	10.854 (-0.058)	10.878 (-0.034)

Table 4.10: MAE, RMSE, and MaxE of IPs (in eV) obtained with sd-LRMP2 and ab-LRMP2 with respect to the ones obtained with RMP2.

	sd-LRMP2			ab-LRMP2		
	default	domsel	cpldel	default	domsel	cpldel
MAE	0.038	0.036	0.038	0.025	0.027	0.024
RMSE	0.049	0.048	0.049	0.032	0.035	0.030
MaxE	-0.131	-0.146	0.124	-0.090	-0.094	-0.079

Table 4.11: EAs (in eV) obtained with RMP2, sd-LRMP2 and ab-LRMP2 methods. The deviations from the canonical values are given in parenthesis. Parameters are set as 'domsel=0.985' and 'cpldel=1'.

	RMP2	sd-LRMP2	ab-LRMP2
M01	-0.642	-0.641 (0.001)	-0.637 (0.004)
M02	-0.640	-0.641 (-0.001)	-0.631 (0.009)
M03	-0.713	-0.713 (-0.000)	-0.701 (0.012)
M04	-0.690	-0.690 (-0.000)	-0.654 (0.037)
M05	-0.647	-0.648 (-0.000)	-0.636 (0.011)
M06	-0.679	-0.680 (-0.001)	-0.652 (0.027)
M07	-0.720	-0.720 (-0.000)	-0.705 (0.015)
M08	-0.329	-0.330 (-0.001)	-0.302 (0.026)
M09	-0.540	-0.538 (0.002)	-0.378 (0.162)
M10	-0.671	-0.672 (-0.001)	-0.629 (0.042)
M11	-0.632	-0.634 (-0.002)	-0.606 (0.026)
M12	-0.644	-0.646 (-0.002)	-0.606 (0.038)
M13	-0.361	-0.363 (-0.002)	-0.335 (0.025)
M14	-0.625	-0.628 (-0.002)	-0.596 (0.029)
M15	-0.683	-0.684 (-0.001)	-0.671 (0.012)
M16	-0.553	-0.553 (-0.000)	-0.530 (0.023)
M17	-0.493	-0.495 (-0.001)	-0.482 (0.012)
M18	-0.700	-0.700 (-0.000)	-0.676 (0.024)
M19	-0.634	-0.635 (-0.001)	-0.584 (0.050)
M20	-0.575	-0.575 (-0.000)	-0.525 (0.050)
M21	1.738	1.741 (0.003)	1.745 (0.007)
M22	-0.559	-0.560 (-0.001)	-0.538 (0.022)
M23	-0.545	-0.565 (-0.020)	-0.543 (0.002)
M24	-0.692	-0.693 (-0.000)	-0.670 (0.022)
M25	-0.636	-0.638 (-0.002)	-0.592 (0.044)
M26	-0.489	-0.489 (-0.001)	-0.437 (0.052)
M27	-0.392	-0.394 (-0.002)	-0.337 (0.054)
M28	-0.668	-0.669 (-0.001)	-0.649 (0.020)
M29	-0.635	-0.635 (-0.000)	-0.570 (0.065)
M30	-0.659	-0.660 (-0.001)	-0.592 (0.066)

Table 4.12: MAE, RMSE, and MaxE of EAs (in eV) obtained with sd-LRMP2 and ab-LRMP2 with respect to the ones obtained with RMP2.

	sd-LRMP2			ab-LRMP2		
	default	domsel	cpldel	default	domsel	cpldel
MAE	0.005	0.001	0.002	0.043	0.061	0.033
RMSE	0.019	0.001	0.004	0.054	0.071	0.044
MaxE	-0.100	0.004	-0.020	0.185	0.127	0.162

the summation of the square of the errors divided by the number of the samples.

Table 4.8 and Table 4.10 show that the sd-localization errors are larger than the ab-localization errors for RSEs and IPs. In the default case, for radical stabilization energies the mean absolute error (MAE) is 0.26 kcal/mol for sd-LRMP2 compared to 0.17 kcal/mol for ab-LRMP2. For vertical ionization energies the MAE is 0.038 eV for sd-LRMP2 compared to 0.025 eV for ab-LRMP2. However, for molecular electron affinities the local error for sd-LRMP2 is much smaller than ab-LRMP2. The MAE is 0.005 eV for sd-LRMP2 compared to 0.043 eV for ab-LRMP2. Adding an additional electron to the molecules, the influence to the other electrons is rather small. As a result, the localization in neutral molecules and closed shell part of anions for sd-localization are quite similar, and the domains and pair lists are also quite similar. This leads to a nice cancelation of domain errors and pair errors. Therefore, the localization errors for sd-LRMP2 in the calculation of molecular electron affinities are comparatively small. The same behavior is also found for the RMSEs and MaxEs.

In column 'domsel', the parameter 'domsel' changes from 0.985 to 0.990. The accuracy is not improved. In RSE calculations, the MAE increases from 0.26 kcal/mol to 0.34 kcal/mol for sd-LRMP2 and from 0.17 kcal/mol to 0.26 kcal/mol for ab-LRMP2. In IP calculations, the MAE decreases from 0.038 eV to 0.036 eV for sd-LRMP2 and increases from 0.025 eV to 0.027 eV for ab-LRMP2. In EA calculations, the MAE decreases from 0.005 eV to 0.001 eV for sd-LRMP2 and increases from 0.043 eV to 0.061 eV for ab-LRMP2. Therefore, 0.985 is a better choice for parameter 'domsel'. In all the following calculation, 'domsel=0.985' will always be used.

Comparing the column 'default' and 'cpldel', the influence of parameter 'cpldel' can be studied. As discussed before, 'cpldel' affects the PM localization, 'cpldel=1' should lead to better localization, in particular for diffuse basis sets. Changing from 0 to 1, the local error of sd-LRMP2 and ab-LRMP2 are slightly smaller. In RSE calculations, the MAE decreases from 0.26 kcal/mol to 0.25 kcal/mol for sd-LRMP2 and from 0.17 kcal/mol to 0.14 kcal/mol for ab-LRMP2. In IP calculations, the MAE are both 0.038 eV for sd-LRMP2 and decrease from 0.025 eV to 0.024 eV for ab-LRMP2. In EA calculations, the MAE decreases from 0.005 eV to 0.002 eV for sd-LRMP2 and from 0.043 eV to 0.033 eV for ab-LRMP2. Therefore, 1 is a better choice for parameter 'cpldel'. In all the following calculation, 'cpldel=1' will always be the choice.

It is also interesting to see the errors with respect to the results obtained with the UCCSD(T) method which is generally regarded as the golden standard. In Table 4.13, Table 4.14, and Table 4.15, the statistic of local errors for RMP2, sd-LRMP2,

and ab-LRMP2 with respect to UCCSD(T) are listed and compared for different options. In column 'default', 'domsel=0.985' and 'cpldel=0'. In column 'domsel', 'domsel=0.990' and 'cpldel=0'. In column 'cpldel', 'domsel=0.985' and 'cpldel=1'.

Table 4.13: MAE, RMSE, and MaxE of RSE (in kcal/mol) obtained with RMP2, sd-LRMP2 and ab-LRMP2 with respect to the ones obtained with UCCSD(T).

	RMP2	sd-LRMP2			ab-LRMP2		
		default	domsel	cpldel	default	domsel	cpldel
MAE	0.48	0.40	0.36	0.41	0.50	0.43	0.46
RMSE	0.65	0.64	0.59	0.64	0.70	0.66	0.66
MaxE	-2.12	-2.49	-2.49	-2.48	-2.39	-2.87	-2.38

Table 4.14: MAE, RMSE, and MaxE of IP (in eV) obtained with RMP2, sd-LRMP2 and ab-LRMP2 with respect to the ones obtained with UCCSD(T).

	RMP2	sd-LRMP2			ab-LRMP2		
		default	domsel	cpldel	default	domsel	cpldel
MAE	0.175	0.171	0.173	0.170	0.171	0.172	0.170
RMSE	0.237	0.234	0.231	0.232	0.232	0.230	0.231
MaxE	0.602	0.555	0.575	0.564	0.567	0.583	0.576

Table 4.15: MAE, RMSE, and MaxE of EA (in eV) obtained with RMP2, sd-LRMP2 and ab-LRMP2 with respect to the ones obtained with UCCSD(T).

	RMP2	sd-LRMP2			ab-LRMP2		
		default	domsel	cpldel	default	domsel	cpldel
MAE	0.050	0.054	0.050	0.051	0.028	0.036	0.030
RMSE	0.064	0.070	0.064	0.066	0.058	0.060	0.057
MaxE	0.259	0.263	0.260	0.262	0.271	0.265	0.266

The above three tables show the performance of sd-LRMP2 and ab-LRMP2 compared to RMP2. In the calculations of RSEs, the MAE is 0.48 kcal/mol for RMP2 compared to 0.40 kcal/mol for sd-LRMP2 and 0.50 kcal/mol for ab-LRMP2. In the calculations of IPs, the MAE is 0.175 eV for RMP2 compared to 0.171 eV for sd-LRMP2 and 0.171 eV for ab-LRMP2. In the calculations of EAs, the MAE is 0.050 eV for RMP2 compared to 0.054 eV for sd-LRMP2 and 0.028 eV for ab-LRMP2. All the above numbers prove that both sd-LRMP2 and ab-LRMP2 are reliable methods, and fortuitously, they are always even closer to the UCCSD(T)

results because of the error composition. Therefore, it can be concluded that the local errors are small as compared to the error of RMP2 itself.

A study of the local error of sd-LRMP2 and ab-LRMP2 are also done for the discussed 10 larger molecules. The differences between the RMP2 and LRMP2 for larger molecules are listed in Table 4.16.

Table 4.16: IPs of 10 larger molecules for RMP2, sd-LRMP2, and ab-LRMP2 calculations. The deviations from the canonical values are given in parenthesis.

Molecular Name	RHF	RMP2	sd-LRMP2	ab-LRMP2
glutathione	8.525	9.351	9.319 (-0.032)	9.325 (-0.027)
androstenedione	8.191	9.573	9.510 (-0.063)	9.535 (-0.038)
testosterone	8.038	9.440	9.378 (-0.062)	9.408 (-0.032)
progesterone	8.118	9.513	9.450 (-0.063)	9.475 (-0.038)
pregnenolone	7.349	8.870	8.828 (-0.042)	8.851 (-0.019)
testosterone propionate	8.156	9.553	9.490 (-0.063)	9.520 (-0.033)
androstenedione precursor	7.096	7.755	7.710 (-0.045)	7.717 (-0.038)
cholesterol	7.230	8.765	8.723 (-0.042)	8.747 (-0.018)
borrelidin	7.578	8.434	8.416 (-0.018)	8.422 (-0.012)
glutathione disulfide	8.893	8.961	8.934 (-0.027)	8.939 (-0.022)
MAE			0.046	0.028
RMSE			0.048	0.029
MaxE			-0.063	-0.038

The MAEs are 0.046 eV for sd-LRMP2 and 0.028 eV for ab-LRMP2 for 10 larger molecules. The errors for smaller and larger molecules are in the same range. Considering that the size of 10 larger molecules is twice or even three times larger than for the 30 smaller ones, there appears to be no explicit correlation between the molecular size and the local error. Therefore, sd-LRMP2 and ab-LRMP2 are proven to be reliable for both small and larger systems.

4.3 Accuracy of LUCCSD

4.3.1 Default Settings of LUCCSD

For the same systems as discussed in the LRMP2 part, a systematical study of the accuracy of LUCCSD is also performed. In Table 4.17, Table 4.19, and Table

Table 4.17: RSEs (in kcal/mol) obtained with UCCSD, sd-LUCCSD and ab-LUCCSD methods. The deviations from the canonical values are given in parenthesis. Parameters are set as 'domsel=0.985', 'cpldel=1', 'nomp2=0', 'keepcls=0', 'igskip=0'.

	UCCSD	sd-LUCCSD	ab-LUCCSD
R01	1.73	1.79 (0.06)	1.88 (0.15)
R02	-2.59	-2.05 (0.54)	-1.82 (0.77)
R03	-1.19	-0.93 (0.26)	-0.90 (0.29)
R04	-1.60	-1.17 (0.43)	-1.09 (0.51)
R05	-16.23	-15.55 (0.68)	-16.11 (0.12)
R06	-9.21	-8.65 (0.56)	-8.76 (0.44)
R07	-7.35	-6.50 (0.85)	-6.62 (0.72)
R08	-5.93	-5.62 (0.31)	-5.16 (0.76)
R09	-5.90	-5.52 (0.37)	-5.28 (0.62)
R10	-6.01	-5.71 (0.31)	-5.23 (0.78)
R11	-5.91	-5.63 (0.28)	-5.59 (0.32)
R12	-5.45	-4.86 (0.59)	-4.87 (0.58)
R13	-3.04	-2.86 (0.18)	-2.42 (0.62)
R14	-11.29	-10.68 (0.61)	-10.85 (0.44)
R15	4.87	5.31 (0.44)	5.20 (0.33)
R16	-11.79	-11.08 (0.71)	-11.14 (0.65)
R17	-10.03	-9.27 (0.76)	-9.40 (0.63)
R18	-11.87	-11.63 (0.24)	-11.44 (0.42)
R19	-2.64	-2.01 (0.63)	-1.29 (1.35)
R20	-3.31	-2.85 (0.45)	-2.82 (0.48)
R21	-8.13	-7.91 (0.23)	-8.15 (-0.01)
R22	-3.79	-3.38 (0.41)	-3.36 (0.43)
R23	-4.16	-3.75 (0.41)	-3.69 (0.46)
R24	-8.14	-7.52 (0.62)	-7.37 (0.76)
R25	0.89	0.95 (0.07)	0.95 (0.06)
R26	2.92	3.13 (0.21)	3.10 (0.18)
R27	-8.63	-8.34 (0.29)	-8.76 (-0.13)
R28	0.47	0.82 (0.36)	0.78 (0.32)
R29	-2.34	-1.38 (0.96)	-1.16 (1.18)
R30	-11.79	-10.53 (1.26)	-10.91 (0.88)

Table 4.18: MAE, RMSE, and MaxE of RSE (in kcal/mol) obtained with sd-LUCCSD and ab-LUCCSD with respect to the ones obtained with UCCSD.

	sd-LUCCSD				ab-LUCCSD			
	default	nomp2	keepcls	igskip	default	nomp2	keepcls	igskip
MAE	0.47	0.22	0.63	0.49	0.51	0.17	0.55	0.51
RMSE	0.54	0.26	0.71	0.55	0.60	0.22	0.62	0.57
MaxE	1.26	-0.49	1.68	1.23	1.35	-0.67	1.24	1.06

Table 4.19: IPs (in eV) obtained with UCCSD, sd-LUCCSD and ab-LUCCSD methods. The deviations from the canonical values are given in parenthesis. Parameters are set as 'domsel=0.985', 'cpldel=1', 'nomp2=0', 'keepcls=0', 'igskip=0'.

	UCCSD	sd-UCCSD	ab-UCCSD
M01	12.398	12.383 (-0.014)	12.383 (-0.014)
M02	10.746	10.783 (0.036)	10.775 (0.029)
M03	14.314	14.317 (0.003)	14.310 (-0.004)
M04	8.938	8.939 (0.001)	8.936 (-0.002)
M05	9.574	9.606 (0.032)	9.615 (0.041)
M06	11.693	11.704 (0.010)	11.680 (-0.014)
M07	12.757	12.881 (0.124)	12.782 (0.025)
M08	10.054	10.044 (-0.009)	10.072 (0.018)
M09	10.417	11.359 (-0.058)	11.345 (-0.072)
M10	10.022	10.096 (0.074)	10.082 (0.060)
M11	10.654	10.688 (0.034)	10.680 (0.026)
M12	8.887	8.907 (0.020)	8.894 (0.007)
M13	8.850	8.868 (0.018)	8.862 (0.013)
M14	8.921	8.927 (0.006)	8.925 (0.004)
M15	9.061	9.067 (0.006)	9.043 (-0.018)
M16	9.974	10.031 (0.057)	10.047 (0.073)
M17	10.817	10.835 (0.018)	10.864 (0.047)
M18	12.174	12.250 (0.075)	12.229 (0.054)
M19	9.360	9.436 (0.076)	9.426 (0.066)
M20	9.270	9.280 (0.009)	9.265 (-0.005)
M21	11.083	11.090 (0.007)	11.085 (0.002)
M22	9.801	9.850 (0.049)	9.863 (0.062)
M23	8.337	8.345 (0.008)	8.325 (-0.011)
M24	11.587	11.690 (0.102)	11.628 (0.041)
M25	8.254	8.294 (0.040)	8.244 (-0.010)
M26	7.879	7.864 (-0.014)	7.844 (-0.035)
M27	8.216	8.190 (-0.026)	8.161 (-0.055)
M28	11.282	11.365 (0.083)	11.292 (0.010)
M29	10.823	10.964 (0.141)	10.816 (-0.007)
M30	11.038	11.146 (0.107)	11.057 (0.019)

Table 4.20: MAE, RMSE, and MaxE of IP (in eV) obtained with sd-LUCCSD and ab-LUCCSD with respect to the ones obtained with UCCSD.

	sd-LUCCSD				ab-LUCCSD			
	default	nomp2	keepcls	igskip	default	nomp2	keepcls	igskip
MAE	0.042	0.034	0.049	0.047	0.028	0.019	0.025	0.033
RMSE	0.057	0.045	0.065	0.062	0.036	0.025	0.034	0.043
MaxE	0.141	-0.118	-0.150	0.142	0.073	-0.085	0.075	0.098

Table 4.21: EAs (in eV) obtained with UCCSD, sd-LUCCSD and ab-LUCCSD methods. The deviations from the canonical values are given in parenthesis. Parameters are set as 'domsel=0.985', 'cpldel=1', 'nomp2=0', 'keepcls=0', 'igskip=0'.

	UCCSD	sd-LUCCSD	ab-LUCCSD
M01	-0.632	-0.632 (-0.000)	-0.628 (0.004)
M02	-0.625	-0.627 (-0.001)	-0.618 (0.007)
M03	-0.700	-0.700 (-0.000)	-0.690 (0.010)
M04	-0.683	-0.677 (0.006)	-0.662 (0.021)
M05	-0.633	-0.636 (-0.004)	-0.632 (0.001)
M06	-0.667	-0.668 (-0.000)	-0.628 (0.039)
M07	-0.705	-0.703 (0.002)	-0.715 (-0.010)
M08	-0.308	-0.311 (-0.004)	-0.294 (0.014)
M09	-0.530	-0.527 (0.003)	-0.410 (0.119)
M10	-0.657	-0.654 (0.002)	-0.622 (0.034)
M11	-0.613	-0.629 (-0.016)	-0.609 (0.004)
M12	-0.636	-0.643 (-0.007)	-0.637 (-0.001)
M13	-0.365	-0.368 (-0.003)	-0.360 (0.005)
M14	-0.612	-0.620 (-0.008)	-0.530 (-0.018)
M15	-0.684	-0.683 (0.001)	-0.702 (-0.018)
M16	-0.532	-0.533 (-0.001)	-0.536 (-0.004)
M17	-0.470	-0.477 (-0.007)	-0.472 (-0.001)
M18	-0.683	-0.677 (0.005)	-0.685 (-0.002)
M19	-0.616	-0.620 (-0.004)	-0.594 (0.022)
M20	-0.594	-0.589 (0.005)	-0.612 (-0.018)
M21	1.414	1.418 (0.004)	1.451 (0.037)
M22	-0.534	-0.545 (-0.011)	-0.546 (-0.012)
M23	-0.522	-0.509 (0.014)	-0.527 (-0.004)
M24	-0.675	-0.673 (0.002)	-0.697 (-0.023)
M25	-0.638	-0.641 (-0.003)	-0.649 (-0.011)
M26	-0.484	-0.487 (-0.003)	-0.518 (-0.035)
M27	-0.383	-0.397 (-0.014)	-0.391 (-0.007)
M28	-0.650	-0.650 (-0.000)	-0.667 (-0.017)
M29	-0.622	-0.614 (0.008)	-0.656 (-0.034)
M30	-0.640	-0.641 (-0.002)	-0.652 (-0.012)

Table 4.22: MAE, RMSE, and MaxE of EA (in eV) obtained with sd-LUCCSD and ab-LUCCSD with respect to the ones obtained with UCCSD.

	sd-LUCCSD				ab-LUCCSD			
	default	nomp2	keepcls	igskip	default	nomp2	keepcls	igskip
MAE	0.005	0.002	0.005	0.005	0.018	0.028	0.018	0.019
RMSE	0.006	0.004	0.006	0.007	0.028	0.040	0.030	0.029
MaxE	-0.016	-0.020	-0.014	-0.017	0.119	0.168	0.130	0.117

4.21, the RSEs, IPs, and EAs obtained with UCCSD, sd-LUCCSD and ab-LUCCSD methods with 'domsel=0.985', 'cpldel=1', 'nomp2=0', 'keepcls=0', and 'igskip=0' are given. More results are given in Appendix B.

In Tables 4.18, 4.20, and 4.22, the statistics of the local errors for sd-LUCCSD and ab-LUCCSD with respect to UCCSD are listed and compared for different options. In all cases, the parameter 'domsel' is set to 0.985 and the parameter 'cpldel' is set to 1. In the 'default' column, 'nomp2=0', 'keepcls=0', and 'igskip=0'. Keeping other parameters as for the default case, 'nomp2=1' is set in the 'nomp2' column, 'keepcls=1' is set in the 'keepcls' column, and 'igskip=1' is set in the 'igskip' column.

Table 4.18 shows that the sd-localization errors are smaller than ab-localization errors for RSEs, while Table 4.20 shows that the sd-localization errors are larger than ab-localization errors for IP. In the default case, for RSEs the MAE is 0.47 kcal/mol for sd-LUCCSD compared to 0.51 kcal/mol for ab-LUCCSD. For IPs the MAE is 0.042 eV for sd-LUCCSD compared to 0.028 eV for ab-LUCCSD. In 4.22 it is shown that for EA the local error for sd-LUCCSD is again much smaller than ab-LUCCSD for the same reason as discussed in the LRMP2 part. The MAE is 0.005 eV for sd-LUCCSD compared to 0.018 eV for ab-LUCCSD. A similar behaviors is also found for the root mean square errors (RMSE) and maximum errors (MaxE) for the three properties.

Comparing the column 'default' and 'nomp2', the effect of the pair approximation becomes visible. In RSE calculations, the MAE decreases from 0.47 kcal/mol to 0.22 kcal/mol for sd-LUCCSD and from 0.51 kcal/mol to 0.17 kcal/mol for ab-LUCCSD. In IP calculations, the MAE decreases from 0.042 eV to 0.034 eV for sd-LUCCSD and from 0.028 eV to 0.019 eV for ab-LUCCSD. In EA calculations, the MAE decreases from 0.005 eV to 0.002 eV for sd-LUCCSD but increases from 0.018 eV to 0.028 eV for ab-LUCCSD. The local errors are reduced in most cases, in line with intuition. However, the change of the error is not much. The differences between the above errors are the errors of pair approximation. These results show that the pair approximation is an acceptable approximation. Because setting 'nomp2=1' makes the calculations much more expensive, this option will hardly be used in the later applications.

The effect of setting 'keepcls=1' can be seen by comparing columns 'default' and 'keepcls'. In RSE calculations, the MAE increases from 0.47 kcal/mol to 0.63 kcal/mol for sd-LUCCSD and from 0.51 kcal/mol to 0.55 kcal/mol for ab-LUCCSD. In IP calculations, the MAE increases from 0.042 eV to 0.049 eV for sd-LUCCSD but decreases from 0.028 eV to 0.025 eV for ab-LUCCSD. In EA calculations, the MAE

maintains 0.005 eV for sd-LUCCSD and 0.018 eV for ab-LUCCSD. Therefore the local errors are slightly larger. Setting 'keepcls=1' can remove some errors caused by pair approximation, but the errors due to domain approximation remained. Due to the breaking of error compensation, the local error can be larger with this option. For closed-shell systems, this has been already proven and discussed [125,126]. This option will be useful when the domain error is also reduced, i.e., in the LUCCSD-F12 methods.

The errors of setting 'igskip=1' are shown in the column 'igskip'. In RSE calculations, the MAE increases from 0.47 kcal/mol to 0.49 kcal/mol for sd-LUCCSD and maintains 0.51 kcal/mol for ab-LUCCSD. In IP calculations, the MAE increases from 0.042 eV to 0.047 eV for sd-LUCCSD and from 0.028 eV to 0.033 eV for ab-LUCCSD. In EA calculations, the MAE maintains 0.005 eV for sd-LUCCSD and increases from 0.018 eV to 0.019 eV for ab-LUCCSD. It is shown that the changes of local errors are within statistical uncertainties. All the above results show that the 'igskip=1' approximation is acceptable for the application.

Similarly as in the LRMP2 case, the errors with respect to UCCSD(T) are also studied. In Table 4.23, Table 4.24, and Table 4.25 the statistics of local errors for UCCSD, sd-LUCCSD, and ab-LUCCSD with respect to UCCSD(T) are compared. In the calculations of RSEs, the MAE is 0.46 kcal/mol for UCCSD compared to 0.93 kcal/mol for sd-LUCCSD and 0.96 kcal/mol for ab-LUCCSD. In the calculations of IPs, the MAE is 0.061 eV for UCCSD compared to 0.071 eV for sd-LUCCSD and 0.063 eV for ab-LUCCSD. In the calculations of EAs, the MAE is 0.031 eV for UCCSD compared to 0.033 eV for sd-LUCCSD and 0.035 eV for ab-LUCCSD. With respect to UCCSD(T) the errors of LUCCSD are slightly larger than the errors of UCCSD. However, the differences are not large and the above results prove that both sd-LUCCSD and ab-LUCCSD are still reliable methods.

Table 4.23: MAE, RMSE, and MaxE of RSE (in kcal/mol) obtained with UCCSD, sd-LUCCSD, and ab-LUCCSD with respect to the ones obtained with UCCSD(T).

	UCCSD	sd-LUCCSD			ab-LUCCSD		
		default	nomp2	igskip	default	nomp2	igskip
MAE	0.46	0.93	0.36	0.94	0.96	0.44	0.95
RMSE	0.53	1.04	0.48	1.16	1.06	0.53	1.04
MaxE	1.03	2.25	1.20	2.23	1.88	1.01	1.86

Table 4.24: MAE, RMSE, and MaxE of IP (in eV) obtained with UCCSD, sd-LUCCSD, and ab-LUCCSD with respect to the ones obtained with UCCSD(T).

	UCCSD	sd-LUCCSD			ab-LUCCSD		
		default	nomp2	igskip	default	nomp2	igskip
MAE	0.061	0.071	0.066	0.074	0.063	0.062	0.064
RMSE	0.077	0.099	0.075	0.100	0.074	0.073	0.075
MaxE	0.248	0.282	0.170	0.283	0.176	0.204	0.162

Table 4.25: MAE, RMSE, and MaxE of EA (in eV) obtained with sd-LUCCSD and ab-LUCCSD with respect to the ones obtained with UCCSD(T).

	UCCSD	sd-LUCCSD			ab-LUCCSD		
		default	nomp2	igskip	default	nomp2	igskip
MAE	0.031	0.033	0.031	0.034	0.035	0.018	0.036
RMSE	0.033	0.034	0.033	0.035	0.040	0.030	0.041
MaxE	-0.065	-0.061	-0.064	-0.056	-0.071	0.119	-0.074

4.4 Accuracy of LUCCSD(T)

Before testing the accuracy of LUCCSD(T), it is necessary to analyze how many percent of (T) correction is obtained by the local non-iterative (T) approximation. In Table 4.26, Table 4.27, and Table 4.28 the percentage of the (T) correction obtained with sd-LUCCSD(T) and ab-LUCCSD(T) methods as compared to UCCSD(T) is shown. For radicals and cations, the average percentages are 93% for sd-LUCCSD(T) and 92% for ab-LUCCSD(T). For anions, the average percentages are both 94% for sd-LUCCSD(T) and ab-LUCCSD(T). The absolute (T) correction ranges from -3 kcal/mol to -47 kcal/mol. The errors of the absolute (T) correction energies is about 5 kcal/mol and the error of energies difference is suspected to be in the range of 0.5 - 1.0 kcal/mol. This prediction will be practically checked in the next sections by checking the local errors of LUCCSD(T).

Table 4.26: Average, maximum, and minimum percent of (T) correction in the energies of 30 radicals obtained with sd-LUCCSD(T) and ab-LUCCSD(T) methods with respect to UCCSD(T) method. The 30 radicals are the ones involved in the calculations of RSE.

	sd-LUCCSD(T)	ab-LUCCSD(T)
Average	93%	92%
Maximum	99%	99%
Minimum	78%	76%

Table 4.27: Average, maximum, and minimum percent of (T) correction in the energies of 30 cations obtained with sd-LUCCSD(T) and ab-LUCCSD(T) methods with respect to UCCSD(T) method. The 30 cations are the ones involved in the calculations of IP.

	sd-LUCCSD(T)	ab-LUCCSD(T)
Average	93%	92%
Maximum	97%	97%
Minimum	87%	86%

Table 4.28: Average, maximum, and minimum percent of (T) correction in the energies of 30 anions obtained with sd-LUCCSD(T) and ab-LUCCSD(T) methods with respect to UCCSD(T) method. The 30 anions are the ones involved in the calculations of EA.

	sd-LUCCSD(T)	ab-LUCCSD(T)
Average	94%	94%
Maximum	98%	99%
Minimum	86%	86%

In Table 4.26, it is shown that for some molecules, the percentage of (T) is rather low, i.e., below 85%. The reason for this is that there are larger atoms in these molecules, i.e., P, S, and Cl, which makes the distance criteria in PM localization not fit any more. Alternatively, choosing bond separations for defining pairs by setting 'use_dist=0' in `Molpro` can solve this problem. Table 4.29 shows the great improvement of (T) percentage for these molecules by using bond criteria.

Table 4.29: Percent of (T) correction in the energies of 6 radicals obtained with sd-LUCCSD(T) and ab-LUCCSD(T) methods with respect to UCCSD(T) method. The different between using distant criteria and bond criteria have been compared.

	distant criteria		bond criteria	
	sd-LUCCSD(T)	ab-LUCCSD(T)	sd-LUCCSD(T)	ab-LUCCSD(T)
R02	85%	83%	96%	95%
R25	85%	85%	97%	97%
R26	84%	78%	96%	96%
R27	89%	81%	97%	97%
R28	83%	81%	94%	93%
R29	78%	76%	93%	95%

In Table 4.30, Table 4.32, and Table 4.34, the RSEs, IPs, and EAs obtained with UCCSD(T), sd-LUCCSD(T) and ab-LUCCSD(T) methods with 'domsel=0.985', 'cpldel=1', 'nomp2=0', 'keepcls=0', and 'igskip=0' are given. Table 4.31, Table 4.33, and Table 4.35 show that the local errors of LUCCSD(T) are similar to those of LUCCSD.

Table 4.30: RSEs (in kcal/mol) obtained with UCCSD(T), sd-LUCCSD(T) and ab-LUCCSD(T) methods. The deviations from the canonical values are given in parenthesis. Parameters are set as 'domsel=0.985', 'cpldel=1', 'nomp2=0', 'keepcls=0', 'igskip=0'.

	UCCSD(T)	sd-LUCCSD(T)	ab-LUCCSD(T)
R01	1.60	1.34 (-0.26)	1.80 (0.20)
R02	-2.99	-2.53 (0.46)	-2.05 (0.94)
R03	-1.36	-1.13 (0.23)	-0.91 (0.46)
R04	-1.69	-1.36 (0.33)	-1.16 (0.53)
R05	-17.26	-16.61 (0.65)	-17.20 (0.06)
R06	-9.80	-9.21 (0.60)	-9.30 (0.51)
R07	-8.17	-7.26 (0.92)	-7.45 (0.73)
R08	-6.22	-5.99 (0.24)	-5.45 (0.77)
R09	-6.23	-5.87 (0.36)	-5.60 (0.63)
R10	-6.36	-6.11 (0.25)	-5.56 (0.80)
R11	-6.23	-6.04 (0.19)	-6.01 (0.23)
R12	-5.93	-5.53 (0.41)	-5.48 (0.45)
R13	-3.44	-3.23 (0.21)	-2.68 (0.76)
R14	-11.88	-11.17 (0.71)	-11.31 (0.57)
R15	4.81	5.27 (0.47)	5.18 (0.37)
R16	-12.47	-11.79 (0.67)	-11.67 (0.80)
R17	-10.77	-10.03 (0.74)	-10.10 (0.67)
R18	-12.59	-12.59 (-0.01)	-12.09 (0.50)
R19	-3.15	-2.47 (0.68)	-1.59 (1.56)
R20	-3.66	-2.62 (1.04)	-2.78 (0.88)
R21	-8.71	-8.58 (0.14)	-8.70 (0.01)
R22	-4.31	-3.81 (0.50)	-3.63 (0.69)
R23	-4.71	-4.02 (0.69)	-3.91 (0.80)
R24	-8.67	-7.99 (0.68)	-7.76 (0.92)
R25	0.94	0.59 (-0.36)	0.58 (-0.37)
R26	2.86	2.69 (-0.17)	2.66 (-0.21)
R27	-9.26	-9.82 (-0.56)	-9.45 (-0.19)
R28	0.14	-0.04 (-0.18)	0.60 (0.45)
R29	-2.80	-1.92 (0.88)	-1.04 (1.76)
R30	-12.79	-11.44 (1.35)	-11.80 (0.98)

Table 4.31: MAE, RMSE, and MaxE of RSE (in kcal/mol) obtained with sd-LUCCSD(T) and ab-LUCCSD(T) with respect to the ones obtained with UCCSD(T).

	sd-LUCCSD(T)				ab-LUCCSD(T)			
	default	nomp2	keepcls	igskip	default	nomp2	keepcls	igskip
MAE	0.50	0.25	0.68	0.50	0.63	0.20	0.66	0.62
RMSE	0.58	0.30	0.78	0.59	0.73	0.26	0.75	0.69
MaxE	1.35	-0.57	1.84	1.29	1.76	-0.84	1.77	1.57

Table 4.32: IPs (in eV) obtained with UCCSD(T), sd-LUCCSD(T) and ab-LUCCSD(T) methods. The deviations from the canonical values are given in parenthesis. Parameters are set as 'domsel=0.985', 'cpldel=1', 'nomp2=0', 'keepcls=0', 'igskip=0'.

	UCCSD(T)	sd-LUCCSD(T)	ab-LUCCSD(T)
M01	12.475	12.454 (-0.021)	12.454 (-0.021)
M02	10.803	10.841 (0.038)	10.833 (0.030)
M03	14.348	14.354 (0.005)	14.347 (-0.001)
M04	8.902	8.900 (-0.001)	8.898 (-0.003)
M05	9.634	9.663 (0.030)	9.674 (0.041)
M06	11.725	11.729 (0.004)	11.707 (-0.018)
M07	12.698	12.826 (0.127)	12.726 (0.028)
M08	10.039	10.030 (-0.009)	10.056 (0.017)
M09	11.169	11.135 (-0.033)	11.120 (-0.049)
M10	10.065	10.151 (0.086)	10.137 (0.071)
M11	10.691	10.721 (0.030)	10.714 (0.023)
M12	8.962	8.980 (0.018)	8.967 (0.005)
M13	8.934	8.946 (0.013)	8.942 (0.008)
M14	8.987	9.022 (0.034)	9.019 (0.032)
M15	9.149	9.155 (0.006)	9.130 (-0.019)
M16	9.997	10.065 (0.068)	10.087 (0.090)
M17	10.844	10.862 (0.015)	11.864 (0.020)
M18	12.102	12.176 (0.074)	12.164 (0.062)
M19	9.491	9.582 (0.091)	9.571 (0.080)
M20	9.351	9.354 (0.002)	9.339 (-0.012)
M21	11.053	11.088 (0.034)	11.078 (0.025)
M22	9.825	9.876 (0.051)	9.900 (0.075)
M23	8.333	8.334 (0.000)	8.325 (-0.008)
M24	11.565	11.684 (0.120)	11.630 (0.066)
M25	8.324	8.371 (0.047)	8.324 (0.001)
M26	7.902	7.878 (-0.025)	7.867 (-0.036)
M27	8.225	8.183 (-0.039)	8.184 (-0.039)
M28	11.221	11.327 (0.106)	11.268 (0.047)
M29	10.682	10.800 (0.117)	10.684 (0.001)
M30	10.949	11.097 (0.148)	11.025 (0.075)

Table 4.33: MAE, RMSE, and MaxE of IP (in eV) obtained with sd-LUCCSD(T) and ab-LUCCSD(T) with respect to the ones obtained with UCCSD(T).

	sd-LUCCSD(T)				ab-LUCCSD(T)			
	default	nomp2	keepcls	igskip	default	nomp2	keepcls	igskip
MAE	0.047	0.039	0.054	0.053	0.033	0.022	0.031	0.040
RMSE	0.063	0.051	0.072	0.068	0.042	0.030	0.040	0.049
MaxE	0.148	-0.132	0.171	0.149	0.090	-0.091	0.083	0.091

Table 4.34: EAs (in eV) obtained with UCCSD(T), sd-LUCCSD(T) and ab-LUCCSD(T) methods. The deviations from the canonical values are given in parenthesis. Parameters are set as 'domsel=0.985', 'cpldel=1', 'nomp2=0', 'keepcls=0', 'igskip=0'.

	UCCSD(T)	sd-LUCCSD(T)	ab-LUCCSD(T)
M01	-0.609	-0.609 (-0.000)	-0.603 (0.006)
M02	-0.615	-0.617 (-0.001)	-0.605 (0.010)
M03	-0.683	-0.682 (-0.000)	-0.669 (0.013)
M04	-0.651	-0.646 (0.005)	-0.629 (0.022)
M05	-0.609	-0.615 (-0.006)	-0.607 (0.002)
M06	-0.648	-0.649 (-0.001)	-0.600 (0.048)
M07	-0.682	-0.680 (0.003)	-0.690 (-0.008)
M08	-0.280	-0.288 (-0.007)	-0.270 (0.011)
M09	-0.481	-0.480 (0.001)	-0.364 (0.118)
M10	-0.633	-0.632 (0.001)	-0.591 (0.041)
M11	-0.588	-0.609 (-0.021)	-0.583 (0.005)
M12	-0.607	-0.618 (-0.010)	-0.596 (0.011)
M13	-0.339	-0.345 (-0.005)	-0.324 (0.016)
M14	-0.578	-0.591 (-0.012)	-0.588 (-0.010)
M15	-0.653	-0.654 (-0.000)	-0.669 (-0.016)
M16	-0.497	-0.502 (-0.005)	-0.505 (-0.008)
M17	-0.442	-0.454 (-0.012)	-0.445 (-0.003)
M18	-0.655	-0.650 (0.005)	-0.652 (0.003)
M19	-0.583	-0.590 (-0.007)	-0.548 (0.035)
M20	-0.552	-0.547 (0.004)	-0.562 (-0.010)
M21	1.479	1.475 (-0.004)	1.511 (0.032)
M22	-0.498	-0.515 (-0.017)	-0.514 (-0.016)
M23	-0.478	-0.528 (-0.049)	-0.543 (-0.064)
M24	-0.645	-0.645 (0.001)	-0.668 (-0.022)
M25	-0.601	-0.608 (-0.008)	-0.607 (-0.006)
M26	-0.447	-0.457 (-0.009)	-0.473 (-0.026)
M27	-0.348	-0.370 (-0.022)	-0.347 (0.001)
M28	-0.619	-0.621 (-0.002)	-0.639 (-0.020)
M29	-0.586	-0.579 (0.006)	-0.608 (-0.022)
M30	-0.607	-0.612 (-0.005)	-0.616 (-0.010)

Table 4.35: MAE, RMSE, and MaxE of EA (in eV) obtained with sd-LUCCSD(T) and ab-LUCCSD(T) with respect to the ones obtained with UCCSD(T).

	sd-LUCCSD(T)				ab-LUCCSD(T)			
	default	nomp2	keepcls	igskip	default	nomp2	keepcls	igskip
MAE	0.008	0.003	0.007	0.009	0.021	0.030	0.020	0.021
RMSE	0.012	0.005	0.012	0.013	0.031	0.043	0.032	0.031
MaxE	-0.049	-0.025	-0.053	-0.051	0.118	0.180	0.130	0.116

The reason that the MAE of EAs for sd-LUCCSD(T) is comparatively small has been discussed in the LRMP2 part. In the default case, for the RSEs the MAE is 0.50 kcal/mol for sd-LUCCSD(T) compared to 0.63 kcal/mol for ab-LUCCSD(T). For IPs the MAE is 0.047 eV for sd-LUCCSD(T) compared to 0.033 eV for ab-LUCCSD(T). In 4.35 it is shown that for EAs the local error for sd-LUCCSD(T) is again much smaller than ab-LUCCSD(T) for the same reason as discussed in the LRMP2 part. The MAE is 0.008 eV for sd-LUCCSD(T) compared to 0.021 eV for ab-LUCCSD. A similar behavior is also found for the root mean square errors (RMSE) and maximum errors (MaxE). All the MAEs are about 1 kcal/mol (equal to 0.043 eV). The maximum errors are about 1-4 kcal/mol. Therefore, the conclusion is that the newly developed open-shell LUCCSD(T) is the method with a mean error of about 1 kcal/mol and maximum error of about 1-4 kcal/mol.

For different options, similar conclusions can be obtained for LUCCSD(T) as the ones for LUCCSD. For 'nomp2=1', the errors are smaller but still similar compared to default case. Therefore, it is sufficient to only include strong pairs for LUCCSD(T) calculations (for triples there are close pairs included as discussed in the theory part). For 'keepcls=1', the errors are not smaller and sometimes even bigger. This indicates that 'keepcls=1' is not really needed for current applications but maybe useful for later LUCCSD(T)-F12 applications. For 'igskip=1', the errors are comparable to the default case. This indicates that the highly efficient implementation 'igskip=1' is also a acceptable approximation.

5 Applications

5.1 Formation Energy of Copper-Oxygen Complex

The stability of complexes can be studied by comparing the formation energies of them. The formation energy of copper-oxygen complex with ligands L is defined as

$$\mathtt{(CuL)}^{+} + \mathtt{O}_2 \rightarrow \mathtt{(CuLO_2)}^{+}. \tag{5.1}$$

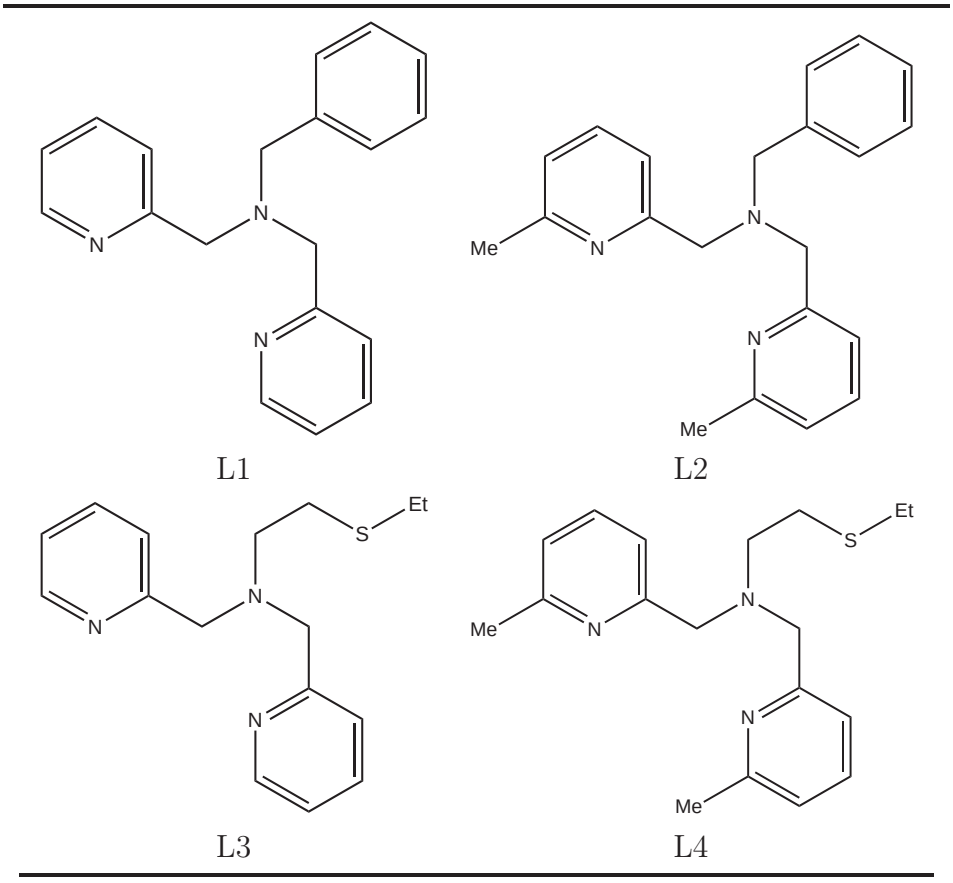

Figure 5.1: Structures of 4 large ligand in copper-oxygen complexes.

Starting from the model molecule $[Cu(NH_3)_4O_2]^+$ where the ligand $(NH_3)_4$ is denoted as L0, the calculation has been done for four larger ligands L1, L2, L3, and L4. The structures of the larger ligands are given in Figure 5.1. From the study of model molecule, it is known that the ground state of $(CuL)^+$ is a closed shell singlet, but the ground state of $(CuLO_2)^+$ can be either a high-spin open-shell triplet or a low-spin open-shell singlet. To deal with low-spin open-shell singlet states, multi-reference methods must be used. Unfortunately, for the copper-oxygen complexes with the four large ligands in Figure 5.1, it is still impossible to perform any multi reference calculation. Therefore, only the formation energies of the high-spin open-shell triplet states of the copper-oxygen complexes with large ligands have been calculated.

Aron Bona provided all the geometries of copper complexes, which are optimized using DFT/B3LYP methods with the cc-pVTZ basis set. The relativistic effective core potential, ECP10MDF, is used for Cu. Using the optimized B3LYP geometries, the energies of every involved molecule are obtained with the HF, RMP2, sd-LRMP2, and ab-LRMP2 methods. In the above single point energy calculations, ECP10MDF [127, 128] and cc-pVTZ-PP basis sets are used for Cu and aug-cc-pVTZ basis sets are used for other atoms. The formation energies, which are defined as the reaction energies of the above reactions, are given in Table 5.1. All the energies of related molecules are listed in Table B.58, B.59, and B.60 in Appendix B.

Table 5.1: Formation energies (in kcal/mol) of copper-oxygen complexes (high-spin open-shell triplet state) obtained with HF, RMP2, sd-LRMP2, ab-LRMP2, sd-LUCCSD, and sd-LUCCSD(T) methods. The deviations of LRMP2 from the RMP2 values are given in parenthesis.

	HF	RMP2	sd-LRMP2	ab-LRMP2	sd-LUCCSD	sd-LUCCSD(T)
L0	28.33	15.66	16.05 (0.39)	16.06 (0.40)	9.96	6.80
L1	16.35	9.47	9.54 (0.06)	10.20 (0.73)	1.74	-0.38
L2	20.59	14.42	14.66 (0.24)	15.27 (0.85)	4.91	3.61
L3	20.69	16.06	16.48 (0.43)	17.10 (1.04)	5.11	7.43
L4	24.69	22.39	22.41 (0.01)	23.08 (0.68)	8.38	11.59

Comparing the formation energies obtained with sd-LRMP2 and ab-LRMP2 with RMP2, the accuracy of local methods in copper complexes can be demonstrated. All the local errors are below 1 kcal/mol except one which is 1.04 kcal/mol. This is convincing evidence that the local methods are sufficient for these molecules. Furthermore, sd-LRMP2 always gives smaller errors in this case. Therefore, sd-localization is chosen for the LUCCSD(T) calculations. In Table 5.1, formation energies obtained with sd-LUCCSD and sd-LUCCSD(T) are also given. The sd-

LUCCSD(T) value only allows to conclude that the copper-oxygen complex with ligand L1 is stable while others are easy to dissociate. It is furthermore important to recall that these calculations are done for the gas phase, which is not the real case in experiments. The solvent effect is believed to be also important, and will further bring the formation energies down. Studies of solvent effects in these systems are planned to be done but will not be discussed in this work.

5.2 Inter Conversion of (S)-glutamate

Glutamate mutase (GluM) is an important enzyme in anaerobic bacteria (e.g. *Clostridium tetanomorphum*). The secondary structure of it is provided in Figure 5.2.

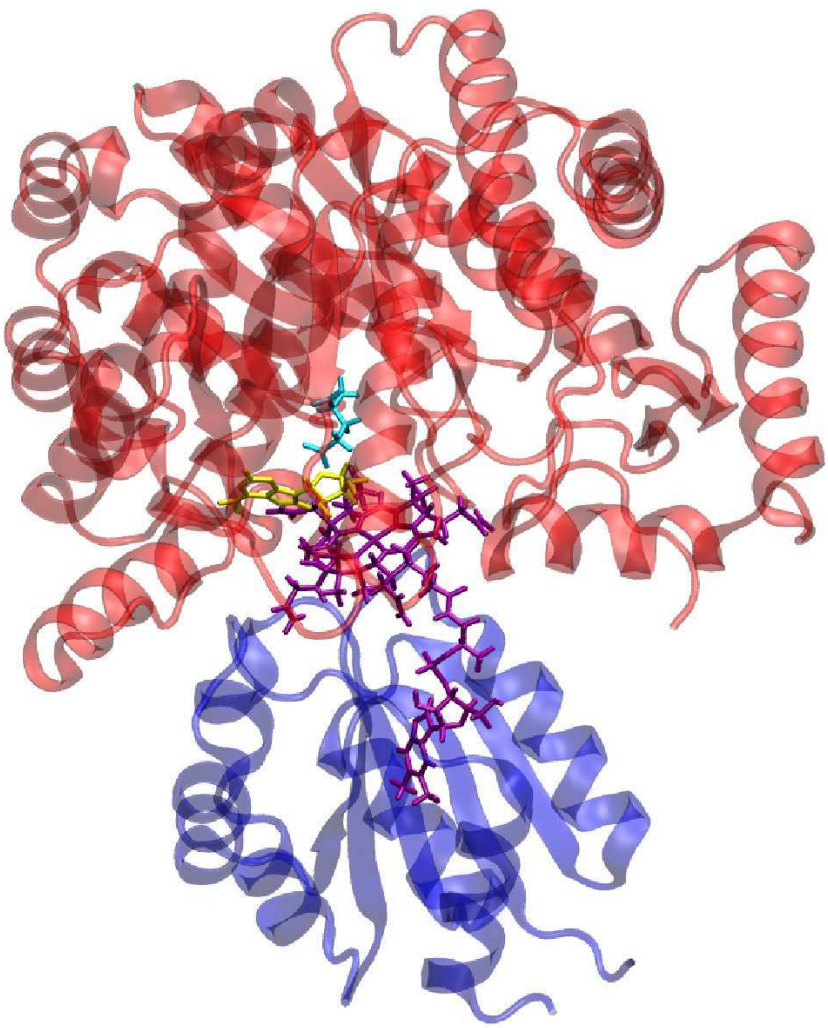

Figure 5.2: One $\sigma\epsilon-$subunit of Glutamate mutase (GluM) from anaerobic bacteria (e.g. *Clostridium tetanomorphum*) with coenzyme B12 and Glutamate substrate (green).

Clostridium spec. bacteria use glutamate as a carbon and energy source, to degrade it to butyrate, CO_2, NH_4^+, H_2, and in biosynthetic pathways of various peptidyl antibiotics. [129] The inter-conversion of (S)-glutamate to (2S,3S)-3-methylaspartate (right) has been studied using different methods and technologies. [130] The reaction is shown in Figure 5.3. The QM part of the transition states and intermediates, including 3 intermediates and 4 transition states (TS) is provided in Figure 5.4.

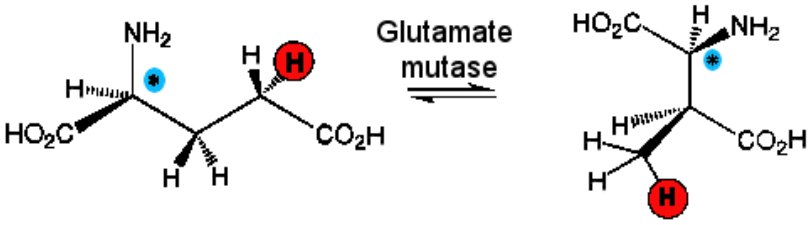

Figure 5.3: Inter-conversion of (S)-glutamate (left) to (2S,3S)-3-methylaspartate (right).

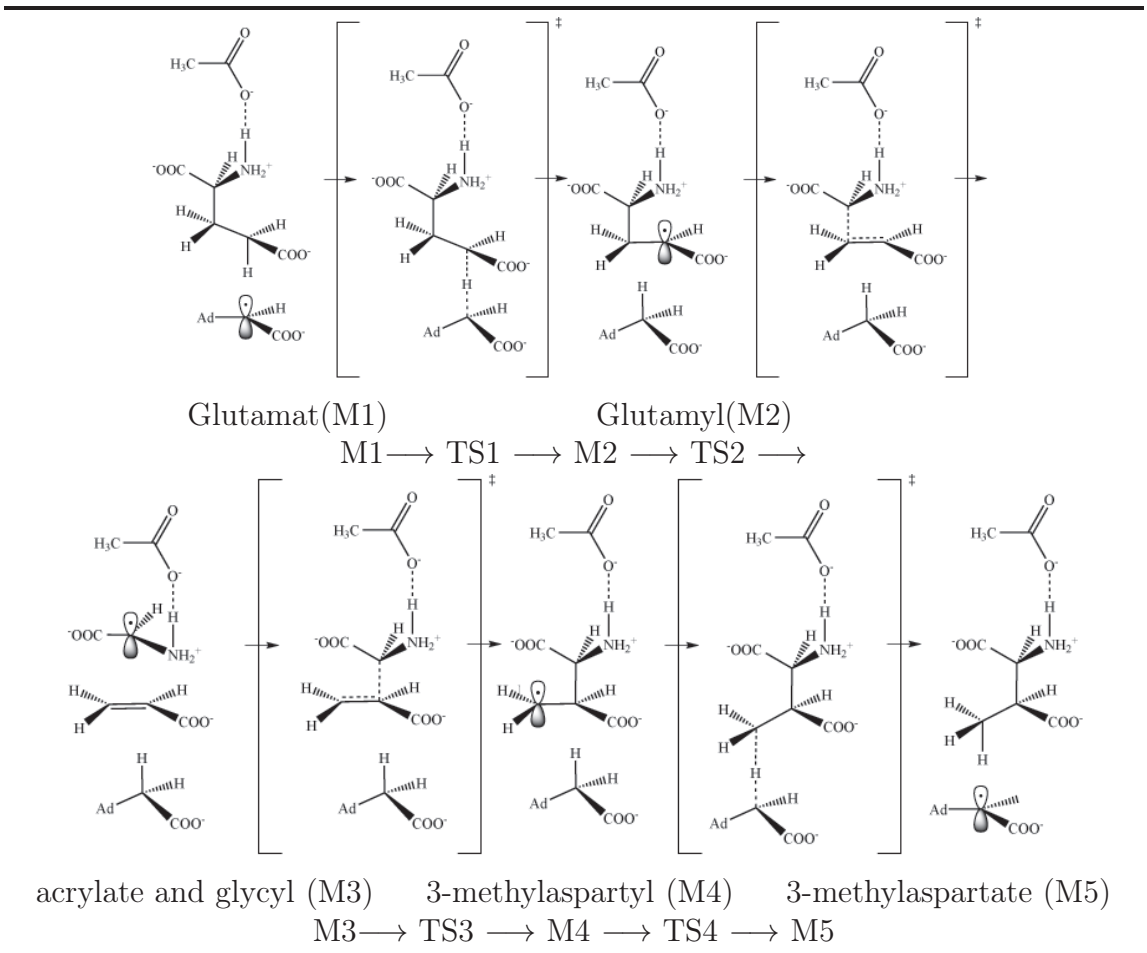

Figure 5.4: Transition states and intermediates of the inter-conversion of (S)-glutamate.

All the structures and the MM part have been provided by Judith Rommel. The structure of the GluM is taken from a PDB-file (X-ray diffraction), together with additional water and cations. Classical molecular dynamics (MD) simulations in NAMD have been done for QM/MM inital structures with CHARMM22 [131] force field in DL_POLY [132] for 50 ns at 300 K and 1 bar. The protein and solvent comprised 63411 atoms, including 17899 water molecules. For the QM part, the results obtained with HF, RMP2, sd-LRMP2, and ab-LRMP2 are given in Table 5.2. In all the QM calculations, charge fields from MM calculations and aug-cc-pVTZ basis sets have been used.

Table 5.2: Relative energies (in kcal/mol) for transition states and intermediates for inter-conversion of (S)-glutamate to (2S,3S)-3-methylaspartate obtained with HF, RMP2, sd-LRMP2, and ab-LRMP2. The deviations of LRMP2 from RMP2 values are given in parenthesis.

	HF	RMP2	sd-LRMP2	ab-LRMP2
M1	0.00	0.00	0.00 (0.00)	0.00 (0.00)
TS1	42.20	21.50	19.59 (-1.91)	18.42 (-3.08)
M2	3.37	2.25	0.10 (-2.15)	-0.23 (-2.48)
TS2	30.97	20.81	16.98 (-3.83)	16.58 (-4.23)
M3	5.90	8.50	5.03 (-3.47)	4.40 (-4.09)
TS3	32.99	18.07	15.25 (-2.82)	13.92 (-4.15)
M4	5.65	5.39	2.67 (-2.71)	2.24 (-3.14)
TS4	47.93	24.79	22.17 (-2.62)	20.51 (-4.27)
M5	2.81	3.39	2.18 (-1.21)	1.94 (-1.46)

Table 5.2 shows that the local errors are smaller for sd-LRMP2 compared to ab-LRMP2. However, all the above errors are quite large and need to be improved.

In a straightforward sense, using extended domains to reduce the domain errors is a possible option. The results using sd-LRMP2 with 'iext=1' are listed in Table 5.3. The absolute errors with 'iext=1' are all below 1 kcal/mol. Using 'iext=1' makes sd-LUCCSD(T) rather expensive, especially due to the large consumption of disk space. However, it is still possible to do the calculation within acceptable time. The calculations using sd-LUCCSD(T) with 'iext=1' are still not finished and will not be shown in this thesis. They will be given and discussed in the coming paper for sd-LUCCSD(T) and ab-LUCCSD(T). In the following contexts, the sd-LUCCSD(T) calculations with default options ('iext=0') will be discussed.

In Table 5.4, the transition states and intermediates obtained with sd-LUCCSD, sd-LUCCSD(T), and DFT with B3LYP functional are displayed.

Table 5.3: Relative energies (in kcal/mol) for transition states and intermediates for inter-conversion of (S)-glutamate to (2S,3S)-3-methylaspartate obtained with HF, RMP2, and sd-LRMP2 with 'iext=1'. The deviations of LRMP2 from RMP2 values are given in parenthesis.

	HF	RMP2	sd-LRMP2
M1	0.00	0.00	0.00 (0.00)
TS1	42.20	21.50	21.82 (0.32)
M2	3.37	2.25	1.70 (-0.55)
TS2	30.97	20.81	19.99 (-0.82)
M3	5.90	8.50	7.57 (-0.93)
TS3	32.99	18.07	17.54 (-0.53)
M4	5.65	5.39	4.68 (-0.70)
TS4	47.93	24.79	25.19 (0.40)
M5	2.81	3.39	2.72 (-0.68)

Table 5.4: Relative energies (in kcal/mol) for transition states and intermediates for inter-conversion of (S)-glutamate to (2S,3S)-3-methylaspartate obtained with sd-LUCCSD, sd-LUCCSD(T), and DFT-B3LYP.

	sd-LUCCSD	sd-LUCCSD(T)	DFT-B3LYP
M1	0.00	0.00	0.00
TS1	23.38	21.36	20.14
M2	1.50	0.36	0.05
TS2	22.00	19.59	11.54
M3	6.87	5.29	-1.22
TS3	20.16	17.37	11.41
M4	4.45	3.24	5.39
TS4	29.56	26.10	24.92
M5	3.24	2.41	2.41

Table 5.5: Relative energies (in kcal/mol) for transition states and intermediates for inter-conversion of (S)-glutamate to (2S,3S)-3-methylaspartate obtained with MM, RMP2/MM, LUCCSD(T)/MM, and DFT-B3LYP/MM.

	MM	RMP2/MM	LUCCSD(T)/MM	DFT-B3LYP/MM
M1	0.00	0.00	0.00	0.00
TS1	-3.77	17.72	17.58	16.36
M2	-3.06	-0.81	-2.70	-3.01
TS2	-0.69	20.12	18.90	10.85
M3	3.80	12.30	9.09	2.59
TS3	2.43	20.50	19.80	13.84
M4	-2.69	2.69	0.54	2.70
TS4	-2.19	22.60	23.91	22.73
M5	-0.76	2.63	1.65	1.65

Finally, the energy of the MM part should be added to the QM part. In Table 5.5, the results of MM part, RMP2/MM, LUCCSD(T)/MM, and DFT-B3LYP/MM methods are provided. Using the data in Table 5.5, the relative energies of the stationary point are drawn in Figure 5.5.

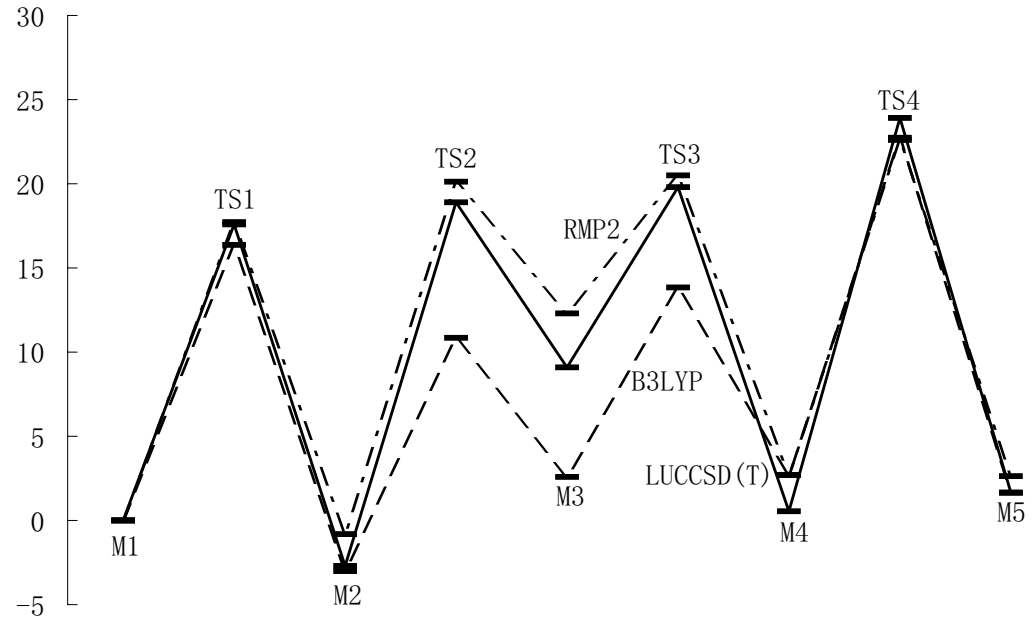

Figure 5.5: Transition states and intermediates of inter-conversion from (S)-glutamate obtained with RMP2/MM, LUCCSD(T)/MM, and DFT-B3LYP/MM methods.

Figure 5.5 shows that except for the second intermediate 'acrylate and glycyl (M3)' and the transition state before and after it, the transition states and intermediates obtained with three different QM methods are quite similar. For 'acrylate and glycyl', compared to LUCCSD(T) results, RMP2 is about 3 kcal/mol too high and DFT-B3LYP is about 7 kcal/mol too low. Despite the fact that the local error is in the range of 2-3 kcal/mol, the LUCCSD(T) curve should be more believable than the DFT-B3LYP one.

Finally, credit is due to Miss Judith Rommel in our institute for doing all MM work in this section.

6 Summary

The aim of this research was to expand the closed shell local electron correlation methods to open shell systems. A whole set of open shell local methods has been developed and coded into the `Molpro` software package. These methods are denoted as DF-LRMP2, LDF-LRMP2, DF-LUCCSD, and DF-LUCCSD(T) respectively. Two localization schemes, i.e., sd-localization and ab-localization have been implemented. In the presented tests, linear scaling has been achieved for LDF-LRMP2, the iteration part of DF-LRMP2, and the iteration part of DF-LUCCSD with additional linear scaling approximations.

The local errors of DF-LRMP2, DF-LUCCSD, and DF-LUCCSD(T) have been tested by calculating 30 radical stabilization energies, 30 vertical ionization potentials, and 30 molecular electron affinities. The mean errors are below 1 kcal/mol and the maximum errors are about 2-4 kcal/mol. Compared to UCCSD(T), the error of DF-LRMP2 and DF-LUCCSD methods are not significantly larger than those of RMP2 and UCCSD respectively. The error of sd-localization is similar to the one of ab-localization. In some cases, sd-localization has larger errors while in other cases, ab-localization holds larger errors.

Two preliminary applications have been made. In the calculation of dissociation energies of copper-oxygen (triplet) complexes, the local error of DF-LRMP2 is below 1 kcal/mol and the sd-localization method has smaller errors. In the calculation of the transition states and intermediates for inter conversion from (S)-glutamate to (2S,3S)-3-methylaspartate, the local error of DF-LRMP2 is about 2-3 kcal/mol for transition states and intermediates. For the second intermediate (Acrylate and glycyl in GluM) and the transition states before and after it, the energies obtained with LUCCSD(T) are about 8 kcal/mol higher than the ones obtained with DFT/B3LYP. For the other transition states and intermediates, the results obtained with LUCCSD(T) and DFT are as close as about 1 kcal/mol. The conclusion is that the DFT/B3LYP energy of the second intermediate is not plausible. The LUCCSD(T) transition states and intermediates are closer to the exact one.

The newly developed DF-LUCCSD(T) method has expanded the applicability of

the UCCSD(T) method to the system with 100-150 correlated orbitals and 2000-4000 basis functions. With respect to UCCSD(T), the mean error of DF-LUCCSD(T) is below 2 kcal/mol and the maximum error of it is about 2-4 kcal/mol. However, these errors are still not satisfying in every case. The F12 method [133] is supposed to be able to bring these errors together with basis set errors to below 1 kcal/mol. The DF-LRMP2-F12, DF-LUCCSD-F12, and DF-LUCCSD(T)-F12 methods are under development by Dr. Filipe Agapito in our group.

Appendix A
Optimized Stationary Points Structures

In this Appendix, the structures for the molecules included in Chapter 5 are provided. All stationary points were optimized at the DFT/B3LYP level of theory, with the cc-pV(T+d)Z basis set. Structure A.1 and Structure A.2 are the structure of methane and the structure of the methyl radical. From the Structure A.3 to Structure A.62, the structure of molecules and radicals involved in the 30 radical stabilization energy calculations are provided. From Structure A.63 to Structure A.92, the structure of molecules involved in IP and EA calculations are provided. The structurs of molecules involved in the calculation of formation energies of copper-oxygen complexes (high-spin open-shell triplet state) are given in structures from Structure A.93 to A.103. The QM part of molecules involved in the calculation of the transition states and intermediates of the inter-conversion of glutamate are provided in structures from Structure A.104 to A.112.

Structure A.1: R00-H, CH_4

```
   5
DFT-B3LYP/VTZ+D  ENERGY=-40.50228455
 H          0.6285247168        0.6285247336       -0.6285245243
 C          0.0000000000        0.0000000000        0.0000000000
 H         -0.6285247168       -0.6285247336       -0.6285245243
 H          0.6285247168       -0.6285247336        0.6285245243
 H         -0.6285247168        0.6285247336        0.6285245243
```

Structure A.2: R00, $\cdot CH_3$

```
   4
DFT-B3LYP/VTZ+D  ENERGY=-39.82481121
 C          0.0001042567        0.0000000000        0.0000000000
 H          0.5388526750       -0.9336081431        0.0000000000
 H          0.5388526750        0.9336081431        0.0000000000
 H         -1.0778096068        0.0000000000        0.0000000000
```

Structure A.3: R01-H, CH_3-CF_3

```
   8
DFT-B3LYP/VTZ+D  ENERGY=-377.55690790
 C         -0.0001308212        0.0000000000       -0.8244957310
 C         -0.0000616542        0.0000000000        0.6776668468
 H          1.0263577052        0.0000000000       -1.1843229417
 H         -0.5131373242        0.8889396788       -1.1848291526
 H         -0.5131373242       -0.8889396788       -1.1848291526
 F          0.6268242570        1.0856804362        1.1790722978
 F         -1.2535390955        0.0000000000        1.1794095354
 F          0.6268242570       -1.0856804362        1.1790722978
```

Structure A.4: R01, $\cdot CH_2-CF_3$

```
   7
DFT-B3LYP/VTZ+D  ENERGY=-376.87967339
 C          0.9396423918       -0.0084350970        0.0217971269
 C         -0.5363733533        0.0075087537        0.0530570469
 H          1.4691568408        0.9192176065       -0.1183214837
 H          1.4519098614       -0.9561336155        0.0158585842
 F         -1.0735111258       -0.0655147559       -1.1927656116
 F         -1.0346066195       -1.0355132444        0.7483756585
 F         -1.0142279953        1.1386983526        0.6117476787
```

Structure A.5: R02-H, CH_3-CH_2-Cl

```
   8
DFT-B3LYP/VTZ+D  ENERGY=-539.36983398
 C         -0.6523116054       -0.4914230251       -0.0021876450
 C          0.4499907001        0.5463998328        0.0012493197
 H         -0.5893164412       -1.1284409983       -0.8837081951
 H         -0.5595680071       -1.1219754120        0.8856386192
 H         -1.6348016879       -0.0208735310        0.0131840029
 Cl         0.3511973539        1.6305106890       -1.4494303700
 H          0.3913396522        1.2022121653        0.8658447506
 H          1.4375530354        0.0940122795       -0.0334044823
```

Structure A.6: R02, $\cdot CH_2-CH_2-Cl$

```
   7
DFT-B3LYP/VTZ+D  ENERGY=-538.70103754
 C         -0.7894363620        0.5121603576       -0.0054185648
 C          0.2286611486       -0.5291686300       -0.0041164471
 H         -1.0335137415        1.0359830589       -0.9177510978
 H         -1.1695394967        0.9052987152        0.9258530186
 Cl         1.9344120473        0.2320259952        0.1764200671
 H          0.2914984263       -1.0814487173       -0.9358054990
 H          0.1599729780       -1.2078247797        0.8395125230
```

Structure A.7: R03-H, CH_3-CH_2-F

```
   8
DFT-B3LYP/VTZ+D  ENERGY=-179.03953132
 C         -0.6718834949       -0.3941115847        0.0025838103
 C          0.5916834421        0.4335917356       -0.0075944311
 H         -0.7122479314       -1.0248958756        0.8908072325
 H         -0.7036444547       -1.0374817549       -0.8791315171
 H         -1.5531865548        0.2474765002       -0.0083776910
 F          0.6343443173        1.2523784080        1.1243599538
 H          0.6391211483        1.0864827975       -0.8818619529
 H          1.4854255278       -0.1937682261        0.0121185954
```

Structure A.8: R03, $\cdot CH_2-CH_2-F$

```
   7
DFT-B3LYP/VTZ+D  ENERGY=-178.36628016
 C         -0.7584938320        0.4603930823       -0.0040185926
 C          0.4598363595       -0.3745345629       -0.0028615810
 H         -1.2189772116        0.7585496479        0.9266057612
 H         -1.2957661746        0.6486171251       -0.9220405284
 F          0.1195335506       -1.7429313798        0.1326662514
 H          1.1165659270       -0.1356966559        0.8350376156
 H          1.0167433810       -0.2849992566       -0.9364259261
```

Structure A.9: R04-H, CH_3-CH_2-OH

```
   9
DFT-B3LYP/VTZ+D  ENERGY=-155.01051820
 C         -0.9306360741       -0.3891680879        0.0000000000
 C          0.3334058266        0.4456968169        0.0000000000
 H         -1.8128501290        0.2531576427        0.0000000000
 H         -0.9671351001       -1.0270204156       -0.8837230767
 H         -0.9671351001       -1.0270204156        0.8837230767
 H          0.3551019984        1.0932893056        0.8850561045
 H          0.3551019984        1.0932893056       -0.8850561045
 O          1.4498889029       -0.4428963038        0.0000000000
 H          2.2580926771        0.0772981521        0.0000000000
```

Structure A.10: R04, $\cdot CH_2-CH_2-OH$

```
   8
DFT-B3LYP/VTZ+D  ENERGY=-154.33805712
 C         -1.0395544862       -0.4645799383        0.0000000000
 C          0.1881864592        0.3564331917        0.0000000000
 H         -2.0093022296        0.0095408510        0.0000000000
 H         -0.9672813584       -1.5408112836        0.0000000000
 H          0.1989614517        1.0222757106       -0.8800296749
 H          0.1989614517        1.0222757106        0.8800296749
 O          1.3267527376       -0.4976214816        0.0000000000
 H          2.1182979742        0.0472242393        0.0000000000
```

Structure A.11: R05-H, $CH_3{-}CH{=}CH_2$

```
   9
DFT-B3LYP/VTZ+D  ENERGY=-117.86943251
 C         -1.4234781540       -0.1695153705        0.0000000000
 C         -0.2453843400        0.4408366712        0.0000000000
 C          1.0859867644       -0.2443382166        0.0000000000
 H         -1.5028530259       -1.2507581789        0.0000000000
 H         -2.3511139227        0.3875749461        0.0000000000
 H         -0.2199649507        1.5272434620        0.0000000000
 H          0.9784004372       -1.3293329313        0.0000000000
 H          1.6740385958        0.0419653090       -0.8764009433
 H          1.6740385958        0.0419653090        0.8764009433
```

Structure A.12: R05, $\cdot CH_2{-}CH{=}CH_2$

```
   8
DFT-B3LYP/VTZ+D  ENERGY=-117.22162847
 C         -1.2527104682        0.0000000000       -0.1536252692
 C         -0.0021792025        0.0000000000        0.4252676575
 C          1.1913503018        0.0000000000       -0.2635769786
 H         -1.3701880620        0.0000000000       -1.2296765448
 H         -2.1516473448        0.0000000000        0.4452125829
 H          0.0469298645        0.0000000000        1.5103622187
 H          2.1402433146        0.0000000000        0.2523478527
 H          1.2122165965        0.0000000000       -1.3457645192
```

Structure A.13: R06-H, $CH_3{-}CHO$

```
   7
DFT-B3LYP/VTZ+D  ENERGY=-153.80502100
 C         -0.5948193943        0.2488804424        0.0000000000
 H         -1.3479316848       -0.5359248064        0.0000000000
 H         -0.7205230780        0.8903098551       -0.8767144997
 H         -0.7205230780        0.8903098551        0.8767144997
 C          0.7877992053       -0.3374839392        0.0000000000
 H          1.6124822418        0.4070764570        0.0000000000
 O          1.0335307881       -1.5157768640        0.0000000000
```

Structure A.14: R06, $\cdot CH_2{-}CHO$

```
   6
DFT-B3LYP/VTZ+D  ENERGY=-153.14591197
 C         -0.6649210148        0.2952691888        0.0000000000
 C          0.6397581266       -0.2835418383        0.0000000000
 O          1.6705227168        0.3809499702        0.0000000000
 H         -0.7647128653        1.3719771320        0.0000000000
 H         -1.5516710323       -0.3235648217        0.0000000000
 H          0.6873280690       -1.3879816308        0.0000000000
```

Structure A.15: R07-H, $CH_3{-}CN$

```
   6
DFT-B3LYP/VTZ+D  ENERGY=-132.72589934
 C         -0.0000234865        0.0000000000       -0.4820151843
 C          0.0000081379        0.0000000000        0.9733143113
 H         -0.5114828903       -0.8856414048       -0.8583641108
 N          0.0001313860        0.0000000000        2.1231955240
 H         -0.5114828903        0.8856414048       -0.8583641108
 H          1.0228497432        0.0000000000       -0.8579794294
```

Structure A.16: R07, $\cdot CH_2{-}CN$

```
   5
DFT-B3LYP/VTZ+D  ENERGY=-132.06505351
 C          0.9344262064        0.0000000000       -1.1104929597
 C         -0.2590708219        0.0000000000       -0.4168928209
 H          1.8717067763        0.0000000000       -0.5755930243
 H          0.9340183164        0.0000000000       -2.1896189726
 N         -1.2644194772        0.0000000000        0.1686597774
```

Structure A.17: R08-H, $CH_3{-}CO{-}NH_2$

```
   9
DFT-B3LYP/VTZ+D  ENERGY=-209.18456162
 C         -1.1015453444        0.0834563019        0.0000000000
 C          0.3611267778        0.4885863708        0.0000000000
 N          1.2595563310       -0.5378713711        0.0000000000
 H         -1.2612352723       -0.9943250657        0.0000000000
 H         -1.5804151458        0.5155571925        0.8781054856
 H         -1.5804151458        0.5155571925       -0.8781054856
 O          0.7089064363        1.6535069094        0.0000000000
 H          2.2399908276       -0.3134533374        0.0000000000
 H          0.9794925356       -1.5006031928        0.0000000000
```

Structure A.18: R08, $\cdot CH_2{-}CO{-}NH_2$

```
   8
DFT-B3LYP/VTZ+D  ENERGY=-208.51991554
 C         -1.1985172114       -0.2513774573        0.0000000000
 C          0.0283479606        0.5307305741        0.0000000000
 O          0.0200951590        1.7564499377        0.0000000000
 N          1.1983922326       -0.1858185247        0.0000000000
 H         -1.2054772019       -1.3324867332        0.0000000000
 H         -2.1333801149        0.2853084026        0.0000000000
 H          1.2210085890       -1.1883924152        0.0000000000
 H          2.0652855872        0.3222902161        0.0000000000
```

Structure A.19: R09-H, $CH_3{-}CO{-}NH{-}CH_3$

```
  12
DFT-B3LYP/VTZ+D  ENERGY=-248.47658952
 C         -1.8723361724        0.0012414962        0.3445319544
 C         -0.5561105305        0.0095963506       -0.4099384411
 N          0.5701342254        0.0243818500        0.3533645830
 C          1.8906254593        0.0328075764       -0.2505309410
 H         -1.7601037123        0.0087127188        1.4287018735
 H         -2.4531574817        0.8721013795        0.0416320450
 H         -2.4359503782       -0.8843863682        0.0520903643
 O         -0.5091286753        0.0033732803       -1.6286304715
 H          0.4884079468        0.0297058287        1.3535624901
 H          2.0226381017        0.9102155837       -0.8845544276
 H          2.6397371844        0.0454967774        0.5384648662
 H          2.0400030329       -0.8505934736       -0.8723368951
```

Structure A.20: R09, $\cdot CH_2-CO-NH-CH_3$

```
  11
DFT-B3LYP/VTZ+D  ENERGY=-247.81219343
 C         -2.0037402262        0.0022640783        0.4205952682
 C         -0.7759004855        0.0142954509       -0.3572431948
 N          0.3893021488        0.0385716300        0.3633764743
 C          1.6797882746        0.0520110858       -0.2959134715
 H         -2.9384284682       -0.0172563849       -0.1162427890
 H         -2.0132823501        0.0120668679        1.5018585802
 O         -0.7728998361        0.0034461964       -1.5859931672
 H          0.3511072901        0.0472415659        1.3664298665
 H          1.7823090602        0.9289904927       -0.9371548512
 H          2.4626312834        0.0685921283        0.4595514684
 H          1.8068213089       -0.8309761114       -0.9243011837
```

Structure A.21: R10-H, $CH_3-CO-O-CH_3$

```
  11
DFT-B3LYP/VTZ+D  ENERGY=-268.34778121
 C         -1.7900204273       -0.4073734265        0.0000000000
 C         -0.4888839730        0.3498487133        0.0000000000
 O         -0.3751054022        1.5489961441        0.0000000000
 O          0.5632786071       -0.4973187230        0.0000000000
 C          1.8611196268        0.1193501389        0.0000000000
 H         -1.8475348084       -1.0505850989        0.8786180710
 H         -2.6175967036        0.2952677427        0.0000000000
 H         -1.8475348084       -1.0505850989       -0.8786180710
 H          1.9915899106        0.7388235301        0.8860124022
 H          2.5739720677       -0.6999784520        0.0000000000
 H          1.9915899106        0.7388235301       -0.8860124022
```

Structure A.22: R10, $\cdot CH_2-CO-O-CH_3$

```
  10
DFT-B3LYP/VTZ+D  ENERGY=-267.68368682
 C         -1.9175238931       -0.5242426004        0.0000000000
 C         -0.6939300651        0.2443586443        0.0000000000
 O          0.4033571883       -0.5554036944        0.0000000000
 C          1.6636246982        0.1283993190        0.0000000000
 H         -2.8541109011        0.0091622491        0.0000000000
 H         -1.8976575397       -1.6027207661        0.0000000000
 O         -0.6368468496        1.4580396933        0.0000000000
 H          1.7605464369        0.7557597240        0.8853039607
 H          2.4205784884       -0.6504572928        0.0000000000
 H          1.7605464369        0.7557597240       -0.8853039607
```

Structure A.23: R11-H, $CH_3-CO-OH$

```
   8
DFT-B3LYP/VTZ+D  ENERGY=-229.06236641
 C         -0.9599916974        0.0869053239        0.0000000000
 C          0.5336344631        0.2534322725        0.0000000000
 O          1.1672847193       -0.9463867913        0.0000000000
 H         -1.2694665109       -0.4805557006        0.8780787955
 H         -1.4349741582        1.0627435178        0.0000000000
 H         -1.2694665109       -0.4805557006       -0.8780787955
 O          1.1300847309        1.2982815883        0.0000000000
 H          2.1177829641       -0.7588945098        0.0000000000
```

Structure A.24: R11, $\cdot CH_2{-}CO{-}OH$

```
   7
DFT-B3LYP/VTZ+D  ENERGY=-228.39782687
 C         -1.0664943343       -0.1628827594        0.0000000000
 C          0.2985358118        0.3078509417        0.0000000000
 O          1.2041435389       -0.7086669743        0.0000000000
 H         -1.2934559534       -1.2174501781        0.0000000000
 H         -1.8559532673        0.5706213945        0.0000000000
 O          0.6307454621        1.4758071438        0.0000000000
 H          2.0796467423       -0.2956775682        0.0000000000
```

Structure A.25: R12-H, $CH_3{-}CH({-}CH_2)_2$

```
  12
DFT-B3LYP/VTZ+D  ENERGY=-157.15636508
 C         -1.4728858809        0.1154343124       -0.0000192311
 C         -0.1097482559       -0.5326473563       -0.0045912191
 C          1.0309158294        0.0916175119       -0.7610083923
 C          1.0348392348        0.0897457464        0.7474494039
 H         -2.0514940656       -0.1696403168       -0.8818676686
 H         -2.0472239463       -0.1735964775        0.8833392489
 H         -1.3886688876        1.2043370866        0.0022560794
 H         -0.1299625362       -1.6164427452       -0.0059144237
 H          1.7287232471       -0.5554841926       -1.2744267701
 H          0.8466277576        1.0321080910       -1.2637999039
 H          1.7352264510       -0.5585586851        1.2557527429
 H          0.8529840526        1.0288830251        1.2536271339
```

Structure A.26: R12, $\cdot CH_2{-}CH({-}CH_2)_2$

```
  11
DFT-B3LYP/VTZ+D  ENERGY=-156.49132285
 C         -0.1918790233       -0.2415887178        0.1235513509
 C          0.9782248292       -0.0092694515       -0.8319961895
 C          1.2289726242        0.0024436760        0.6374829261
 C         -1.2250085687        0.7623423703        0.2916671927
 H         -0.9838036668        1.8147485443        0.2366472287
 H         -2.2460176960        0.4835621893        0.5002050138
 H         -0.5252147703       -1.2691889483        0.1908274408
 H          1.3210782092       -0.8561810076       -1.4106714118
 H          0.9931330203        0.9330986536       -1.3618988047
 H          1.4139144328        0.9527174878        1.1187774220
 H          1.7450786095       -0.8367507963        1.0838548309
```

Structure A.27: R13-H, $CH_3{-}F$

```
   5
DFT-B3LYP/VTZ+D  ENERGY=-139.73297048
 C         -0.0001062940        0.0000000000        0.0699414837
 F         -0.0000159624        0.0000000000       -1.3169291578
 H          0.5155325103        0.8925546791        0.4262127522
 H         -1.0309417642        0.0000000000        0.4261481696
 H          0.5155325103       -0.8925546791        0.4262127522
```

Structure A.28: R13, $\cdot CH_2-F$

```
   4
DFT-B3LYP/VTZ+D  ENERGY=-139.06389849
 C          0.0714910288        0.0583980012       -0.0498111337
 F         -1.2276003772       -0.2626561806        0.0145311230
 H          0.4840550302        0.0785546594       -1.0479537908
 H          0.4266573182        0.6737365201        0.7638848016
```

Structure A.29: R14-H, CH_3-NH_2

```
   7
DFT-B3LYP/VTZ+D  ENERGY=-95.83425038
 C         -0.5531654177        0.0713212598        0.0000000000
 N          0.9061152602        0.1944959188        0.0000000000
 H         -0.9383814356       -0.9572296124        0.0000000000
 H         -0.9568617410        0.5789619436       -0.8770676887
 H         -0.9568617410        0.5789619436        0.8770676887
 H          1.2986460376       -0.2685692267       -0.8108804221
 H          1.2986460376       -0.2685692267        0.8108804221
```

Structure A.30: R14, $\cdot CH_2-NH_2$

```
   6
DFT-B3LYP/VTZ+D  ENERGY=-95.17990392
 C          0.7109702394        0.1255433859       -0.0437084579
 N         -0.6819377067        0.1103240107       -0.0074887389
 H          1.2188857538        0.1265820089        0.9094589671
 H          1.1782329036       -0.3827429400       -0.8743595232
 H         -1.1019015322        0.6893468468        0.7039810773
 H         -1.1386026578        0.2399536878       -0.8977103244
```

Structure A.31: R15-H, $CH_3-NH_3^+$

```
   8
DFT-B3LYP/VTZ+D  ENERGY=-96.19179968
 C         -0.0000612105        0.0000000000       -0.7900657870
 N         -0.0000220783        0.0000000000        0.7232257472
 H          0.5156874937        0.8928977326       -1.1295592079
 H          0.5156874937       -0.8928977326       -1.1295592079
 H         -1.0311753332        0.0000000000       -1.1296137434
 H         -0.4761931063        0.8246254247        1.0966871087
 H         -0.4761931063       -0.8246254247        1.0966871087
 H          0.9522698472        0.0000000000        1.0965399816
```

Structure A.32: R15, $\cdot CH_2-NH_3^+$

```
   7
DFT-B3LYP/VTZ+D  ENERGY=-95.50842652
 C         -0.8944964416        0.0966088219       -0.0252192791
 N          0.5711094842        0.0296438995       -0.0043723573
 H         -1.3847022189       -0.3750244089       -0.8594167713
 H         -1.3747011977        0.4067022430        0.8867891251
 H          0.9640733652        0.1232203549       -0.9468578705
 H          0.9724435611        0.7766232941        0.5718432635
 H          0.9178614477       -0.8624602044        0.3772338896
```

Structure A.33: R16-H, $CH_3{-}NH{-}CH_3$

```
  10
DFT-B3LYP/VTZ+D  ENERGY=-135.12505511
 C         -0.0936547699       -0.0321771188       -1.2434572731
 N          0.6522000050       -0.1636998382       -0.0011879421
 C         -0.1768016907       -0.0213105766        1.1859720949
 H          0.5888435580       -0.0939866661       -2.0917494084
 H         -0.6652567707        0.9065883474       -1.3294250581
 H         -0.8039574249       -0.8575767122       -1.3308073506
 H          1.3994567044        0.5183547461        0.0213668291
 H          0.4457063184       -0.0777481145        2.0795210977
 H         -0.8932553729       -0.8448216769        1.2308466365
 H         -0.7512745568        0.9187836099        1.2248733740
```

Structure A.34: R16, $\cdot CH_2{-}NH{-}CH_3$

```
   9
DFT-B3LYP/VTZ+D  ENERGY=-134.47190402
 C         -1.4199465801       -0.1733584199       -0.1114614439
 N         -0.2476646166        0.3390653312        0.4154260076
 C          1.0058900147       -0.3427180338        0.1576148487
 H         -2.3141835664        0.4160983974        0.0269058819
 H         -1.5071505852       -1.2505046660       -0.1414941283
 H         -0.1803539417        1.3447140332        0.3897547327
 H          0.9285282109       -1.3781509784        0.4940875750
 H          1.2808320666       -0.3533008532       -0.9053125552
 H          1.8065169977        0.1343021894        0.7219520815
```

Structure A.35: R17-H, $CH_3{-}NH{-}CHO$

```
   9
DFT-B3LYP/VTZ+D  ENERGY=-209.16758145
 C         -1.1362999297       -0.0240451911        0.0017070525
 N          0.2273273584        0.4628778908       -0.0044804127
 C          1.3352126743       -0.3205941845       -0.0017319471
 O          2.4768500233        0.0864814272       -0.0067867443
 H         -1.1215700089       -1.1132128886        0.0057889653
 H         -1.6786089791        0.3104810646        0.8886741023
 H         -1.6839297693        0.3039523181       -0.8843413867
 H          0.3942598669        1.4577770569       -0.0114045995
 H          1.0844267642       -1.3979014934        0.0058279701
```

Structure A.36: R17, $\cdot CH_2{-}NH{-}CHO$

```
   8
DFT-B3LYP/VTZ+D  ENERGY=-208.51161656
 C         -1.2805084531       -0.0414327701        0.0000000000
 N          0.0214416144        0.3981593230        0.0000000000
 C          1.1478714235       -0.3850585600        0.0000000000
 O          2.2766564143        0.0570590715        0.0000000000
 H          0.2037792057        1.3924874065        0.0000000000
 H         -2.0701646827        0.6863775555        0.0000000000
 H         -1.4699595237       -1.1002519697        0.0000000000
 H          0.9123920015       -1.4619620566        0.0000000000
```

Structure A.37: R18-H, $CH_3{-}N({-}CH_3)_2$

```
  13
DFT-B3LYP/VTZ+D  ENERGY=-174.41798452
 C         -0.7046604632        1.2199605146       -0.0338048602
 N          0.0015299180        0.0048973372       -0.3999056078
 C          1.3992132564        0.0535376545       -0.0090027220
 C         -0.6606186374       -1.1791569729        0.1174604607
 H         -0.7415385014        1.3853347189        1.0583036793
 H         -0.2179458181        2.0838541720       -0.4886937964
 H         -1.7306625449        1.1768352995       -0.4019804957
 H          1.9122947525       -0.8451480345       -0.3543864631
 H          1.8834762128        0.9171232013       -0.4670166867
 H          1.5387649064        0.1255557378        1.0847150323
 H         -1.6880897980       -1.2201936903       -0.2469338144
 H         -0.1434414683       -2.0751054517       -0.2285928951
 H         -0.6898388148       -1.2094234862        1.2217851691
```

Structure A.38: R18, $\cdot CH_2{-}N({-}CH_3)_2$

```
  12
DFT-B3LYP/VTZ+D  ENERGY=-173.76536396
 C         -1.5756299267        0.3461400767       -0.0023211723
 N         -0.2254754416        0.0596283240        0.0219844567
 C          0.4050004982       -0.0807412838        1.3194627989
 C          0.6040130108        0.6665153604       -0.9999338947
 H         -2.0230358871        0.5052210565       -0.9721410015
 H         -2.1781997741       -0.0695287536        0.7917653415
 H         -0.2290430611       -0.6823377654        1.9700484407
 H          1.3659375267       -0.5852649155        1.2119947271
 H          0.5749105753        0.8898907348        1.8083088359
 H          1.5638939164        0.1514961900       -1.0513808408
 H          0.7919922676        1.7328530049       -0.8063079922
 H          0.1124892957        0.5777789713       -1.9683086993
```

Structure A.39: R19-H, $CH_3{-}NO_2$

```
   7
DFT-B3LYP/VTZ+D  ENERGY=-244.99016744
 C          0.6602284319       -0.0079394737       -0.0105836192
 N         -0.8394023249       -0.0171762673       -0.0061498730
 O         -1.3803578779       -0.0038416071        1.0856246035
 O         -1.4076034391       -0.0371687819       -1.0836757536
 H          1.0008535165       -0.0211531721       -1.0386202963
 H          0.9771228875        0.8893127721        0.5136726813
 H          0.9878848060       -0.8855554700        0.5397312573
```

Structure A.40: R19, $\cdot CH_2{-}NO_2$

```
   6
DFT-B3LYP/VTZ+D  ENERGY=-244.32103065
 C          0.0000000000        0.0000000000        0.7327375580
 N          0.0000000000        0.0000000000       -0.6786869434
 O          1.0952471630        0.0000000000       -1.2430182811
 O         -1.0952471630        0.0000000000       -1.2430182811
 H          0.9603624185        0.0000000000        1.2183379737
 H         -0.9603624185        0.0000000000        1.2183379737
```

Structure A.41: R20-H, $CH_3{-}O{-}CF_3$

```
   9
DFT-B3LYP/VTZ+D  ENERGY=-452.76604716
 C         -1.2330278445        0.0437257737        0.0007900099
 O         -0.0027316925        0.7912471384        0.0021883818
 C          1.1267130384        0.0706092248        0.0035022337
 H         -2.0211793417        0.7895130138        0.0001687106
 H         -1.3067400366       -0.5737562067        0.8950294147
 H         -1.3049781317       -0.5733339576       -0.8938797687
 F          1.2359683643       -0.7339657132       -1.0779438232
 F          2.1613236222        0.9073813528        0.0044968909
 F          1.2336550221       -0.7338006258        1.0852439504
```

Structure A.42: R20, $\cdot CH_2{-}O{-}CF_3$

```
   8
DFT-B3LYP/VTZ+D  ENERGY=-452.09742903
 F          1.2768963102       -1.0019146649        0.7105813591
 F          1.9629204691        0.9738945511        0.1303121074
 F          0.9969255776       -0.3198245914       -1.3216705579
 C          0.9979091685        0.0777005926       -0.0361257977
 O         -0.1760821465        0.6588943309        0.3193232782
 C         -1.3221709445       -0.0968386518        0.2013752636
 H         -2.2068168566        0.4616644482        0.4511287651
 H         -1.3179785780       -0.9253170148       -0.4892284178
```

Structure A.43: R21-H, $CH_3{-}O{-}CH_3$

```
   9
DFT-B3LYP/VTZ+D  ENERGY=-154.99439779
 C          0.0000000000        1.1737943995        0.0430694345
 O          0.0000000000        0.0000000003        0.8241171628
 C          0.0000000000       -1.1737943994        0.0430694350
 H         -0.8900273788        1.2342018569       -0.5970610797
 H          0.0000000000        2.0210003596        0.7269141430
 H          0.8900273788        1.2342018569       -0.5970610797
 H          0.8900273787       -1.2342018566       -0.5970610793
 H          0.0000000000       -2.0210003605        0.7269141427
 H         -0.8900273787       -1.2342018566       -0.5970610793
```

Structure A.44: R21, $\cdot CH_2{-}O{-}CH_3$

```
   8
DFT-B3LYP/VTZ+D  ENERGY=-154.33415990
 H         -1.1346031100       -0.6585016073        0.6799901996
 C         -1.2962464736        0.0162887270       -0.1526338666
 H         -2.2672039050        0.1176160829       -0.6121762993
 O         -0.5326842618        1.1304785010       -0.2381258927
 C          0.7147777491        1.0641625747        0.4389849662
 H          1.1986119771        2.0293813432        0.3096239406
 H          1.3453379785        0.2781389789        0.0146455700
 H          0.5670540457        0.8708733995        1.5065083822
```

Structure A.45: R22-H, $CH_3-O-CHO$

```
   8
DFT-B3LYP/VTZ+D  ENERGY=-229.03736614
 H         -1.1434897767       -0.5061946628        0.8866592152
 H         -1.1434897767       -0.5061946628       -0.8866592152
 C         -1.0263767650        0.1144893942        0.0000000000
 H         -1.7501567689        0.9234002344        0.0000000000
 O          0.2661820426        0.7515501299        0.0000000000
 C          1.3207097587       -0.0735463815        0.0000000000
 H          2.2415611091        0.5234992225        0.0000000000
 O          1.2767971770       -1.2720452738        0.0000000000
```

Structure A.46: R22, $\cdot CH_2-O-CHO$

```
   7
DFT-B3LYP/VTZ+D  ENERGY=-228.37085404
 H         -1.9783306720        0.8950587236        0.0000000000
 C         -1.2144725253        0.1401505374        0.0000000000
 H         -1.3648436035       -0.9245334510        0.0000000000
 O          0.0551393718        0.6336989870        0.0000000000
 C          1.0986592138       -0.2415657190        0.0000000000
 H          2.0297341575        0.3332302911        0.0000000000
 O          1.0040660576       -1.4332793691        0.0000000000
```

Structure A.47: R23-H, $CH_3-CO-O-CH_3$

```
  11
DFT-B3LYP/VTZ+D  ENERGY=-268.34778589
 C          0.9897452247       -0.8389650272        0.0000004017
 C          1.0208893601        0.6663125002       -0.0000022673
 O          2.0147657204        1.3469218387       -0.0000122465
 H          2.0056411410       -1.2219716809        0.0000133596
 H          0.4549786271       -1.2016565326       -0.8782387469
 H          0.4549545861       -1.2016565680        0.8782244815
 O         -0.2294936655        1.1768029680        0.0000101256
 C         -0.3142794655        2.6113388818        0.0000026158
 H          0.1674114206        3.0225433050        0.8858679259
 H          0.1674048813        3.0225348028       -0.8858702374
 H         -1.3754848302        2.8424765121        0.0000045880
```

Structure A.48: R23, $\cdot CH_2-CO-O-CH_3$

```
  10
DFT-B3LYP/VTZ+D  ENERGY=-267.68185952
 C          0.8692818130       -0.7875056734        0.0008541869
 H          1.9000791175       -1.1278482422        0.0010293171
 H          0.3495591744       -1.1721638016       -0.8773564161
 H          0.3494536181       -1.1716472880        0.8792283724
 C          0.8387748750        0.7131195697        0.0004414320
 O          1.7848081255        1.4514098857        0.0003924714
 O         -0.4611483830        1.1623239465        0.0001111645
 C         -0.6839117352        2.5056375038       -0.0003384274
 H          0.1583426535        3.1735785879       -0.0004887555
 H         -1.7222692587        2.7802495115       -0.0004963453
```

Structure A.49: R24-H, $CH_3{-}OH$

```
   6
DFT-B3LYP/VTZ+D  ENERGY=-115.70598509
 C         -0.3324600101        0.1019565241        0.0000000000
 O          1.0839385788        0.2097705486        0.0000000000
 H          1.4571930805       -0.6756646417        0.0000000000
 H         -0.7268031815        1.1169702916        0.0000000000
 H         -0.7119602338       -0.4119448613        0.8899773779
 H         -0.7119602338       -0.4119448613       -0.8899773779
```

Structure A.50: R24, $\cdot CH_2{-}OH$

```
   5
DFT-B3LYP/VTZ+D  ENERGY=-115.04580207
 C         -0.4154090077        0.1286225708        0.0549358321
 O          0.8759098435       -0.2404167820        0.3020427866
 H         -0.8334691375       -0.0540663236       -0.9263569698
 H         -1.0403830820        0.1247113742        0.9338386828
 H          1.3591783836       -0.2987868395       -0.5275523318
```

Structure A.51: R25-H, $CH_3{-}PH_3^+$

```
   8
DFT-B3LYP/VTZ+D  ENERGY=-382.75377391
 C         -0.0001431880        0.0000000934       -0.9848699108
 P         -0.0000481741        0.0000000359        0.8112333580
 H          0.5150309541       -0.8916295066       -1.3424195943
 H         -1.0298763029        0.0000035204       -1.3425280895
 H          0.5150364626        0.8916265896       -1.3424194277
 H          1.2955119452        0.0000044978        1.3359137317
 H         -0.6477588396        1.1219303917        1.3361202164
 H         -0.6477538573       -1.1219336221        1.3361197163
```

Structure A.52: R25, $\cdot CH_2{-}PH_3^+$

```
   7
DFT-B3LYP/VTZ+D  ENERGY=-382.07720767
 C         -1.0978474677        0.0272364673       -0.0003075448
 P          0.6560242282        0.0063079844       -0.0010497316
 H         -1.6384843392       -0.0220798701       -0.9355336711
 H         -1.6370965556        0.0321836385        0.9369950447
 H          1.1720469327        0.6206571916       -1.1466709539
 H          1.1729976353        0.6688572203        1.1168259817
 H          1.1967115663       -1.2902956320        0.0258118750
```

Structure A.53: R26-H, $CH_3{-}SH_2^+$

```
   7
DFT-B3LYP/VTZ+D  ENERGY=-438.96643924
 C         -0.7437096423        0.1797683222        0.0000000000
 S          1.0808362636        0.3103607271        0.0000000000
 H         -1.0519018721       -0.8604411525        0.0000000000
 H         -1.0793687366        0.7046738205        0.8918336074
 H         -1.0793687366        0.7046738205       -0.8918336074
 H          1.3834653620       -0.5611787688        0.9887751295
 H          1.3834653620       -0.5611787688       -0.9887751295
```

Structure A.54: R26, $\cdot CH_2{-}SH_2^+$

```
   6
DFT-B3LYP/VTZ+D  ENERGY=-438.28689060
 S          0.9116395197        0.2631188310       -0.0286986100
 C         -0.8331522348        0.1801132973        0.0142572037
 H         -1.3349177793        0.4188069792       -0.9113619922
 H         -1.3421851314       -0.0864875049        0.9273024225
 H          1.1985756666        0.1545110022        1.2889989324
 H          1.2699529592       -1.0247596049       -0.3051899562
```

Structure A.55: R27-H, $CH_3{-}SH$

```
   6
DFT-B3LYP/VTZ+D  ENERGY=-438.66020147
 C         -0.4626170987        0.1714940664        0.0000000000
 S          1.3608394811        0.2574181951        0.0000000000
 H          1.5911549935       -1.0648717473        0.0000000000
 H         -0.8137712909        1.2013712112        0.0000000000
 H         -0.8350960425       -0.3256333627        0.8924455403
 H         -0.8350960425       -0.3256333627       -0.8924455403
```

Structure A.56: R27, $\cdot CH_2{-}SH$

```
   5
DFT-B3LYP/VTZ+D  ENERGY=-438.00063481
 C         -0.5228744074       -0.2395646487        0.0000000000
 S          1.1943201546       -0.2950358202        0.0000000000
 H          1.4293062088        1.0265134535        0.0000000000
 H         -1.0606367062        0.6920288633        0.0000000000
 H         -1.0401152499       -1.1839418479        0.0000000000
```

Structure A.57: R28-H, $CH_3{-}SO{-}O{-}CH_3$

```
  11
DFT-B3LYP/VTZ+D  ENERGY=-628.38887134
 C          0.0000000000        1.3568509600       -0.3313689779
 S          0.0000000000        0.0026199382        0.8408677082
 C          0.0000000000       -1.4570552984       -0.1969243021
 H          0.0000000000        2.2649677103        0.2687385261
 H          0.8995866840        1.3120929457       -0.9408546317
 H         -0.8995866840        1.3120929457       -0.9408546317
 O          1.2512646521        0.0369175353        1.5578564935
 O         -1.2512646521        0.0369175353        1.5578564935
 H          0.0000000000       -2.3038935133        0.4870322220
 H          0.8997153664       -1.4702863794       -0.8076709500
 H         -0.8997153664       -1.4702863794       -0.8076709500
```

Structure A.58: R28, $\cdot CH_2{-}SO{-}O{-}CH_3$

```
  10
DFT-B3LYP/VTZ+D  ENERGY=-627.71416724
 C        -1.2613677909       -0.7737144107       -0.2042408058
 S        -0.3756778457        0.6467012165        0.2550825952
 C         1.3270459932        0.2188181503       -0.0791220893
 H        -2.2968036769       -0.6281504397       -0.4711736177
 H        -0.8578638857       -1.7555281113       -0.0091750647
 O        -0.7611481696        1.7175517546       -0.6309614261
 O        -0.5118318982        0.8184472277        1.6843305727
 H         1.4504050559        0.0198566185       -1.1408620823
 H         1.9109401814        1.0903606328        0.2128015214
 H         1.6116690365       -0.6385176388        0.5264503966
```

Structure A.59: R29-H, $CH_3{-}SO{-}CH_3$

```
  10
DFT-B3LYP/VTZ+D  ENERGY=-553.15316159
 C         0.2228427573       -0.0284411128        1.2280588266
 S        -0.8830683745       -0.8186513183        0.0159399378
 C        -0.0351046085       -0.1974970715       -1.4713660144
 H         0.2169879220        1.0488110909        1.0649018662
 H        -0.1822679940       -0.2557338612        2.2120561435
 H         1.2292888157       -0.4369344906        1.1386073003
 O        -2.1847616393       -0.1045493221        0.0954394031
 H         0.9751021497       -0.6031849592       -1.5231167716
 H        -0.6156913742       -0.5405756631       -2.3253014153
 H        -0.0232726542        0.8917097079       -1.4448542763
```

Structure A.60: R29, $\cdot CH_2{-}SO{-}CH_3$

```
   9
DFT-B3LYP/VTZ+D  ENERGY=-552.48400548
 C        -0.8053109214       -1.0744121734        0.2744357287
 S        -0.5289333017        0.2241503849       -0.8252150918
 C         0.9934872855        0.9255239081       -0.0923203055
 H        -0.0486838769       -1.8448643522        0.3421255099
 H        -1.8388260659       -1.3110756720        0.4832299319
 O        -1.5972839639        1.2439930747       -0.7348142510
 H         1.7580743838        0.1525936229       -0.0354472383
 H         1.3116517735        1.7252887312       -0.7576163368
 H         0.7486976870        1.3155634758        0.8930230529
```

Structure A.61: R30-H, $CH_3{-}C{\equiv}CH$

```
   7
DFT-B3LYP/VTZ+D  ENERGY=-116.62322242
 C        -0.0056577374        0.0099615611       -0.0039910008
 H         0.0085069703       -0.0150819613        1.0871233015
 H         1.0277564253       -0.0147637442       -0.3544476802
 H        -0.5012153586       -0.8972622907       -0.3543218269
 C        -0.6916475438        1.1982906015       -0.4888735189
 C        -1.2568209891        2.1773463165       -0.8889018202
 H        -1.7574217668        3.0433665170       -1.2427104546
```

Structure A.62: R30, $\cdot CH_2{-}C{\equiv}CH$

```
   6
DFT-B3LYP/VTZ+D  ENERGY=-115.97031347
 C         -0.0044826458        0.0000000000       -0.0024592708
 H          0.0114582895        0.0000000000        1.0781581778
 H          0.9391444370        0.0000000000       -0.5293892679
 C         -1.1880084470        0.0000000000       -0.6856559725
 C         -2.2422965229        0.0000000000       -1.2949243333
 H         -3.1613451108        0.0000000000       -1.8251763333
```

Structure A.63: M01, water, H_2O

```
   3
DFT-B3LYP/VTZ+D  ENERGY=-76.42271960
 H          0.0000000000        0.7605297729        0.8279979837
 O          0.0000000000        0.0000000000        0.2396078137
 H          0.0000000000       -0.7605297729        0.8279979837
```

Structure A.64: M02, formaldehyde, CH_2O

```
   4
DFT-B3LYP/VTZ+D  ENERGY=-114.49013093
 C          0.0000000000        0.0000000000       -0.5296889368
 O          0.0000000000        0.0000000000        0.6695864923
 H          0.0000000000       -0.9373964964       -1.1188113300
 H          0.0000000000        0.9373964964       -1.1188113300
```

Structure A.65: M03, methane, CH_4

```
   5
DFT-B3LYP/VTZ+D  ENERGY=-40.50228032
 H          0.6292770544        0.6292770544       -0.6292770544
 C          0.0000000000        0.0000000000        0.0000000000
 H         -0.6292770544       -0.6292770544       -0.6292770544
 H          0.6292770544       -0.6292770544        0.6292770544
 H         -0.6292770544        0.6292770544        0.6292770544
```

Structure A.66: M04, hydrazine, N_2H_4

```
   6
DFT-B3LYP/VTZ+D  ENERGY=-111.84519878
 N          0.0938524857       -0.7367579064        0.0000000000
 N         -0.0938524857        0.7367579064        0.0000000000
 H         -0.4561253949       -1.0533130942        0.7949907850
 H         -0.4561253949       -1.0533130942       -0.7949907850
 H          0.4561253949        1.0533130942       -0.7949907850
 H          0.4561253949        1.0533130942        0.7949907850
```

Structure A.67: M05, methylamine, CH_5N

```
   7
DFT-B3LYP/VTZ+D  ENERGY=-95.83429378
 C          0.0088476452        0.0042343948        0.0000000000
 N          1.4733078975       -0.0051885911        0.0000000000
 H         -0.4552103383        0.9997357933        0.0000000000
 H         -0.3545029758       -0.5330947308       -0.8771138273
 H         -0.3545029758       -0.5330947308        0.8771138273
 H          1.8283998736        0.4873784324        0.8108346709
 H          1.8283998736        0.4873784324       -0.8108346709
```

Structure A.68: M06, oxirane, C_2H_4O

```
   7
DFT-B3LYP/VTZ+D  ENERGY=-153.76031030
 C          0.0022481676       -0.1820401419        0.0000000000
 C          1.4658966389       -0.1836352145        0.0000000000
 O          0.7354125333        1.0435308181        0.0000000000
 H         -0.5330147151       -0.4022972530       -0.9179014017
 H         -0.5330147151       -0.4022972530        0.9179014017
 H          2.0006780452       -0.4050669778        0.9179001870
 H          2.0006780452       -0.4050669778       -0.9179001870
```

Structure A.69: M07, ethane, C_2H_6

```
   8
DFT-B3LYP/VTZ+D  ENERGY=-79.79915182
 C         -0.2287657583        0.2222831097       -0.0114604358
 C          1.2987655922        0.2120173542        0.0056203117
 H         -0.6193505409        1.2413779733       -0.0117347450
 H         -0.6394702189       -0.2871462896        0.8619687070
 H         -0.6196811650       -0.2797412361       -0.8981935027
 H          1.6896812927        0.7140434639        0.8923524316
 H          1.6893504801       -0.8070775258        0.0058971940
 H          1.7094703181        0.7214441503       -0.8678099607
```

Structure A.70: M08, urea, CH_4ON_2

```
   8
DFT-B3LYP/VTZ+D  ENERGY=-225.24305565
 O          1.9533685786       -1.1254837560        0.0000000000
 C          1.3442465772       -0.0708555347        0.0000000000
 N          1.9784181043        1.1469560352        0.0000000000
 N         -0.0275206087       -0.0112749508        0.0000000000
 H          2.9808597804        1.1381202289        0.0000000000
 H         -0.5211342139       -0.8837631583        0.0000000000
 H          1.4989894261        2.0271470199        0.0000000000
 H         -0.5495816441        0.8442621158        0.0000000000
```

Structure A.71: M09, oxalic acid, $C_2H_2O_4$

```
   8
DFT-B3LYP/VTZ+D  ENERGY=-378.31012355
 C          0.0012646014        0.0281239532        0.0000000000
 C          1.5431368954       -0.0281239001        0.0000000000
 O          2.2064290760        0.9747865045        0.0000000000
 O         -0.6620269779       -0.9747869696        0.0000000000
 O          2.0223555052       -1.2629253687        0.0000000000
 O         -0.4779564823        1.2629246167        0.0000000000
 H          1.2581145016       -1.8686162850        0.0000000000
 H          0.2862828804        1.8686174490        0.0000000000
```

Structure A.72: M10, dimethylether, C_2H_6O

```
   9
DFT-B3LYP/VTZ+D  ENERGY=-154.99439778
 C          0.0000000000        1.1738374410        0.0430612007
 O          0.0000000000        0.0000000000        0.8240610920
 C          0.0000000000       -1.1738374410        0.0430612007
 H         -0.8900320266        1.2342841898       -0.5970733937
 H          0.0000000000        2.0209378398        0.7269750407
 H          0.8900320266        1.2342841898       -0.5970733937
 H          0.8900320266       -1.2342841898       -0.5970733937
 H          0.0000000000       -2.0209378398        0.7269750407
 H         -0.8900320266       -1.2342841898       -0.5970733937
```

Structure A.73: M11, ethanol, C_2H_6O

```
   9
DFT-B3LYP/VTZ+D  ENERGY=-155.01051820
 C         -0.9306360741       -0.3891680879        0.0000000000
 C          0.3334058266        0.4456968169        0.0000000000
 H         -1.8128501290        0.2531576427        0.0000000000
 H         -0.9671351001       -1.0270204156       -0.8837230767
 H         -0.9671351001       -1.0270204156        0.8837230767
 H          0.3551019984        1.0932893056        0.8850561045
 H          0.3551019984        1.0932893056       -0.8850561045
 O          1.4498889029       -0.4428963038        0.0000000000
 H          2.2580926771        0.0772981521        0.0000000000
```

Structure A.74: M12, furan, C_4H_4O

```
   9
DFT-B3LYP/VTZ+D  ENERGY=-229.97559173
 O          0.0024787185        0.0035701257        0.0000000000
 C          1.3640571504        0.0001464721        0.0000000000
 C          1.8406374080        1.2683997259        0.0000000000
 C          0.6929495822        2.1253501902        0.0000000000
 C         -0.3877511014        1.3081656311        0.0000000000
 H          1.8324234143       -0.9674090696        0.0000000000
 H         -1.4484802965        1.4826764271        0.0000000000
 H          2.8758782070        1.5630169194        0.0000000000
 H          0.6812109174        3.2016595782        0.0000000000
```

Structure A.75: M13, imidazole, $C_3H_4N_2$

```
   9
DFT-B3LYP/VTZ+D  ENERGY=-226.16817125
 N         -1.1969247215        0.1266962331        0.0000000000
 C         -0.2925967839        1.0746288709        0.0000000000
 N          0.9701960761        0.5622299280        0.0000000000
 C          0.8537525978       -0.8091410286        0.0000000000
 C         -0.4914518169       -1.0534324301        0.0000000000
 H         -0.4861005031        2.1348739752        0.0000000000
 H          1.8278294918        1.0860989768        0.0000000000
 H          1.7105288067       -1.4585456615        0.0000000000
 H         -0.9910208017       -2.0073822975        0.0000000000
```

Structure A.76: M14, thiophene, C_4H_4S

```
   9
DFT-B3LYP/VTZ+D  ENERGY=-552.93686083
 S          0.0000000044        0.0000000000        1.1379205819
 C          1.2358551828        0.0000000000       -0.0573789674
 C          0.7113463181        0.0000000000       -1.3171816144
 C         -0.7113463216        0.0000000000       -1.3171815886
 C         -1.2358551787        0.0000000000       -0.0573789572
 H          2.2726311621        0.0000000000        0.2339563855
 H          1.3151780845        0.0000000000       -2.2127649361
 H         -1.3151780898        0.0000000000       -2.2127648893
 H         -2.2726311617        0.0000000000        0.2339563354
```

Structure A.77: M15, butadiene, C_4H_6

```
  10
DFT-B3LYP/VTZ+D  ENERGY=-155.94633228
 C          1.8406702838        0.1184396624        0.0000000000
 C          0.6094711233       -0.3956807982        0.0000000000
 C         -0.6094711233        0.3956807982        0.0000000000
 C         -1.8406702838       -0.1184396624        0.0000000000
 H          2.0082346672        1.1890042581        0.0000000000
 H          2.7198071134       -0.5150465733        0.0000000000
 H          0.4831444797       -1.4718907941        0.0000000000
 H         -0.4831444797        1.4718907941        0.0000000000
 H         -2.0082346672       -1.1890042581        0.0000000000
 H         -2.7198071134        0.5150465733        0.0000000000
```

Structure A.78: M16, glycine, $C_2H_5O_2N$

```
  10
DFT-B3LYP/VTZ+D  ENERGY=-284.40023129
 N          0.1872669131        0.1004923770        1.6467939120
 C         -0.4745512166       -0.0495772996        0.3680139628
 C          0.4304570747       -0.0087987774       -0.8542172576
 O         -0.2776968664       -0.1609243346       -1.9980913091
 H          0.3537610931       -0.1237687638       -2.7319867562
 H          0.6995438905        0.9743756452        1.6726313397
 H          0.8813012341       -0.6278796141        1.7673289920
 H         -1.2294304082        0.7308460001        0.2438836003
 H         -1.0241375235       -0.9936317993        0.3396611132
 O          1.6246648093        0.1385455667       -0.8376245972
```

Structure A.79: M17, propionyl chloride, C_3H_5OCl

```
  10
DFT-B3LYP/VTZ+D  ENERGY=-652.69595862
 C          0.0650142971        0.0033577200        0.0774476606
 O          0.2253754550        0.0171256136        1.2469949947
 Cl         1.5073728421       -0.0330126657       -1.0439866947
 C         -1.2328832057        0.0119748548       -0.6835459293
 C         -2.4560100600        0.0431497125        0.2262563026
 H         -1.2025944620        0.8712475920       -1.3575964898
 H         -1.2285222419       -0.8663492113       -1.3332819544
 H         -3.3651680090        0.0493425333       -0.3746129866
 H         -2.4824954123       -0.8275653019        0.8801720969
 H         -2.4548692034        0.9316551527        0.8563519999
```

Structure A.80: M18, propane, C_3H_8

```
  11
DFT-B3LYP/VTZ+D  ENERGY=-119.09793677
 C          0.0000000484        0.0000000000       -0.5772534554
 C         -1.2748930582        0.0000000000        0.2656465152
 C          1.2748928676        0.0000000000        0.2656465091
 H         -0.0000000848       -0.8737158971       -1.2350651571
 H         -0.0000000848        0.8737158971       -1.2350651571
 H         -2.1691246096        0.0000000000       -0.3600607585
 H         -1.3208664101       -0.8811254827        0.9098961802
 H         -1.3208664101        0.8811254827        0.9098961802
 H          2.1691245029        0.0000000000       -0.3600605507
 H          1.3208666193        0.8811253876        0.9098962118
 H          1.3208666193       -0.8811253876        0.9098962118
```

Structure A.81: M19, isobutene, C_4H_8

```
  12
DFT-B3LYP/VTZ+D  ENERGY=-157.17330775
 C         -0.0000000013        0.0000000000        0.1000809085
 C         -0.0000000018        0.0000000000        1.4306264582
 C         -1.2738002893        0.0000000000       -0.6998472057
 C          1.2738002902        0.0000000000       -0.6998472037
 H         -0.9223478843        0.0000000000        1.9977742279
 H          0.9223478804        0.0000000000        1.9977742286
 H         -1.3255798270        0.8766164020       -1.3524838145
 H         -1.3255798270       -0.8766164020       -1.3524838145
 H         -2.1540145344        0.0000000000       -0.0581006873
 H          1.3255798255        0.8766164014       -1.3524838135
 H          1.3255798255       -0.8766164014       -1.3524838135
 H          2.1540145435        0.0000000000       -0.0581006936
```

Structure A.82: M20, benzene, C_6H_6

```
  12
DFT-B3LYP/VTZ+D  ENERGY=-232.17901211
 C          0.6285811217        1.2406955739        0.0014619157
 C          1.3886058128        0.0755889634        0.0032056664
 C          0.7598547531       -1.1652944558        0.0036839044
 C         -0.6291522065       -1.2411445737        0.0023572559
 C         -1.3891772426       -0.0760358177        0.0006140979
 C         -0.7604239515        1.1648465967        0.0001376326
 H          1.1180774650        2.2060550278        0.0011340372
 H          2.4693663032        0.1345606548        0.0041906955
 H          1.3514527604       -2.0716664322        0.0050926860
 H         -1.1186497991       -2.2065053929        0.0026819416
 H         -2.4699383781       -0.1350077470       -0.0003707693
 H         -1.3520216385        2.0712176027       -0.0012690638
```

Structure A.83: M21, benzoquinone, $C_6H_4O_2$

```
  12
DFT-B3LYP/VTZ+D  ENERGY=-381.38417864
 C          0.0000000000        1.2655770320       -0.6679445091
 H          0.0000000000        2.1760329835       -1.2533079526
 C          0.0000000000        1.2655770216        0.6679445082
 H          0.0000000000        2.1760329681        1.2533079522
 C          0.0000000000        0.0000000009        1.4400321650
 O          0.0000000000        0.0000000154        2.6582516630
 C          0.0000000000       -1.2655770303        0.6679445097
 H          0.0000000000       -2.1760329937        1.2533079422
 C          0.0000000000       -1.2655770200       -0.6679445088
 H          0.0000000000       -2.1760329784       -1.2533079418
 C          0.0000000000        0.0000000068       -1.4400321650
 O          0.0000000000       -0.0000000058       -2.6582516630
```

Structure A.84: M22, alanine, $C_3H_7O_2N$

```
  13
DFT-B3LYP/VTZ+D  ENERGY=-323.70090448
 O         -0.3057123106        2.2972847369        0.2743575320
 C          0.4577581270        1.3795115669        0.1161034073
 O          1.8023782917        1.5442373493        0.0902638742
 H          1.9741948885        2.4918166876        0.1991087966
 C          0.0556140959       -0.0791965039       -0.0992679465
 N         -1.2944635176       -0.3794509604        0.3509031158
 H         -1.9471283885        0.2615897248       -0.0882063844
 H         -1.3765668425       -0.2149471093        1.3476396861
 H          0.7543610176       -0.6930797064        0.4730309297
 C          0.2113588302       -0.4273546566       -1.5856903080
 H         -0.0360981106       -1.4766655064       -1.7360181444
 H          1.2286837545       -0.2443904875       -1.9285986609
 H         -0.4697778354        0.1751628648       -2.1901768975
```

Structure A.85: M23, thiophenol, C_6H_6S

```
  13
DFT-B3LYP/VTZ+D  ENERGY=-630.34240602
 C          0.4601405087        0.0233785561        0.0000000000
 S          2.2351319717       -0.0362681534        0.0000000000
 C         -0.2609643023        1.2179653753        0.0000000000
 H          0.2578602367        2.1675328073        0.0000000000
 C         -1.6502232980        1.1921876858        0.0000000000
 H         -2.1974153601        2.1260100694        0.0000000000
 C         -2.3351113306       -0.0173973596        0.0000000000
 H         -3.4164783488       -0.0328147967        0.0000000000
 C         -1.6158324581       -1.2075422120        0.0000000000
 H         -2.1360063974       -2.1565844473        0.0000000000
 C         -0.2275558865       -1.1921405042        0.0000000000
 H          0.3230480338       -2.1240552923        0.0000000000
 H          2.4470810261        1.2881071594        0.0000000000
```

Structure A.86: M24, butane, C_4H_{10}

```
  14
DFT-B3LYP/VTZ+D  ENERGY=-158.39678461
 C          0.5702810342       -0.5095628969        0.0000000000
 C          1.9567008758        0.1329960040        0.0000000000
 C         -0.5702810763        0.5095629707        0.0000000000
 C         -1.9567008559       -0.1329960425        0.0000000000
 H          0.4691571935       -1.1605441351       -0.8743932786
 H          0.4691571935       -1.1605441351        0.8743932786
 H          2.7466878526       -0.6198675515        0.0000000000
 H          2.0995172576        0.7630872638       -0.8808690365
 H          2.0995172576        0.7630872638        0.8808690365
 H         -0.4691572591        1.1605442088        0.8743932813
 H         -0.4691572591        1.1605442088       -0.8743932813
 H         -2.7466878709        0.6198674645        0.0000000000
 H         -2.0995171717       -0.7630873116       -0.8808690421
 H         -2.0995171717       -0.7630873116        0.8808690421
```

Structure A.87: M25, hexatriene, C_6H_8

```
  14
DFT-B3LYP/VTZ+D  ENERGY=-233.32925002
 C         -3.0657629478        0.1366675653        0.0000000000
 C         -1.8578170827       -0.4359906615        0.0000000000
 C         -0.6073457894        0.2898242385        0.0000000000
 C          0.6073458827       -0.2898262068        0.0000000000
 C          1.8578165332        0.4359898195        0.0000000000
 C          3.0657633232       -0.1366663605        0.0000000000
 H         -3.1794894325        1.2141572116        0.0000000000
 H         -3.9728676848       -0.4513611086        0.0000000000
 H         -1.7851073400       -1.5197612624        0.0000000000
 H         -0.6734395580        1.3747231063        0.0000000000
 H          0.6734399569       -1.3747250763        0.0000000000
 H          1.7851051839        1.5197603250        0.0000000000
 H          3.1794921894       -1.2141557943        0.0000000000
 H          3.9728667660        0.4513642042        0.0000000000
```

Structure A.88: M26, aniline, C_6H_7N

```
  14
DFT-B3LYP/VTZ+D  ENERGY=-287.52884233
 C          2.1502983444       -1.2013566593       -0.2687920278
 C          1.3808812944       -0.0323394081       -0.3030239823
 C          2.0415600222        1.2014402907       -0.3366978936
 C          3.4279490839        1.2590684893       -0.3370058014
 C          4.1887079196        0.0949558592       -0.3042483536
 C          3.5363979556       -1.1331523686       -0.2701391846
 N         -0.0121608516       -0.0934311847       -0.2420779779
 H         -0.4910479314        0.7142250761       -0.6075620848
 H         -0.4178568064       -0.9518298025       -0.5794292729
 H          1.4612433556        2.1163133955       -0.3577130323
 H          3.9169051954        2.2246175845       -0.3650202911
 H          5.2688708033        0.1442300030       -0.3060153168
 H          4.1106949033       -2.0505789467       -0.2448005506
 H          1.6552807117       -2.1647713287       -0.2356452303
```

Structure A.89: M27, catechol, $C_6H_6O_2$

```
  14
DFT-B3LYP/VTZ+D  ENERGY=-382.62313209
 C         -0.0162710592       -1.3978740589        0.0020238277
 C          1.1878149135       -0.7127592471        0.0005098979
 C          1.2060244645        0.6871186098       -0.0016321449
 C          0.0066158385        1.3839314715       -0.0021153834
 C         -1.2032616653        0.6952878593       -0.0005741479
 C         -1.2181710878       -0.6929796225        0.0016031622
 O          2.4247622483       -1.3184352559        0.0008130514
 O          2.3880013969        1.3652829537       -0.0031667528
 H          0.0383666833        2.4650334520       -0.0036228959
 H         -2.1321846475        1.2492160170       -0.0010904370
 H         -2.1551726390       -1.2325744012        0.0029344339
 H         -0.0163492123       -2.4822706628        0.0034879740
 H          2.3216640747       -2.2743647955        0.0033229315
 H          3.1050736913        0.7191836805       -0.0024945167
```

Structure A.90: M28, pentane, C_5H_{12}

```
  17
DFT-B3LYP/VTZ+D  ENERGY=-197.69537268
 C         -0.0000000950        0.0000000000       -0.3182606618
 C         -1.2817458631        0.0000000000        0.5164574288
 C          1.2817458154        0.0000000000        0.5164572707
 C          2.5553810475        0.0000000000       -0.3282709027
 C         -2.5553809694        0.0000000000       -0.3282708797
 H         -0.0000001313       -0.8747607467       -0.9782069639
 H         -0.0000001313        0.8747607467       -0.9782069639
 H         -1.2819694290       -0.8743163554        1.1750540119
 H         -1.2819694290        0.8743163554        1.1750540119
 H          1.2819693686       -0.8743163517        1.1750538619
 H          1.2819693686        0.8743163517        1.1750538619
 H          3.4497852259        0.0000000000        0.2971516194
 H          2.6020669706       -0.8811069315       -0.9723201872
 H          2.6020669706        0.8811069315       -0.9723201872
 H         -3.4497852472        0.0000000000        0.2971515089
 H         -2.6020667360        0.8811069292       -0.9723201675
 H         -2.6020667360       -0.8811069292       -0.9723201675
```

Structure A.91: M29, cyclohexane, C_6H_{12}

```
  18
DFT-B3LYP/VTZ+D  ENERGY=-235.79016673
 C          1.2677663162       -0.7319385326        0.2273164157
 C          1.2677663049        0.7319385367       -0.2273164173
 C          0.0000000037        1.4638217177        0.2280388670
 C         -1.2677663101        0.7319385409       -0.2273164110
 C         -1.2677663065       -0.7319385374        0.2273164096
 C          0.0000000085       -1.4638217185       -0.2280388633
 H          2.1560761550       -1.2449685001       -0.1493584627
 H          1.3290076931       -0.7682471499        1.3206502529
 H          2.1560761438        1.2449684912        0.1493584666
 H          1.3290076829        0.7682471561       -1.3206502543
 H          0.0000000057        1.5362352675        1.3213151572
 H          0.0000000038        2.4891180509       -0.1502868899
 H         -2.1560761691        1.2449684890        0.1493584592
 H         -1.3290076837        0.7682471597       -1.3206502486
 H         -1.3290076812       -0.7682471551        1.3206502472
 H         -2.1560761631       -1.2449684912       -0.1493584593
 H          0.0000000099       -1.5362352656       -1.3213151538
 H         -0.0000000139       -2.4891180594        0.1502868846
```

Structure A.92: M30, hexane, C_6H_{14}

```
  20
DFT-B3LYP/VTZ+D  ENERGY=-236.99396289
 C         -0.6656341749       -0.3762819404        0.0000000000
 C         -1.8912990858        0.5393318339        0.0000000000
 C          0.6656341468        0.3762819551        0.0000000000
 C          1.8912990740       -0.5393318166        0.0000000000
 C         -3.2163127740       -0.2222507366        0.0000000000
 C          3.2163127899        0.2222507171        0.0000000000
 H         -0.7098944558       -1.0346288322       -0.8746689403
 H         -0.7098944558       -1.0346288322        0.8746689403
 H         -1.8495236605        1.1965159262       -0.8743576422
 H         -1.8495236605        1.1965159262        0.8743576422
 H          0.7098944309        1.0346288466       -0.8746689404
 H          0.7098944309        1.0346288466        0.8746689404
 H          1.8495236545       -1.1965159137        0.8743576451
 H          1.8495236545       -1.1965159137       -0.8743576451
 H         -4.0688409171        0.4591297526        0.0000000000
 H         -3.3048125953       -0.8620711088        0.8810567475
 H         -3.3048125953       -0.8620711088       -0.8810567475
 H          4.0688409247       -0.4591297826        0.0000000000
 H          3.3048126345        0.8620710905        0.8810567493
 H          3.3048126345        0.8620710905       -0.8810567493
```

Structure A.93: oxygen, O_2

```
   2
DFT-B3LYP/VTZ+D  ENERGY=-150.26891311
 O          0.0000000000        0.0000000000       -0.6083560000
 O          0.0000000000        0.0000000000        0.6083560000
```

Structure A.94: $(CuL0)^+$, $[Cu(NH_3)_4]^+$

```
  17
DFT-B3LYP/VTZ+D  ENERGY=-423.36217082
 N          1.2829181000        1.6796477000       -0.4436284000
 Cu        -0.0025588000        0.0030591000       -0.0002627000
 N          0.6419612000       -0.9266140000        1.8396037000
 N         -2.0401679000        0.6840373000        0.2095617000
 N          0.1152260000       -1.4365487000       -1.6055209000
 H         -0.3114605000       -2.3380206000       -1.3760182000
 H          1.0749083000       -1.6558803000       -1.8852173000
 H         -0.3514484000       -1.1273832000       -2.4622864000
 H          2.2782735000        1.4686106000       -0.3339852000
 H          1.1118414000        2.4916749000        0.1553338000
 H          1.1846600000        2.0256934000       -1.4017648000
 H         -2.2673677000        1.4795063000       -0.3929720000
 H         -2.7342065000       -0.0328022000       -0.0182785000
 H         -2.2715246000        0.9904314000        1.1582619000
 H          0.7874288000       -0.2606388000        2.6029807000
 H          1.5270058000       -1.4327559000        1.7511228000
 H         -0.0254886000       -1.6120170000        2.2030699000
```

Structure A.95: $(CuL0O_2)^+$, $[Cu(NH_3)_4O_2]^+$

```
  19
DFT-B3LYP/VTZ+D  ENERGY=-573.63817749
 Cu        -0.1127867000       -0.0579900000        0.0000000000
 O         -0.1003947000       -2.1933672000        0.0000000000
 O          1.0231231000       -2.7322530000        0.0000000000
 N         -2.2339878000       -0.4056542000        0.0000000000
 N         -0.2283025000        2.1300903000        0.0000000000
 H         -2.3628238000       -1.4221515000        0.0000000000
 H          0.6906471000        2.5812738000        0.0000000000
 N          1.1105757000       -0.2782534000        1.7801998000
 N          1.1105757000       -0.2782534000       -1.7801998000
 H         -0.7182213000        2.5087416000        0.8154010000
 H         -0.7182213000        2.5087416000       -0.8154010000
 H         -2.7446232000       -0.0585248000        0.8163467000
 H         -2.7446232000       -0.0585248000       -0.8163467000
 H          0.5721042000       -0.4779801000        2.6276941000
 H          0.5721042000       -0.4779801000       -2.6276941000
 H          1.6814346000       -1.1136627000        1.6150774000
 H          1.6814346000       -1.1136627000       -1.6150774000
 H          1.7609927000        0.4697054000        2.0333004000
 H          1.7609927000        0.4697054000       -2.0333004000
```

Structure A.96: (CuL1)$^+$, [Cu($C_{18}N_4H_{18}$)]$^+$

```
  41
DFT-B3LYP/VTZ+D  ENERGY=-1112.64499511
 C          0.0068490000       -0.0073476000        0.0235675000
 C         -0.0080738000        0.0251439000        1.4213841000
 N          1.1375520000        0.0533567000        2.1373709000
 C          2.3132625000        0.0385801000        1.4872964000
 C          2.4090069000       -0.0090338000        0.0971319000
 C          1.2301763000       -0.0298570000       -0.6502185000
 Cu         0.8268113000        0.3298650000        4.1511242000
 C         -1.3234823000       -0.0450929000        2.1915834000
 N         -1.2971065000        0.6785689000        3.4586924000
 C         -2.0749518000        0.0891353000        4.5439580000
 C         -1.4242542000       -1.1459458000        5.1605628000
 C         -2.2043557000       -2.1715254000        5.7036520000
 C         -1.5795206000       -3.2467903000        6.3395240000
 C         -0.1853291000       -3.2698587000        6.4062245000
 C          0.5243575000       -2.2180219000        5.8284930000
 N         -0.0751137000       -1.1801552000        5.2216715000
 C         -1.3436252000        2.1344029000        3.3616243000
 C         -0.5374233000        2.8397035000        4.4479966000
 C         -0.9400022000        4.0803615000        4.9513670000
 C         -0.1354950000        4.7362455000        5.8862578000
 C          1.0497439000        4.1251612000        6.2986591000
 C          1.3770766000        2.8806977000        5.7615542000
 N          0.6074447000        2.2510671000        4.8585540000
 H          3.2140859000        0.0667019000        2.1068490000
 H          3.3895854000       -0.0225785000       -0.3827196000
 H         -1.5116840000       -1.1084767000        2.4199840000
 H         -2.1524468000        0.2775136000        1.5309384000
 H         -2.1590250000        0.8464689000        5.3425089000
 H         -0.9025327000        2.4171848000        2.3901844000
 H         -2.3780925000        2.5313553000        3.3558960000
 H         -3.1133370000       -0.1545302000        4.2438102000
 H         -3.2934863000       -2.1230393000        5.6305669000
 H         -2.1734199000       -4.0557154000        6.7719964000
 H          0.3497511000       -4.0891479000        6.8903802000
 H          1.6177254000       -2.2047999000        5.8515340000
 H          2.2922308000        2.3654825000        6.0669503000
 H          1.7108733000        4.5959060000        7.0289418000
 H         -0.4334390000        5.7073443000        6.2890654000
 H         -1.8763005000        4.5278913000        4.6093247000
 H          1.2608433000       -0.0586213000       -1.7421741000
 H         -0.9351615000       -0.0183819000       -0.5299360000
```

Structure A.97: $(CuL1O_2)^+$, $[Cu(C_{18}N_4H_{18})O_2]^+$

```
 43
DFT-B3LYP/VTZ+D  ENERGY=-1262.93391414
 C          0.0528878000       -0.4933425000       -3.8348885000
 C          0.0650403000       -0.4450888000       -2.4376687000
 N          1.2198288000       -0.4077113000       -1.7458239000
 C          2.3871255000       -0.4345029000       -2.4052576000
 C          2.4596471000       -0.4979346000       -3.7969129000
 C          1.2680174000       -0.5230235000       -4.5242297000
 Cu         0.9726405000       -0.1071539000        0.3443336000
 O          2.8627477000       -0.2253002000        1.0176877000
 O          3.4042603000       -1.3450347000        0.9208808000
 C         -1.2196044000       -0.5136543000       -1.6252847000
 N         -1.1305071000        0.2170374000       -0.3558779000
 C         -1.9528918000       -0.3490795000        0.7198725000
 C         -1.3572699000       -1.6231091000        1.2997012000
 C         -2.1618293000       -2.6358950000        1.8296249000
 C         -1.5539689000       -3.7503989000        2.4140115000
 C         -0.1601011000       -3.8254245000        2.4399086000
 C          0.5729485000       -2.7796795000        1.8781362000
 N         -0.0132248000       -1.7061714000        1.3287360000
 C         -1.2471337000        1.6730415000       -0.4946116000
 C         -0.4859022000        2.4264271000        0.5851822000
 C         -0.9053500000        3.6765625000        1.0485861000
 C         -0.1149938000        4.3554592000        1.9800031000
 C          1.0678387000        3.7621670000        2.4259245000
 C          1.4106236000        2.5057844000        1.9258677000
 N          0.6516357000        1.8588570000        1.0296140000
 H          3.2930907000       -0.4088965000       -1.7928740000
 H          3.4316503000       -0.5212505000       -4.2933422000
 H         -1.4041946000       -1.5750355000       -1.3872439000
 H         -2.0771151000       -0.1798709000       -2.2401634000
 H         -2.0036721000        0.3986063000        1.5298597000
 H         -0.8081248000        1.9515200000       -1.4680085000
 H         -2.3017177000        2.0084328000       -0.5214753000
 H         -2.9964785000       -0.5301309000        0.3979282000
 H         -3.2501075000       -2.5504810000        1.7864313000
 H         -2.1634448000       -4.5526375000        2.8374955000
 H          0.3570709000       -4.6800039000        2.8803941000
 H          1.6669770000       -2.7964353000        1.8584989000
 H          2.3231895000        1.9941751000        2.2465380000
 H          1.7148829000        4.2565368000        3.1531168000
 H         -0.4225951000        5.3348719000        2.3547550000
 H         -1.8373628000        4.1127754000        0.6814532000
 H          1.2823674000       -0.5631284000       -5.6162821000
 H         -0.8968804000       -0.5118794000       -4.3745964000
```

Structure A.98: (CuL2)$^+$, [Cu($C_{20}N_4H_{22}$)]$^+$

```
 47
DFT-B3LYP/VTZ+D  ENERGY=-1191.25275278
 N          0.6187715000        2.2313378000        4.8488409000
 C         -0.5196536000        2.8276345000        4.4323148000
 C         -0.9101529000        4.0773160000        4.9235869000
 C         -0.1012512000        4.7339455000        5.8535501000
 C          1.0774457000        4.1148111000        6.2730833000
 C          1.3929577000        2.8627645000        5.7469551000
 C         -1.3361683000        2.1215332000        3.3547191000
 N         -1.2990489000        0.6673566000        3.4616496000
 C         -2.0865558000        0.0927199000        4.5473828000
 C         -1.4561609000       -1.1516516000        5.1648305000
 C         -2.2528347000       -2.1637898000        5.7041655000
 C         -1.6351009000       -3.2392619000        6.3459339000
 C         -0.2435378000       -3.2744146000        6.4191326000
 C          0.5021066000       -2.2378518000        5.8415790000
 N         -0.1088697000       -1.2012560000        5.2310673000
 Cu         0.8244211000        0.2893288000        4.1548836000
 N          1.1252772000        0.0504445000        2.1260698000
 C         -0.0233208000        0.0199977000        1.4177585000
 C         -0.0213186000        0.0054539000        0.0213032000
 C          1.2020413000        0.0059501000       -0.6519870000
 C          2.3823129000        0.0328376000        0.0895290000
 C          2.3150332000        0.0611739000        1.4890353000
 C         -1.3307819000       -0.0638880000        2.1990348000
 C          3.5463580000        0.1058186000        2.3501098000
 H          3.3547423000        0.0401231000       -0.4065561000
 H         -1.5053639000       -1.1275877000        2.4364680000
 H         -2.1693166000        0.2468043000        1.5446766000
 H         -2.1575645000        0.8522135000        5.3452282000
 H         -0.8999177000        2.3962485000        2.3788312000
 H         -2.3679023000        2.5259923000        3.3536461000
 H         -3.1291037000       -0.1333483000        4.2475264000
 H         -3.3407672000       -2.1044072000        5.6265125000
 H         -2.2334054000       -4.0429202000        6.7821427000
 H          0.2703005000       -4.1009806000        6.9135512000
 C          2.0052044000       -2.2322181000        5.8520663000
 H          2.3032916000        2.3423748000        6.0582146000
 H          1.7418493000        4.5854707000        7.0003337000
 H         -0.3906060000        5.7113131000        6.2474768000
 H         -1.8416768000        4.5300211000        4.5755660000
 H          1.2339348000       -0.0073319000       -1.7442170000
 H         -0.9656081000       -0.0076206000       -0.5275570000
 H          2.3943729000       -2.4404172000        4.8402594000
 H          2.3829164000       -1.2421107000        6.1534706000
 H          2.4134715000       -2.9899836000        6.5348790000
 H          4.4644416000        0.1698405000        1.7501637000
 H          3.5057657000        0.9764821000        3.0255991000
 H          3.6085767000       -0.7963032000        2.9816995000
```

Structure A.99: $(CuL2O_2)^+$, $[Cu(C_{20}N_4H_{22})O_2]^+$

```
 49
DFT-B3LYP/VTZ+D  ENERGY=-1341.53415794
 N          0.7128761000        1.8071768000        1.0975239000
 C         -0.3720741000        2.3741293000        0.5312255000
 C         -0.8209460000        3.6467897000        0.8898608000
 C         -0.1109873000        4.3595415000        1.8568389000
 C          1.0061895000        3.7683946000        2.4412175000
 C          1.3981466000        2.4787379000        2.0499125000
 C         -1.0748434000        1.5928790000       -0.5658885000
 N         -1.0147645000        0.1447658000       -0.3467829000
 C         -1.8927936000       -0.3253258000        0.7292788000
 C         -1.3856190000       -1.6097439000        1.3601244000
 C         -2.2574080000       -2.5368375000        1.9387507000
 C         -1.7278986000       -3.6690121000        2.5622945000
 C         -0.3432317000       -3.8467632000        2.5746522000
 C          0.4580483000       -2.8825061000        1.9628753000
 N         -0.0511114000       -1.7887569000        1.3763265000
 Cu         1.0362323000       -0.2357044000        0.3497395000
 O          2.8589552000       -0.7334481000        1.0383308000
 O          3.2189003000       -1.9011542000        0.7822119000
 N          1.2907791000       -0.3262497000       -1.8368304000
 C          0.1085140000       -0.5230463000       -2.4548227000
 C          0.0013908000       -0.6415374000       -3.8414302000
 C          1.1629925000       -0.5619643000       -4.6108296000
 C          2.3787842000       -0.3398712000       -3.9699968000
 C          2.4193204000       -0.2154000000       -2.5721057000
 C         -1.1231940000       -0.6479439000       -1.5753073000
 C          3.7185313000        0.0453315000       -1.8636582000
 H          3.3035751000       -0.2515954000       -4.5432698000
 H         -1.2346087000       -1.7058458000       -1.2825008000
 H         -2.0281477000       -0.3875662000       -2.1576550000
 H         -1.9149753000        0.4532725000        1.5105946000
 H         -0.5660212000        1.8098889000       -1.5198290000
 H         -2.1154590000        1.9531034000       -0.6772886000
 H         -2.9374708000       -0.4546544000        0.3866197000
 H         -3.3366846000       -2.3711716000        1.9005663000
 H         -2.3895604000       -4.4055137000        3.0250115000
 H          0.1155150000       -4.7200086000        3.0424057000
 H          1.5455130000       -2.9890393000        1.9301533000
 C          2.5827944000        1.8071423000        2.6837809000
 H          1.5778800000        4.2932837000        3.2088165000
 H         -0.4322326000        5.3597505000        2.1579474000
 H         -1.7106971000        4.0689117000        0.4175543000
 H          1.1169555000       -0.6556332000       -5.6986561000
 H         -0.9753524000       -0.7911361000       -4.3068163000
 H          2.2936128000        0.8385413000        3.1200565000
 H          3.3648471000        1.5960101000        1.9384282000
 H          3.0161254000        2.4328049000        3.4752053000
 H          4.4890571000        0.3869164000       -2.5679308000
 H          3.5899443000        0.8056589000       -1.0793269000
 H          4.0870464000       -0.8695176000       -1.3729104000
```

Structure A.100: (CuL3)$^+$, [Cu($C_{16}N_3SH_{21}$)]$^+$

```
  42
DFT-B3LYP/VTZ+D  ENERGY=-1381.66594047
 N          2.9093087000       -0.0182086000       -3.8261807000
 C          1.8268380000       -0.0530541000       -3.0167965000
 C          1.9533419000       -0.1810997000       -1.6308367000
 C          3.2250036000       -0.2496355000       -1.0593479000
 C          4.3406378000       -0.1912685000       -1.8972253000
 C          4.1348022000       -0.0824798000       -3.2707132000
 C          0.4549265000        0.1483572000       -3.6512349000
 N          0.3500203000       -0.3506491000       -5.0286713000
 C          0.0797133000       -1.7940030000       -5.1197899000
 C          0.5053298000       -2.4189313000       -6.4579799000
 S          2.2393162000       -2.0513772000       -7.0158190000
 C          3.1950978000       -3.5232491000       -6.4143323000
 C          3.2590819000       -3.7501182000       -4.9097388000
 Cu         2.4462775000       -0.0917061000       -5.8172256000
 C         -0.4751942000        0.4995303000       -5.8943630000
 C          0.2715490000        1.7257981000       -6.4092605000
 C         -0.4195508000        2.8983245000       -6.7244578000
 C          0.2738245000        3.9777009000       -7.2749417000
 C          1.6476383000        3.8525642000       -7.4899225000
 C          2.2698647000        2.6572838000       -7.1354452000
 N          1.6047725000        1.6136520000       -6.6043687000
 H          2.7689870000       -4.3901008000       -6.9388027000
 H          4.1955895000       -3.3485246000       -6.8349304000
 H          3.6686217000       -2.8768247000       -4.3856248000
 H          2.2718945000       -3.9832248000       -4.4864327000
 H          3.9125873000       -4.6117238000       -4.7051817000
 H          0.3911166000       -3.5101789000       -6.4082163000
 H         -0.1315620000       -2.0721410000       -7.2820610000
 H          0.6287556000       -2.2752647000       -4.3008643000
 H         -0.9943378000       -2.0182312000       -4.9653935000
 H          0.2686686000        1.2329499000       -3.6731091000
 H         -0.7818097000       -0.0909417000       -6.7694684000
 H         -1.4091239000        0.8204579000       -5.4000133000
 H         -0.3196515000       -0.2842039000       -2.9935236000
 H          1.0597123000       -0.2210976000       -1.0064487000
 H          3.3419515000       -0.3465649000        0.0208770000
 H          5.3545468000       -0.2358826000       -1.5001512000
 H          4.9794497000       -0.0462704000       -3.9596468000
 H          3.3425671000        2.5239150000       -7.2790345000
 H          2.2336574000        4.6650458000       -7.9188760000
 H         -0.2499207000        4.9001310000       -7.5292788000
 H         -1.4932214000        2.9609725000       -6.5417762000
```

Structure A.101: $(CuL3O_2)^+$, $[Cu(C_{16}N_3SH_{21})O_2]^+$

```
 44
DFT-B3LYP/VTZ+D  ENERGY=-1531.94836685
 C          2.9139893000       -0.0839486000       -3.8524744000
 C          1.8067130000       -0.0322654000       -3.0038368000
 N          1.9332274000       -0.1399911000       -1.6651770000
 C          3.1569141000       -0.3104956000       -1.1343934000
 C          4.3083013000       -0.3889125000       -1.9167416000
 C          4.1841060000       -0.2709968000       -3.3022590000
 C          0.3944226000        0.0860654000       -3.5544079000
 N         -0.5177695000        0.7488398000       -2.6030853000
 C         -0.3433565000        2.2157918000       -2.6113398000
 C         -0.6545323000        2.8583847000       -1.2712862000
 C         -1.1205739000        4.1719570000       -1.1843942000
 C         -1.2854620000        4.7522896000        0.0752425000
 C         -0.9814592000        3.9984205000        1.2107745000
 C         -0.5368085000        2.6880500000        1.0410079000
 N         -0.3805539000        2.1286811000       -0.1715236000
 Cu         0.1537871000        0.1297075000       -0.5733746000
 S         -1.4996220000       -1.6549019000       -0.8100205000
 C         -2.2366269000       -1.0893977000       -2.4088688000
 C         -1.9378796000        0.3704738000       -2.7710201000
 O          0.6544401000       -0.4190395000        1.2763859000
 O          1.6839957000        0.1524109000        1.7392596000
 C         -2.9027236000       -1.5348155000        0.3932560000
 C         -3.5303389000       -0.1608903000        0.5859245000
 H         -3.6419632000       -2.2809928000        0.0706306000
 H         -2.4491719000       -1.9030613000        1.3242774000
 H         -2.7887847000        0.5799963000        0.9116412000
 H         -4.0150345000        0.2031940000       -0.3312257000
 H         -4.3093822000       -0.2290620000        1.3600463000
 H         -3.3229151000       -1.2405953000       -2.3637592000
 H         -1.8551321000       -1.7831536000       -3.1687745000
 H         -2.5212455000        1.0354930000       -2.1218914000
 H         -2.2721564000        0.5530165000       -3.8102939000
 H          0.7110008000        2.4274373000       -2.8434867000
 H          0.0209114000       -0.9293667000       -3.7449933000
 H          0.4119582000        0.5998215000       -4.5308682000
 H         -0.9432398000        2.6888437000       -3.4074464000
 H         -1.3439269000        4.7340679000       -2.0921553000
 H         -1.6449899000        5.7781568000        0.1671198000
 H         -1.0887344000        4.4114758000        2.2133884000
 H         -0.2896642000        2.0604419000        1.8973985000
 H          3.2036207000       -0.3753954000       -0.0470690000
 H          5.2789181000       -0.5317192000       -1.4424527000
 H          5.0628058000       -0.3184068000       -3.9470328000
 H          2.7815117000        0.0183891000       -4.9303952000
```

Structure A.102: (CuL4)$^+$, [Cu($C_{18}N_3SH_{25}$)]$^+$

```
  48
DFT-B3LYP/VTZ+D  ENERGY=-1460.27373570
 N          1.5771934000        1.6282295000       -6.6276061000
 C          0.2440612000        1.7259587000       -6.4283351000
 C         -0.4733794000        2.8690423000       -6.7828827000
 C          0.2020605000        3.9315473000       -7.3840473000
 C          1.5734372000        3.8167942000       -7.6061672000
 C          2.2419696000        2.6521003000       -7.2123444000
 C         -0.4856347000        0.5092792000       -5.8677916000
 N          0.3574999000       -0.3246307000       -5.0045553000
 Cu         2.4426227000       -0.0396892000       -5.7852985000
 S          2.2477109000       -2.0239306000       -6.9712916000
 C          3.2095231000       -3.4915035000       -6.3691464000
 C          3.2376899000       -3.7377075000       -4.8663044000
 C          0.4700899000        0.1899780000       -3.6332146000
 C          1.8295142000       -0.0538495000       -2.9899895000
 N          2.9204771000       -0.0067039000       -3.7891933000
 C          4.1534983000       -0.1112809000       -3.2429788000
 C          4.3206805000       -0.2859188000       -1.8631464000
 C          3.2005799000       -0.3575767000       -1.0381271000
 C          1.9330831000       -0.2392992000       -1.6119113000
 C          0.0934915000       -1.7698576000       -5.0776861000
 C          0.5168486000       -2.4021349000       -6.4127495000
 H          2.8095307000       -4.3573737000       -6.9151673000
 H          4.2176302000       -3.2984554000       -6.7625427000
 H          3.6045429000       -2.8603636000       -4.3182774000
 H          2.2454911000       -4.0045330000       -4.4764804000
 H          3.9092105000       -4.5829504000       -4.6523410000
 H          0.4090884000       -3.4937782000       -6.3575244000
 H         -0.1233137000       -2.0634887000       -7.2375380000
 H          0.6495117000       -2.2402134000       -4.2572067000
 H         -0.9785830000       -1.9977168000       -4.9145368000
 H          0.3223430000        1.2798899000       -3.6744162000
 H         -0.8152803000       -0.0978883000       -6.7228268000
 H         -1.4066501000        0.8407169000       -5.3567918000
 H         -0.3224622000       -0.2073491000       -2.9744750000
 H          1.0327646000       -0.2887901000       -0.9986637000
 H          3.3112868000       -0.5052222000        0.0370773000
 H          5.3253601000       -0.3711477000       -1.4490592000
 C          5.3346602000       -0.0067466000       -4.1680861000
 C          3.7216905000        2.4829775000       -7.4167379000
 H          2.1319763000        4.6256356000       -8.0769340000
 H         -0.3334947000        4.8363815000       -7.6744752000
 H         -1.5462842000        2.9206467000       -6.5941805000
 H          6.2339508000       -0.4443314000       -3.7176044000
 H          5.1276237000       -0.5102132000       -5.1225438000
 H          5.5527311000        1.0492774000       -4.3916998000
 H          3.9274060000        1.5831772000       -8.0148733000
 H          4.1533802000        3.3499276000       -7.9306988000
 H          4.2327066000        2.3623372000       -6.4498699000
```

Structure A.103: $(CuL4O_2)^+$, $[Cu(C_{18}N_3SH_{25})O_2]^+$

```
  50
DFT-B3LYP/VTZ+D  ENERGY=-1610.54737270
 N          2.0777142000       -0.2077158000       -1.7227882000
 C          1.7819292000       -0.2537708000       -3.0401887000
 C          2.7171302000       -0.6119602000       -4.0093925000
 C          4.0080078000       -0.9496768000       -3.6014508000
 C          4.3167100000       -0.8894880000       -2.2459118000
 C          3.3364599000       -0.5050665000       -1.3192730000
 C          0.3538069000        0.0644918000       -3.4444102000
 N         -0.2851155000        1.0161444000       -2.5171236000
 Cu         0.3590299000        0.4117911000       -0.5236975000
 O          0.7482074000       -0.2721569000        1.2978030000
 O          0.8670425000       -1.5319144000        1.3380664000
 C          3.6695280000       -0.4205991000        0.1435396000
 C          0.2642241000        2.3777042000       -2.6721058000
 C          0.1377606000        3.2086583000       -1.4099115000
 N          0.2974963000        2.5685804000       -0.2297865000
 C          0.2942877000        3.2904027000        0.9173275000
 C          0.1155863000        4.6812141000        0.8926485000
 C         -0.0704591000        5.3376040000       -0.3205739000
 C         -0.0600122000        4.5860228000       -1.4960145000
 C          0.4978592000        2.5735335000        2.2226024000
 C         -1.7622026000        1.0275927000       -2.6184339000
 C         -2.4205890000       -0.2819515000       -2.1717362000
 S         -1.7318923000       -0.9581103000       -0.5996747000
 C         -2.9799801000       -0.4619642000        0.6755424000
 C         -3.2946655000        1.0242219000        0.7871552000
 H         -3.8822985000       -1.0531376000        0.4668493000
 H         -2.5398584000       -0.8517624000        1.6039774000
 H         -2.3909286000        1.6173880000        0.9781429000
 H         -3.7835725000        1.4110115000       -0.1183818000
 H         -3.9919006000        1.1817627000        1.6237755000
 H         -3.5002772000       -0.1276433000       -2.0507626000
 H         -2.2993994000       -1.0754341000       -2.9197275000
 H         -2.1168537000        1.8510094000       -1.9861142000
 H         -2.0751023000        1.2519461000       -3.6559140000
 H          1.3334296000        2.2860859000       -2.9109890000
 H         -0.2217586000       -0.8710022000       -3.4337875000
 H          0.3337114000        0.4356544000       -4.4839155000
 H         -0.2069413000        2.9053562000       -3.5186591000
 H         -0.1978322000        5.0595309000       -2.4684781000
 H         -0.2209468000        6.4176376000       -0.3516425000
 H          0.1198474000        5.2360452000        1.8305671000
 H          5.3196130000       -1.1285891000       -1.8927307000
 H          4.7638818000       -1.2412480000       -4.3319634000
 H          2.4373540000       -0.6245196000       -5.0632569000
 H          3.2340617000        0.4785411000        0.5968682000
 H          3.2666736000       -1.2879045000        0.6849006000
 H          4.7561255000       -0.4015254000        0.2882357000
 H          0.4645051000        3.2819071000        3.0581394000
 H         -0.2708872000        1.8064774000        2.3835114000
 H          1.4671305000        2.0575032000        2.2407296000
```

Structure A.104: M1, glutamate in GluM, $C_{17}N_6O_9H_{23}$

```
 55
DFT-B3LYP/VTZ+D  ENERGY=-1667.29820611
 C        -7.5691623562        0.0339805756        8.4209202034
 H        -7.9197374162       -0.8539526951        7.8744270122
 H        -8.2929511973        0.8370683914        8.2381269370
 C        -6.2165983825        0.3720179647        7.7794523474
 O        -6.2374176591        1.2156993425        6.8154988940
 O        -5.1596558511       -0.2337197381        8.1263037975
 C        -3.4086215634        2.9310287927        6.6727760387
 O        -4.3885413758        3.4540304237        6.0676735455
 O        -2.8166157287        3.4444578927        7.6768126142
 N        -3.9660167973        0.7241147374        5.6734867848
 H        -3.7240340398       -0.2495725084        5.9357940347
 H        -4.1101323945        0.7853019105        4.6591804534
 H        -4.9578882940        0.9928859996        6.1791668223
 C        -2.8429433181        1.6220517013        6.1086940134
 H        -2.2827312663        1.0970590896        6.8898104487
 C        -1.9303918991        1.9337882846        4.9085654819
 H        -1.7347284316        1.0044287097        4.3507003674
 H        -2.4898182608        2.6043598514        4.2363593658
 C        -0.5810266332        2.5542353911        5.3039499017
 H        -0.1409265931        3.0232455696        4.4147170259
 H        -0.7177334440        3.3234345569        6.0718454265
 C         0.3719158812        1.4571542362        5.7956952903
 O         0.9454746272        0.7781676822        4.8951192790
 O         0.4616783950        1.2680078694        7.0514595536
 C         2.9023578234        6.3038913098        3.4957526286
 H         3.3784864944        6.0569117852        2.5425298413
 O         2.2786682183        7.5751283963        3.3905359913
 H         2.8710648448        8.1211209449        2.8043276858
 C         1.8312395846        4.0196936800        3.0089810785
 H         1.9269839530        3.0225751666        3.4429805818
 H         1.4330488984        4.1152944302        1.9964686441
 C         1.8503373002        5.2212607951        3.8783966737
 H         0.8678774312        5.7341705975        3.8355983803
 O         2.1130253377        4.8321022600        5.2422462180
 C         3.1196746941        5.6675827776        5.8081710036
 H         2.6976397669        6.5193412687        6.3627650986
 N         3.8505706490        4.8670308866        6.7623915306
 C         4.8585814272        4.0983871424        8.5706970551
 N         4.8880768666        3.0686475431        7.6421026064
 C         4.2823478681        3.5674952339        6.5864080496
 H         4.0788274198        3.0389085699        5.6628440667
 N         5.1414905613        5.3991067206       10.5257332350
 C         4.5123963150        6.4003170578        9.8924353238
 H         4.3855718967        7.3160418573       10.4717707533
 N         4.0168399988        6.4145258569        8.6468361922
 C         4.2187766191        5.2298392349        8.0403751078
 C         5.3369933658        4.2103669239        9.8987718808
 N         5.9534842863        3.2176890879       10.5615929834
 H         6.2537182221        2.3607958020       10.0827702698
 H         6.3966220798        3.4066262986       11.4611152269
 C         3.9545366948        6.2047679320        4.6371070984
 H         4.6887076124        5.4236269942        4.3517441815
 O         4.5763738226        7.3939311419        5.0262293839
 H         4.9193129045        7.9096031400        4.2393824502
 H        -7.5140654799       -0.2161951466        9.4803745838
```

Structure A.105: TS1, $C_{17}N_6O_9H_{23}$

```
 55
DFT-B3LYP/VTZ+D  ENERGY=-1667.26611322
 C        -7.5218051893        0.0669795491        8.4341426033
 H        -7.8862629724       -0.8061755413        7.8723308656
 H        -8.2207370230        0.8889035062        8.2376652593
 C        -6.1518484704        0.3626260764        7.8263232266
 O        -6.1843707962        1.0916676348        6.7382088548
 O        -5.0886142367       -0.1238805313        8.2573374419
 C        -3.3851431428        2.9539832733        6.6958680275
 O        -4.4110198211        3.4678049448        6.1513787000
 O        -2.7815902944        3.4566242284        7.6999251531
 N        -3.8869217863        0.7850537251        5.6073821881
 H        -3.5951572536       -0.1846284357        5.8018904181
 H        -4.0502247232        0.8818988834        4.6008239822
 H        -5.1621225609        1.0165379581        6.2564618643
 C        -2.7974879595        1.6938033696        6.0573375950
 H        -2.2095476350        1.1601620282        6.8128993819
 C        -1.8583499033        2.1211072007        4.8858680777
 H        -1.6846430169        1.2464784983        4.2416618967
 H        -2.3968367897        2.8773039945        4.2904752189
 C        -0.5136610762        2.6335499206        5.3702450216
 H         0.0764776423        3.2972334166        4.3941831349
 H        -0.5911562302        3.4087394123        6.1396564194
 C         0.4237035264        1.5063418274        5.7614788705
 O         0.8084278133        0.7356988851        4.8382372093
 O         0.6930992261        1.3947121960        7.0041033386
 C         2.5013777846        6.0783801075        3.4955147820
 H         2.8522623458        5.5661151349        2.5855551646
 O         1.9461919213        7.3354375330        3.1384342007
 H         2.6618656529        7.8523580944        2.6756809422
 C         0.7988551698        4.0773539754        3.4378326526
 H         1.4943977738        3.3072670897        3.0838970357
 H         0.0600662528        4.3808185059        2.6941093080
 C         1.4129983937        5.2097692396        4.1977380322
 H         0.6267740428        5.9180091894        4.5205661639
 O         2.0649041135        4.6488332830        5.3605738637
 C         3.0403804938        5.5756149858        5.8049053033
 H         2.6066974532        6.4069213519        6.3876062004
 N         3.9187356042        4.8620704760        6.6988203579
 C         4.9168519379        4.1089997139        8.5211272206
 N         5.0062314447        3.0932047076        7.5801676502
 C         4.4023310317        3.5814819719        6.5191110770
 H         4.2407034358        3.0567421564        5.5852067784
 N         5.1084218405        5.3955635699       10.4986563231
 C         4.4532378412        6.3786601076        9.8629787419
 H         4.2808655928        7.2834385226       10.4484369598
 N         3.9793376289        6.3868569701        8.6085173553
 C         4.2436925255        5.2203466166        7.9906589340
 C         5.3571819105        4.2207827767        9.8628238561
 N         5.9859754826        3.2402458277       10.5320657623
 H         6.2996762075        2.3839216011       10.0611406822
 H         6.3979333540        3.4296087945       11.4455417274
 C         3.6763783525        6.1853543326        4.5433835119
 H         4.5254475106        5.5573044618        4.2174836356
 O         4.0803952779        7.4821337209        4.8780656952
 H         4.6057610730        7.9354338067        4.1569379539
 H        -7.4907680551       -0.1892604276        9.4931255646
```

Structure A.106: M2, glutamyl in GluM, $C_{17}N_6O_9H_{23}$

```
 55
DFT-B3LYP/VTZ+D  ENERGY=-1667.29812506
 C        -7.5651148153        0.0645520296        8.4388919633
 H        -7.9360313824       -0.8049257642        7.8759361475
 H        -8.2712245359        0.8840610276        8.2590072489
 C        -6.2112969282        0.3717608939        7.8060472119
 O        -6.2786324757        1.0833602599        6.7116444589
 O        -5.1307655983       -0.0936583410        8.2240783719
 C        -3.4616007813        2.8831653203        6.6694164843
 O        -4.4627805645        3.4291118660        6.1098302839
 O        -2.8293407648        3.3811069171        7.6571139088
 N        -4.0311885670        0.7343132789        5.5530520547
 H        -3.7628608065       -0.2482024079        5.7071372009
 H        -4.1746200081        0.8887969224        4.5502016555
 H        -5.2537803142        0.9833847640        6.1931352856
 C        -2.9287512926        1.5840779115        6.0695163341
 H        -2.4175025887        1.0195759423        6.8559808254
 C        -1.8971212914        1.9405040798        4.9443569668
 H        -1.6936571953        1.0242698931        4.3705678675
 H        -2.3922127458        2.6615885538        4.2706251089
 C        -0.6146938077        2.4518185403        5.4961400032
 H         1.1631718518        3.0910356157        3.5426329913
 H        -0.5637506390        3.4440030896        5.9400039377
 C         0.4570092213        1.4810376174        5.8039693371
 O         0.8380533544        0.7226923768        4.8598896247
 O         0.8808244730        1.4506776759        7.0091127412
 C         2.8225871419        6.2134936195        3.5107250176
 H         3.3082838182        5.9448650692        2.5651042087
 O         2.1885931103        7.4807134652        3.3574683564
 H         2.8152126317        8.0387164318        2.8213547870
 C         1.8761275652        3.8288928677        3.1493177323
 H         2.8742310125        3.3714711751        3.2849874310
 H         1.6550605726        3.9770962111        2.0795710517
 C         1.7848711283        5.1493347188        3.9079896833
 H         0.7817899534        5.5853395276        3.7783299195
 O         1.9811679074        4.8739099124        5.3176828250
 C         3.0317998302        5.6718658187        5.8477109067
 H         2.6527760780        6.5421619037        6.4034525385
 N         3.7617121060        4.8615310419        6.8003472057
 C         4.8207446775        4.1053969161        8.5853107049
 N         4.8106284545        3.0639953587        7.6700828431
 C         4.1705630700        3.5548233403        6.6305430050
 H         3.9159366022        3.0098746048        5.7298097385
 N         5.1518488550        5.4171506193       10.5246591802
 C         4.5194865887        6.4197132763        9.8957312612
 H         4.4121104790        7.3404799216       10.4708326993
 N         3.9986818757        6.4289661670        8.6609216161
 C         4.1749944386        5.2367443961        8.0603405051
 C         5.3268996957        4.2233148921        9.9018145519
 N         5.9468148703        3.2291282833       10.5614245026
 H         6.2379372266        2.3700508918       10.0819595065
 H         6.4047947243        3.4214322075       11.4524937776
 C         3.8693533104        6.1779577533        4.6610082622
 H         4.6313920381        5.4107256641        4.4170756043
 O         4.4572704769        7.3942051000        5.0281090936
 H         4.8524604864        7.8796036137        4.2472726118
 H        -7.5141383411       -0.1973863497        9.4957064344
```

Structure A.107: TS2, $C_{17}N_6O_9H_{23}$

```
  55
DFT-B3LYP/VTZ+D  ENERGY=-1667.27982282
 C        -7.6023693999        0.0663094415        8.4525228577
 H        -7.9717168906       -0.7989804622        7.8822325889
 H        -8.3114567519        0.8852335927        8.2818457918
 C        -6.2579593074        0.3804215267        7.8260036425
 O        -6.3703108365        1.0553083713        6.6892969522
 O        -5.1608261684       -0.0156527279        8.2393454070
 C        -3.4852068623        2.8931713684        6.7260888607
 O        -4.4804609985        3.4544370719        6.1352561613
 O        -2.8194571939        3.4467932225        7.6734345598
 N        -3.9651138600        0.7930461531        5.5133061007
 H        -3.6585778057       -0.1827375061        5.4692054284
 H        -4.1857594847        1.1674480929        4.5864813863
 H        -5.4356315266        1.0177616548        6.2299955628
 C        -3.0594339683        1.5761103370        6.2618576968
 H        -2.3798976755        1.0145402435        6.8970741937
 C        -1.5617772320        2.3465751063        4.7635128257
 H        -1.6314031750        1.4194071032        4.1925884812
 H        -2.2371880435        3.1523377864        4.4716342637
 C        -0.4121826432        2.5991445849        5.4608254230
 H         1.1522688247        3.1596236740        3.4921542312
 H        -0.2636411199        3.5501831639        5.9681573184
 C         0.5167233135        1.4849851486        5.8077107377
 O         0.8858514444        0.7121796163        4.8772012791
 O         0.8133730234        1.3836223424        7.0454323757
 C         2.8661945443        6.2525580648        3.5104116852
 H         3.3465263726        5.9881483287        2.5613042391
 O         2.2344359685        7.5223464216        3.3674350264
 H         2.8500732125        8.0754026648        2.8140171440
 C         1.8861631577        3.8860975826        3.1191300462
 H         2.8716275077        3.4014166309        3.2504772126
 H         1.6720554355        4.0649508310        2.0525430343
 C         1.8257114416        5.1900246364        3.9064872850
 H         0.8254450837        5.6397436248        3.8073324009
 O         2.0495621914        4.8803231402        5.3050319516
 C         3.0881270841        5.6904376225        5.8397780313
 H         2.6983881245        6.5541629521        6.3982135741
 N         3.8230481814        4.8828764916        6.7892433265
 C         4.8477552908        4.1111445533        8.5871190944
 N         4.8669123901        3.0823757201        7.6580852769
 C         4.2486914204        3.5826614286        6.6102110757
 H         4.0297435803        3.0506356717        5.6924985072
 N         5.1402823708        5.4053184986       10.5449101592
 C         4.5085381307        6.4091667522        9.9169180186
 H         4.3851714146        7.3232148878       10.4998391067
 N         4.0063801234        6.4276470160        8.6743035863
 C         4.2039510062        5.2440312240        8.0632640044
 C         5.3328938982        4.2189765047        9.9126011480
 N         5.9513329905        3.2227738058       10.5700130984
 H         6.2495187950        2.3681807568       10.0866653616
 H         6.3992169414        3.4091660751       11.4675975119
 C         3.9191555473        6.2070478379        4.6540950135
 H         4.6772132023        5.4391827342        4.3979057335
 O         4.5149516114        7.4181402725        5.0254307178
 H         4.8863501270        7.9130871002        4.2389986693
 H        -7.5391510693       -0.2011817506        9.5072830421
```

Structure A.108: M3, acrylate and glycyl in GluM, $C_{17}N_6O_9H_{23}$

```
 55
DFT-B3LYP/VTZ+D  ENERGY=-1667.30014600
 C        -7.6331092325        0.0506784781        8.4471772774
 H        -7.9891488017       -0.8254403240        7.8848568868
 H        -8.3459924004        0.8631005502        8.2654706045
 C        -6.2843073331        0.3628033967        7.8397154156
 O        -6.3737287387        1.1078671277        6.7396632755
 O        -5.2004140541       -0.0829812426        8.2308795534
 C        -3.4794018068        2.9451437849        6.9063087202
 O        -4.4109915958        3.4797878501        6.1913383600
 O        -2.8326470014        3.5866970093        7.8207596770
 N        -3.8090296751        0.8218440597        5.7285971873
 H        -3.4924440690       -0.1505652172        5.6750473843
 H        -3.9319058237        1.2821331519        4.8243107261
 H        -5.4492090757        1.0879784558        6.3080541353
 C        -3.1523848876        1.5602373903        6.6961325948
 H        -2.4588964093        1.0459580894        7.3531392740
 C        -1.2603299966        2.4070171552        4.1001037011
 H        -1.0557934673        1.5895102586        3.4067293286
 H        -2.0314018915        3.1306803534        3.8298014064
 C        -0.6166532791        2.4830173174        5.2716808795
 H         1.4251110038        2.9827697799        3.6203919404
 H        -0.8354412691        3.2769313253        5.9847759485
 C         0.3396648819        1.4169007760        5.7310803711
 O         0.9087325082        0.7168916710        4.8436626494
 O         0.4605359868        1.2786238662        6.9943256656
 C         2.8956442185        6.1930135509        3.5132338221
 H         3.3994749668        5.9392790504        2.5729945488
 O         2.2249847331        7.4405195302        3.3529578929
 H         2.8325931577        8.0122285517        2.8097180280
 C         2.0832826710        3.7562518652        3.2048220945
 H         3.1151453547        3.3843953148        3.3501105736
 H         1.8427656594        3.8435231934        2.1312012642
 C         1.8924063948        5.0962532629        3.9070622810
 H         0.8747102964        5.4728735256        3.7251143133
 O         2.0389573208        4.8894071916        5.3341934051
 C         3.0941779748        5.6824641852        5.8582118356
 H         2.7170992197        6.5500794824        6.4181281592
 N         3.8271021004        4.8705367379        6.8087444499
 C         4.8526454666        4.0988633122        8.6054488641
 N         4.8546966836        3.0633297211        7.6835161920
 C         4.2351201839        3.5646081832        6.6359957611
 H         3.9997595457        3.0276098107        5.7249908377
 N         5.1632132694        5.3998444414       10.5547207524
 C         4.5390085926        6.4064557875        9.9240535564
 H         4.4251394340        7.3237835225       10.5035077182
 N         4.0346017112        6.4244784035        8.6827442236
 C         4.2186897187        5.2353830550        8.0777531524
 C         5.3442440097        4.2093826929        9.9278127223
 N         5.9574203655        3.2105512540       10.5856672529
 H         6.2510463497        2.3553034408       10.1001806688
 H         6.4121748503        3.3958521102       11.4800943047
 C         3.9319253970        6.1903505948        4.6725524078
 H         4.7112211761        5.4363003374        4.4429103151
 O         4.4952466736        7.4212585696        5.0312300464
 H         4.8742913127        7.9093631785        4.2438645133
 H        -7.5684289831       -0.2060408652        9.5045224367
```

Structure A.109: TS3, $C_{17}N_6O_9H_{23}$

```
 55
DFT-B3LYP/VTZ+D  ENERGY=-1667.28001516
 C        -7.5489946805        0.0624377766        8.4542968875
 H        -7.8940891098       -0.8155659938        7.8880187593
 H        -8.2553127439        0.8759298497        8.2499663641
 C        -6.1797638189        0.3707270169        7.8740682068
 O        -6.2295201428        1.0747743388        6.7533493303
 O        -5.1083570845       -0.0581178394        8.3210587066
 C        -3.4319817882        3.0062918787        6.9450353863
 O        -4.4044146411        3.4922040002        6.2701215467
 O        -2.8424169193        3.6386235103        7.8973471200
 N        -3.7190445702        0.8613286759        5.7719510787
 H        -3.4007768522       -0.1154892336        5.7893210629
 H        -3.7999996301        1.2134079219        4.8131677454
 H        -5.2657867592        1.0533525414        6.3462160584
 C        -2.9162146202        1.6746677299        6.5961301487
 H        -2.3567653840        1.1502420026        7.3670625566
 C        -1.5521590744        2.5794116405        4.2641186978
 H        -1.4101124807        1.7978987637        3.5171218190
 H        -2.1180090203        3.4717772575        3.9934011247
 C        -1.1501072117        2.3634655404        5.5683421408
 H         1.0820981088        3.1407213368        3.5238445995
 H        -1.0904276807        3.2050358371        6.2575276843
 C        -0.2119818744        1.2179670866        5.9023367887
 O         0.1281537945        0.4680561635        4.9478352943
 O         0.1524572866        1.1138481375        7.1216973444
 C         2.8562850506        6.2036903487        3.5092743319
 H         3.3412020338        5.9184820890        2.5680403718
 O         2.2178049627        7.4647426583        3.3310953996
 H         2.8383493797        8.0187672468        2.7834886214
 C         1.8342126764        3.8449664988        3.1415006350
 H         2.8116405508        3.3403197076        3.2552819574
 H         1.6064483109        4.0265733214        2.0785795306
 C         1.8148780722        5.1486475330        3.9311713162
 H         0.8184287642        5.6129590549        3.8594241595
 O         2.0734793747        4.8255859527        5.3188812592
 C         3.0947847668        5.6626675415        5.8450066508
 H         2.6893412553        6.5202147999        6.4027170941
 N         3.8485455020        4.8707599234        6.7925238500
 C         4.8635552710        4.0991510801        8.5958933834
 N         4.8943284220        3.0724451031        7.6643360768
 C         4.2835089840        3.5743048542        6.6129284287
 H         4.0827169433        3.0480012854        5.6878795573
 N         5.1443708534        5.3926426120       10.5549314511
 C         4.5102350318        6.3939324970        9.9255787109
 H         4.3806425475        7.3064239546       10.5093457049
 N         4.0126985222        6.4122626304        8.6810132520
 C         4.2185493870        5.2303413149        8.0700396149
 C         5.3439538908        4.2074048834        9.9231462987
 N         5.9663353965        3.2136586560       10.5792534846
 H         6.2647924303        2.3596215759       10.0945289582
 H         6.4110876424        3.3985393668       11.4790255941
 C         3.9103582930        6.1915982795        4.6545020847
 H         4.6886175636        5.4423908245        4.4047777812
 O         4.4732734722        7.4199659782        5.0186056729
 H         4.8565068056        7.9095593525        4.2341681896
 H        -7.5167441241       -0.1901548618        9.5141195153
```

Structure A.110: M4, 3-methylaspartyl in GluM, $C_{17}N_6O_9H_{23}$

```
 55
DFT-B3LYP/VTZ+D  ENERGY=-1667.28961403
 C        -7.7949838453      -0.0663719472       8.3213820659
 H        -7.9056638259      -1.0417226800       7.8269584303
 H        -8.7120826294       0.5095924534       8.1595390281
 C        -6.6363979813       0.6417302543       7.6205907258
 O        -6.8532197256       1.6729517025       6.9743740155
 O        -5.4583512247       0.0528781056       7.6895634152
 C        -3.4244424063       3.1242416127       6.9928916732
 O        -4.3784938939       3.5307011106       6.2752146537
 O        -2.8944789327       3.7764458808       7.9580923556
 N        -3.6960901482       0.8527770987       6.0352824336
 H        -3.2269716340      -0.0541992509       5.8554388459
 H        -4.0800176179       1.2388639256       5.1652792315
 H        -4.5605857934       0.5866268068       6.7699656436
 C        -2.7460122921       1.8052501325       6.6631724366
 H        -2.3757718111       1.3437273100       7.5853080119
 C        -1.8086343828       2.2576581377       4.3415938298
 H        -1.4163525373       1.5433146690       3.6212953993
 H        -2.4949339762       3.0386839704       4.0128962682
 C        -1.4834385399       2.1094086552       5.7791162001
 H         1.0228693748       3.1511678827       3.5102073662
 H        -1.0996892051       3.0653336776       6.1823595434
 C        -0.3461787415       1.0954311133       6.0799661634
 O         0.2447551182       0.5810352727       5.0964242274
 O        -0.1020954685       0.9004864695       7.3136578480
 C         2.8302641901       6.1965470766       3.4853787079
 H         3.3104704887       5.8966133423       2.5462790317
 O         2.1998751250       7.4581267943       3.2938419052
 H         2.8291218305       8.0087154969       2.7516447475
 C         1.7697716043       3.8542435761       3.1186208695
 H         2.7426505392       3.3370300084       3.2120669316
 H         1.5292955658       4.0461782103       2.0612031443
 C         1.7815893809       5.1527684757       3.9181783332
 H         0.7912451384       5.6330536695       3.8651580678
 O         2.0611612313       4.8132594929       5.2982491282
 C         3.0811235119       5.6562714826       5.8222609711
 H         2.6745409699       6.5138835057       6.3794750822
 N         3.8401862363       4.8691065627       6.7683788815
 C         4.8574692247       4.1040436848       8.5737507706
 N         4.8918065197       3.0757824226       7.6433671145
 C         4.2806186088       3.5739837865       6.5903550125
 H         4.0835693757       3.0459973922       5.6651773100
 N         5.1343327358       5.4032967936      10.5301160951
 C         4.4993379347       6.4019573268       9.8985745993
 H         4.3679973700       7.3161411156      10.4794417658
 N         4.0026046716       6.4153942678       8.6533278343
 C         4.2098936713       5.2324283280       8.0456981832
 C         5.3363115390       4.2165825741       9.9017000793
 N         5.9591165144       3.2265425286      10.5621897299
 H         6.2605357505       2.3701290491      10.0833821508
 H         6.4001806592       3.4152825462      11.4626768631
 C         3.8890909742       6.1900016920       4.6289161476
 H         4.6732571391       5.4484738716       4.3767626880
 O         4.4383649764       7.4234873376       4.9940747963
 H         4.8380446238       7.9092014913       4.2150510571
 H        -7.6565582240      -0.2459854753       9.3875173620
```

Structure A.111: TS4, $C_{17}N_6O_9H_{23}$

```
 55
DFT-B3LYP/VTZ+D  ENERGY=-1667.25849787
 C        -7.6413287874       -0.0750507885        8.3389777259
 H        -7.7508933635       -1.0505763653        7.8452064210
 H        -8.5463756842        0.5134594409        8.1524313880
 C        -6.4580901514        0.6356634902        7.6683755059
 O        -6.6575699386        1.7075331933        7.0826604627
 O        -5.2922887750        0.0253589960        7.6875663093
 C        -3.3504038301        3.2258802163        7.0230185687
 O        -4.3070452920        3.6100534004        6.2974222876
 O        -2.8536216942        3.8770976412        8.0060476736
 N        -3.5365906148        0.9624519562        6.0233352223
 H        -3.0410817939        0.0821883275        5.7950674384
 H        -3.9683241998        1.3703518454        5.1860731235
 H        -4.3695535138        0.6369071524        6.7476856074
 C        -2.6228041534        1.9322774696        6.6895862871
 H        -2.2935927234        1.4591559397        7.6222075866
 C        -1.4919523017        2.6707485603        4.4647920953
 H        -1.5357707093        1.8254647033        3.7705791046
 H        -2.2647409494        3.4277654340        4.2825619561
 C        -1.3067913816        2.2915750179        5.9106076995
 H        -0.3631346445        3.2903148912        4.0269103493
 H        -0.9158059344        3.1561847783        6.4698069995
 C        -0.2737684007        1.1633942355        6.1460879813
 O         0.1511305036        0.5446499985        5.1383340644
 O         0.0323977101        0.9696144522        7.3668093336
 C         2.3773414455        5.9104815380        3.4387403718
 H         2.7641724064        5.3624752082        2.5641418795
 O         1.8082756266        7.1354354770        3.0045747667
 H         2.5414259087        7.6761432100        2.5997628580
 C         0.7616809841        3.8479513650        3.4155037005
 H         1.4361388736        2.9838128590        3.4202847569
 H         0.3767547727        4.0777068860        2.4174446554
 C         1.2939257922        5.0441074423        4.1563061636
 H         0.4756846116        5.7442382463        4.4127152618
 O         1.9204498001        4.5610891608        5.3653665696
 C         2.8993961233        5.5034856997        5.7807532901
 H         2.4722397204        6.3427826473        6.3564259753
 N         3.7999129963        4.8125566363        6.6732079337
 C         4.8617983211        4.1025148480        8.4795525187
 N         4.9460033206        3.0767530729        7.5484445190
 C         4.3064546387        3.5401800645        6.4974190811
 H         4.1378837663        3.0031518708        5.5717384551
 N         5.0736971335        5.4146188268       10.4395310627
 C         4.3958380134        6.3815488207        9.8046667666
 H         4.2256219941        7.2925687090       10.3812693338
 N         3.8953622676        6.3673024281        8.5595836024
 C         4.1567581479        5.1955965313        7.9517042936
 C         5.3251965717        4.2348414234        9.8132030646
 N         5.9773201489        3.2723126247       10.4853103754
 H         6.2914984278        2.4085617383       10.0288025804
 H         6.3877855464        3.4768683095       11.3955621034
 C         3.5218003271        6.1043915707        4.5058038031
 H         4.4159098837        5.5259819452        4.2153380510
 O         3.8290624863        7.4369958300        4.8028819398
 H         4.4247200265        7.8769597115        4.1289527861
 H        -7.5455740892       -0.2559057739        9.4095801982
```

Structure A.112: M5, 3-methylaspartate in GluM, $C_{17}N_6O_9H_{23}$

```
 55
DFT-B3LYP/VTZ+D  ENERGY=-1667.29436168
 C        -7.7759762379      -0.0675878729       8.3258612725
 H        -7.8928502476      -1.0421093658       7.8309521066
 H        -8.6877276057       0.5157220137       8.1601179588
 C        -6.6096199538       0.6303085939       7.6269912037
 O        -6.8211997140       1.6540940904       6.9661577971
 O        -5.4321309212       0.0430495945       7.7099623734
 C        -3.4051948123       3.1146273276       6.9676947120
 O        -4.3608721461       3.5180767768       6.2491932089
 O        -2.8822486851       3.7697127528       7.9345682469
 N        -3.6901804079       0.8453066900       6.0259065693
 H        -3.2302723133      -0.0627035434       5.8310243053
 H        -4.1096085655       1.2379776167       5.1763345938
 H        -4.5341127136       0.5774335353       6.7757521525
 C        -2.7236793177       1.7946772884       6.6403191069
 H        -2.3681510190       1.3353617820       7.5698377955
 C        -1.7720222865       2.1918107775       4.2773364231
 H        -2.0414857459       1.2230867355       3.8374670322
 H        -2.5809257245       2.9123736006       4.0842081847
 C        -1.4685711054       2.0849624103       5.7689880888
 H        -0.8742811595       2.5234467932       3.7436542703
 H        -1.0897127860       3.0555039039       6.1274326418
 C        -0.3207486374       1.0957488037       6.0976547632
 O         0.3070285085       0.6010962364       5.1250962635
 O        -0.0989824927       0.8932185775       7.3357361870
 C         2.8901336977       6.3064448266       3.4758648782
 H         3.3593580396       6.0355604010       2.5255358125
 O         2.2748864599       7.5778225479       3.3455414277
 H         2.8725027789       8.1151978399       2.7557792308
 C         1.7417726667       4.0590292538       2.9956654472
 H         1.7440725225       3.0578480973       3.4272867973
 H         1.3647719770       4.1924422010       1.9798254596
 C         1.8287816763       5.2415925310       3.8842659081
 H         0.8579192349       5.7803142595       3.8929361797
 O         2.1403310967       4.8137635439       5.2254080650
 C         3.1352014538       5.6672241290       5.7878505859
 H         2.7021601460       6.5117049683       6.3454946911
 N         3.8823608000       4.8771214247       6.7365564819
 C         4.8709413831       4.1037219810       8.5540967016
 N         4.9251419160       3.0822045024       7.6170081248
 C         4.3329026246       3.5847605606       6.5556700066
 H         4.1606968992       3.0656894937       5.6202726583
 N         5.1234721717       5.3968914914      10.5186199376
 C         4.4916017270       6.3955153278       9.8845646940
 H         4.3508630407       7.3072405671      10.4671999069
 N         4.0086900974       6.4120363481       8.6336297320
 C         4.2280818927       5.2329409522       8.0232745643
 C         5.3348216166       4.2125922560       9.8882265099
 N         5.9541268376       3.2231161873      10.5521186874
 H         6.2612301814       2.3674422692      10.0752055642
 H         6.3869388020       3.4116410150      11.4566038884
 C         3.9519109432       6.2210788206       4.6124629025
 H         4.6987620465       5.4544516601       4.3215822451
 O         4.5537724438       7.4198458981       5.0016715076
 H         4.8996653098       7.9343728848       4.2149467011
 H        -7.6429305973      -0.2485171884       9.3924589389
```

Appendix B
Supplementary Data

The data included in Chapter 5 and Chapter 6 are provided in this appendix. The radical stabilization energies (RSEs), the energies of the radicals and molecules involved, and the errors of different methods are given in tables from Table B.1 to B.19. The vertical ionization potentials (IPs), the energies of molecules and cations involved, and the errors of different methods are give in tables from Table B.20 to B. 38. The molecular electron affinities (EAs), the energies of molecules and anions involved, and the errors of different methods are given in tables from Table B.39 to B.57. Formation energies of copper-oxygen complexes (high-spin open-shell triplet state), molecules involved, and errors of different methods are given in tables from Table B.58 to B.60. In Table B.61 and Table B.62, the energies involved in the calculation of the transition states and intermediates of the inter-conversion of glutamate are provided.

Table B.1: Radical stabilization energies (RSEs, in kcal/mol) obtained with HF and RMP2 methods. The energies (in Hartree) of related molecules and radicals are given. The aug-cc-pVTZ basis set have been used. The radicals are numbered from R00 to R30 as discussed in Chapter 5.

	HF			RMP2		
	Molecule	Radical	RSE	Molecule	Radical	RSE
R00	-40.213 588	-39.573 468	0.00	-40.414 444	-39.738 765	0.00
R01	-375.971 263	-375.327 538	2.26	-377.082 634	-376.403 979	1.87
R02	-538.201 157	-537.562 949	-1.20	-538.759 088	-538.086 803	-2.13
R03	-178.152 180	-177.512 611	-0.35	-178.771 765	-178.097 806	-1.08
R04	-154.145 369	-153.506 344	-0.69	-154.758 337	-154.084 832	-1.36
R05	-117.117 545	-116.488 905	-7.20	-117.633 837	-116.989 045	-19.38
R06	-152.977 182	-152.345 475	-5.28	-153.554 104	-152.892 911	-9.09
R07	-131.975 308	-131.338 852	-2.30	-132.497 385	-131.834 198	-7.84
R08	-208.063 360	-207.430 157	-4.34	-208.854 253	-208.187 666	-5.71
R09	-247.103 676	-246.470 284	-4.22	-248.070 607	-247.403 984	-5.68
R10	-266.940 574	-266.307 099	-4.17	-267.930 101	-267.263 859	-5.92
R11	-227.905 874	-227.272 326	-4.12	-228.722 479	-228.055 997	-5.77
R12	-156.151 916	-155.516 510	-2.96	-156.853 275	-156.186 449	-5.56
R13	-139.097 177	-138.459 625	-1.61	-139.541 492	-138.871 245	-3.41
R14	-95.255 395	-94.628 416	-8.25	-95.667 151	-95.010 388	-11.87
R15	-95.618 446	-94.969 541	5.51	-96.020 746	-95.337 441	4.79
R16	-134.294 539	-133.667 345	-8.11	-134.880 989	-134.224 866	-12.27
R17	-208.043 866	-207.413 016	-5.82	-208.834 438	-208.175 505	-10.51
R18	-173.335 356	-172.707 679	-7.81	-174.100 476	-173.444 093	-12.11
R19	-243.761 513	-243.120 909	0.30	-244.642 963	-243.972 321	-3.16
R20	-450.854 569	-450.217 386	-1.84	-452.198 835	-451.528 445	-3.32
R21	-154.128 707	-153.497 195	-5.40	-154.737 682	-154.075 192	-8.28
R22	-227.880 054	-227.241 512	-0.99	-228.694 764	-228.025 451	-3.99
R23	-266.940 569	-266.302 543	-1.31	-267.930 123	-267.261 507	-4.43
R24	-115.091 991	-114.460 941	-5.69	-115.528 953	-114.866 842	-8.51
R25	-381.889 484	-381.247 844	0.95	-382.227 446	-381.549 358	1.51
R26	-438.069 197	-437.422 656	4.03	-438.432 600	-437.751 742	3.25
R27	-437.759 662	-437.126 509	-4.37	-438.130 382	-437.468 852	-8.88
R28	-626.570 386	-625.927 614	1.66	-627.613 802	-626.936 226	1.19
R29	-551.662 818	-551.022 742	-0.03	-552.461 309	-551.787 410	-1.12
R30	-115.909 632	-115.277 817	-5.21	-116.397 471	-115.741 437	-12.33

Table B.2: RSEs (in kcal/mol) obtained with UCCSD and UCCSD(T) methods. The energies (in Hartree) of related molecules and radicals are given. The aug-cc-pVTZ basis set have been used. The radicals are numbered from R00 to R30 as discussed in Chapter 5.

	UCCSD			UCCSD(T)		
	Molecule	Radical	RSE	Molecule	Radical	RSE
R00	-40.434 374	-39.758 581	0.00	-40.440 926	-39.763 639	0.00
R01	-377.096 745	-376.418 193	1.73	-377.135 923	-376.456 089	1.60
R02	-538.799 139	-538.127 480	-2.59	-538.823 756	-538.151 237	-2.99
R03	-178.797 473	-178.123 574	-1.19	-178.819 666	-178.144 553	-1.36
R04	-154.785 911	-154.112 668	-1.60	-154.809 527	-154.134 935	-1.69
R05	-117.666 895	-117.016 970	-16.23	-117.690 124	-117.040 343	-17.26
R06	-153.573 158	-152.912 035	-9.21	-153.598 295	-152.936 632	-9.80
R07	-132.510 822	-131.846 735	-7.35	-132.536 530	-131.872 269	-8.17
R08	-208.873 292	-208.206 944	-5.93	-208.908 426	-208.241 058	-6.22
R09	-248.099 870	-247.433 472	-5.90	-248.143 045	-247.475 691	-6.23
R10	-267.955 021	-267.288 809	-6.01	-267.998 431	-267.331 278	-6.36
R11	-228.736 122	-228.069 742	-5.91	-228.771 526	-228.104 170	-6.23
R12	-156.892 238	-156.225 128	-5.45	-156.922 969	-156.255 134	-5.93
R13	-139.556 772	-138.885 825	-3.04	-139.571 278	-138.899 471	-3.44
R14	-95.690 453	-95.032 650	-11.29	-95.706 117	-95.047 761	-11.88
R15	-96.047 965	-95.364 403	4.87	-96.061 958	-95.377 009	4.81
R16	-134.914 729	-134.257 725	-11.79	-134.938 160	-134.280 738	-12.47
R17	-208.853 836	-208.194 031	-10.03	-208.889 182	-208.229 051	-10.77
R18	-174.143 293	-173.486 414	-11.87	-174.175 039	-173.517 808	-12.59
R19	-244.641 071	-243.969 479	-2.64	-244.685 147	-244.012 882	-3.15
R20	-452.211 089	-451.540 565	-3.31	-452.259 902	-451.588 448	-3.66
R21	-154.766 611	-154.103 780	-8.13	-154.790 216	-154.126 815	-8.71
R22	-228.709 374	-228.039 616	-3.79	-228.745 100	-228.074 688	-4.31
R23	-267.955 040	-267.285 872	-4.16	-267.998 453	-267.328 667	-4.71
R24	-115.546 469	-114.883 641	-8.14	-115.562 345	-114.898 876	-8.67
R25	-382.266 167	-381.588 959	0.89	-382.279 072	-381.600 281	0.94
R26	-438.469 766	-437.789 318	2.92	-438.485 171	-437.803 321	2.86
R27	-438.163 758	-437.501 712	-8.63	-438.180 460	-437.517 928	-9.26
R28	-627.636 511	-626.959 976	0.47	-627.684 383	-627.006 868	0.14
R29	-552.494 142	-551.822 071	-2.34	-552.531 491	-551.858 667	-2.80
R30	-116.418 319	-115.761 313	-11.79	-116.442 610	-115.785 698	-12.79

Table B.3: RSEs (in kcal/mol) obtained with sd-LRMP2 and ab-LRMP2 methods. The energies (in Hartree) of related molecules and radicals are given. The aug-cc-pVTZ basis set have been used. Parameters are set as default, i.e., 'domsel=0.985' and 'cpldel=0'.

	sd-LRMP2, default			ab-LRMP2, default		
	Molecule	Radical	RSE	Molecule	Radical	RSE
R00	-40.412 426	-39.737 601	0.00	-40.412 425	-39.737 601	0.00
R01	-377.073 401	-376.396 426	1.35	-377.073 400	-376.395 660	1.83
R02	-538.752 143	-538.081 475	-2.61	-538.752 143	-538.081 079	-2.36
R03	-178.765 694	-178.092 831	-1.23	-178.765 694	-178.092 628	-1.10
R04	-154.751 114	-154.078 588	-1.44	-154.751 114	-154.078 371	-1.31
R05	-117.627 077	-116.983 728	-19.75	-117.627 077	-116.683 576	-19.66
R06	-153.549 023	-152.889 031	-9.31	-153.549 023	-152.888 887	-9.22
R07	-132.492 962	-131.830 893	-8.00	-132.492 962	-131.830 758	-7.92
R08	-208.846 439	-208.181 307	-6.08	-208.846 439	-208.180 931	-5.85
R09	-248.059 325	-247.394 114	-6.03	-248.059 325	-247.393 749	-5.80
R10	-267.919 896	-267.255 109	-6.30	-267.919 896	-267.254 733	-6.06
R11	-228.715 470	-228.050 465	-6.16	-228.715 470	-228.050 084	-5.92
R12	-156.841 921	-156.176 467	-5.88	-156.841 921	-156.176 096	-5.65
R13	-139.538 665	-138.869 478	-3.54	-139.538 665	-138.869 123	-3.31
R14	-95.662 651	-95.006 427	-11.67	-95.662 651	-95.006 405	-11.66
R15	-96.016 276	-95.333 786	4.81	-96.016 276	-95.333 629	4.91
R16	-134.873 148	-134.218 472	-12.64	-134.873 148	-134.218 370	-12.58
R17	-208.826 827	-208.169 664	-11.08	-208.826 827	-208.169 423	-10.93
R18	-174.090 398	-173.434 074	-11.61	-174.090 399	-173.433 879	-11.49
R19	-244.636 753	-243.966 295	-2.74	-244.636 753	-243.965 874	-2.48
R20	-452.188 039	-451.518 477	-3.30	-452.188 039	-451.518 439	-3.28
R21	-154.731 568	-154.069 758	-8.17	-154.731 567	-154.069 577	-8.05
R22	-228.688 117	-228.019 742	-4.05	-228.688 117	-228.019 644	-3.99
R23	-267.919 914	-267.252 173	-4.44	-267.919 915	-267.252 089	-4.39
R24	-115.525 067	-114.863 725	-8.46	-115.525 067	-114.863 641	-8.41
R25	-382.223 019	-381.546 032	1.36	-382.223 019	-381.546 038	1.35
R26	-438.428 114	-437.748 340	3.11	-438.428 114	-437.748 348	3.10
R27	-438.125 936	-437.466 160	-9.44	-438.125 936	-437.465 748	-9.18
R28	-627.602 532	-626.926 520	0.74	-627.602 531	-626.925 894	1.14
R29	-552.452 154	-551.779 170	-1.16	-552.452 155	-551.779 058	-1.08
R30	-116.392 103	-115.736 832	-12.27	-116.392 103	-115.736 723	-12.20

Table B.4: RSEs (in kcal/mol) obtained with sd-LRMP2 and ab-LRMP2 methods. The energies (in Hartree) of related molecules and radicals are given. The aug-cc-pVTZ basis set have been used. Parameters are set as 'domsel=0.990' and 'cpldel=0'.

	sd-LRMP2, domsel=0.990			ab-LRMP2, domsel=0.990		
	Molecule	Radical	RSE	Molecule	Radical	RSE
R00	-40.412 426	-39.737 601	0.00	-40.412 425	-39.737 601	0.00
R01	-377.073 401	-376.396 426	1.35	-377.073 400	-376.396 014	1.61
R02	-538.752 143	-538.081 475	-2.61	-538.752 143	-538.081 079	-2.36
R03	-178.765 694	-178.093 232	-1.48	-178.765 694	-178.092 843	-1.24
R04	-154.751 114	-154.078 588	-1.44	-154.751 114	-154.078 614	-1.46
R05	-117.627 077	-116.983 728	-19.75	-117.627 078	-116.984 336	-20.13
R06	-153.549 023	-152.889 031	-9.31	-153.549 023	-152.888 887	-9.22
R07	-132.492 962	-131.830 893	-8.00	-132.492 962	-131.830 758	-7.92
R08	-208.846 439	-208.181 307	-6.08	-208.846 439	-208.180 931	-5.85
R09	-248.060 193	-247.395 061	-6.08	-248.060 193	-247.394 615	-5.80
R10	-267.919 896	-267.255 109	-6.30	-267.919 896	-267.254 733	-6.06
R11	-228.715 470	-228.050 465	-6.16	-228.715 470	-228.050 084	-5.92
R12	-156.841 921	-156.176 467	-5.88	-156.841 922	-156.176 096	-5.65
R13	-139.538 665	-138.869 478	-3.54	-139.538 665	-138.869 123	-3.31
R14	-95.662 651	-95.007 225	-12.17	-95.662 651	-95.006 858	-11.94
R15	-96.016 276	-95.333 786	4.81	-96.016 276	-95.333 629	4.91
R16	-134.874 553	-134.218 472	-11.76	-134.874 553	-134.218 669	-11.89
R17	-208.827 243	-208.169 664	-10.82	-208.827 243	-208.169 631	-10.80
R18	-174.090 398	-173.435 466	-12.48	-174.090 399	-173.434 822	-12.08
R19	-244.637 408	-243.968 525	-3.73	-244.637 408	-243.968 531	-3.73
R20	-452.188 039	-451.518 477	-3.30	-452.188 039	-451.518 626	-3.40
R21	-154.731 568	-154.069 758	-8.17	-154.731 567	-154.069 577	-8.05
R22	-228.688 117	-228.020 559	-4.56	-228.688 117	-228.020 518	-4.53
R23	-267.919 914	-267.253 370	-5.20	-267.919 915	-267.253 321	-5.17
R24	-115.525 502	-114.864 402	-8.61	-115.525 502	-114.864 427	-8.63
R25	-382.223 019	-381.546 032	1.36	-382.223 019	-381.546 038	1.35
R26	-438.428 114	-437.748 340	3.11	-438.428 114	-437.748 348	3.10
R27	-438.125 936	-437.466 160	-9.44	-438.125 936	-437.466 219	-9.48
R28	-627.602 532	-626.926 520	0.74	-627.602 531	-626.926 457	0.78
R29	-552.452 154	-551.780 029	-1.69	-552.452 155	-551.780 269	-1.84
R30	-116.392 103	-115.737 621	-12.77	-116.392 103	-115.737 259	-12.54

Table B.5: RSEs (in kcal/mol) obtained with sd-LRMP2 and ab-LRMP2 methods. The energies (in Hartree) of related molecules and radicals are given. The aug-cc-pVTZ basis set have been used. Parameters are set as 'domsel=0.985' and 'cpldel=1'.

	sd-LRMP2, cpldel=1			ab-LRMP2, cpldel=1		
	Molecule	Radical	RSE	Molecule	Radical	RSE
R00	-40.412 426	-39.737 601	0.00	-40.412 425	-39.737 601	0.00
R01	-377.073 408	-376.396 425	1.35	-377.073 408	-376.395 660	1.83
R02	-538.752 149	-538.081 482	-2.61	-538.752 149	-538.081 086	-2.36
R03	-178.765 697	-178.092 836	-1.23	-178.765 697	-178.092 630	-1.10
R04	-154.751 119	-154.078 598	-1.45	-154.751 119	-154.078 378	-1.31
R05	-117.627 096	-116.983 730	-19.74	-117.627 096	-116.983 578	-19.65
R06	-153.549 025	-152.889 020	-9.30	-153.549 025	-152.888 875	-9.21
R07	-132.492 966	-131.830 897	-8.00	-132.492 966	-131.830 762	-7.92
R08	-208.846 450	-208.181 297	-6.07	-208.846 450	-208.180 918	-5.83
R09	-248.059 347	-247.394 097	-6.01	-248.059 347	-247.393 724	-5.77
R10	-267.919 942	-267.255 106	-6.27	-267.919 942	-267.254 725	-6.03
R11	-228.715 485	-228.050 454	-6.15	-228.715 485	-228.050 071	-5.91
R12	-156.842 003	-156.176 531	-5.87	-156.842 003	-156.176 164	-5.64
R13	-139.538 665	-138.869 478	-3.54	-139.538 665	-138.869 120	-3.31
R14	-95.662 645	-95.007 231	-12.18	-95.662 645	-95.006 852	-11.94
R15	-96.016 275	-95.333 783	4.81	-96.016 275	-95.333 626	4.91
R16	-134.873 144	-134.218 483	-12.65	-134.873 144	-134.218 624	-12.74
R17	-208.826 837	-208.169 672	-11.08	-208.826 837	-208.169 431	-10.93
R18	-174.090 418	-173.434 098	-11.61	-174.090 418	-173.434 515	-11.87
R19	-244.636 759	-243.967 447	-3.46	-244.636 759	-243.967 026	-3.19
R20	-452.188 044	-451.518 482	-3.30	-452.188 044	-451.518 444	-3.28
R21	-154.731 578	-154.069 761	-8.16	-154.731 578	-154.069 581	-8.05
R22	-228.688 121	-228.019 741	-4.04	-228.688 121	-228.019 645	-3.98
R23	-267.919 961	-267.252 212	-4.44	-267.919 961	-267.252 125	-4.39
R24	-115.525 065	-114.863 721	-8.46	-115.525 065	-114.863 635	-8.41
R25	-382.223 028	-381.546 038	1.36	-382.223 028	-381.546 044	1.36
R26	-438.428 122	-437.748 353	3.10	-438.428 122	-437.748 360	3.10
R27	-438.125 942	-437.466 171	-9.45	-438.125 942	-437.465 760	-9.19
R28	-627.602 546	-626.926 535	0.74	-627.602 546	-626.925 912	1.14
R29	-552.452 198	-551.779 227	-1.16	-552.452 198	-551.779 342	-1.24
R30	-116.392 165	-115.736 894	-12.27	-116.392 165	-115.736 789	-12.20

Table B.6: RSEs (in kcal/mol) obtained with sd-LUCCSD and ab-LUCCSD methods. The energies (in Hartree) of related molecules and radicals are given. The aug-cc-pVTZ basis set have been used. Parameters are set as 'domsel=0.985', 'cpldel=1', 'nomp2=0', 'keepcls=0', and 'igskip=0'.

	sd-LUCCSD, default			ab-LUCCSD, default		
	Molecule	Radical	RSE	Molecule	Radical	RSE
R00	-40.432 711	-39.757 694	0.00	-40.432 711	-39.757 694	0.00
R01	-377.092 487	-376.414 620	1.79	-377.092 489	-376.414 475	1.88
R02	-538.797 819	-538.126 072	-2.05	-538.797 819	-538.125 705	-1.82
R03	-178.794 596	-178.121 060	-0.93	-178.794 596	-178.121 008	-0.90
R04	-154.783 340	-154.110 189	-1.17	-154.783 340	-154.110 059	-1.09
R05	-117.664 785	-117.014 549	-15.55	-117.664 786	-117.015 442	-16.11
R06	-153.570 762	-152.909 528	-8.65	-153.570 761	-152.909 707	-8.76
R07	-132.509 859	-131.845 199	-6.50	-132.509 857	-131.845 395	-6.62
R08	-208.870 009	-208.203 941	-5.62	-208.870 010	-208.203 222	-5.16
R09	-248.096 696	-247.430 480	-5.52	-248.096 695	-247.430 090	-5.28
R10	-267.951 808	-267.285 885	-5.71	-267.951 811	-267.285 135	-5.23
R11	-228.733 170	-228.067 122	-5.63	-228.733 169	-228.067 062	-5.59
R12	-156.890 402	-156.223 131	-4.86	-156.890 181	-156.222 919	-4.87
R13	-139.554 845	-138.884 386	-2.86	-139.554 846	-138.883 689	-2.42
R14	-95.688 692	-95.030 690	-10.68	-95.688 691	-95.030 959	-10.85
R15	-96.045 751	-95.362 271	5.31	-96.045 751	-95.362 442	5.20
R16	-134.912 830	-134.255 473	-11.08	-134.912 830	-134.255 558	-11.14
R17	-208.851 282	-208.191 043	-9.27	-208.851 283	-208.191 250	-9.40
R18	-174.140 761	-173.484 272	-11.63	-174.140 761	-173.483 982	-11.44
R19	-244.638 872	-243.967 051	-2.01	-244.638 875	-243.965 911	-1.29
R20	-452.207 222	-451.536 755	-2.85	-452.207 236	-451.536 719	-2.82
R21	-154.763 951	-154.101 536	-7.91	-154.763 736	-154.101 705	-8.15
R22	-228.706 981	-228.037 352	-3.38	-228.706 981	-228.037 320	-3.36
R23	-267.951 827	-267.282 786	-3.75	-267.951 830	-267.282 698	-3.69
R24	-115.544 533	-114.881 501	-7.52	-115.544 533	-114.881 266	-7.37
R25	-382.263 168	-381.586 630	0.95	-382.263 169	-381.586 644	0.95
R26	-438.467 357	-437.787 348	3.13	-438.467 357	-437.787 403	3.10
R27	-438.161 981	-437.500 253	-8.34	-438.161 980	-437.500 925	-8.76
R28	-627.630 995	-626.954 668	0.82	-627.630 594	-626.954 326	0.78
R29	-552.490 208	-551.817 383	-1.38	-552.490 209	-551.817 037	-1.16
R30	-116.417 019	-115.758 788	-10.53	-116.417 021	-115.759 388	-10.91

Table B.7: RSEs (in kcal/mol) obtained with sd-LUCCSD and ab-LUCCSD methods. The energies (in Hartree) of related molecules and radicals are given. The aug-cc-pVTZ basis set have been used. Parameters are set as 'domsel=0.985', 'cpldel=1', 'nomp2=1', 'keepcls=0', and 'igskip=0'.

	sd-LUCCSD, nomp2=1			ab-LUCCSD, nomp2=1		
	Molecule	Radical	RSE	Molecule	Radical	RSE
R00	-40.432 711	-39.757 694	0.00	-40.432 711	-39.757 694	0.00
R01	-377.088 287	-376.411 212	1.29	-377.088 287	-376.410 514	1.73
R02	-538.793 389	-538.123 138	-2.99	-538.793 083	-538.122 577	-2.83
R03	-178.792 217	-178.119 312	-1.33	-178.791 882	-178.119 082	-1.39
R04	-154.779 713	-154.107 325	-1.65	-154.779 676	-154.107 148	-1.56
R05	-117.661 253	-117.012 596	-16.54	-117.661 205	-117.012 485	-16.50
R06	-153.568 903	-152.908 808	-9.36	-153.569 047	-152.908 067	-8.81
R07	-132.507 147	-131.843 992	-7.44	-132.507 147	-131.843 608	-7.20
R08	-208.866 719	-208.201 603	-6.21	-208.866 719	-208.201 294	-6.02
R09	-248.090 264	-247.425 033	-6.14	-248.090 264	-247.424 727	-5.95
R10	-267.946 279	-267.281 270	-6.28	-267.946 279	-267.280 960	-6.09
R11	-228.730 196	-228.065 071	-6.21	-228.730 196	-228.064 758	-6.01
R12	-156.882 662	-156.216 679	-5.67	-156.882 662	-156.216 405	-5.50
R13	-139.554 391	-138.884 344	-3.12	-139.554 391	-138.884 043	-2.93
R14	-95.686 712	-95.030 069	-11.53	-95.686 712	-95.029 832	-11.38
R15	-96.044 175	-95.361 331	4.91	-96.044 175	-95.361 195	5.00
R16	-134.908 090	-134.252 331	-12.08	-134.908 090	-134.252 418	-12.14
R17	-208.847 414	-208.189 136	-10.50	-208.847 414	-208.188 881	-10.34
R18	-174.134 767	-173.477 889	-11.38	-174.134 767	-173.478 191	-11.57
R19	-244.635 864	-243.965 430	-2.88	-244.634 822	-243.965 070	-3.30
R20	-452.201 216	-451.531 334	-3.22	-452.201 216	-451.531 284	-3.19
R21	-154.761 430	-154.099 152	-7.99	-154.761 430	-154.098 984	-7.89
R22	-228.703 696	-228.034 638	-3.74	-228.703 519	-228.034 446	-3.73
R23	-267.946 295	-267.277 782	-4.08	-267.946 295	-267.277 607	-3.97
R24	-115.543 181	-114.880 926	-8.01	-115.543 181	-114.880 895	-7.99
R25	-382.262 460	-381.586 233	0.76	-382.262 460	-381.586 244	0.75
R26	-438.466 101	-437.786 608	2.81	-438.466 101	-437.786 626	2.80
R27	-438.160 207	-437.499 714	-9.11	-438.160 207	-437.499 342	-8.88
R28	-627.626 818	-626.951 617	0.12	-627.626 818	-626.951 041	0.48
R29	-552.486 492	-551.815 079	-2.26	-552.486 492	-551.815 169	-2.32
R30	-116.413 840	-115.757 380	-11.65	-116.413 317	-115.757 374	-11.97

Table B.8: RSEs (in kcal/mol) obtained with sd-LUCCSD and ab-LUCCSD methods. The energies (in Hartree) of related molecules and radicals are given. The aug-cc-pVTZ basis set have been used. Parameters are set as 'domsel=0.985', 'cpldel=1', 'nomp2=0', 'keepcls=1', and 'igskip=0'.

	sd-LUCCSD, keepcls=1			ab-LUCCSD, keepcls=1		
	Molecule	Radical	RSE	Molecule	Radical	RSE
R00	-40.432 711	-39.757 694	0.00	-40.432 711	-39.757 694	0.00
R01	-377.093 979	-376.416 012	1.85	-377.094 223	-376.416 164	1.91
R02	-538.798 038	-538.126 116	-1.94	-538.798 083	-538.126 037	-1.86
R03	-178.795 463	-178.121 811	-0.86	-178.795 572	-178.121 807	-0.79
R04	-154.784 075	-154.110 731	-1.05	-154.784 144	-154.110 683	-0.98
R05	-117.665 041	-117.014 772	-15.53	-117.665 086	-117.015 251	-15.80
R06	-153.571 354	-152.909 850	-8.48	-153.571 515	-152.910 507	-8.79
R07	-132.510 105	-131.845 047	-6.25	-132.510 186	-131.845 910	-6.74
R08	-208.871 058	-208.204 771	-5.48	-208.871 503	-208.204 722	-5.17
R09	-248.098 215	-247.431 758	-5.37	-248.098 593	-247.431 997	-5.28
R10	-267.953 590	-267.287 259	-5.45	-267.954 001	-267.287 173	-5.14
R11	-228.734 407	-228.068 013	-5.41	-228.734 841	-228.068 649	-5.54
R12	-156.891 754	-156.223 943	-4.52	-156.891 534	-156.224 340	-4.91
R13	-139.555 935	-138.884 995	-2.56	-139.556 000	-138.884 891	-2.45
R14	-95.689 575	-95.031 312	-10.51	-95.689 573	-95.031 859	-10.86
R15	-96.046 612	-95.362 692	5.59	-96.046 607	-95.363 061	5.35
R16	-134.913 536	-134.256 188	-11.09	-134.913 517	-134.256 314	-11.18
R17	-208.852 498	-208.191 965	-9.09	-208.852 680	-208.192 687	-9.43
R18	-174.142 006	-173.485 242	-11.45	-174.142 053	-173.485 142	-11.36
R19	-244.640 574	-243.968 386	-1.78	-244.641 077	-243.968 285	-1.40
R20	-452.209 304	-451.538 482	-2.63	-452.209 625	-451.538 852	-2.66
R21	-154.764 981	-154.102 433	-7.82	-154.764 798	-154.102 705	-8.11
R22	-228.708 355	-228.038 267	-3.09	-228.708 604	-228.038 569	-3.13
R23	-267.953 609	-267.284 130	-3.48	-267.954 021	-267.284 561	-3.49
R24	-115.545 566	-114.881 991	-7.18	-115.545 590	-114.882 352	-7.39
R25	-382.263 168	-381.586 630	0.95	-382.263 169	-381.586 644	0.95
R26	-438.467 357	-437.787 348	3.13	-438.467 357	-437.787 403	3.10
R27	-438.161 981	-437.500 253	-8.34	-438.161 980	-437.500 925	-8.76
R28	-627.632 116	-626.955 784	0.83	-627.631 844	-626.955 587	0.78
R29	-552.490 887	-551.818 071	-1.38	-552.490 930	-551.817 745	-1.15
R30	-116.417 023	-115.758 111	-10.11	-116.417 044	-115.759 267	-10.82

Table B.9: RSEs (in kcal/mol) obtained with sd-LUCCSD and ab-LUCCSD methods. The energies (in Hartree) of related molecules and radicals are given. The aug-cc-pVTZ basis set have been used. Parameters are set as 'domsel=0.985', 'cpldel=1', 'nomp2=0', 'keepcls=0', and 'igskip=1'.

	sd-LUCCSD, igskip=1			ab-LUCCSD, igskip=1		
	Molecule	Radical	RSE	Molecule	Radical	RSE
R00	-40.432 690	-39.757 734	0.00	-40.432 690	-39.757 734	0.00
R01	-377.092 602	-376.414 791	1.79	-377.092 605	-376.414 206	2.16
R02	-538.797 797	-538.126 033	-2.00	-538.797 797	-538.125 698	-1.79
R03	-178.794 675	-178.121 194	-0.93	-178.794 675	-178.121 156	-0.90
R04	-154.783 325	-154.110 205	-1.15	-154.783 325	-154.110 317	-1.22
R05	-117.664 795	-117.015 030	-15.81	-117.664 796	-117.015 942	-16.38
R06	-153.570 912	-152.909 720	-8.64	-153.570 911	-152.909 872	-8.73
R07	-132.509 949	-131.845 341	-6.49	-132.509 947	-131.845 539	-6.62
R08	-208.870 026	-208.203 999	-5.60	-208.870 027	-208.203 595	-5.35
R09	-248.096 718	-247.430 543	-5.51	-248.096 719	-247.430 137	-5.25
R10	-267.951 866	-267.285 994	-5.70	-267.951 868	-267.285 611	-5.46
R11	-228.733 196	-228.067 199	-5.62	-228.733 195	-228.066 820	-5.38
R12	-156.890 366	-156.223 106	-4.83	-156.890 367	-156.222 906	-4.70
R13	-139.554 951	-138.884 542	-2.85	-139.554 952	-138.883 818	-2.40
R14	-95.688 652	-95.030 590	-10.60	-95.688 651	-95.030 878	-10.78
R15	-96.045 725	-95.362 277	5.33	-96.045 725	-95.362 465	5.21
R16	-134.912 808	-134.255 380	-11.00	-134.912 807	-134.255 767	-11.24
R17	-208.851 339	-208.191 053	-9.21	-208.851 339	-208.191 042	-9.20
R18	-174.140 695	-173.484 195	-11.58	-174.140 692	-173.483 931	-11.42
R19	-244.638 739	-243.966 916	-1.97	-244.638 742	-243.966 298	-1.58
R20	-452.207 325	-451.536 832	-2.80	-452.207 325	-451.537 033	-2.93
R21	-154.763 962	-154.101 573	-7.89	-154.763 962	-154.101 669	-7.95
R22	-228.707 083	-228.037 496	-3.37	-228.707 084	-228.037 804	-3.56
R23	-267.951 885	-267.282 877	-3.73	-267.951 889	-267.283 137	-3.89
R24	-115.544 539	-114.881 538	-7.50	-115.544 539	-114.881 308	-7.36
R25	-382.263 066	-381.586 547	0.98	-382.263 066	-381.586 562	0.97
R26	-438.467 249	-437.787 247	3.17	-438.467 248	-437.787 303	3.13
R27	-438.161 915	-437.500 079	-8.23	-438.161 914	-437.500 778	-8.67
R28	-627.630 965	-626.954 671	0.84	-627.630 958	-626.954 342	1.04
R29	-552.490 153	-551.817 291	-1.31	-552.490 153	-551.817 309	-1.32
R30	-116.417 124	-115.758 991	-10.56	-116.417 126	-115.759 588	-10.93

Table B.10: RSEs (in kcal/mol) obtained with sd-LUCCSD(T) and ab-LUCCSD(T) methods. The energies (in Hartree) of related molecules and radicals are given. The aug-cc-pVTZ basis set have been used. Parameters are set as 'domsel=0.985', 'cpldel=1', 'nomp2=0', 'keepcls=0', and 'igskip=0'.

	sd-LUCCSD(T), default			ab-LUCCSD(T), default		
	Molecule	Radical	RSE	Molecule	Radical	RSE
R00	-40.439 049	-39.762 648	0.00	-40.439 049	-39.762 648	0.00
R01	-377.126 525	-376.447 985	1.34	-377.126 528	-376.447 256	1.80
R02	-538.818 642	-538.146 277	-2.53	-538.818 643	-538.145 515	-2.05
R03	-178.815 522	-178.140 923	-1.13	-178.815 522	-178.140 565	-0.91
R04	-154.805 586	-154.131 358	-1.36	-154.805 586	-154.131 033	-1.16
R05	-117.687 106	-117.037 180	-16.61	-117.687 106	-117.038 119	-17.20
R06	-153.595 120	-152.933 392	-9.21	-153.595 119	-152.933 538	-9.30
R07	-132.535 003	-131.870 170	-7.26	-132.535 001	-131.870 465	-7.45
R08	-208.903 492	-208.236 633	-5.99	-208.903 492	-208.235 776	-5.45
R09	-248.137 024	-247.469 977	-5.87	-248.137 024	-247.469 554	-5.60
R10	-267.992 122	-267.325 457	-6.11	-267.992 125	-267.324 583	-5.56
R11	-228.766 817	-228.100 048	-6.04	-228.766 816	-228.099 986	-6.01
R12	-156.919 411	-156.251 816	-5.53	-156.919 166	-156.251 504	-5.48
R13	-139.568 855	-138.897 607	-3.23	-139.568 856	-138.896 730	-2.68
R14	-95.703 866	-95.045 267	-11.17	-95.703 865	-95.045 484	-11.31
R15	-96.059 345	-95.374 540	5.27	-96.059 346	-95.374 689	5.18
R16	-134.934 965	-134.277 355	-11.79	-134.934 964	-134.277 162	-11.67
R17	-208.884 757	-208.224 339	-10.03	-208.884 757	-208.224 446	-10.10
R18	-174.169 643	-173.513 308	-12.59	-174.169 643	-173.512 501	-12.09
R19	-244.681 239	-244.008 779	-2.47	-244.681 244	-244.007 385	-1.59
R20	-452.250 115	-451.577 889	-2.62	-452.250 130	-451.578 160	-2.78
R21	-154.786 082	-154.123 349	-8.58	-154.785 845	-154.123 315	-8.70
R22	-228.740 531	-228.070 204	-3.81	-228.992 143	-228.069 912	-3.63
R23	-267.992 139	-267.322 142	-4.02	-267.992 143	-267.321 965	-3.91
R24	-115.559 870	-114.896 209	-7.99	-115.559 870	-114.895 828	-7.76
R25	-382.273 569	-381.596 233	0.59	-382.273 570	-381.596 250	0.58
R26	-438.479 784	-437.799 092	2.69	-438.479 783	-437.799 151	2.66
R27	-438.175 414	-437.514 657	-9.82	-438.175 413	-437.514 074	-9.45
R28	-627.670 082	-626.993 746	-0.04	-627.669 613	-626.992 263	0.60
R29	-552.519 426	-551.846 078	-1.92	-552.519 427	-551.844 682	-1.04
R30	-116.441 014	-115.782 843	-11.44	-116.441 016	-115.783 427	-11.80

Table B.11: RSEs (in kcal/mol) obtained with sd-LUCCSD(T) and ab-LUCCSD(T) methods. The energies (in Hartree) of related molecules and radicals are given. The aug-cc-pVTZ basis set have been used. Parameters are set as 'domsel=0.985', 'cpldel=1', 'nomp2=1', 'keepcls=0', and 'igskip=0'.

	sd-LUCCSD(T), nomp2=1			ab-LUCCSD(T), nomp2=1		
	Molecule	Radical	RSE	Molecule	Radical	RSE
R00	-40.439 049	-39.762 648	0.00	-40.439 049	-39.762 648	0.00
R01	-377.125 500	-376.447 355	1.09	-377.125 500	-376.446 548	1.60
R02	-538.816 939	-538.146 062	-3.47	-538.816 590	-538.145 388	-3.26
R03	-178.813 452	-178.139 351	-1.44	-178.813 076	-178.139 066	-1.50
R04	-154.802 166	-154.128 581	-1.77	-154.802 125	-154.128 370	-1.66
R05	-117.683 625	-117.035 336	-17.64	-117.683 574	-117.035 194	-17.58
R06	-153.593 179	-152.932 695	-9.99	-153.593 353	-152.931 818	-9.33
R07	-132.532 153	-131.868 960	-8.29	-132.532 153	-131.868 522	-8.01
R08	-208.900 450	-208.234 511	-6.56	-208.900 450	-208.234 164	-6.35
R09	-248.131 464	-247.465 474	-6.53	-248.131 464	-247.465 129	-6.32
R10	-267.987 671	-267.321 935	-6.69	-267.987 671	-267.321 585	-6.47
R11	-228.764 136	-228.098 236	-6.59	-228.764 136	-228.097 887	-6.37
R12	-156.911 710	-156.245 215	-6.22	-156.911 710	-156.244 876	-6.00
R13	-139.568 375	-138.897 569	-3.51	-139.568 375	-138.897 201	-3.28
R14	-95.701 646	-95.044 571	-12.13	-95.701 646	-95.044 266	-11.94
R15	-96.057 598	-95.373 489	4.84	-96.057 598	-95.373 321	4.94
R16	-134.930 302	-134.274 304	-12.80	-134.930 302	-134.274 337	-12.82
R17	-208.881 323	-208.222 985	-11.34	-208.881 323	-208.222 675	-11.14
R18	-174.164 921	-173.507 719	-12.05	-174.164 921	-173.508 000	-12.22
R19	-244.678 102	-244.007 152	-3.42	-244.676 790	-244.006 758	-4.00
R20	-452.247 546	-451.576 800	-3.55	-452.247 546	-451.576 722	-3.50
R21	-154.783 970	-154.121 200	-8.55	-154.783 970	-154.120 970	-8.41
R22	-228.737 929	-228.068 288	-4.24	-228.737 687	-228.068 056	-4.25
R23	-267.987 689	-267.318 638	-4.61	-267.987 689	-267.318 424	-4.48
R24	-115.558 360	-114.895 552	-8.53	-115.558 360	-114.895 481	-8.49
R25	-382.274 755	-381.597 135	0.77	-382.274 755	-381.597 143	0.76
R26	-438.480 729	-437.800 002	2.71	-438.480 729	-437.800 015	2.71
R27	-438.176 125	-437.515 333	-9.79	-438.176 125	-437.514 922	-9.54
R28	-627.672 216	-626.996 277	-0.29	-627.672 216	-626.995 589	0.14
R29	-552.521 797	-551.849 744	-2.73	-552.521 797	-551.849 780	-2.75
R30	-116.437 551	-115.781 315	-12.65	-116.436 949	-115.781 309	-13.03

Table B.12: RSEs (in kcal/mol) obtained with sd-LUCCSD(T) and ab-LUCCSD(T) methods. The energies (in Hartree) of related molecules and radicals are given. The aug-cc-pVTZ basis set have been used. Parameters are set as 'domsel=0.985', 'cpldel=1', 'nomp2=0', 'keepcls=1', and 'igskip=0'.

	sd-LUCCSD(T), keepcls=1			ab-LUCCSD(T), keepcls=1		
	Molecule	Radical	RSE	Molecule	Radical	RSE
R00	-40.439 049	-39.762 648	0.00	-40.439 049	-39.762 648	0.00
R01	-377.128 236	-376.449 583	1.41	-377.128 404	-376.449 079	1.84
R02	-538.818 934	-538.146 355	-2.40	-538.818 938	-538.145 889	-2.10
R03	-178.816 548	-178.141 804	-1.04	-178.816 614	-178.141 467	-0.79
R04	-154.806 470	-154.132 017	-1.22	-154.806 499	-154.131 754	-1.04
R05	-117.687 449	-117.037 474	-16.58	-117.687 445	-117.038 058	-16.95
R06	-153.595 822	-152.933 774	-9.01	-153.595 937	-152.934 486	-9.38
R07	-132.535 352	-131.870 050	-6.96	-132.535 380	-131.871 002	-7.54
R08	-208.904 714	-208.237 597	-5.83	-208.905 147	-208.237 480	-5.48
R09	-248.138 810	-247.471 484	-5.69	-248.139 153	-247.471 743	-5.64
R10	-267.994 186	-267.327 048	-5.81	-267.994 571	-267.326 901	-5.48
R11	-228.768 252	-228.101 077	-5.79	-228.768 671	-228.101 797	-5.98
R12	-156.921 088	-156.252 885	-5.14	-156.920 745	-156.253 210	-5.56
R13	-139.570 075	-138.898 297	-2.90	-139.570 125	-138.898 047	-2.71
R14	-95.704 875	-95.045 981	-10.99	-95.704 843	-95.046 525	-11.35
R15	-96.060 322	-95.375 018	5.59	-96.060 293	-95.375 384	5.34
R16	-134.935 832	-134.278 221	-11.79	-134.935 756	-134.278 048	-11.73
R17	-208.886 179	-208.225 389	-9.80	-208.886 341	-208.226 109	-10.15
R18	-174.171 116	-173.514 491	-12.41	-174.171 123	-173.513 846	-12.00
R19	-244.683 121	-244.010 220	-2.20	-244.683 618	-244.010 011	-1.75
R20	-452.252 482	-451.579 844	-2.36	-452.252 722	-451.580 463	-2.60
R21	-154.787 277	-154.124 388	-8.48	-154.787 055	-154.124 445	-8.65
R22	-228.742 107	-228.071 279	-3.50	-228.742 371	-228.071 341	-3.37
R23	-267.994 203	-267.323 708	-3.71	-267.994 588	-267.324 034	-3.67
R24	-115.561 031	-114.896 777	-7.62	-115.561 037	-114.897 025	-7.77
R25	-382.273 569	-381.596 233	0.59	-382.273 570	-381.596 250	0.58
R26	-438.479 784	-437.799 092	2.69	-438.479 783	-437.799 151	2.66
R27	-438.175 414	-437.514 657	-9.82	-438.175 413	-437.514 074	-9.45
R28	-627.671 327	-626.994 988	-0.04	-627.671 018	-626.993 684	0.59
R29	-552.520 186	-551.846 852	-1.92	-552.520 244	-551.845 485	-1.03
R30	-116.441 099	-115.782 148	-10.95	-116.441 055	-115.783 386	-11.75

Table B.13: RSEs (in kcal/mol) obtained with sd-LUCCSD(T) and ab-LUCCSD(T) methods. The energies (in Hartree) of related molecules and radicals are given. The aug-cc-pVTZ basis set have been used. Parameters are set as 'domsel=0.985', 'cpldel=1', 'nomp2=0', 'keepcls=0', and 'igskip=1'.

	sd-LUCCSD(T), igskip=1			ab-LUCCSD(T), igskip=1		
	Molecule	Radical	RSE	Molecule	Radical	RSE
R00	-40.439 025	-39.762 693	0.00	-40.439 025	-39.762 693	0.00
R01	-377.126 686	-376.448 214	1.34	-377.126 688	-376.446 991	2.11
R02	-538.818 616	-538.146 237	-2.48	-538.818 616	-538.145 512	-2.03
R03	-178.815 627	-178.141 094	-1.13	-178.815 627	-178.140 751	-0.91
R04	-154.805 575	-154.131 384	-1.34	-154.805 575	-154.131 326	-1.31
R05	-117.687 119	-117.037 904	-17.02	-117.687 119	-117.038 850	-17.61
R06	-153.595 339	-152.933 690	-9.21	-153.595 339	-152.933 805	-9.29
R07	-132.535 116	-131.870 367	-7.27	-132.535 115	-131.870 666	-7.46
R08	-208.903 554	-208.236 757	-5.98	-208.903 554	-208.236 282	-5.69
R09	-248.137 091	-247.470 103	-5.86	-248.137 091	-247.469 660	-5.59
R10	-267.992 236	-267.325 648	-6.11	-267.992 239	-267.325 217	-5.84
R11	-228.766 894	-228.100 202	-6.05	-228.766 894	-228.099 757	-5.77
R12	-156.919 367	-156.251 788	-5.49	-156.919 367	-156.251 488	-5.30
R13	-139.568 991	-138.897 805	-3.23	-139.568 992	-138.896 894	-2.66
R14	-95.703 820	-95.045 157	-11.09	-95.703 819	-95.045 396	-11.24
R15	-96.059 317	-95.374 547	5.29	-96.059 317	-95.374 714	5.19
R16	-134.934 939	-134.277 253	-11.70	-134.934 938	-134.277 403	-11.80
R17	-208.884 869	-208.224 400	-9.95	-208.884 870	-208.224 257	-9.86
R18	-174.169 571	-173.513 223	-12.54	-174.169 567	-173.512 452	-12.06
R19	-244.681 138	-244.008 692	-2.44	-244.681 143	-244.007 981	-1.99
R20	-452.250 265	-451.578 011	-2.56	-452.250 266	-451.578 560	-2.90
R21	-154.786 109	-154.123 410	-8.56	-154.786 109	-154.123 292	-8.48
R22	-228.740 703	-228.070 421	-3.80	-228.740 704	-228.070 542	-3.87
R23	-267.992 252	-267.322 294	-4.00	-267.992 257	-267.322 541	-4.15
R24	-115.559 884	-114.896 264	-7.98	-115.559 884	-114.895 885	-7.74
R25	-382.273 459	-381.596 145	0.62	-382.273 459	-381.596 164	0.60
R26	-438.479 664	-437.798 981	2.73	-438.479 663	-437.799 042	2.69
R27	-438.175 338	-437.514 461	-9.70	-438.175 337	-437.513 911	-9.35
R28	-627.670 109	-626.993 828	-0.03	-627.670 100	-626.992 351	0.89
R29	-552.519 403	-551.846 020	-1.85	-552.519 403	-551.845 032	-1.23
R30	-116.441 137	-115.783 118	-11.49	-116.441 139	-115.783 705	-11.86

Table B.14: (T) correction (in kcal/mol) of the radicals involved in RSEs obtained with sd-LUCCSD(T), ab-LUCCSD(T), and UCCSD(T) methods. Numbers in parenthesis indicate percent of the conventional (T) correction.

	UCCSD(T)	sd-LUCCSD(T)	ab-LUCCSD(T)
R01	-23.78	-20.94(88%)	-20.57(87%)
R02	-14.91	-12.68(85%)	-12.43(83%)
R03	-13.16	-12.46(95%)	-12.27(93%)
R04	-13.97	-13.28(95%)	-13.16(94%)
R05	-14.67	-14.20(97%)	-14.23(97%)
R06	-15.43	-14.98(97%)	-14.95(97%)
R07	-16.02	-15.67(98%)	-15.73(98%)
R08	-21.41	-20.51(96%)	-20.43(95%)
R09	-26.49	-24.78(94%)	-24.76(93%)
R10	-26.65	-24.83(93%)	-24.75(93%)
R11	-21.60	-20.66(96%)	-20.66(96%)
R12	-18.83	-18.00(96%)	-17.94(95%)
R13	-8.56	-8.30(97%)	-8.18(96%)
R14	-9.48	-9.15(96%)	-9.11(96%)
R15	-7.91	-7.70(97%)	-7.68(97%)
R16	-14.44	-13.73(95%)	-13.56(94%)
R17	-21.98	-20.89(95%)	-20.83(95%)
R18	-19.70	-18.22(92%)	-17.90(91%)
R19	-27.24	-26.18(96%)	-26.03(96%)
R20	-30.05	-25.81(86%)	-26.00(87%)
R21	-14.45	-13.69(95%)	-13.56(94%)
R22	-22.01	-20.61(94%)	-20.45(94%)
R23	-26.85	-24.70(92%)	-24.64(92%)
R24	-9.56	-9.23(97%)	-9.14(96%)
R25	-7.10	-6.03(85%)	-6.03(85%)
R26	-8.79	-7.37(84%)	-7.37(78%)
R27	-10.18	-9.04(89%)	-8.25(81%)
R28	-29.43	-24.52(83%)	-23.81(81%)
R29	-22.96	-18.01(78%)	-17.35(76%)
R30	-15.30	-15.09(99%)	-15.08(99%)
Ave		93%	92%
Max		99%	99%
Min		78%	76%

Table B.15: Errors of RSEs (in kcal/mol) obtained with sd-LRMP2 and ab-LRMP2 with respect to the ones obtained with RMP2.

	sd-LRMP2			ab-LRMP2		
	default	domsel	cpldel	default	domsel	cpldel
RSE01	-0.52	-0.52	-0.51	-0.04	-0.26	-0.03
RSE02	-0.48	-0.48	-0.48	-0.23	-0.23	-0.23
RSE03	-0.15	-0.40	-0.15	-0.02	-0.16	-0.02
RSE04	-0.08	-0.08	-0.08	0.06	-0.09	0.06
RSE05	-0.37	-0.37	-0.36	-0.27	-0.75	-0.26
RSE06	-0.22	-0.22	-0.21	-0.13	-0.13	-0.12
RSE07	-0.17	-0.17	-0.17	-0.08	-0.08	-0.08
RSE08	-0.38	-0.38	-0.36	-0.14	-0.14	-0.13
RSE09	-0.35	-0.40	-0.33	-0.12	-0.12	-0.09
RSE10	-0.38	-0.38	-0.35	-0.14	-0.14	-0.11
RSE11	-0.39	-0.39	-0.37	-0.15	-0.15	-0.13
RSE12	-0.33	-0.33	-0.31	-0.09	-0.09	-0.08
RSE13	-0.13	-0.13	-0.13	0.09	0.09	0.10
RSE14	0.20	-0.30	-0.31	0.21	-0.07	-0.07
RSE15	0.02	0.02	0.03	0.12	0.12	0.12
RSE16	-0.37	0.51	-0.38	-0.31	0.39	-0.47
RSE17	-0.57	-0.31	-0.57	-0.42	-0.29	-0.42
RSE18	0.50	-0.37	0.50	0.62	0.03	0.23
RSE19	0.42	-0.57	-0.30	0.68	-0.57	-0.03
RSE20	0.02	0.02	0.02	0.04	-0.08	0.04
RSE21	0.11	0.11	0.11	0.22	0.22	0.23
RSE22	-0.05	-0.57	-0.05	0.01	-0.54	0.01
RSE23	-0.01	-0.76	-0.01	0.04	-0.73	0.05
RSE24	0.05	-0.10	0.05	0.11	-0.11	0.11
RSE25	-0.16	-0.16	-0.15	-0.16	-0.16	-0.16
RSE26	-0.14	-0.14	-0.15	-0.15	-0.15	-0.15
RSE27	-0.57	-0.57	-0.57	-0.31	-0.60	-0.31
RSE28	-0.45	-0.45	-0.45	-0.05	-0.41	-0.06
RSE29	-0.04	-0.58	-0.05	0.03	-0.73	-0.12
RSE30	0.06	-0.44	0.06	0.13	-0.21	0.12
MAE	0.26	0.34	0.25	0.17	0.26	0.14
RMSE	0.31	0.39	0.31	0.24	0.34	0.18
MAX	-0.57	-0.76	-0.57	0.68	-0.75	-0.47

Table B.16: Errors of RSEs (in kcal/mol) obtained with sd-LUCCSD and ab-LUCCSD with respect to the ones obtained with UCCSD.

	sd-LUCCSD				ab-LUCCSD			
	default	nomp2	keepcls	igskip	default	nomp2	keepcls	igskip
RSE01	0.06	-0.44	0.12	0.06	0.15	0.00	0.18	0.43
RSE02	0.54	-0.40	0.65	0.59	0.77	-0.24	0.73	0.80
RSE03	0.26	-0.14	0.33	0.26	0.29	-0.20	0.40	0.29
RSE04	0.43	-0.05	0.55	0.45	0.51	0.04	0.62	0.38
RSE05	0.68	-0.31	0.70	0.43	0.12	-0.27	0.43	-0.15
RSE06	0.56	-0.16	0.73	0.57	0.44	0.40	0.41	0.47
RSE07	0.85	-0.10	1.10	0.85	0.72	0.14	0.61	0.73
RSE08	0.31	-0.29	0.45	0.32	0.76	-0.09	0.76	0.58
RSE09	0.37	-0.24	0.52	0.39	0.62	-0.05	0.61	0.64
RSE10	0.31	-0.27	0.56	0.31	0.78	-0.07	0.87	0.55
RSE11	0.28	-0.30	0.50	0.29	0.32	-0.10	0.37	0.52
RSE12	0.59	-0.22	0.93	0.62	0.58	-0.05	0.54	0.75
RSE13	0.18	-0.08	0.48	0.19	0.62	0.11	0.59	0.64
RSE14	0.61	-0.24	0.78	0.69	0.44	-0.09	0.43	0.51
RSE15	0.44	0.04	0.71	0.45	0.33	0.12	0.48	0.34
RSE16	0.71	-0.29	0.70	0.79	0.65	-0.35	0.61	0.55
RSE17	0.76	-0.47	0.94	0.83	0.63	-0.31	0.61	0.83
RSE18	0.24	0.49	0.41	0.29	0.42	0.30	0.51	0.45
RSE19	0.63	-0.24	0.86	0.67	1.35	-0.67	1.24	1.06
RSE20	0.45	0.08	0.67	0.51	0.48	0.12	0.64	0.38
RSE21	0.23	0.14	0.31	0.25	-0.01	0.25	0.02	0.19
RSE22	0.41	0.05	0.69	0.42	0.43	0.06	0.66	0.23
RSE23	0.41	0.08	0.68	0.42	0.46	0.19	0.67	0.26
RSE24	0.62	0.13	0.96	0.63	0.76	0.15	0.74	0.78
RSE25	0.07	-0.13	0.07	0.09	0.06	-0.14	0.06	0.08
RSE26	0.21	-0.11	0.21	0.25	0.18	-0.12	0.18	0.21
RSE27	0.29	-0.49	0.29	0.39	-0.13	-0.25	-0.13	-0.05
RSE28	0.36	-0.35	0.36	0.37	0.32	0.01	0.31	0.58
RSE29	0.96	0.07	0.95	1.02	1.18	0.02	1.19	1.01
RSE30	1.26	0.14	1.68	1.23	0.88	-0.18	0.97	0.86
MAE	0.47	0.22	0.63	0.49	0.51	0.17	0.55	0.51
RMSE	0.54	0.26	0.71	0.55	0.60	0.22	0.62	0.57
MAX	1.26	-0.49	1.68	1.23	1.35	-0.67	1.24	1.06

Table B.17: Errors of RSEs (in kcal/mol) obtained with sd-LUCCSD(T) and ab-LUCCSD(T) with respect to the ones obtained with UCCSD(T).

	sd-LUCCSD(T)				ab-LUCCSD(T)			
	default	nomp2	keepcls	igskip	default	nomp2	keepcls	igskip
RSE01	-0.26	-0.50	-0.18	-0.26	0.20	0.00	0.24	0.51
RSE02	0.46	-0.47	0.59	0.51	0.94	-0.27	0.89	0.97
RSE03	0.23	-0.08	0.32	0.23	0.46	-0.14	0.58	0.45
RSE04	0.33	-0.08	0.47	0.35	0.53	0.03	0.65	0.38
RSE05	0.65	-0.38	0.68	0.24	0.06	-0.32	0.31	-0.35
RSE06	0.60	-0.18	0.80	0.59	0.51	0.48	0.42	0.52
RSE07	0.92	-0.11	1.21	0.91	0.73	0.16	0.63	0.72
RSE08	0.24	-0.34	0.40	0.24	0.77	-0.12	0.74	0.54
RSE09	0.36	-0.30	0.54	0.37	0.63	-0.08	0.59	0.65
RSE10	0.25	-0.33	0.55	0.24	0.80	-0.11	0.88	0.52
RSE11	0.19	-0.36	0.44	0.18	0.23	-0.14	0.25	0.46
RSE12	0.41	-0.28	0.79	0.44	0.45	-0.07	0.37	0.63
RSE13	0.21	-0.07	0.54	0.21	0.76	0.16	0.73	0.78
RSE14	0.71	-0.25	0.89	0.79	0.57	-0.06	0.53	0.64
RSE15	0.47	0.03	0.78	0.49	0.37	0.14	0.53	0.38
RSE16	0.67	-0.34	0.68	0.76	0.80	-0.36	0.74	0.67
RSE17	0.74	-0.57	0.97	0.81	0.67	-0.37	0.62	0.90
RSE18	-0.01	0.54	0.18	0.05	0.50	0.36	0.59	0.53
RSE19	0.68	-0.27	0.96	0.71	1.56	-0.84	1.40	1.16
RSE20	1.04	0.11	1.30	1.10	0.88	0.16	1.06	0.76
RSE21	0.14	0.16	0.23	0.16	0.01	0.30	0.06	0.23
RSE22	0.50	0.07	0.82	0.52	0.69	0.07	0.94	0.44
RSE23	0.69	0.10	1.00	0.71	0.80	0.23	1.04	0.56
RSE24	0.68	0.14	1.05	0.69	0.92	0.19	0.90	0.93
RSE25	-0.36	-0.18	-0.36	-0.33	-0.37	-0.18	-0.37	-0.34
RSE26	-0.17	-0.15	-0.17	-0.13	-0.21	-0.16	-0.21	-0.17
RSE27	-0.56	-0.54	-0.56	-0.44	-0.19	-0.28	-0.19	-0.10
RSE28	-0.18	-0.43	-0.18	-0.18	0.45	0.00	0.44	0.75
RSE29	0.88	0.07	0.88	0.95	1.76	0.05	1.77	1.57
RSE30	1.35	0.13	1.84	1.29	0.98	-0.24	1.03	0.93
MAE	0.50	0.25	0.68	0.50	0.63	0.20	0.66	0.62
RMSE	0.58	0.30	0.78	0.59	0.73	0.26	0.75	0.69
MAX	1.35	-0.57	1.84	1.29	1.76	-0.84	1.77	1.57

Table B.18: Errors of RSEs (in kcal/mol) obtained with UCCSD, RMP2, sd-LRMP2, and ab-LRMP2 with respect to the ones obtained with UCCSD(T).

	UCCSD	RMP2	sd-LRMP2			ab-LRMP2		
			default	domsel	cpldel	default	domsel	cpldel
RSE01	0.13	0.27	-0.25	-0.25	-0.24	0.23	0.01	0.24
RSE02	0.40	0.86	0.38	0.38	0.38	0.63	0.63	0.63
RSE03	0.18	0.28	0.13	-0.12	0.13	0.26	0.13	0.26
RSE04	0.09	0.33	0.25	0.25	0.25	0.38	0.23	0.38
RSE05	1.03	-2.12	-2.49	-2.49	-2.48	-2.39	-2.87	-2.38
RSE06	0.60	0.71	0.50	0.50	0.51	0.59	0.59	0.60
RSE07	0.83	0.34	0.17	0.17	0.17	0.26	0.26	0.26
RSE08	0.30	0.52	0.14	0.14	0.15	0.38	0.38	0.39
RSE09	0.34	0.55	0.20	0.15	0.23	0.43	0.43	0.46
RSE10	0.35	0.44	0.06	0.06	0.09	0.30	0.30	0.33
RSE11	0.33	0.46	0.07	0.07	0.09	0.31	0.31	0.33
RSE12	0.48	0.38	0.05	0.05	0.06	0.28	0.28	0.29
RSE13	0.40	0.03	-0.10	-0.10	-0.10	0.12	0.12	0.13
RSE14	0.59	0.01	0.21	-0.29	-0.30	0.22	-0.06	-0.06
RSE15	0.07	-0.02	0.00	0.00	0.00	0.10	0.10	0.10
RSE16	0.68	0.19	-0.18	0.70	-0.19	-0.11	0.58	-0.28
RSE17	0.73	0.26	-0.32	-0.06	-0.32	-0.16	-0.03	-0.16
RSE18	0.72	0.48	0.98	0.10	0.97	1.10	0.51	0.71
RSE19	0.52	-0.01	0.41	-0.58	-0.31	0.68	-0.58	-0.04
RSE20	0.35	0.34	0.36	0.36	0.36	0.38	0.26	0.38
RSE21	0.58	0.44	0.55	0.55	0.55	0.66	0.66	0.66
RSE22	0.53	0.32	0.27	-0.25	0.27	0.33	-0.22	0.33
RSE23	0.55	0.28	0.26	-0.49	0.27	0.32	-0.46	0.32
RSE24	0.54	0.16	0.21	0.06	0.21	0.26	0.04	0.27
RSE25	-0.06	0.57	0.41	0.41	0.42	0.41	0.41	0.41
RSE26	0.06	0.39	0.24	0.24	0.24	0.24	0.24	0.24
RSE27	0.63	0.38	-0.18	-0.18	-0.19	0.07	-0.22	0.07
RSE28	0.32	1.05	0.60	0.60	0.60	0.99	0.64	0.99
RSE29	0.47	1.68	1.65	1.11	1.64	1.72	0.96	1.57
RSE30	1.00	0.46	0.52	0.02	0.52	0.58	0.25	0.58
MAE	0.46	0.48	0.40	0.36	0.41	0.50	0.43	0.46
RMSE	0.53	0.65	0.64	0.59	0.64	0.70	0.66	0.66
MAX	1.03	-2.12	-2.49	-2.49	-2.48	-2.39	-2.87	-2.38

Table B.19: Errors of RSEs (in kcal/mol) obtained with sd-LUCCSD and ab-LUCCSD with respect to the ones obtained with UCCSD(T).

	sd-LUCCSD				ab-LUCCSD			
	default	nomp2	keepcls	igskip	default	nomp2	keepcls	igskip
RSE01	0.19	-0.31	0.25	0.19	0.28	0.13	0.31	0.56
RSE02	0.94	0.00	1.05	0.99	1.17	0.16	1.13	1.20
RSE03	0.43	0.04	0.51	0.44	0.47	-0.03	0.58	0.46
RSE04	0.52	0.04	0.64	0.54	0.60	0.13	0.72	0.47
RSE05	1.71	0.72	1.73	1.45	1.15	0.76	1.46	0.88
RSE06	1.16	0.44	1.33	1.17	1.04	1.00	1.01	1.07
RSE07	1.68	0.73	1.93	1.68	1.55	0.97	1.43	1.56
RSE08	0.61	0.01	0.75	0.62	1.06	0.20	1.06	0.88
RSE09	0.71	0.09	0.86	0.72	0.95	0.28	0.95	0.98
RSE10	0.65	0.08	0.91	0.66	1.13	0.27	1.22	0.90
RSE11	0.60	0.03	0.82	0.61	0.64	0.22	0.69	0.85
RSE12	1.07	0.26	1.41	1.10	1.07	0.43	1.02	1.23
RSE13	0.58	0.32	0.88	0.59	1.02	0.51	0.99	1.04
RSE14	1.20	0.35	1.37	1.28	1.03	0.50	1.02	1.10
RSE15	0.50	0.10	0.78	0.52	0.40	0.19	0.54	0.40
RSE16	1.38	0.38	1.38	1.47	1.33	0.33	1.29	1.22
RSE17	1.49	0.26	1.68	1.56	1.36	0.42	1.34	1.57
RSE18	0.96	1.20	1.13	1.01	1.14	1.01	1.22	1.17
RSE19	1.15	0.28	1.38	1.19	1.86	-0.15	1.76	1.58
RSE20	0.81	0.44	1.03	0.86	0.84	0.47	1.00	0.73
RSE21	0.81	0.72	0.89	0.83	0.57	0.82	0.60	0.77
RSE22	0.93	0.58	1.22	0.95	0.95	0.58	1.19	0.75
RSE23	0.96	0.63	1.23	0.97	1.01	0.74	1.22	0.81
RSE24	1.15	0.66	1.49	1.17	1.30	0.68	1.28	1.31
RSE25	0.01	-0.18	0.01	0.04	0.00	-0.19	0.00	0.03
RSE26	0.27	-0.05	0.27	0.30	0.24	-0.07	0.24	0.27
RSE27	0.92	0.14	0.92	1.03	0.50	0.38	0.50	0.59
RSE28	0.68	-0.03	0.68	0.70	0.64	0.33	0.64	0.90
RSE29	1.43	0.54	1.42	1.49	1.64	0.48	1.65	1.48
RSE30	2.25	1.14	2.68	2.23	1.88	0.82	1.97	1.86
MAE	0.93	0.36	1.09	0.94	0.96	0.44	1.00	0.95
RMSE	1.04	0.48	1.21	1.16	1.06	0.53	1.10	1.04
MAX	2.25	1.20	2.68	2.23	1.88	1.01	1.97	1.86

Table B.20: Vertical ionization potentials (IPs, in eV) obtained with HF and RMP2 methods. The energies (in Hartree) of related molecules and cations (removing one electron from the corresponding molecules and maintaining the geometry unchanged) are given. The cc-pVTZ basis set have been used. The molecules are numbered from M01 to M30 as discussed in Chapter 5.

	HF			RMP2		
	Molecule	Cation	IP	Molecule	Cation	IP
M01	-76.056 833	-75.651 298	11.035	-76.318 551	-75.853 839	12.645
M02	-113.911 993	-113.557 457	9.647	-114.306 834	-113.894 071	11.232
M03	-40.213 305	-39.717 159	13.501	-40.411 566	-39.884 629	14.339
M04	-111.217 577	-110.906 935	8.453	-111.659 896	-111.337 873	8.763
M05	-95.253 097	-94.941 906	8.468	-95.657 496	-95.297 705	9.790
M06	-152.925 746	-152.530 608	10.752	-153.500 885	-153.069 282	11.745
M07	-79.259 808	-78.802 308	12.449	-79.629 756	-79.166 865	12.596
M08	-224.078 120	-223.741 106	9.171	-224.886 216	-224.498 402	10.553
M09	-376.521 989	-376.090 841	11.732	-377.762 823	-377.367 792	10.749
M10	-154.126 126	-153.795 331	9.001	-154.724 154	-154.341 451	10.414
M11	-154.142 460	-153.789 438	9.606	-154.743 997	-154.336 481	11.089
M12	-228.707 064	-228.421 029	7.783	-229.575 739	-229.244 140	9.023
M13	-224.894 672	-224.612 098	7.689	-225.775 693	-225.438 211	9.183
M14	-551.382 301	-551.091 269	7.919	-552.195 273	-551.861 609	9.079
M15	-154.977 769	-154.685 035	7.966	-155.627 499	-155.294 786	9.054
M16	-282.947 230	-282.618 433	8.947	-283.956 317	-283.581 342	10.204
M17	-650.976 602	-650.612 398	9.911	-651.902 765	-651.482 142	11.446
M18	-118.307 710	-117.872 833	11.834	-118.851 568	-118.404 535	12.164
M19	-156.168 515	-155.874 630	7.997	-156.853 598	-156.501 320	9.586
M20	-230.779 631	-230.476 125	8.259	-231.729 092	-231.382 979	9.418
M21	-379.364 738	-378.987 269	10.271	-380.736 588	-380.332 141	11.006
M22	-321.996 503	-321.674 397	8.765	-323.182 261	-322.812 950	10.049
M23	-628.325 456	-628.043 299	7.678	-629.449 547	-629.142 766	8.348
M24	-157.355 481	-156.953 054	10.951	-158.073 529	-157.641 937	11.744
M25	-231.891 733	-231.626 847	7.208	-232.858 001	-232.552 695	8.308
M26	-285.832 505	-285.569 126	7.167	-286.993 665	-286.700 566	7.976
M27	-380.557 600	-380.282 626	7.482	-381.979 158	-381.673 296	8.323
M28	-196.403 166	-196.005 547	10.820	-197.295 432	-196.884 068	11.194
M29	-234.286 024	-233.893 301	10.687	-235.328 718	-234.946 642	10.397
M30	-235.450 858	-235.059 193	10.658	-236.517 379	-236.116 377	10.912

Table B.21: IPs (in eV) obtained with UCCSD and UCCSD(T) methods. The energies (in Hartree) of related molecules and cations (removing one electron from the corresponding molecules and maintaining the geometry unchanged) are given. The cc-pVTZ basis set have been used. The molecules are numbered from M01 to M30 as discussed in Chapter 5.

	UCCSD			UCCSD(T)		
	Molecule	Cation	IP	Molecule	Cation	IP
M01	-76.324 501	-75.868 895	12.398	-76.332 180	-75.873 716	12.475
M02	-114.317 241	-113.922 325	10.746	-114.333 707	-113.936 719	10.803
M03	-40.431 809	-39.905 773	14.314	-40.438 097	-39.910 805	14.348
M04	-111.678 299	-111.349 820	8.938	-111.695 249	-111.368 111	8.902
M05	-95.681 858	-95.330 016	9.574	-95.696 649	-95.342 624	9.634
M06	-153.519 497	-153.089 772	11.693	-153.543 661	-153.112 780	11.725
M07	-79.660 969	-79.192 161	12.757	-79.674 438	-79.207 786	12.698
M08	-224.899 456	-224.529 996	10.054	-224.933 468	-224.564 537	10.039
M09	-377.760 613	-377.341 052	11.417	-377.815 869	-377.405 424	11.169
M10	-154.754 323	-154.386 021	10.022	-154.776 697	-154.406 798	10.065
M11	-154.773 009	-154.381 487	10.654	-154.795 281	-154.402 403	10.691
M12	-229.590 609	-229.264 020	8.887	-229.634 841	-229.305 489	8.962
M13	-225.786 241	-225.461 020	8.850	-225.832 073	-225.503 764	8.934
M14	-552.219 195	-551.891 373	8.921	-552.265 630	-551.935 347	8.987
M15	-155.663 545	-155.330 552	9.061	-155.695 634	-155.359 431	9.149
M16	-283.975 386	-283.608 847	9.974	-284.017 882	-283.650 493	9.997
M17	-651.939 435	-651.541 933	10.817	-651.982 598	-651.584 089	10.844
M18	-118.893 017	-118.445 614	12.174	-118.914 009	-118.469 272	12.102
M19	-156.896 897	-156.552 922	9.360	-156.927 193	-156.578 405	9.491
M20	-231.753 906	-231.413 224	9.270	-231.805 665	-231.462 007	9.351
M21	-380.756 141	-380.348 840	11.083	-380.828 066	-380.421 866	11.053
M22	-323.210 606	-322.850 421	9.801	-323.261 165	-322.900 091	9.825
M23	-629.483 843	-629.177 481	8.337	-629.483 843	-629.240 451	8.333
M24	-158.125 148	-157.699 318	11.587	-158.125 148	-157.728 733	11.565
M25	-232.904 238	-232.600 913	8.254	-232.904 238	-232.648 083	8.324
M26	-287.019 779	-286.730 233	7.879	-287.081 134	-286.790 727	7.902
M27	-381.996 216	-381.694 280	8.216	-382.067 425	-381.765 160	8.225
M28	-197.357 225	-196.942 627	11.282	-197.393 400	-196.981 029	11.221
M29	-235.389 672	-234.991 922	10.823	-235.434 711	-235.042 141	10.682
M30	-236.589 340	-236.183 689	11.038	-236.633 122	-236.230 739	10.949

Table B.22: IPs (in eV) obtained with sd-LRMP2 and ab-LRMP2 methods. The energies (in Hartree) of related molecules and cations (removing one electron from the corresponding molecules and maintaining the geometry unchanged) are given. The cc-pVTZ basis set have been used. Parameters are set as default, i.e., 'domsel= 0.985' and 'cpldel=0'.

	sd-LRMP2, default			ab-LRMP2, default		
	Molecule	Cation	IP	Molecule	Cation	IP
M01	-76.317 081	-75.853 065	12.627	-76.317 081	-75.853 065	12.627
M02	-114.305 137	-113.892 377	11.232	-114.305 137	-113.892 447	11.230
M03	-40.409 873	-39.883 430	14.325	-40.409 873	-39.883 233	14.331
M04	-111.655 808	-111.335 047	8.728	-111.655 818	-111.334 484	8.744
M05	-95.653 021	-95.294 214	9.764	-95.653 021	-95.294 209	9.764
M06	-153.495 956	-153.065 820	11.705	-153.495 956	-153.065 402	11.716
M07	-79.625 392	-79.159 242	12.685	-79.625 392	-79.162 188	12.604
M08	-224.879 448	-224.494 198	10.483	-224.879 448	-224.493 286	10.508
M09	-377.753 849	-377.361 941	10.664	-377.753 848	-377.360 525	10.703
M10	-154.718 502	-154.335 551	10.421	-154.718 503	-154.335 816	10.413
M11	-154.736 907	-154.331 175	11.041	-154.736 907	-154.330 819	11.050
M12	-229.567 723	-229.236 037	9.026	-229.567 724	-229.236 237	9.020
M13	-225.766 790	-225.429 122	9.188	-225.766 791	-225.429 594	9.176
M14	-552.187 293	-551.853 811	9.075	-552.187 293	-551.853 834	9.074
M15	-155.620 178	-155.288 135	9.035	-155.620 178	-155.287 947	9.040
M16	-283.946 431	-283.573 138	10.158	-283.946 430	-283.572 787	10.167
M17	-651.893 791	-651.474 883	11.399	-651.893 791	-651.474 453	11.411
M18	-118.844 160	-118.398 198	12.135	-118.844 161	-118.397 805	12.146
M19	-156.844 002	-156.492 418	9.567	-156.844 002	-156.492 311	9.570
M20	-231.718 013	-231.371 934	9.417	-231.718 013	-231.371 591	9.427
M21	-380.724 306	-380.320 094	11.000	-380.724 331	-380.320 069	11.001
M22	-323.168 543	-322.801 723	9.982	-323.168 543	-322.801 021	10.001
M23	-629.435 400	-629.131 197	8.278	-629.435 400	-629.130 369	8.300
M24	-158.062 969	-157.631 787	11.733	-158.062 969	-157.631 744	11.734
M25	-232.846 360	-232.541 995	8.282	-232.846 362	-232.541 659	8.291
M26	-286.978 196	-286.687 709	7.905	-286.978 196	-286.686 865	7.928
M27	-381.962 755	-381.658 378	8.283	-381.962 755	-381.658 381	8.282
M28	-197.281 694	-196.872 212	11.143	-197.281 694	-196.871 487	11.162
M29	-235.310 354	-234.933 095	10.266	-235.310 354	-234.931 596	10.307
M30	-236.500 444	-236.101 593	10.853	-236.500 444	-236.100 697	10.878

Table B.23: IPs (in eV) obtained with sd-LRMP2 and ab-LRMP2 methods. The energies (in Hartree) of related molecules and cations (removing one electron from the corresponding molecules and maintaining the geometry unchanged) are given. The cc-pVTZ basis set have been used. Parameters are set as 'domsel=0.990' and 'cpldel=0'.

	sd-LRMP2, domsel=0.990			ab-LRMP2, domsel=0.990		
	Molecule	Cation	IP	Molecule	Cation	IP
M01	-76.317 081	-75.853 065	12.627	-76.317 081	-75.853 065	12.627
M02	-114.305 137	-113.892 977	11.215	-114.305 137	-113.892 916	11.217
M03	-40.409 873	-39.883 430	14.325	-40.409 873	-39.883 233	14.331
M04	-111.657 984	-111.335 047	8.788	-111.657 983	-111.334 484	8.803
M05	-95.653 533	-95.294 629	9.766	-95.653 533	-95.294 438	9.771
M06	-153.495 956	-153.065 820	11.705	-153.495 956	-153.065 402	11.716
M07	-79.625 392	-79.162 979	12.583	-79.625 392	-79.162 904	12.585
M08	-224.879 448	-224.494 485	10.475	-224.879 448	-224.494 248	10.482
M09	-377.754 644	-377.361 941	10.686	-377.754 644	-377.360 760	10.718
M10	-154.719 059	-154.336 971	10.397	-154.719 060	-154.336 675	10.405
M11	-154.738 164	-154.331 175	11.075	-154.738 165	-154.330 819	11.084
M12	-229.567 723	-229.236 373	9.016	-229.567 724	-229.236 382	9.016
M13	-225.767 557	-225.430 700	9.166	-225.767 558	-225.430 625	9.168
M14	-552.187 900	-551.854 828	9.063	-552.187 900	-551.854 699	9.067
M15	-155.620 178	-155.288 135	9.035	-155.620 178	-155.288 870	9.015
M16	-283.947 077	-283.573 681	10.161	-283.947 077	-283.573 043	10.178
M17	-651.895 253	-651.475 615	11.419	-651.895 253	-651.475 313	11.427
M18	-118.844 160	-118.398 198	12.135	-118.844 160	-118.397 805	12.146
M19	-156.844 762	-156.492 418	9.588	-156.844 762	-156.492 311	9.591
M20	-231.718 013	-231.372 717	9.396	-231.718 013	-231.372 031	9.415
M21	-380.725 805	-380.322 111	10.985	-380.725 805	-380.322 502	10.974
M22	-323.169 564	-322.801 723	10.009	-323.169 564	-322.801 211	10.023
M23	-629.436 265	-629.131 197	8.301	-629.436 265	-629.130 588	8.318
M24	-158.062 969	-157.633 612	11.683	-158.062 969	-157.632 970	11.701
M25	-232.847 279	-232.541 995	8.307	-232.847 279	-232.542 936	8.282
M26	-286.978 810	-286.688 745	7.893	-286.978 810	-286.688 114	7.910
M27	-381.965 168	-381.659 630	8.314	-381.965 168	-381.659 559	8.316
M28	-197.281 694	-196.873 606	11.105	-197.281 694	-196.872 432	11.137
M29	-235.314 168	-234.934 809	10.323	-235.314 168	-234.933 606	10.356
M30	-236.500 444	-236.104 802	10.766	-236.500 444	-236.102 883	10.818

Table B.24: IPs (in eV) obtained with sd-LRMP2 and ab-LRMP2 methods. The energies (in Hartree) of related molecules and cations (removing one electron from the corresponding molecules and maintaining the geometry unchanged) are given. The cc-pVTZ basis set have been used. Parameters are set as 'domsel=0.985' and 'cpldel=1'.

	sd-LRMP2, cpldel=1			ab-LRMP2, cpldel=1		
	Molecule	Cation	IP	Molecule	Cation	IP
M01	-76.317 027	-75.853 035	12.626	-76.317 027	-75.853 035	12.626
M02	-114.305 131	-113.892 366	11.232	-114.305 131	-113.892 437	11.230
M03	-40.409 873	-39.883 427	14.325	-40.409 873	-39.883 231	14.331
M04	-111.655 749	-111.335 038	8.727	-111.655 749	-111.334 440	8.743
M05	-95.652 996	-95.294 205	9.763	-95.653 000	-95.294 192	9.764
M06	-153.495 956	-153.065 415	11.716	-153.495 956	-153.065 021	11.726
M07	-79.625 392	-79.157 930	12.720	-79.625 391	-79.161 919	12.612
M08	-224.879 463	-224.494 187	10.484	-224.879 463	-224.493 279	10.509
M09	-377.753 673	-377.360 557	10.697	-377.753 673	-377.359 531	10.725
M10	-154.718 500	-154.335 526	10.421	-154.718 500	-154.335 792	10.414
M11	-154.736 860	-154.331 154	11.040	-154.736 861	-154.330 793	11.050
M12	-229.567 705	-229.235 999	9.026	-229.567 705	-229.236 199	9.021
M13	-225.767 375	-225.429 636	9.190	-225.767 375	-225.430 105	9.178
M14	-552.187 274	-551.853 775	9.075	-552.187 274	-551.853 798	9.074
M15	-155.620 181	-155.288 138	9.035	-155.620 180	-155.287 951	9.040
M16	-283.946 347	-283.573 077	10.157	-283.946 347	-283.572 706	10.167
M17	-651.894 047	-651.474 815	11.408	-651.894 047	-651.474 386	11.420
M18	-118.844 160	-118.398 200	12.135	-118.844 161	-118.397 802	12.146
M19	-156.844 005	-156.492 396	9.568	-156.844 005	-156.492 295	9.571
M20	-231.717 990	-231.371 911	9.417	-231.717 990	-231.371 568	9.427
M21	-380.724 254	-380.320 562	10.985	-380.724 254	-380.320 336	10.991
M22	-323.168 448	-322.801 196	9.993	-323.168 448	-322.800 663	10.008
M23	-629.435 352	-629.131 142	8.278	-629.435 352	-629.130 313	8.301
M24	-158.062 970	-157.631 791	11.733	-158.062 970	-157.631 737	11.734
M25	-232.846 362	-232.541 997	8.282	-232.846 362	-232.541 659	8.291
M26	-286.978 175	-286.687 740	7.903	-286.978 175	-286.686 865	7.927
M27	-381.962 612	-381.658 799	8.267	-381.692 612	-381.658 554	8.274
M28	-197.281 697	-196.872 209	11.143	-197.281 697	-196.871 480	11.163
M29	-235.310 359	-234.932 466	10.283	-235.310 359	-234.931 176	10.318
M30	-236.500 452	-236.101 588	10.854	-236.500 452	-236.100 688	10.878

Table B.25: IPs (in eV) obtained with sd-LUCCSD and ab-LUCCSD methods. The energies (in Hartree) of related molecules and cations (removing one electron from the corresponding molecules and maintaining the geometry unchanged) are given. The cc-pVTZ basis set have been used. Parameters are set as 'domsel=0.985', 'cpldel=1', 'nomp2=0', 'keepcls=0', and 'igskip=0'.

	sd-LUCCSD, default			ab-LUCCSD, default		
	Molecule	Cation	IP	Molecule	Cation	IP
M01	-76.323 334	-75.868 255	12.383	-76.323 334	-75.868 255	12.383
M02	-114.315 776	-113.919 522	10.783	-114.315 776	-113.919 810	10.775
M03	-40.430 405	-39.904 272	14.317	-40.430 405	-39.904 510	14.310
M04	-111.676 685	-111.348 168	8.939	-111.676 685	-111.348 290	8.936
M05	-95.679 999	-95.326 978	9.606	-95.679 999	-95.326 654	9.615
M06	-153.517 491	-153.087 381	11.704	-153.517 490	-153.088 262	11.680
M07	-79.658 996	-79.185 637	12.881	-79.658 997	-79.189 258	12.782
M08	-224.896 154	-224.527 042	10.044	-224.896 157	-224.526 033	10.072
M09	-377.756 955	-377.339 534	11.359	-377.756 953	-377.340 048	11.345
M10	-154.751 868	-154.380 846	10.096	-154.751 869	-154.381 351	10.082
M11	-154.770 321	-154.377 554	10.688	-154.770 321	-154.377 844	10.680
M12	-229.588 018	-229.260 680	8.907	-229.588 018	-229.261 158	8.894
M13	-225.784 736	-225.458 843	8.868	-225.784 736	-225.459 048	8.862
M14	-552.217 201	-551.889 148	8.927	-552.217 201	-551.889 226	8.925
M15	-155.660 167	-155.326 950	9.067	-155.660 167	-155.327 838	9.043
M16	-283.972 170	-283.603 548	10.031	-283.972 171	-283.602 961	10.047
M17	-651.639 517	-651.541 402	10.835	-651.939 513	-651.540 739	10.864
M18	-118.890 742	-118.440 578	12.250	-118.890 743	-118.441 338	12.229
M19	-156.895 417	-156.548 654	9.436	-156.895 421	-156.549 024	9.426
M20	-231.750 504	-231.409 488	9.280	-231.750 504	-231.410 018	9.265
M21	-380.751 516	-380.343 950	11.090	-380.751 517	-380.344 142	11.085
M22	-323.207 015	-322.845 025	9.850	-323.207 801	-322.844 562	9.863
M23	-629.481 876	-629.175 220	8.345	-629.481 876	-629.175 935	8.325
M24	-158.122 552	-157.692 955	11.690	-158.122 552	-157.695 215	11.628
M25	-232.900 033	-232.595 241	8.294	-232.900 034	-232.597 071	8.244
M26	-287.016 156	-286.727 141	7.864	-287.016 157	-286.727 902	7.844
M27	-381.992 041	-381.691 062	8.190	-381.991 228	-381.691 318	8.161
M28	-197.354 286	-196.936 632	11.365	-197.354 285	-196.939 314	11.292
M29	-235.388 252	-234.985 317	10.964	-235.388 251	-234.990 773	10.816
M30	-236.586 051	-236.176 457	11.146	-236.586 051	-236.179 715	11.057

Table B.26: IPs (in eV) obtained with sd-LUCCSD and ab-LUCCSD methods. The energies (in Hartree) of related molecules and cations (removing one electron from the corresponding molecules and maintaining the geometry unchanged) are given. The cc-pVTZ basis set have been used. Parameters are set as 'domsel=0.985', 'cpldel=1', 'nomp2=1', 'keepcls=0', and 'igskip=0'.

	sd-LUCCSD, nomp2=1			ab-LUCCSD, nomp2=1		
	Molecule	Cation	IP	Molecule	Cation	IP
M01	-76.323 334	-75.868 255	12.383	-76.323 334	-75.868 255	12.383
M02	-114.315 786	-113.920 601	10.754	-114.315 786	-113.920 807	10.748
M03	-40.430 405	-39.904 272	14.317	-40.430 405	-39.904 510	14.310
M04	-111.674 806	-111.347 414	8.909	-111.674 806	-111.347 004	8.920
M05	-95.678 036	-95.326 731	9.560	-95.678 036	-95.326 754	9.559
M06	-153.515 128	-153.086 743	11.657	-153.515 128	-153.086 351	11.668
M07	-79.657 188	-79.185 376	12.839	-79.657 188	-79.188 066	12.765
M08	-224.893 466	-224.526 061	9.998	-224.893 466	-224.525 198	10.021
M09	-377.752 395	-377.335 704	11.339	-377.752 395	-377.334 443	11.373
M10	-154.749 311	-154.380 292	10.042	-154.749 311	-154.380 664	10.031
M11	-154.766 739	-154.376 319	10.624	-154.766 739	-154.375 953	10.634
M12	-229.583 403	-229.256 656	8.891	-229.583 403	-229.256 847	8.886
M13	-225.778 274	-225.452 747	8.858	-225.778 274	-225.453 157	8.847
M14	-552.212 184	-551.884 483	8.891	-552.212 184	-551.884 492	8.917
M15	-155.657 068	-155.324 607	9.047	-155.657 068	-155.324 474	9.050
M16	-283.966 564	-283.600 872	9.951	-283.966 564	-283.600 534	9.960
M17	-651.931 648	-651.535 420	10.782	-651.931 648	-651.534 943	10.795
M18	-118.886 525	-118.439 723	12.158	-118.886 525	-118.439 454	12.165
M19	-156.888 467	-156.544 806	9.351	-156.888 467	-156.544 740	9.353
M20	-231.744 125	-231.403 342	9.273	-231.744 125	-231.403 092	9.280
M21	-380.745 007	-380.337 794	11.081	-380.745 007	-380.337 765	11.082
M22	-323.198 420	-322.839 891	9.756	-323.198 420	-322.839 166	9.776
M23	-629.471 691	-629.167 187	8.286	-629.471 691	-629.166 589	8.302
M24	-158.115 867	-157.691 809	11.539	-158.115 867	-157.690 114	11.585
M25	-232.893 930	-232.591 227	8.237	-232.893 930	-232.591 042	8.242
M26	-287.006 357	-286.718 724	7.827	-287.006 357	-286.718 182	7.842
M27	-381.891 988	-381.681 345	8.181	-381.981 988	-381.681 359	8.181
M28	-197.348 812	-196.937 769	11.185	-197.345 141	-196.931 509	11.256
M29	-235.373 521	-234.980 092	10.706	-235.373 521	-234.978 901	10.738
M30	-236.574 440	-236.170 508	10.992	-236.574 440	-236.169 791	11.011

Table B.27: IPs (in eV) obtained with sd-LUCCSD and ab-LUCCSD methods. The energies (in Hartree) of related molecules and cations (removing one electron from the corresponding molecules and maintaining the geometry unchanged) are given. The cc-pVTZ basis set have been used. Parameters are set as 'domsel=0.985', 'cpldel=1', 'nomp2=0', 'keepcls=1', and 'igskip=0'.

	sd-LUCCSD, keepcls=1			ab-LUCCSD, keepcls=1		
	Molecule	Cation	IP	Molecule	Cation	IP
M01	-76.323 334	-75.868 255	12.383	-76.323 334	-75.868 255	12.383
M02	-114.316 209	-113.919 699	10.790	-114.316 239	-113.920 929	10.757
M03	-40.430 405	-39.904 272	14.317	-40.430 405	-39.904 510	14.310
M04	-111.678 000	-111.349 271	8.945	-111.678 021	-111.349 303	8.945
M05	-95.681 004	-95.327 562	9.618	-95.681 024	-95.327 792	9.612
M06	-153.519 667	-153.087 454	11.761	-153.519 762	-153.089 033	11.721
M07	-79.659 734	-79.186 073	12.889	-79.659 783	-79.189 762	12.790
M08	-224.897 501	-224.528 147	10.051	-224.897 959	-224.528 425	10.056
M09	-377.758 833	-377.340 663	11.379	-377.759 773	-377.341 956	11.369
M10	-154.753 045	-154.381 059	10.122	-154.753 100	-154.382 957	10.072
M11	-154.771 158	-154.377 912	10.701	-154.771 259	-154.378 337	10.692
M12	-229.589 782	-229.262 653	8.902	-229.589 968	-229.263 155	8.893
M13	-225.786 578	-225.460 617	8.870	-225.786 814	-225.461 045	8.865
M14	-552.218 078	-551.889 871	8.931	-552.218 200	-551.889 990	8.931
M15	-155.660 859	-155.327 539	9.070	-155.660 997	-155.328 150	9.057
M16	-283.973 731	-283.604 856	10.038	-283.974 229	-283.605 204	10.042
M17	-651.939 745	-651.539 748	10.884	-651.939 975	-651.539 713	10.892
M18	-118.891 290	-118.440 920	12.255	-118.891 380	-118.442 145	12.224
M19	-156.895 779	-156.548 969	9.437	-156.895 918	-156.549 598	9.424
M20	-231.751 892	-231.410 941	9.278	-231.752 023	-231.441 327	9.271
M21	-380.753 730	-380.346 082	11.093	-380.754 253	-380.346 770	11.088
M22	-323.208 777	-322.846 676	9.853	-323.209 308	-322.846 928	9.861
M23	-629.483 288	-629.176 497	8.348	-629.483 537	-629.177 455	8.329
M24	-158.123 361	-157.692 102	11.735	-158.123 488	-157.695 875	11.636
M25	-232.901 179	-232.596 264	8.297	-232.901 334	-232.597 967	8.255
M26	-287.017 999	-286.728 860	7.868	-287.018 388	-286.729 519	7.861
M27	-381.994 390	-381.692 966	8.202	-381.994 825	-381.693 533	8.199
M28	-197.355 362	-196.937 845	11.361	-197.355 526	-196.940 779	11.286
M29	-235.389 750	-234.986 477	10.974	-235.389 961	-234.992 063	10.827
M30	-236.587 396	-236.177 985	11.141	-236.587 596	-236.181 449	11.052

Table B.28: IPs (in eV) obtained with sd-LUCCSD and ab-LUCCSD methods. The energies (in Hartree) of related molecules and cations (removing one electron from the corresponding molecules and maintaining the geometry unchanged) are given. The cc-pVTZ basis set have been used. Parameters are set as 'domsel=0.985', 'cpldel=1', 'nomp2=0', 'keepcls=0', and 'igskip=1'.

	sd-LUCCSD, igskip=1			ab-LUCCSD, igskip=1		
	Molecule	Cation	IP	Molecule	Cation	IP
M01	-76.323 317	-75.868 289	12.382	-76.323 317	-75.868 289	12.382
M02	-114.315 977	-113.918 927	10.804	-114.315 977	-113.919 207	10.797
M03	-40.430 394	-39.904 233	14.318	-40.430 394	-39.904 471	14.311
M04	-111.676 653	-111.348 297	8.935	-111.676 653	-111.348 423	8.932
M05	-95.679 984	-95.326 877	9.609	-95.679 984	-95.326 621	9.616
M06	-153.517 521	-153.087 480	11.702	-153.517 520	-153.088 377	11.678
M07	-79.658 972	-79.185 743	12.877	-79.658 972	-79.189 381	12.778
M08	-224.896 156	-224.526 314	10.064	-224.896 158	-224.525 340	10.090
M09	-377.757 107	-377.340 219	11.344	-377.757 104	-377.340 695	11.331
M10	-154.751 888	-154.380 634	10.102	-154.751 889	-154.381 139	10.089
M11	-154.770 311	-154.376 843	10.707	-154.770 311	-154.377 144	10.699
M12	-229.588 062	-229.260 862	8.904	-229.588 062	-229.261 320	8.891
M13	-225.784 755	-225.458 819	8.869	-225.784 755	-225.459 021	8.864
M14	-552.217 130	-551.889 141	8.925	-552.217 130	-551.889 219	8.923
M15	-155.660 216	-155.327 167	9.063	-155.660 215	-155.328 056	9.039
M16	-283.972 203	-283.603 490	10.033	-283.972 203	-283.602 969	10.047
M17	-651.939 121	-651.538 601	10.899	-651.939 123	-651.538 029	10.914
M18	-118.890 712	-118.440 144	12.261	-118.890 712	-118.441 013	12.237
M19	-156.895 441	-156.548 564	9.439	-156.895 446	-156.548 988	9.428
M20	-231.750 553	-231.409 652	9.276	-231.750 553	-231.410 167	9.262
M21	-380.751 755	-380.344 197	11.090	-380.751 756	-380.344 403	11.085
M22	-323.207 043	-322.844 804	9.857	-323.207 040	-322.844 412	9.868
M23	-629.481 883	-629.175 236	8.344	-629.481 882	-629.175 960	8.325
M24	-158.122 516	-157.692 750	11.695	-158.122 516	-157.694 958	11.634
M25	-232.900 127	-232.595 277	8.295	-232.900 127	-232.597 135	8.245
M26	-287.016 161	-286.727 198	7.863	-287.016 161	-286.727 883	7.844
M27	-381.992 065	-381.691 211	8.183	-381.992 064	-381.691 402	8.178
M28	-197.354 245	-196.936 533	11.367	-197.354 244	-196.939 277	11.292
M29	-235.388 209	-234.985 248	10.965	-235.388 208	-234.990 777	10.815
M30	-236.586 004	-236.176 345	11.147	-236.586 004	-236.179 686	11.056

Table B.29: IPs (in eV) obtained with sd-LUCCSD(T) and ab-LUCCSD(T) methods. The energies (in Hartree) of related molecules and cations (removing one electron from the corresponding molecules and maintaining the geometry unchanged) are given. The cc-pVTZ basis set have been used. Parameters are set as 'domsel=0.985', 'cpldel=1', 'nomp2=0', 'keepcls=0', and 'igskip=0'.

	sd-LUCCSD(T), default			ab-LUCCSD(T), default		
	Molecule	Cation	IP	Molecule	Cation	IP
M01	-76.330 591	-75.872 917	12.454	-76.330 591	-75.872 917	12.454
M02	-114.331 838	-113.933 455	10.841	-114.331 838	-113.933 748	10.833
M03	-40.436 465	-39.908 974	14.354	-40.436 465	-39.909 227	14.347
M04	-111.692 775	-111.365 688	8.900	-111.692 775	-111.365 765	8.898
M05	-95.694 119	-95.339 001	9.663	-95.694 119	-95.338 596	9.674
M06	-153.540 748	-153.109 708	11.729	-153.540 747	-153.110 510	11.707
M07	-79.672 014	-79.200 679	12.826	-79.672 014	-79.204 346	12.726
M08	-224.928 451	-224.559 868	10.030	-224.928 455	-224.558 912	10.056
M09	-377.807 992	-377.398 774	11.135	-377.807 989	-377.399 352	11.120
M10	-154.772 679	-154.399 619	10.151	-154.772 680	-154.400 160	10.137
M11	-154.791 003	-154.397 030	10.721	-154.791 003	-154.397 271	10.714
M12	-229.630 006	-229.299 979	8.980	-229.630 006	-229.300 472	8.967
M13	-225.828 284	-225.499 509	8.946	-225.828 284	-225.499 690	8.942
M14	-552.258 940	-551.927 405	9.022	-552.258 940	-551.927 480	9.019
M15	-155.690 841	-155.354 400	9.155	-155.690 841	-155.355 329	9.130
M16	-284.011 516	-283.641 628	10.065	-284.011 517	-283.640 815	10.087
M17	-651.976 461	-651.578 301	10.862	-651.976 457	-651.577 222	10.864
M18	-118.910 536	-118.463 084	12.176	-118.910 536	-118.463 535	12.164
M19	-156.923 541	-156.571 398	9.582	-156.923 546	-156.571 806	9.571
M20	-231.799 453	-231.455 712	9.354	-231.799 453	-231.456 253	9.339
M21	-380.819 026	-380.411 562	11.088	-380.819 028	-380.411 926	11.078
M22	-323.252 846	-322.889 894	9.876	-323.252 843	-322.889 018	9.900
M23	-629.538 686	-629.232 434	8.334	-629.538 686	-629.232 733	8.325
M24	-158.149 106	-157.719 717	11.684	-158.149 106	-157.721 705	11.630
M25	-232.946 777	-232.639 158	8.371	-232.946 778	-232.640 872	8.324
M26	-287.073 317	-286.783 820	7.878	-287.073 317	-286.784 216	7.867
M27	-382.057 337	-381.756 613	8.183	-382.056 365	-381.756 467	8.184
M28	-197.387 599	-196.971 338	11.327	-197.387 598	-196.973 504	11.268
M29	-235.428 961	-235.032 077	10.800	-235.428 960	-235.036 338	10.684
M30	-236.626 119	-236.218 310	11.097	-236.626 119	-236.220 967	11.025

Table B.30: IPs (in eV) obtained with sd-LUCCSD(T) and ab-LUCCSD(T) methods. The energies (in Hartree) of related molecules and cations (removing one electron from the corresponding molecules and maintaining the geometry unchanged) are given. The cc-pVTZ basis set have been used. Parameters are set as 'domsel=0.985', 'cpldel=1', 'nomp2=1', 'keepcls=0', and 'igskip=0'.

	sd-LUCCSD(T), nomp2=1			ab-LUCCSD(T), nomp2=1		
	Molecule	Cation	IP	Molecule	Cation	IP
M01	-76.330 591	-75.872 917	12.454	-76.330 591	-75.872 917	12.454
M02	-114.331 825	-113.934 618	10.809	-114.331 825	-113.934 837	10.803
M03	-40.436 465	-39.908 974	14.354	-40.436 465	-39.909 227	14.347
M04	-111.690 681	-111.364 812	8.867	-111.690 681	-111.364 334	8.880
M05	-95.691 933	-95.338 779	9.610	-95.691 933	-95.338 796	9.609
M06	-153.538 060	-153.108 991	11.676	-153.538 060	-153.108 363	11.693
M07	-79.669 994	-79.200 475	12.776	-79.669 994	-79.202 996	12.708
M08	-224.925 895	-224.559 436	9.972	-224.925 895	-224.558 475	9.998
M09	-377.804 809	-377.397 424	11.085	-377.804 809	-377.395 871	11.128
M10	-154.770 461	-154.399 999	10.081	-154.770 461	-154.400 392	10.070
M11	-154.787 545	-154.396 153	10.650	-154.787 545	-154.395 755	10.661
M12	-229.625 711	-229.296 345	8.963	-229.625 711	-229.296 560	8.957
M13	-225.821 978	-225.493 543	8.937	-225.821 978	-225.494 023	8.924
M14	-552.256 580	-551.926 622	8.979	-552.256 580	-551.926 619	8.979
M15	-155.688 005	-155.352 573	9.128	-155.688 005	-155.352 399	9.132
M16	-284.006 556	-283.640 242	9.968	-284.006 556	-283.639 835	9.979
M17	-651.972 628	-651.575 696	10.801	-651.972 628	-651.575 136	10.816
M18	-118.906 331	-118.462 206	12.085	-118.906 331	-118.461 869	12.094
M19	-156.917 176	-156.568 941	9.476	-156.917 176	-156.568 848	9.479
M20	-231.793 874	-231.450 315	9.349	-231.793 874	-231.450 027	9.357
M21	-380.814 146	-380.407 963	11.053	-380.814 146	-380.407 915	11.054
M22	-323.245 738	-322.886 708	9.770	-323.245 738	-322.885 847	9.793
M23	-629.531 488	-629.227 660	8.268	-629.531 488	-629.226 898	8.288
M24	-158.142 703	-157.719 859	11.506	-158.142 703	-157.717 856	11.561
M25	-232.941 666	-232.636 738	8.298	-232.941 666	-232.636 441	8.306
M26	-287.064 583	-286.776 674	7.834	-287.064 583	-286.775 974	7.853
M27	-382.049 620	-381.749 170	8.176	-382.049 620	-381.749 094	8.178
M28	-197.379 014	-196.970 571	11.114	-197.379 014	-196.967 635	11.194
M29	-235.415 375	-235.027 640	10.551	-235.415 375	-235.026 146	10.591
M30	-236.615 353	-236.214 857	10.898	-236.615 353	-236.213 900	10.924

Table B.31: IPs (in eV) obtained with sd-LUCCSD(T) and ab-LUCCSD(T) methods. The energies (in Hartree) of related molecules and cations (removing one electron from the corresponding molecules and maintaining the geometry unchanged) are given. The cc-pVTZ basis set have been used. Parameters are set as 'domsel= 0.985', 'cpldel=1', 'nomp2=0', 'keepcls=1', and 'igskip=0'.

	sd-LUCCSD(T), keepcls=1			ab-LUCCSD(T), keepcls=1		
	Molecule	Cation	IP	Molecule	Cation	IP
M01	-76.330 591	-75.872 917	12.454	-76.330 591	-75.872 917	12.454
M02	-114.332 312	-113.933 656	10.848	-114.332 338	-113.935 011	10.812
M03	-40.436 465	-39.908 974	14.354	-40.436 465	-39.909 227	14.347
M04	-111.694 261	-111.366 942	8.907	-111.694 261	-111.366 959	8.906
M05	-95.695 260	-95.339 678	9.676	-95.695 248	-95.339 871	9.670
M06	-153.543 253	-153.109 791	11.795	-153.543 320	-153.111 413	11.753
M07	-79.672 862	-79.201 168	12.835	-79.672 877	-79.204 916	12.734
M08	-224.929 993	-224.561 098	10.038	-224.930 464	-224.561 506	10.040
M09	-377.810 107	-377.400 802	11.138	-377.811 075	-377.401 514	10.145
M10	-154.774 032	-154.399 907	10.180	-154.774 069	-154.401 975	10.125
M11	-154.791 996	-154.397 460	10.736	-154.792 055	-154.397 837	10.727
M12	-229.632 017	-229.302 233	8.974	-229.632 197	-229.302 777	8.964
M13	-225.830 401	-225.501 513	8.949	-225.830 635	-225.502 001	8.943
M14	-552.259 956	-551.928 240	9.026	-552.260 071	-551.928 333	9.027
M15	-155.691 634	-155.355 079	9.158	-155.691 790	-155.355 825	9.142
M16	-284.013 321	-283.643 164	10.072	-284.013 806	-283.643 369	10.080
M17	-651.976 878	-651.576 914	10.884	-651.977 033	-651.576 466	10.900
M18	-118.911 226	-118.463 481	12.184	-118.911 259	-118.464 480	12.157
M19	-156.924 029	-156.571 786	9.585	-156.924 106	-156.572 468	9.569
M20	-231.801 043	-231.457 355	9.352	-231.801 127	-231.457 828	9.342
M21	-380.821 522	-380.413 953	11.091	-380.822 136	-380.414 997	11.079
M22	-323.254 900	-322.891 818	9.880	-323.255 413	-322.891 694	9.897
M23	-629.540 336	-629.233 915	8.338	-629.540 541	-629.234 469	8.329
M24	-158.150 123	-157.718 838	11.736	-158.150 169	-157.722 473	11.638
M25	-232.948 083	-232.640 341	8.374	-232.948 266	-232.642 060	8.332
M26	-287.075 474	-286.785 811	7.882	-287.075 835	-286.786 260	7.880
M27	-382.060 021	-381.758 776	8.197	-382.060 452	-381.759 081	8.201
M28	-197.388 947	-196.972 810	11.324	-197.389 007	-196.975 254	11.259
M29	-235.430 828	-235.033 454	10.813	-235.430 908	-235.037 895	10.694
M30	-236.627 803	-236.220 170	11.092	-236.627 875	-236.223 035	11.016

Table B.32: IPs (in eV) obtained with sd-LUCCSD(T) and ab-LUCCSD(T) methods. The energies (in Hartree) of related molecules and cations (removing one electron from the corresponding molecules and maintaining the geometry unchanged) are given. The cc-pVTZ basis set have been used. Parameters are set as 'domsel= 0.985', 'cpldel=1', 'nomp2=0', 'keepcls=0', and 'igskip=1'.

	sd-LUCCSD(T), igskip=1			ab-LUCCSD(T), igskip=1		
	Molecule	Cation	IP	Molecule	Cation	IP
M01	-76.330 573	-75.872 955	12.452	-76.330 573	-75.872 955	12.452
M02	-114.332 115	-113.932 768	10.867	-114.332 115	-113.932 768	10.859
M03	-40.436 453	-39.908 933	14.355	-40.436 453	-39.908 933	14.348
M04	-111.692 739	-111.365 851	8.895	-111.692 739	-111.365 851	8.893
M05	-95.694 102	-95.338 889	9.666	-95.694 102	-95.338 562	9.675
M06	-153.540 798	-153.109 857	11.726	-153.540 797	-153.110 674	11.704
M07	-79.671 985	-79.200 802	12.822	-79.671 986	-79.204 489	12.721
M08	-224.928 492	-224.559 010	10.054	-224.928 495	-224.558 094	10.079
M09	-377.808 263	-377.400 597	11.093	-377.808 260	-377.400 313	11.101
M10	-154.772 712	-154.399 382	10.159	-154.772 712	-154.399 922	10.144
M11	-154.790 995	-154.396 214	10.743	-154.790 994	-154.396 470	10.736
M12	-229.630 075	-229.300 257	8.975	-229.630 075	-229.300 727	8.962
M13	-225.828 315	-225.499 531	8.947	-225.828 315	-225.499 714	8.942
M14	-552.258 860	-551.927 458	9.018	-552.258 860	-551.927 533	9.016
M15	-155.690 904	-155.354 751	9.147	-155.690 904	-155.355 685	9.122
M16	-284.011 597	-283.641 606	10.068	-284.011 598	-283.640 871	10.088
M17	-651.976 174	-651.575 505	10.903	-651.976 177	-651.574 524	10.930
M18	-118.910 500	-118.462 589	12.188	-118.910 500	-118.463 164	12.173
M19	-156.923 570	-156.571 298	9.586	-156.923 575	-156.571 766	9.573
M20	-231.799 525	-231.455 976	9.348	-231.799 525	-231.456 503	9.334
M21	-380.819 391	-380.411 979	11.086	-380.819 393	-380.412 365	11.076
M22	-323.252 921	-322.889 674	9.884	-323.252 918	-322.888 886	9.906
M23	-629.538 708	-629.232 536	8.331	-629.538 707	-629.232 839	8.323
M24	-158.149 063	-157.719 489	11.689	-158.149 064	-157.721 417	11.637
M25	-232.946 902	-232.639 269	8.371	-232.946 902	-232.641 028	8.323
M26	-287.073 333	-286.784 023	7.873	-287.073 334	-286.784 319	7.864
M27	-382.057 386	-381.756 914	8.176	-382.057 385	-381.756 688	8.182
M28	-197.387 549	-196.971 236	11.328	-197.387 548	-196.973 471	11.268
M29	-235.428 907	-235.032 011	10.800	-235.428 907	-235.036 349	10.682
M30	-236.626 063	-236.218 194	11.099	-236.626 063	-236.220 943	11.024

Table B.33: (T) correction (in kcal/mol) of the cations involved in IPs obtained with sd-LUCCSD(T), ab-LUCCSD(T), and UCCSD(T) methods. Numbers in parenthesis indicate percent of the conventional (T) correction.

	UCCSD(T)	sd-LUCCSD(T)	ab-LUCCSD(T)
M01	-3.03	-2.93(97%)	-2.93(97%)
M02	-9.03	-8.74(97%)	-8.75(97%)
M03	-3.16	-2.95(93%)	-2.96(94%)
M04	-11.48	-10.99(96%)	-10.97(96%)
M05	-7.91	-7.54(95%)	-7.49(95%)
M06	-14.44	-14.01(97%)	-13.96(97%)
M07	-9.80	-9.44(96%)	-9.47(97%)
M08	-21.68	-20.60(95%)	-20.63(95%)
M09	-40.39	-37.17(92%)	-37.21(92%)
M10	-13.04	-11.78(90%)	-11.80(91%)
M11	-13.13	-12.22(93%)	-12.19(93%)
M12	-26.02	-24.66(95%)	-24.67(95%)
M13	-26.82	-25.52(95%)	-25.50(95%)
M14	-27.59	-24.01(87%)	-24.00(87%)
M15	-18.12	-16.79(93%)	-17.25(95%)
M16	-26.13	-23.90(91%)	-23.75(91%)
M17	-26.31	-23.15(88%)	-22.89(87%)
M18	-14.85	-14.12(95%)	-13.93(94%)
M19	-15.99	-14.27(89%)	-14.30(89%)
M20	-30.61	-29.01(95%)	-29.01(95%)
M21	-45.82	-42.43(93%)	-42.54(93%)
M22	-31.17	-28.16(90%)	-27.90(90%)
M23	-39.51	-35.90(91%)	-35.64(90%)
M24	-18.46	-16.79(91%)	-16.62(90%)
M25	-29.60	-27.56(93%)	-27.48(93%)
M26	-37.96	-35.57(94%)	-35.34(93%)
M27	-47.56	-41.39(87%)	-41.13(86%)
M28	-24.10	-21.78(90%)	-21.45(89%)
M29	-31.51	-29.34(93%)	-28.59(91%)
M30	-29.52	-26.26(89%)	-25.89(88%)
Ave		93%	92%
Max		97%	97%
Min		87%	86%

Table B.34: Errors of IPs (in eV) obtained with sd-LRMP2 and ab-LRMP2 with respect to the ones obtained with RMP2.

	sd-LRMP2			ab-LRMP2		
	default	domsel	cpldel	default	domsel	cpldel
IP01	-0.019	-0.019	-0.020	-0.019	-0.019	-0.020
IP02	0.000	-0.016	0.000	-0.002	-0.015	-0.002
IP03	-0.013	-0.013	-0.013	-0.008	-0.008	-0.008
IP04	-0.034	0.025	-0.036	-0.019	0.040	-0.019
IP05	-0.027	-0.024	-0.027	-0.027	-0.019	-0.027
IP06	-0.040	-0.040	-0.029	-0.029	-0.029	-0.018
IP07	0.089	-0.013	0.124	0.009	-0.011	0.016
IP08	-0.070	-0.078	-0.069	-0.045	-0.071	-0.044
IP09	-0.085	-0.063	-0.052	-0.046	-0.031	-0.024
IP10	0.007	-0.017	0.007	0.000	-0.009	0.000
IP11	-0.049	-0.014	-0.049	-0.039	-0.005	-0.039
IP12	0.002	-0.007	0.003	-0.003	-0.007	-0.003
IP13	0.005	-0.017	0.007	-0.008	-0.015	-0.006
IP14	-0.005	-0.016	-0.004	-0.006	-0.013	-0.005
IP15	-0.018	-0.018	-0.018	-0.013	-0.038	-0.013
IP16	-0.046	-0.043	-0.046	-0.036	-0.026	-0.036
IP17	-0.047	-0.027	-0.038	-0.035	-0.019	-0.026
IP18	-0.029	-0.029	-0.029	-0.018	-0.018	-0.018
IP19	-0.019	0.002	-0.018	-0.016	0.005	-0.015
IP20	-0.001	-0.022	-0.001	0.008	-0.004	0.008
IP21	-0.006	-0.020	-0.021	-0.005	-0.031	-0.014
IP22	-0.068	-0.040	-0.056	-0.049	-0.026	-0.042
IP23	-0.070	-0.047	-0.070	-0.048	-0.030	-0.047
IP24	-0.011	-0.061	-0.011	-0.010	-0.043	-0.010
IP25	-0.026	-0.001	-0.026	-0.016	-0.026	-0.016
IP26	-0.071	-0.083	-0.072	-0.048	-0.065	-0.049
IP27	-0.040	-0.009	-0.056	-0.040	-0.007	-0.049
IP28	-0.051	-0.089	-0.051	-0.032	-0.057	-0.031
IP29	-0.131	-0.074	-0.114	-0.090	-0.041	-0.079
IP30	-0.059	-0.146	-0.058	-0.034	-0.094	-0.034
MAE	0.038	0.036	0.038	0.025	0.027	0.024
RMSE	0.049	0.048	0.049	0.032	0.035	0.030
MAX	-0.131	-0.146	0.124	-0.090	-0.094	-0.079

Table B.35: Errors of IPs (in eV) obtained with sd-LUCCSD and ab-LUCCSD with respect to the ones obtained with UCCSD.

	sd-LUCCSD				ab-LUCCSD			
	default	nomp2	keepcls	igskip	default	nomp2	keepcls	igskip
IP01	-0.014	-0.014	-0.014	-0.016	-0.014	-0.014	-0.014	-0.016
IP02	0.036	0.007	0.043	0.058	0.029	0.002	0.011	0.050
IP03	0.003	0.003	0.003	0.003	-0.004	-0.004	-0.004	-0.003
IP04	0.001	-0.030	0.007	-0.003	-0.002	-0.018	0.007	-0.007
IP05	0.032	-0.015	0.044	0.034	0.041	-0.015	0.038	0.041
IP06	0.010	-0.036	0.068	0.009	-0.014	-0.026	0.027	-0.016
IP07	0.124	0.082	0.132	0.120	0.025	0.009	0.033	0.021
IP08	-0.009	-0.056	-0.003	0.010	0.018	-0.032	0.002	0.037
IP09	-0.058	-0.078	-0.038	-0.073	-0.072	-0.044	-0.047	-0.086
IP10	0.074	0.020	0.100	0.080	0.060	0.009	0.050	0.067
IP11	0.034	-0.030	0.047	0.053	0.026	-0.020	0.038	0.045
IP12	0.020	0.004	0.015	0.017	0.007	-0.001	0.006	0.004
IP13	0.018	0.008	0.020	0.019	0.013	-0.003	0.015	0.014
IP14	0.006	-0.029	0.010	0.005	0.004	-0.004	0.011	0.002
IP15	0.006	-0.014	0.009	0.001	-0.018	-0.011	-0.004	-0.023
IP16	0.057	-0.023	0.064	0.059	0.073	-0.014	0.068	0.073
IP17	0.018	-0.035	0.068	0.082	0.047	-0.022	0.075	0.098
IP18	0.075	-0.016	0.081	0.086	0.054	-0.009	0.050	0.062
IP19	0.076	-0.009	0.077	0.079	0.066	-0.007	0.064	0.068
IP20	0.009	0.003	0.007	0.006	-0.005	0.010	0.000	-0.008
IP21	0.007	-0.002	0.009	0.007	0.002	-0.002	0.005	0.001
IP22	0.049	-0.045	0.052	0.056	0.062	-0.025	0.060	0.066
IP23	0.008	-0.051	0.012	0.008	-0.011	-0.034	-0.008	-0.012
IP24	0.102	-0.048	0.148	0.107	0.041	-0.002	0.049	0.047
IP25	0.040	-0.017	0.043	0.041	-0.010	-0.012	0.001	-0.009
IP26	-0.014	-0.052	-0.011	-0.016	-0.035	-0.037	-0.018	-0.034
IP27	-0.026	-0.035	-0.014	-0.033	-0.055	-0.036	-0.018	-0.039
IP28	0.083	-0.097	0.079	0.085	0.010	-0.026	0.004	0.010
IP29	0.141	-0.118	0.150	0.142	-0.007	-0.085	0.004	-0.009
IP30	0.107	-0.047	0.102	0.109	0.019	-0.027	0.013	0.018
MAE	0.042	0.034	0.049	0.047	0.028	0.019	0.025	0.033
RMSE	0.057	0.045	0.065	0.062	0.036	0.025	0.034	0.043
MAX	0.141	-0.118	-0.150	0.142	0.073	-0.085	0.075	0.098

Table B.36: Errors of IPs (in eV) obtained with sd-LUCCSD(T) and ab-LUCCSD(T) with respect to the ones obtained with UCCSD(T).

	sd-LUCCSD(T)				ab-LUCCSD(T)			
	default	nomp2	keepcls	igskip	default	nomp2	keepcls	igskip
IP01	-0.021	-0.021	-0.021	-0.023	-0.021	-0.021	-0.021	-0.023
IP02	0.038	0.006	0.045	0.064	0.030	0.000	0.009	0.056
IP03	0.005	0.005	0.005	0.006	-0.001	-0.001	-0.001	-0.001
IP04	-0.001	-0.035	0.005	-0.007	-0.003	-0.022	0.004	-0.009
IP05	0.030	-0.024	0.042	0.032	0.041	-0.024	0.037	0.041
IP06	0.004	-0.049	0.070	0.002	-0.018	-0.032	0.028	-0.021
IP07	0.127	0.078	0.137	0.123	0.028	0.009	0.036	0.023
IP08	-0.009	-0.067	-0.001	0.015	0.017	-0.041	0.001	0.040
IP09	-0.033	-0.083	-0.031	-0.076	-0.049	-0.041	-0.024	-0.068
IP10	0.086	0.015	0.115	0.093	0.071	0.005	0.060	0.079
IP11	0.030	-0.040	0.045	0.052	0.023	-0.030	0.036	0.045
IP12	0.018	0.000	0.012	0.013	0.005	-0.005	0.002	0.000
IP13	0.013	0.003	0.016	0.013	0.008	-0.010	0.009	0.008
IP14	0.034	-0.009	0.039	0.030	0.032	-0.009	0.040	0.028
IP15	0.006	-0.021	0.010	-0.001	-0.019	-0.016	-0.007	-0.027
IP16	0.068	-0.029	0.075	0.071	0.090	-0.018	0.083	0.091
IP17	0.015	-0.043	0.040	0.054	0.020	-0.028	0.056	0.086
IP18	0.074	-0.017	0.082	0.086	0.062	-0.007	0.056	0.071
IP19	0.091	-0.015	0.094	0.095	0.080	-0.013	0.078	0.082
IP20	0.002	-0.003	0.001	-0.003	-0.012	0.005	-0.010	-0.017
IP21	0.034	0.000	0.037	0.033	0.025	0.001	0.026	0.023
IP22	0.051	-0.056	0.055	0.059	0.075	-0.032	0.072	0.080
IP23	0.000	-0.066	0.005	-0.002	-0.008	-0.045	-0.005	-0.010
IP24	0.120	-0.058	0.171	0.125	0.066	-0.004	0.074	0.072
IP25	0.047	-0.026	0.050	0.048	0.001	-0.018	0.009	0.000
IP26	-0.025	-0.068	-0.020	-0.030	-0.036	-0.049	-0.023	-0.038
IP27	-0.039	-0.047	-0.025	-0.046	-0.039	-0.045	-0.022	-0.040
IP28	0.106	-0.107	0.103	0.107	0.047	-0.027	0.038	0.046
IP29	0.117	-0.132	0.131	0.118	0.001	-0.091	0.012	0.000
IP30	0.148	-0.051	0.143	0.149	0.075	-0.025	0.067	0.074
MAE	0.047	0.039	0.054	0.053	0.033	0.022	0.031	0.040
RMSE	0.063	0.051	0.072	0.068	0.042	0.030	0.040	0.049
MAX	0.148	-0.132	0.171	0.149	0.090	-0.091	0.083	0.091

Table B.37: Errors of IPs (in eV) obtained with UCCSD, RMP2, sd-LRMP2, and ab-LRMP2 with respect to the ones obtained with UCCSD(T).

	UCCSD	RMP2	sd-LRMP2			ab-LRMP2		
			default	domsel	cpldel	default	domsel	cpldel
IP01	-0.078	0.170	0.151	0.151	0.150	0.151	0.151	0.150
IP02	-0.056	0.429	0.429	0.413	0.429	0.427	0.414	0.427
IP03	-0.034	-0.010	-0.023	-0.023	-0.023	-0.018	-0.018	-0.018
IP04	0.036	-0.139	-0.174	-0.114	-0.175	-0.158	-0.099	-0.159
IP05	-0.059	0.157	0.130	0.133	0.130	0.130	0.138	0.130
IP06	-0.031	0.020	-0.020	-0.020	-0.009	-0.009	-0.009	0.001
IP07	0.059	-0.102	-0.014	-0.115	0.022	-0.094	-0.113	-0.087
IP08	0.014	0.514	0.444	0.436	0.445	0.469	0.443	0.469
IP09	0.248	-0.419	-0.504	-0.483	-0.472	-0.466	-0.451	-0.444
IP10	-0.043	0.348	0.355	0.332	0.356	0.348	0.340	0.349
IP11	-0.037	0.398	0.350	0.384	0.349	0.359	0.394	0.359
IP12	-0.075	0.061	0.064	0.054	0.064	0.058	0.054	0.059
IP13	-0.084	0.250	0.255	0.233	0.257	0.242	0.235	0.244
IP14	-0.067	0.092	0.087	0.076	0.088	0.086	0.079	0.087
IP15	-0.087	-0.095	-0.113	-0.113	-0.113	-0.108	-0.133	-0.108
IP16	-0.023	0.206	0.161	0.163	0.160	0.170	0.181	0.170
IP17	-0.027	0.602	0.555	0.575	0.564	0.567	0.583	0.576
IP18	0.073	0.062	0.033	0.033	0.033	0.044	0.044	0.044
IP19	-0.131	0.095	0.076	0.097	0.077	0.079	0.100	0.079
IP20	-0.081	0.067	0.066	0.045	0.066	0.075	0.063	0.075
IP21	0.030	-0.048	-0.053	-0.068	-0.068	-0.053	-0.079	-0.062
IP22	-0.024	0.224	0.156	0.184	0.168	0.175	0.198	0.183
IP23	0.003	0.015	-0.056	-0.032	-0.055	-0.033	-0.015	-0.033
IP24	0.023	0.180	0.168	0.119	0.168	0.170	0.136	0.170
IP25	-0.070	-0.016	-0.041	-0.016	-0.041	-0.032	-0.042	-0.032
IP26	-0.023	0.073	0.002	-0.009	0.001	0.025	0.008	0.025
IP27	-0.009	0.100	0.060	0.092	0.045	0.060	0.094	0.051
IP28	0.061	-0.027	-0.079	-0.117	-0.078	-0.059	-0.085	-0.059
IP29	0.141	-0.290	-0.421	-0.364	-0.403	-0.380	-0.331	-0.368
IP30	0.089	-0.038	-0.096	-0.183	-0.096	-0.072	-0.131	-0.071
MAE	0.061	0.175	0.171	0.173	0.170	0.171	0.172	0.170
RMSE	0.077	0.237	0.234	0.231	0.232	0.232	0.230	0.231
MAX	0.248	0.602	0.555	0.575	0.564	0.567	0.583	0.576

Table B.38: Errors of IPs (in eV) obtained with sd-LUCCSD and ab-LUCCSD with respect to the ones obtained with UCCSD(T).

	sd-LUCCSD				ab-LUCCSD			
	default	nomp2	keepcls	igskip	default	nomp2	keepcls	igskip
IP01	-0.092	-0.092	-0.092	-0.094	-0.092	-0.092	-0.092	-0.094
IP02	-0.020	-0.049	-0.013	0.002	-0.028	-0.055	-0.046	-0.006
IP03	-0.032	-0.032	-0.032	-0.031	-0.038	-0.038	-0.038	-0.037
IP04	0.038	0.007	0.043	0.033	0.034	0.018	0.043	0.030
IP05	-0.027	-0.074	-0.016	-0.025	-0.019	-0.075	-0.022	-0.018
IP06	-0.021	-0.068	0.036	-0.023	-0.045	-0.057	-0.004	-0.047
IP07	0.182	0.140	0.191	0.179	0.084	0.067	0.092	0.080
IP08	0.005	-0.042	0.011	0.025	0.032	-0.018	0.016	0.051
IP09	0.190	0.170	0.210	0.175	0.176	0.204	0.201	0.162
IP10	0.031	-0.024	0.057	0.037	0.017	-0.034	0.007	0.023
IP11	-0.003	-0.067	0.010	0.016	-0.011	-0.057	0.001	0.008
IP12	-0.055	-0.071	-0.060	-0.059	-0.068	-0.076	-0.069	-0.071
IP13	-0.066	-0.076	-0.064	-0.065	-0.071	-0.087	-0.069	-0.070
IP14	-0.061	-0.096	-0.056	-0.062	-0.063	-0.070	-0.056	-0.065
IP15	-0.081	-0.102	-0.078	-0.086	-0.105	-0.098	-0.091	-0.110
IP16	0.034	-0.046	0.040	0.036	0.050	-0.037	0.045	0.050
IP17	-0.009	-0.062	0.040	0.055	0.020	-0.049	0.048	0.070
IP18	0.148	0.056	0.153	0.159	0.127	0.064	0.122	0.135
IP19	-0.055	-0.140	-0.054	-0.052	-0.065	-0.138	-0.067	-0.063
IP20	-0.072	-0.078	-0.074	-0.075	-0.086	-0.071	-0.081	-0.089
IP21	0.037	0.028	0.039	0.037	0.032	0.028	0.035	0.031
IP22	0.025	-0.069	0.028	0.032	0.037	-0.050	0.036	0.042
IP23	0.011	-0.047	0.015	0.011	-0.008	-0.031	-0.004	-0.009
IP24	0.125	-0.025	0.171	0.130	0.064	0.021	0.071	0.070
IP25	-0.030	-0.087	-0.026	-0.028	-0.080	-0.082	-0.069	-0.079
IP26	-0.038	-0.075	-0.034	-0.039	-0.059	-0.061	-0.042	-0.058
IP27	-0.035	-0.044	-0.023	-0.042	-0.064	-0.045	-0.026	-0.047
IP28	0.144	-0.036	0.140	0.145	0.071	0.034	0.065	0.071
IP29	0.282	0.023	0.291	0.283	0.134	0.056	0.145	0.132
IP30	0.196	0.042	0.191	0.198	0.108	0.062	0.102	0.107
MAE	0.071	0.066	0.076	0.074	0.063	0.062	0.060	0.064
RMSE	0.099	0.075	0.104	0.100	0.074	0.073	0.074	0.075
MAX	0.282	0.170	0.291	0.283	0.176	0.204	0.201	0.162

Table B.39: Molecular electron affinities (EAs, in eV) obtained with HF and RMP2 methods. The energies (in Hartree) of related molecules and anions (adding one electron to the corresponding molecules and maintaining the geometry unchanged) are given. The aug-cc-pVTZ basis set have been used. The molecules are numbered from M01 to M30 as discussed in Chapter 5.

	HF			RMP2		
	Molecule	Anion	EA	Molecule	Anion	EA
M01	-76.060 289	-76.031 210	0.791	-76.328 929	-76.305 349	0.642
M02	-113.914 138	-113.888 459	0.699	-114.315 964	-114.292 440	0.640
M03	-40.213 541	-40.182 712	0.839	-40.414 384	-40.388 175	0.713
M04	-111.220 694	-111.188 268	0.882	-111.672 201	-111.646 835	0.690
M05	-95.255 373	-95.226 189	0.794	-95.667 047	-95.643 257	0.647
M06	-152.928 481	-152.898 996	0.802	-153.513 762	-153.488 805	0.679
M07	-79.260 253	-79.227 968	0.879	-79.635 247	-79.608 785	0.720
M08	-224.083 034	-224.066 097	0.461	-224.908 002	-224.895 919	0.329
M09	-376.527 802	-376.498 941	0.785	-377.793 129	-377.773 289	0.540
M10	-154.128 672	-154.098 552	0.820	-154.737 522	-154.712 863	0.671
M11	-154.145 338	-154.116 825	0.776	-154.758 176	-154.734 955	0.632
M12	-228.709 853	-228.680 660	0.794	-229.592 229	-229.568 548	0.644
M13	-224.898 059	-224.879 190	0.513	-225.793 374	-225.780 117	0.361
M14	-551.384 184	-551.355 139	0.790	-552.210 512	-552.187 533	0.625
M15	-154.979 214	-154.947 760	0.856	-155.638 048	-155.612 939	0.683
M16	-282.951 926	-282.925 241	0.726	-283.981 005	-283.960 680	0.553
M17	-650.979 150	-650.955 215	0.651	-651.922 926	-651.904 794	0.493
M18	-118.308 351	-118.276 137	0.877	-118.859 957	-118.834 245	0.700
M19	-156.169 735	-156.139 722	0.817	-156.864 712	-156.841 420	0.634
M20	-230.781 487	-230.751 643	0.812	-231.744 304	-231.723 174	0.575
M21	-379.369 253	-379.392 926	-0.644	-380.764 832	-380.828 708	-1.738
M22	-322.001 249	-321.974 251	0.735	-323.209 986	-323.189 429	0.559
M23	-628.327 759	-628.300 767	0.735	-629.470 364	-629.450 331	0.545
M24	-157.356 313	-157.324 061	0.878	-158.084 887	-158.059 452	0.692
M25	-231.893 771	-231.863 361	0.828	-232.873 943	-232.850 588	0.636
M26	-285.835 905	-285.811 476	0.665	-287.015 406	-286.997 448	0.489
M27	-380.562 859	-380.542 303	0.559	-382.009 460	-381.995 065	0.392
M28	-196.404 192	-196.372 542	0.861	-197.309 793	-197.285 237	0.668
M29	-234.287 173	-234.255 861	0.852	-235.345 862	-235.322 512	0.635
M30	-235.452 078	-235.420 473	0.860	-236.534 756	-236.510 552	0.659

Table B.40: EAs (in eV) obtained with UCCSD and UCCSD(T) methods. The energies (in Hartree) of related molecules and anions (adding one electron to the corresponding molecules and maintaining the geometry unchanged) are given. The aug-cc-pVTZ basis set have been used. The molecules are numbered from M01 to M30 as discussed in Chapter 5.

	UCCSD			UCCSD(T)		
	Molecule	Anion	EA	Molecule	Anion	EA
M01	-76.333 655	-76.310 425	-0.632	-76.342 323	-76.319 950	-0.609
M02	-114.325 378	-114.302 397	-0.625	-114.342 701	-114.320 087	-0.615
M03	-40.434 369	-40.408 641	-0.700	-40.342 701	-40.415 844	-0.683
M04	-111.689 337	-111.664 236	-0.683	-111.707 474	-111.683 548	-0.651
M05	-95.690 452	-95.667 202	-0.633	-95.706 117	-95.683 737	-0.609
M06	-153.531 164	-153.506 636	-0.667	-153.556 544	-153.532 721	-0.648
M07	-79.665 960	-79.640 040	-0.705	-79.679 934	-79.654 861	-0.682
M08	-224.919 148	-224.907 840	-0.308	-224.955 474	-224.945 174	-0.280
M09	-377.788 483	-377.769 024	-0.530	-377.846 804	-377.829 120	-0.481
M10	-154.766 610	-154.742 483	-0.657	-154.790 216	-154.766 972	-0.633
M11	-154.785 911	-154.763 376	-0.613	-154.809 527	-154.787 918	-0.588
M12	-229.605 259	-229.581 889	-0.636	-229.651 049	-229.628 731	-0.607
M13	-225.801 871	-225.788 461	-0.365	-225.280 622	-225.836 920	-0.339
M14	-552.232 467	-552.209 962	-0.612	-552.280 622	-552.259 369	-0.578
M15	-155.672 485	-155.647 366	-0.684	-155.705 643	-155.681 635	-0.653
M16	-283.997 894	-283.978 344	-0.532	-284.042 865	-284.024 585	-0.497
M17	-651.957 867	-651.940 587	-0.470	-652.003 321	-651.987 079	-0.442
M18	-118.900 616	-118.875 519	-0.683	-118.922 382	-118.898 295	-0.655
M19	-156.906 661	-156.884 025	-0.616	-156.938 024	-156.916 596	-0.583
M20	-231.766 867	-231.745 019	-0.594	-231.820 196	-231.799 919	-0.552
M21	-380.781 177	-380.833 129	1.414	-380.855 957	-380.910 299	1.479
M22	-323.235 859	-323.216 232	-0.534	-323.289 190	-323.270 895	-0.498
M23	-629.501 908	-629.482 710	-0.522	-629.567 106	-629.549 525	-0.478
M24	-158.135 416	-158.110 624	-0.675	-158.165 042	-158.141 328	-0.645
M25	-232.917 780	-232.894 331	-0.638	-232.969 134	-232.947 059	-0.601
M26	-287.038 603	-287.020 820	-0.484	-287.102 133	-287.085 696	-0.447
M27	-382.023 001	-382.008 911	-0.383	-382.097 502	-382.084 709	-0.348
M28	-197.370 191	-197.346 302	-0.650	-197.407 695	-197.384 957	-0.619
M29	-235.405 139	-235.382 266	-0.622	-235.451 764	-235.430 240	-0.586
M30	-236.605 017	-236.581 510	-0.640	-236.650 409	-236.628 119	-0.607

Table B.41: EAs (in eV) obtained with sd-LRMP2 and ab-LRMP2 methods. The energies (in Hartree) of related molecules and anions (adding one electron to the corresponding molecules and maintaining the geometry unchanged) are given. The aug-cc-pVTZ basis set have been used. Parameters are set as default, i.e., 'domsel=0.985' and 'cpldel=0'.

	sd-LRMP2, default			ab-LRMP2, default		
	Molecule	Anion	EA	Molecule	Anion	EA
M01	-76.327 661	-76.304 103	-0.641	-76.327 661	-76.304 687	-0.625
M02	-114.314 139	-114.290 589	-0.641	-114.314 139	-114.290 958	-0.631
M03	-40.412 396	-40.386 199	-0.713	-40.412 395	-40.386 614	-0.702
M04	-111.668 180	-111.642 829	-0.690	-111.668 180	-111.644 140	-0.654
M05	-95.662 599	-95.638 798	-0.648	-95.662 598	-95.639 164	-0.638
M06	-153.509 062	-153.484 078	-0.680	-153.509 062	-153.485 546	-0.640
M07	-79.630 388	-79.603 938	-0.720	-79.630 389	-79.604 087	-0.716
M08	-224.901 028	-224.888 910	-0.330	-224.901 027	-224.890 207	-0.294
M09	-377.776 394	-377.756 612	-0.538	-377.776 394	-377.763 349	-0.355
M10	-154.731 465	-154.706 787	-0.672	-154.731 465	-154.708 325	-0.630
M11	-154.751 018	-154.727 715	-0.634	-154.751 018	-154.728 697	-0.607
M12	-229.582 412	-229.558 648	-0.647	-229.582 412	-229.560 232	-0.604
M13	-225.783 470	-225.770 141	-0.363	-225.783 470	-225.771 918	-0.314
M14	-552.200 960	-552.177 885	-0.628	-552.200 960	-552.180 287	-0.563
M15	-155.629 533	-155.604 376	-0.685	-155.629 533	-155.605 008	-0.667
M16	-283.971 000	-283.950 660	-0.553	-283.971 000	-283.952 128	-0.514
M17	-651.912 648	-651.894 474	-0.495	-651.912 648	-651.895 564	-0.465
M18	-118.851 821	-118.826 105	-0.700	-118.851 821	-118.826 994	-0.676
M19	-156.854 335	-156.831 011	-0.635	-156.854 335	-156.832 862	-0.584
M20	-231.734 167	-231.713 049	-0.575	-231.734 167	-231.714 897	-0.524
M21	-380.749 520	-380.813 521	1.742	-380.749 521	-380.813 832	1.750
M22	-323.196 026	-323.175 427	-0.561	-323.196 026	-323.177 751	-0.497
M23	-629.456 538	-629.435 768	-0.565	-629.456 538	-629.438 387	-0.494
M24	-158.073 368	-158.047 917	-0.693	-158.073 368	-158.048 824	-0.668
M25	-232.860 673	-232.837 229	-0.638	-232.860 673	-232.838 791	-0.595
M26	-287.000 740	-286.982 737	-0.490	-287.000 740	-286.985 404	-0.417
M27	-381.993 557	-381.975 483	-0.492	-381.993 557	-381.981 921	-0.317
M28	-197.294 800	-197.270 218	-0.669	-197.294 800	-197.271 778	-0.626
M29	-235.325 897	-235.302 551	-0.635	-235.325 903	-235.305 048	-0.568
M30	-236.516 278	-236.492 039	-0.660	-236.516 278	-236.494 636	-0.589

Table B.42: EAs (in eV) obtained with sd-LRMP2 and ab-LRMP2 methods. The energies (in Hartree) of related molecules and anions (adding one electron to the corresponding molecules and maintaining the geometry unchanged) are given. The aug-cc-pVTZ basis set have been used. Parameters are set as 'domsel=0.990' and 'cpldel=0'.

	sd-LRMP2, domsel=0.990			ab-LRMP2, domsel=0.990		
	Molecule	Anion	EA	Molecule	Anion	EA
M01	-76.327 661	-76.304 103	-0.641	-76.327 661	-76.304 687	-0.625
M02	-114.314 139	-114.290 589	-0.641	-114.314 139	-114.291 186	-0.625
M03	-40.412 396	-40.386 199	-0.713	-40.412 395	-40.386 614	-0.702
M04	-111.668 180	-111.642 829	-0.690	-111.668 180	-111.644 140	-0.654
M05	-95.662 599	-95.638 822	-0.647	-95.662 598	-95.639 948	-0.616
M06	-153.509 062	-153.484 078	-0.680	-153.509 062	-153.485 546	-0.640
M07	-79.630 388	-79.603 938	-0.720	-79.630 389	-79.604 482	-0.705
M08	-224.901 028	-224.888 940	-0.329	-224.901 027	-224.890 714	-0.281
M09	-377.783 773	-377.763 915	-0.540	-377.783 774	-377.765 521	-0.497
M10	-154.731 465	-154.706 787	-0.672	-154.731 465	-154.708 752	-0.618
M11	-154.751 018	-154.727 767	-0.633	-154.751 018	-154.729 458	-0.587
M12	-229.584 775	-229.561 088	-0.645	-229.584 775	-229.563 620	-0.576
M13	-225.784 375	-225.771 055	-0.362	-225.784 375	-225.773 727	-0.290
M14	-552.202 227	-552.179 243	-0.625	-552.202 227	-552.181 643	-0.560
M15	-155.630 447	-155.605 306	-0.684	-155.630 447	-155.607 020	-0.637
M16	-283.971 000	-283.950 660	-0.553	-283.971 000	-283.953 976	-0.463
M17	-651.912 648	-651.894 474	-0.495	-651.912 648	-651.897 633	-0.409
M18	-118.851 821	-118.826 105	-0.700	-118.851 821	-118.827 110	-0.672
M19	-156.854 335	-156.831 011	-0.635	-156.854 335	-156.834 194	-0.548
M20	-231.734 167	-231.713 049	-0.575	-231.734 167	-231.714 897	-0.524
M21	-380.751 919	-380.815 808	1.739	-380.751 919	-380.816 007	1.744
M22	-323.196 026	-323.175 461	-0.560	-323.196 026	-323.179 826	-0.441
M23	-629.456 538	-629.436 437	-0.547	-629.456 538	-629.440 678	-0.432
M24	-158.073 368	-158.047 917	-0.693	-158.073 368	-158.049 505	-0.649
M25	-232.861 662	-232.838 274	-0.636	-232.861 662	-232.841 469	-0.549
M26	-287.001 252	-286.983 236	-0.490	-287.001 252	-287.987 568	-0.372
M27	-381.994 815	-381.980 562	-0.388	-381.994 815	-381.983 579	-0.306
M28	-197.294 800	-197.270 218	-0.669	-197.294 800	-197.272 967	-0.594
M29	-235.325 897	-235.302 551	-0.635	-235.325 903	-235.302 551	-0.509
M30	-236.516 278	-236.492 091	-0.658	-236.516 278	-236.496 553	-0.537

Table B.43: EAs (in eV) obtained with sd-LRMP2 and ab-LRMP2 methods. The energies (in Hartree) of related molecules and anions (adding one electron to the corresponding molecules and maintaining the geometry unchanged) are given. The aug-cc-pVTZ basis set have been used. Parameters are set as 'domsel=0.985' and 'cpldel=1'.

	sd-LRMP2, cpldel=1			ab-LRMP2, cpldel=1		
	Molecule	Anion	EA	Molecule	Anion	EA
M01	-76.327 658	-76.304 100	-0.641	-76.327 658	-76.304 234	-0.637
M02	-114.314 139	-114.290 590	-0.641	-114.314 139	-114.290 962	-0.631
M03	-40.412 396	-40.386 199	-0.713	-40.412 395	-40.386 628	-0.701
M04	-111.668 174	-111.642 824	-0.690	-111.668 174	-111.644 154	-0.654
M05	-95.662 593	-95.638 792	-0.648	-95.662 592	-95.639 202	-0.636
M06	-153.509 094	-153.484 113	-0.680	-153.509 094	-153.485 117	-0.652
M07	-79.630 389	-79.603 939	-0.720	-79.630 390	-79.604 494	-0.705
M08	-224.901 029	-224.888 911	-0.330	-224.901 029	-224.889 914	-0.302
M09	-377.776 399	-377.756 618	-0.538	-377.776 399	-377.762 498	-0.378
M10	-154.731 476	-154.706 799	-0.672	-154.731 476	-154.708 370	-0.629
M11	-154.751 023	-154.727 719	-0.634	-154.751 023	-154.728 756	-0.606
M12	-229.582 510	-229.558 752	-0.646	-229.582 510	-229.560 237	-0.606
M13	-225.783 516	-225.770 186	-0.363	-225.783 516	-225.771 188	-0.335
M14	-552.201 060	-552.177 995	-0.628	-552.201 060	-552.179 145	-0.596
M15	-155.629 558	-155.604 404	-0.684	-155.629 558	-155.604 906	-0.671
M16	-283.970 995	-283.950 655	-0.553	-283.970 995	-283.951 529	-0.530
M17	-651.912 664	-651.894 490	-0.495	-651.912 664	-651.894 963	-0.482
M18	-118.851 831	-118.826 115	-0.700	-118.851 831	-118.826 995	-0.676
M19	-156.854 403	-156.831 085	-0.635	-156.854 403	-156.832 943	-0.584
M20	-231.734 251	-231.713 133	-0.575	-231.734 251	-231.714 964	-0.525
M21	-380.749 570	-380.813 541	1.741	-380.749 571	-380.813 692	1.745
M22	-323.196 019	-323.175 423	-0.560	-323.196 019	-323.176 260	-0.538
M23	-629.456 731	-629.435 981	-0.565	-629.456 732	-629.436 760	-0.543
M24	-158.073 390	-158.047 939	-0.693	-158.073 390	-158.048 757	-0.670
M25	-232.860 801	-232.837 366	-0.638	-232.860 801	-232.839 055	-0.592
M26	-287.000 913	-286.982 926	-0.489	-287.000 913	-286.984 852	-0.437
M27	-381.993 794	-381.979 317	-0.394	-381.993 794	-381.981 394	-0.337
M28	-197.294 855	-197.270 274	-0.669	-197.294 855	-197.271 018	-0.649
M29	-235.325 843	-235.302 493	-0.635	-235.325 843	-235.304 899	-0.570
M30	-236.516 364	-236.492 127	-0.660	-236.516 364	-236.494 600	-0.592

Table B.44: EAs (in eV) obtained with sd-LUCCSD and ab-LUCCSD methods. The energies (in Hartree) of related molecules and anions (adding one electron to the corresponding molecules and maintaining the geometry unchanged) are given. The aug-cc-pVTZ basis set have been used. Parameters are set as 'domsel=0.985', 'cpldel=1', 'nomp2=0', 'keepcls=0', and 'igskip=0'.

	sd-LUCCSD, default			ab-LUCCSD, default		
	Molecule	Anion	EA	Molecule	Anion	EA
M01	-76.332 598	-76.309 374	-0.632	-76.332 598	-76.309 502	-0.628
M02	-114.323 768	-114.300 739	-0.627	-114.323 768	-114.301 045	-0.618
M03	-40.432 695	-40.406 969	-0.700	-40.432 695	-40.407 344	-0.690
M04	-111.687 827	-111.662 944	-0.677	-111.687 827	-111.663 514	-0.662
M05	-95.688 637	-95.665 250	-0.636	-95.688 637	-95.665 414	-0.632
M06	-153.527 673	-153.503 126	-0.668	-153.527 669	-153.504 586	-0.628
M07	-79.663 573	-79.637 733	-0.703	-79.663 573	-79.637 287	-0.715
M08	-224.915 848	-224.904 410	-0.311	-224.915 849	-224.905 041	-0.294
M09	-377.777 837	-377.758 488	-0.527	-377.777 831	-377.762 749	-0.410
M10	-154.763 845	-154.739 799	-0.654	-154.763 846	-154.740 970	-0.622
M11	-154.783 240	-154.760 116	-0.629	-154.783 240	-154.760 846	-0.609
M12	-229.603 127	-229.579 506	-0.643	-229.603 128	-229.579 734	-0.637
M13	-225.799 468	-225.785 945	-0.368	-225.799 467	-225.786 232	-0.360
M14	-552.231 949	-552.209 164	-0.620	-552.231 949	-552.208 793	-0.630
M15	-155.671 186	-155.646 103	-0.683	-155.671 186	-155.645 403	-0.702
M16	-283.994 601	-283.975 011	-0.533	-283.994 602	-283.974 899	-0.536
M17	-651.956 289	-651.938 760	-0.477	-651.956 284	-651.938 952	-0.472
M18	-118.897 799	-118.872 902	-0.677	-118.897 799	-118.872 636	-0.685
M19	-156.904 483	-156.881 713	-0.620	-156.904 477	-156.882 652	-0.594
M20	-231.763 773	-231.742 123	-0.589	-231.763 773	-231.741 279	-0.612
M21	-380.775 888	-380.827 987	1.418	-380.775 888	-380.829 212	1.451
M22	-323.232 177	-323.212 155	-0.545	-323.232 177	-323.212 099	-0.546
M23	-629.499 123	-629.480 429	-0.509	-629.499 124	-629.479 763	-0.527
M24	-158.132 097	-158.107 375	-0.673	-158.132 098	-158.106 470	-0.697
M25	-232.914 347	-232.890 779	-0.641	-232.914 343	-232.890 490	-0.649
M26	-287.036 384	-287.018 485	-0.487	-287.036 385	-287.017 332	-0.518
M27	-382.019 380	-382.004 793	-0.397	-382.019 374	-382.005 011	-0.391
M28	-197.366 291	-197.342 415	-0.650	-197.366 291	-197.341 793	-0.667
M29	-235.402 439	-235.379 871	-0.614	-235.402 438	-235.378 330	-0.656
M30	-236.600 582	-236.577 012	-0.641	-236.600 583	-236.576 627	-0.652

Table B.45: EAs (in eV) obtained with sd-LUCCSD and ab-LUCCSD methods. The energies (in Hartree) of related molecules and anions (adding one electron to the corresponding molecules and maintaining the geometry unchanged) are given. The aug-cc-pVTZ basis set have been used. Parameters are set as 'domsel=0.985', 'cpldel=1', 'nomp2=1', 'keepcls=0', and 'igskip=0'.

	sd-LUCCSD, nomp2=1			ab-LUCCSD, nomp2=1		
	Molecule	Anion	EA	Molecule	Anion	EA
M01	-76.332 598	-76.309 374	-0.632	-76.332 598	-76.309 502	-0.628
M02	-114.323 843	-114.300 869	-0.625	-114.323 843	-114.301 202	-0.616
M03	-40.432 695	-40.406 969	-0.700	-40.432 695	-40.407 344	-0.690
M04	-111.685 913	-111.660 894	-0.681	-111.685 911	-111.661 957	-0.652
M05	-95.686 658	-95.663 479	-0.631	-95.686 658	-95.663 830	-0.621
M06	-153.527 116	-153.502 595	-0.667	-153.527 116	-153.503 481	-0.643
M07	-79.661 780	-79.635 846	-0.706	-79.661 780	-79.636 254	-0.695
M08	-224.913 068	-224.901 874	-0.305	-224.913 068	-224.902 559	-0.286
M09	-377.773 386	-377.754 153	-0.532	-377.772 427	-377.759 129	-0.362
M10	-154.761 325	-154.737 306	-0.654	-154.761 325	-154.738 674	-0.616
M11	-154.779 614	-154.756 934	-0.617	-154.779 614	-154.757 820	-0.593
M12	-229.596 728	-229.573 300	-0.638	-229.596 728	-229.574 343	-0.609
M13	-225.793 214	-225.779 807	-0.365	-225.793 214	-225.780 603	-0.343
M14	-552.224 333	-552.201 770	-0.614	-552.224 333	-552.202 329	-0.599
M15	-155.665 173	-155.640 067	-0.683	-155.665 173	-155.640 437	-0.673
M16	-283.989 047	-283.969 691	-0.527	-283.989 047	-283.970 116	-0.515
M17	-651.948 915	-651.931 741	-0.467	-651.948 915	-651.931 852	-0.464
M18	-118.893 580	-118.868 533	-0.682	-118.893 580	-118.869 140	-0.665
M19	-156.897 769	-156.875 086	-0.617	-156.897 769	-156.876 559	-0.577
M20	-231.757 996	-231.736 293	-0.591	-231.757 996	-231.757 996	-0.553
M21	-380.767 641	-380.819 632	1.415	-380.767 641	-380.819 877	1.421
M22	-323.223 547	-323.203 948	-0.533	-323.223 547	-323.204 329	-0.523
M23	-629.490 054	-629.470 121	-0.542	-629.490 054	-629.469 832	-0.550
M24	-158.125 443	-158.100 652	-0.675	-158.125 443	-158.101 176	-0.660
M25	-232.906 440	-232.882 969	-0.639	-232.906 440	-232.884 351	-0.601
M26	-287.025 956	-287.008 229	-0.482	-287.025 956	-287.009 625	-0.444
M27	-382.009 157	-381.995 021	-0.385	-382.009 157	-381.996 571	-0.342
M28	-197.357 223	-197.333 338	-0.650	-197.357 223	-197.333 693	-0.640
M29	-235.387 730	-235.364 891	-0.621	-235.387 730	-235.366 576	-0.576
M30	-236.589 047	-236.565 519	-0.640	-236.589 047	-236.567 437	-0.588

Table B.46: EAs (in eV) obtained with sd-LUCCSD and ab-LUCCSD methods. The energies (in Hartree) of related molecules and anions (adding one electron to the corresponding molecules and maintaining the geometry unchanged) are given. The aug-cc-pVTZ basis set have been used. Parameters are set as 'domsel=0.985', 'cpldel=1', 'nomp2=0', 'keepcls=1', and 'igskip=0'.

	sd-LUCCSD, keepcls=1			ab-LUCCSD, keepcls=1		
	Molecule	Anion	EA	Molecule	Anion	EA
M01	-76.332 598	-76.309 374	-0.632	-76.332 598	-76.309 502	-0.628
M02	-114.324 165	-114.301 161	-0.626	-114.324 191	-114.301 398	-0.620
M03	-40.432 695	-40.406 969	-0.700	-40.432 695	-40.407 344	-0.690
M04	-111.688 951	-111.664 099	-0.676	-111.688 957	-111.664 919	-0.654
M05	-95.689 520	-95.666 262	-0.633	-95.689 518	-95.666 328	-0.631
M06	-153.529 486	-153.504 979	-0.667	-153.529 603	-153.506 368	-0.632
M07	-79.664 368	-79.638 538	-0.703	-79.664 400	-79.638 258	-0.711
M08	-224.917 147	-224.905 728	-0.311	-224.917 594	-224.906 837	-0.293
M09	-377.779 532	-377.760 225	-0.525	-377.780 461	-377.765 762	-0.400
M10	-154.764 876	-154.740 874	-0.653	-154.764 927	-154.741 836	-0.628
M11	-154.783 976	-154.760 919	-0.627	-154.784 044	-154.761 100	-0.624
M12	-229.604 846	-229.581 294	-0.641	-229.605 226	-229.581 654	-0.641
M13	-225.801 265	-225.787 760	-0.367	-225.801 553	-225.788 027	-0.368
M14	-552.232 579	-552.209 812	-0.620	-552.232 610	-552.209 442	-0.630
M15	-155.671 012	-155.645 974	-0.681	-155.670 790	-155.645 461	-0.689
M16	-283.995 997	-283.976 439	-0.532	-283.996 434	-283.976 687	-0.537
M17	-651.957 098	-651.939 560	-0.477	-651.957 274	-651.939 883	-0.473
M18	-118.898 351	-118.873 442	-0.678	-118.898 408	-118.873 076	-0.689
M19	-156.904 612	-156.881 803	-0.621	-156.904 704	-156.882 227	-0.612
M20	-231.764 647	-231.743 001	-0.589	-231.764 799	-231.742 410	-0.609
M21	-380.777 260	-380.829 619	1.425	-380.777 793	-380.831 531	1.462
M22	-323.233 720	-323.213 711	-0.544	-323.234 173	-323.214 201	-0.543
M23	-629.499 761	-629.480 968	-0.511	-629.499 923	-629.480 633	-0.525
M24	-158.132 899	-158.108 211	-0.672	-158.132 978	-158.107 449	-0.695
M25	-232.914 812	-232.891 322	-0.639	-232.914 885	-232.891 270	-0.643
M26	-287.037 710	-287.019 819	-0.487	-287.037 940	-287.019 106	-0.513
M27	-382.021 167	-382.006 586	-0.397	-382.021 560	-382.007 034	-0.395
M28	-197.367 318	-197.343 481	-0.649	-197.367 420	-197.342 703	-0.673
M29	-235.403 692	-235.381 054	-0.616	-235.403 805	-235.379 371	-0.665
M30	-236.601 849	-236.578 329	-0.640	-236.601 978	-236.577 684	-0.661

Table B.47: EAs (in eV) obtained with sd-LUCCSD and ab-LUCCSD methods. The energies (in Hartree) of related molecules and anions (adding one electron to the corresponding molecules and maintaining the geometry unchanged) are given. The aug-cc-pVTZ basis set have been used. Parameters are set as 'domsel=0.985', 'cpldel=1', 'nomp2=0', 'keepcls=0', and 'igskip=1'.

	sd-LUCCSD, igskip=1			ab-LUCCSD, igskip=1		
	Molecule	Anion	EA	Molecule	Anion	EA
M01	-76.332 581	-76.309 317	-0.633	-76.332 581	-76.309 443	-0.630
M02	-114.323 969	-114.300 925	-0.627	-114.323 969	-114.301 234	-0.619
M03	-40.432 674	-40.406 905	-0.701	-40.432 674	-40.407 282	-0.691
M04	-111.687 747	-111.662 792	-0.679	-111.687 747	-111.663 373	-0.663
M05	-95.688 597	-95.665 162	-0.638	-95.688 597	-95.665 331	-0.633
M06	-153.527 678	-153.503 098	-0.669	-153.527 675	-153.504 560	-0.629
M07	-79.663 536	-79.637 647	-0.704	-79.663 536	-79.637 211	-0.716
M08	-224.915 808	-224.904 269	-0.314	-224.915 810	-224.904 912	-0.297
M09	-377.777 946	-377.758 495	-0.529	-377.777 940	-377.762 792	-0.412
M10	-154.763 856	-154.739 759	-0.656	-154.763 856	-154.740 925	-0.624
M11	-154.783 225	-154.760 073	-0.630	-154.783 225	-154.760 790	-0.610
M12	-229.603 181	-229.579 509	-0.644	-229.603 181	-229.579 703	-0.639
M13	-225.799 460	-225.785 888	-0.369	-225.799 460	-225.786 147	-0.362
M14	-552.231 880	-552.209 005	-0.622	-552.231 880	-552.208 617	-0.633
M15	-155.671 297	-155.646 167	-0.684	-155.671 298	-155.645 471	-0.703
M16	-283.994 604	-283.974 938	-0.535	-283.994 605	-283.974 840	-0.538
M17	-651.956 432	-651.938 829	-0.479	-651.956 428	-651.939 033	-0.473
M18	-118.897 752	-118.872 793	-0.679	-118.897 752	-118.872 536	-0.686
M19	-156.904 483	-156.881 642	-0.622	-156.904 477	-156.882 574	-0.596
M20	-231.764 774	-231.742 059	-0.591	-231.763 774	-231.741 176	-0.615
M21	-380.776 052	-380.828 335	1.423	-380.776 052	-380.829 461	1.453
M22	-323.232 169	-323.212 072	-0.547	-323.232 170	-323.212 025	-0.548
M23	-629.499 055	-629.480 318	-0.510	-629.499 056	-629.479 662	-0.528
M24	-158.132 039	-158.107 264	-0.674	-158.132 040	-158.106 368	-0.699
M25	-232.914 439	-232.890 834	-0.642	-232.914 438	-232.890 506	-0.651
M26	-287.036 346	-287.018 376	-0.489	-287.036 343	-287.017 199	-0.521
M27	-382.019 361	-382.004 706	-0.399	-382.019 355	-382.004 918	-0.393
M28	-197.366 223	-197.342 288	-0.651	-197.366 223	-197.341 687	-0.668
M29	-235.402 372	-235.379 729	-0.616	-235.402 371	-235.378 163	-0.659
M30	-236.600 504	-236.576 875	-0.643	-236.600 505	-236.576 477	-0.654

Table B.48: EAs (in eV) obtained with sd-LUCCSD(T) and ab-LUCCSD(T) methods. The energies (in Hartree) of related molecules and anions (adding one electron to the corresponding molecules and maintaining the geometry unchanged) are given. The aug-cc-pVTZ basis set have been used. Parameters are set as 'domsel=0.985', 'cpldel=1', 'nomp2=0', 'keepcls=0', and 'igskip=0'.

	sd-LUCCSD(T), default			ab-LUCCSD(T), default		
	Molecule	Anion	EA	Molecule	Anion	EA
M01	-76.340 926	-76.318 538	-0.609	-76.340 926	-76.318 771	-0.603
M02	-114.340 701	-114.318 033	-0.617	-114.340 701	-114.318 458	-0.605
M03	-40.439 040	-40.413 961	-0.682	-40.439 040	-40.414 446	-0.669
M04	-111.705 322	-111.681 584	-0.646	-111.705 322	-111.682 214	-0.629
M05	-95.703 808	-95.681 214	-0.615	-95.703 809	-95.681 504	-0.607
M06	-153.552 071	-153.528 211	-0.649	-153.552 066	-153.530 004	-0.600
M07	-79.677 170	-79.652 194	-0.680	-79.677 171	-79.651 806	-0.690
M08	-224.950 620	-224.940 047	-0.288	-224.950 622	-224.940 716	-0.270
M09	-377.831 605	-377.813 951	-0.480	-377.831 599	-377.818 235	-0.364
M10	-154.785 970	-154.762 758	-0.632	-154.785 971	-154.764 247	-0.591
M11	-154.805 480	-154.783 093	-0.609	-154.805 480	-154.784 070	-0.583
M12	-229.647 150	-229.624 453	-0.618	-229.647 151	-229.625 237	-0.596
M13	-225.844 916	-225.832 254	-0.345	-225.844 916	-225.833 027	-0.324
M14	-552.274 585	-552.252 873	-0.591	-552.274 585	-552.252 961	-0.588
M15	-155.702 335	-155.678 312	-0.654	-155.702 336	-155.677 747	-0.669
M16	-284.036 550	-284.018 099	-0.502	-284.036 551	-284.017 993	-0.505
M17	-651.995 238	-651.978 559	-0.454	-651.995 231	-651.978 888	-0.445
M18	-118.918 425	-118.894 533	-0.650	-118.918 426	-118.894 454	-0.652
M19	-156.933 780	-156.912 089	-0.590	-156.933 774	-156.913 646	-0.548
M20	-231.814 585	-231.794 469	-0.547	-231.814 585	-231.793 930	-0.562
M21	-380.844 780	-380.898 979	1.475	-380.844 780	-380.900 293	1.511
M22	-323.280 800	-323.261 890	-0.515	-323.280 801	-323.261 925	-0.514
M23	-629.558 417	-629.539 028	-0.528	-629.558 419	-629.538 468	-0.543
M24	-158.159 756	-158.136 064	-0.645	-158.159 757	-158.135 219	-0.668
M25	-232.961 838	-232.939 477	-0.608	-232.961 834	-232.939 527	-0.607
M26	-287.095 983	-287.079 204	-0.457	-287.095 984	-287.078 596	-0.473
M27	-382.088 261	-382.074 648	-0.370	-382.088 256	-382.075 507	-0.347
M28	-197.400 950	-197.378 135	-0.621	-197.400 949	-197.377 471	-0.639
M29	-235.444 417	-235.423 131	-0.579	-235.444 416	-235.422 085	-0.608
M30	-236.642 263	-236.619 789	-0.612	-236.642 264	-236.619 616	-0.616

Table B.49: EAs (in eV) obtained with sd-LUCCSD(T) and ab-LUCCSD(T) methods. The energies (in Hartree) of related molecules and anions (adding one electron to the corresponding molecules and maintaining the geometry unchanged) are given. The aug-cc-pVTZ basis set have been used. Parameters are set as 'domsel=0.985', 'cpldel=1', 'nomp2=1', 'keepcls=0', and 'igskip=0'.

	sd-LUCCSD(T), nomp2=1			ab-LUCCSD(T), nomp2=1		
	Molecule	Anion	EA	Molecule	Anion	EA
M01	-76.340 926	-76.318 538	-0.609	-76.340 926	-76.318 771	-0.603
M02	-114.340 763	-114.318 165	-0.615	-114.340 763	-114.318 603	-0.603
M03	-40.439 040	-40.413 961	-0.682	-40.439 040	-40.414 446	-0.669
M04	-111.703 180	-111.679 275	-0.650	-111.703 178	-111.680 499	-0.617
M05	-95.701 590	-95.679 258	-0.608	-95.701 590	-95.679 725	-0.595
M06	-153.551 417	-153.527 592	-0.648	-153.551 417	-153.528 688	-0.618
M07	-79.675 164	-79.650 071	-0.683	-79.675 164	-79.650 651	-0.667
M08	-224.947 993	-224.937 800	-0.277	-224.947 993	-224.938 510	-0.258
M09	-377.828 661	-377.811 176	-0.476	-377.827 481	-377.816 405	-0.301
M10	-154.783 859	-154.760 721	-0.630	-154.783 859	-154.762 308	-0.586
M11	-154.802 062	-154.780 244	-0.594	-154.802 062	-154.781 323	-0.564
M12	-229.640 565	-229.618 147	-0.610	-229.640 565	-229.619 358	-0.577
M13	-225.838 700	-225.826 217	-0.340	-225.838 700	-225.827 263	-0.311
M14	-552.270 385	-552.249 026	-0.581	-552.270 385	-552.249 763	-0.561
M15	-155.697 164	-155.673 151	-0.653	-155.697 164	-155.673 615	-0.641
M16	-284.031 870	-284.013 736	-0.493	-284.031 870	-284.014 225	-0.480
M17	-651.992 360	-651.976 233	-0.439	-651.992 360	-651.976 391	-0.435
M18	-118.914 300	-118.890 255	-0.654	-118.914 300	-118.891 062	-0.632
M19	-156.927 770	-156.906 265	-0.585	-156.927 770	-156.908 077	-0.536
M20	-231.809 703	-231.789 545	-0.549	-231.809 703	-231.791 018	-0.508
M21	-380.839 443	-380.893 780	1.479	-380.839 443	-380.893 853	1.481
M22	-323.274 131	-323.255 794	-0.499	-323.274 131	-323.256 247	-0.487
M23	-629.552 767	-629.534 268	-0.503	-629.552 767	-629.533 857	-0.515
M24	-158.153 543	-158.129 809	-0.646	-158.153 543	-158.130 514	-0.627
M25	-232.955 858	-232.933 711	-0.603	-232.955 858	-232.935 210	-0.562
M26	-287.086 859	-287.070 389	-0.448	-287.086 859	-287.071 984	-0.405
M27	-382.080 448	-382.067 543	-0.351	-382.080 448	-382.069 325	-0.303
M28	-197.392 706	-197.369 943	-0.619	-197.392 706	-197.370 432	-0.606
M29	-235.431 490	-235.409 970	-0.586	-235.431 490	-235.411 984	-0.531
M30	-236.631 919	-236.609 570	-0.608	-236.631 919	-236.611 830	-0.547

Table B.50: EAs (in eV) obtained with sd-LUCCSD(T) and ab-LUCCSD(T) methods. The energies (in Hartree) of related molecules and anions (adding one electron to the corresponding molecules and maintaining the geometry unchanged) are given. The aug-cc-pVTZ basis set have been used. Parameters are set as 'domsel= 0.985', 'cpldel=1', 'nomp2=0', 'keepcls=1', and 'igskip=0'.

	sd-LUCCSD(T), keepcls=1			ab-LUCCSD(T), keepcls=1		
	Molecule	Anion	EA	Molecule	Anion	EA
M01	-76.340 926	-76.318 538	-0.609	-76.340 926	-76.318 771	-0.603
M02	-114.341 138	-114.318 497	-0.616	-114.341 163	-114.318 843	-0.607
M03	-40.439 040	-40.413 961	-0.682	-40.439 040	-40.414 446	-0.669
M04	-111.706 603	-111.682 904	-0.645	-111.706 592	-111.683 827	-0.619
M05	-95.704 819	-95.682 379	-0.611	-95.704 786	-95.682 528	-0.606
M06	-153.554 153	-153.530 345	-0.648	-153.554 265	-153.532 045	-0.605
M07	-79.678 087	-79.653 124	-0.679	-79.678 085	-79.652 905	-0.685
M08	-224.952 122	-224.941 576	-0.287	-224.952 586	-224.942 771	-0.267
M09	-377.833 529	-377.815 917	-0.479	-377.834 481	-377.821 586	-0.351
M10	-154.787 165	-154.764 009	-0.630	-154.787 203	-154.765 246	-0.597
M11	-154.806 365	-154.784 066	-0.607	-154.806 393	-154.784 415	-0.598
M12	-229.649 159	-229.626 530	-0.616	-229.649 598	-229.627 514	-0.601
M13	-225.847 016	-225.834 384	-0.344	-225.847 358	-225.835 156	-0.332
M14	-552.275 349	-552.253 661	-0.590	-552.275 373	-552.253 758	-0.588
M15	-155.702 210	-155.678 240	-0.652	-155.701 913	-155.677 933	-0.653
M16	-284.038 192	-284.019 763	-0.501	-284.038 601	-284.020 008	-0.506
M17	-651.996 215	-651.979 526	-0.454	-651.996 301	-651.979 881	-0.447
M18	-118.919 129	-118.895 222	-0.651	-118.919 129	-118.895 000	-0.657
M19	-156.934 004	-156.912 273	-0.591	-156.934 029	-156.913 219	-0.566
M20	-231.815 613	-231.795 497	-0.547	-231.815 734	-231.795 237	-0.558
M21	-380.846 353	-380.900 890	1.484	-380.846 902	-380.902 979	1.526
M22	-323.282 634	-323.263 739	-0.514	-323.283 055	-323.264 313	-0.510
M23	-629.559 181	-629.539 669	-0.531	-629.559 302	-629.539 442	-0.540
M24	-158.160 776	-158.137 127	-0.644	-158.160 773	-158.136 403	-0.663
M25	-232.962 402	-232.940 161	-0.605	-232.962 454	-232.940 508	-0.597
M26	-287.097 548	-287.080 783	-0.456	-287.097 755	-287.080 660	-0.465
M27	-382.090 318	-382.076 725	-0.370	-382.090 712	-382.077 849	-0.350
M28	-197.402 261	-197.379 501	-0.619	-197.402 256	-197.378 548	-0.645
M29	-235.446 049	-235.424 681	-0.581	-235.446 022	-235.423 370	-0.616
M30	-236.643 881	-236.621 475	-0.610	-236.643 877	-236.620 894	-0.625

Table B.51: EAs (in eV) obtained with sd-LUCCSD(T) and ab-LUCCSD(T) methods. The energies (in Hartree) of related molecules and anions (adding one electron to the corresponding molecules and maintaining the geometry unchanged) are given. The aug-cc-pVTZ basis set have been used. Parameters are set as 'domsel= 0.985', 'cpldel=1', 'nomp2=0', 'keepcls=0', and 'igskip=1'.

	sd-LUCCSD(T), igskip=1			ab-LUCCSD(T), igskip=1		
	Molecule	Anion	EA	Molecule	Anion	EA
M01	-76.340 914	-76.318 483	-0.610	-76.340 914	-76.318 713	-0.604
M02	-114.340 982	-114.318 301	-0.617	-114.340 982	-114.318 731	-0.605
M03	-40.439 017	-40.413 890	-0.684	-40.439 017	-40.414 376	-0.671
M04	-111.705 232	-111.681 411	-0.648	-111.705 232	-111.682 053	-0.631
M05	-95.703 763	-95.681 114	-0.616	-95.703 763	-95.681 410	-0.608
M06	-153.552 098	-153.528 202	-0.650	-153.552 094	-153.529 997	-0.601
M07	-79.677 127	-79.652 095	-0.681	-79.677 128	-79.651 717	-0.691
M08	-224.950 614	-224.939 917	-0.291	-224.950 615	-224.940 603	-0.272
M09	-377.831 829	-377.814 065	-0.483	-377.831 822	-377.818 390	-0.366
M10	-154.785 997	-154.762 728	-0.633	-154.785 997	-154.764 211	-0.593
M11	-154.805 469	-154.783 051	-0.610	-154.805 469	-154.784 013	-0.584
M12	-229.647 230	-229.624 474	-0.619	-229.647 232	-229.625 219	-0.599
M13	-225.844 917	-225.832 199	-0.346	-225.844 917	-225.832 938	-0.326
M14	-552.274 508	-552.252 691	-0.594	-552.274 508	-552.252 759	-0.592
M15	-155.702 475	-155.678 397	-0.655	-155.702 476	-155.677 836	-0.670
M16	-284.036 600	-284.018 065	-0.504	-284.036 601	-284.017 976	-0.507
M17	-651.995 450	-651.978 687	-0.456	-651.995 444	-651.979 029	-0.447
M18	-118.918 370	-118.894 408	-0.652	-118.918 370	-118.894 339	-0.654
M19	-156.933 780	-156.912 009	-0.592	-156.933 774	-156.913 557	-0.550
M20	-231.814 597	-231.794 407	-0.549	-231.814 597	-231.793 821	-0.565
M21	-380.845 047	-380.899 507	1.482	-380.845 048	-380.900 694	1.514
M22	-323.280 837	-323.261 843	-0.517	-323.280 838	-323.261 888	-0.516
M23	-629.558 348	-629.538 907	-0.529	-629.558 350	-629.538 360	-0.544
M24	-158.159 687	-158.135 935	-0.646	-158.159 688	-158.135 101	-0.669
M25	-232.961 961	-232.939 555	-0.610	-232.961 960	-232.939 562	-0.609
M26	-287.095 948	-287.079 085	-0.459	-287.095 945	-287.078 449	-0.476
M27	-382.088 260	-382.074 572	-0.372	-382.088 255	-382.075 421	-0.349
M28	-197.400 868	-197.377 988	-0.623	-197.400 868	-197.377 346	-0.640
M29	-235.444 335	-235.422 966	-0.581	-235.444 334	-235.421 890	-0.611
M30	-236.642 169	-236.619 630	-0.613	-236.642 171	-236.619 441	-0.618

Table B.52: (T) correction (in kcal/mol) of the anions involved in EAs obtained with sd-LUCCSD(T), ab-LUCCSD(T), and UCCSD(T) methods. Numbers in parenthesis indicate percent of the conventional (T) correction.

	UCCSD(T)	sd-LUCCSD(T)	ab-LUCCSD(T)
M01	-5.98	-5.75(96%)	-5.82(97%)
M02	-11.10	-10.85(98%)	-10.93(98%)
M03	-4.52	-4.39(97%)	-4.46(99%)
M04	-12.12	-11.70(97%)	-11.73(97%)
M05	-10.38	-10.02(97%)	-10.10(97%)
M06	-16.37	-15.74(96%)	-15.95(97%)
M07	-9.30	-9.07(98%)	-9.11(98%)
M08	-23.43	-22.36(95%)	-22.39(96%)
M09	-37.71	-34.80(92%)	-34.82(92%)
M10	-15.37	-14.41(94%)	-14.61(95%)
M11	-15.40	-14.42(94%)	-14.57(95%)
M12	-29.39	-28.20(96%)	-28.55(97%)
M13	-30.41	-29.06(96%)	-29.36(97%)
M14	-31.00	-27.43(88%)	-27.72(89%)
M15	-21.50	-20.21(94%)	-20.30(94%)
M16	-29.02	-27.04(93%)	-27.04(93%)
M17	-29.17	-24.97(86%)	-25.06(86%)
M18	-14.29	-13.57(95%)	-13.69(96%)
M19	-20.44	-19.06(93%)	-19.45(95%)
M20	-34.45	-32.85(95%)	-33.04(96%)
M21	-48.42	-44.55(92%)	-44.60(92%)
M22	-34.30	-31.21(91%)	-31.27(91%)
M23	-41.93	-36.77(88%)	-36.84(88%)
M24	-19.27	-18.00(93%)	-18.04(94%)
M25	-33.09	-30.56(92%)	-30.77(93%)
M26	-40.71	-38.10(94%)	-38.44(94%)
M27	-46.75	-43.84(94%)	-44.24(95%)
M28	-24.26	-22.41(92%)	-22.39(92%)
M29	-30.10	-27.15(90%)	-27.46(91%)
M30	-29.25	-26.84(92%)	-26.98(92%)
Ave		94%	94%
Max		98%	99%
Min		86%	86%

Table B.53: Errors of EAs (in eV) obtained with sd-LRMP2 and ab-LRMP2 with respect to the ones obtained with RMP2.

	sd-LRMP2			ab-LRMP2		
	default	domsel	cpldel	default	domsel	cpldel
EA01	0.001	0.001	0.001	0.016	0.016	0.004
EA02	-0.001	-0.001	-0.001	0.009	0.016	0.009
EA03	-0.000	-0.000	-0.000	0.012	0.012	0.012
EA04	-0.000	-0.000	-0.000	0.036	0.036	0.037
EA05	-0.000	-0.000	-0.000	0.010	0.031	0.011
EA06	-0.001	-0.001	-0.001	0.039	0.039	0.027
EA07	-0.000	-0.000	-0.000	0.004	0.015	0.015
EA08	-0.001	-0.000	-0.001	0.034	0.048	0.026
EA09	0.002	-0.000	0.002	0.185	0.043	0.162
EA10	-0.001	-0.001	-0.001	0.041	0.053	0.042
EA11	-0.002	-0.001	-0.002	0.025	0.045	0.026
EA12	-0.002	-0.000	-0.002	0.041	0.069	0.038
EA13	-0.002	-0.002	-0.002	0.046	0.071	0.025
EA14	-0.003	-0.000	-0.002	0.063	0.065	0.029
EA15	-0.001	-0.001	-0.001	0.016	0.046	0.012
EA16	-0.000	-0.000	-0.000	0.040	0.090	0.023
EA17	-0.001	-0.001	-0.001	0.029	0.085	0.012
EA18	-0.000	-0.000	-0.000	0.024	0.027	0.024
EA19	-0.001	-0.001	-0.001	0.049	0.086	0.050
EA20	-0.000	-0.000	-0.000	0.051	0.051	0.050
EA21	0.003	-0.000	0.003	0.012	0.006	0.007
EA22	-0.001	-0.000	-0.001	0.062	0.119	0.022
EA23	-0.020	-0.002	-0.020	0.051	0.114	0.002
EA24	-0.000	-0.000	-0.000	0.024	0.043	0.022
EA25	-0.002	-0.001	-0.002	0.040	0.086	0.044
EA26	-0.001	-0.002	-0.001	0.071	0.116	0.052
EA27	-0.100	0.004	-0.002	0.075	0.086	0.054
EA28	-0.001	-0.001	-0.001	0.042	0.074	0.020
EA29	-0.000	-0.000	-0.000	0.068	0.127	0.065
EA30	-0.001	-0.000	-0.001	0.070	0.122	0.066
MAE	0.005	0.001	0.002	0.043	0.061	0.033
RMSE	0.019	0.001	0.004	0.054	0.071	0.044
MAX	-0.100	0.004	-0.020	0.185	0.127	0.162

Table B.54: Errors of EAs (in eV) obtained with sd-LUCCSD and ab-LUCCSD with respect to the ones obtained with UCCSD.

	sd-LUCCSD				ab-LUCCSD			
	default	nomp2	keepcls	igskip	default	nomp2	keepcls	igskip
EA01	-0.000	-0.000	-0.000	-0.001	0.004	0.004	0.004	0.002
EA02	-0.001	-0.000	-0.001	-0.002	0.007	0.009	0.005	0.007
EA03	-0.000	-0.000	-0.000	-0.001	0.010	0.010	0.010	0.009
EA04	0.006	0.002	0.007	0.004	0.021	0.031	0.029	0.020
EA05	-0.004	0.002	-0.000	-0.005	0.001	0.012	0.002	-0.000
EA06	-0.000	-0.000	0.001	-0.001	0.039	0.024	0.035	0.038
EA07	0.002	-0.000	0.002	0.001	-0.010	0.011	-0.006	-0.011
EA08	-0.004	0.003	-0.003	-0.006	0.014	0.022	0.015	0.011
EA09	0.003	0.006	0.004	-0.000	0.119	0.168	0.130	0.117
EA10	0.002	0.003	0.003	0.001	0.034	0.040	0.028	0.033
EA11	-0.016	-0.004	-0.014	-0.017	0.004	0.020	-0.011	0.003
EA12	-0.007	-0.002	-0.005	-0.008	-0.001	0.027	-0.006	-0.003
EA13	-0.003	-0.000	-0.003	-0.004	0.005	0.022	-0.003	0.003
EA14	-0.008	-0.002	-0.007	-0.010	-0.018	0.014	-0.018	-0.021
EA15	0.001	-0.000	0.002	-0.000	-0.018	0.010	-0.006	-0.019
EA16	-0.001	0.005	-0.000	-0.003	-0.004	0.017	-0.005	-0.006
EA17	-0.007	0.003	-0.007	-0.009	-0.001	0.006	-0.003	-0.003
EA18	0.005	0.001	0.005	0.004	-0.002	0.018	-0.006	-0.003
EA19	-0.004	-0.001	-0.005	-0.006	0.022	0.039	0.004	0.020
EA20	0.005	0.004	0.005	0.004	-0.018	0.041	-0.015	-0.020
EA21	0.004	0.001	0.011	0.009	0.037	0.008	0.049	0.040
EA22	-0.011	0.001	-0.010	-0.013	-0.012	0.011	-0.009	-0.014
EA23	0.014	-0.020	0.011	0.013	-0.004	-0.028	-0.002	-0.005
EA24	0.002	-0.000	0.003	-0.000	-0.023	0.014	-0.020	-0.024
EA25	-0.003	-0.001	-0.001	-0.004	-0.011	0.037	-0.005	-0.013
EA26	-0.003	0.002	-0.003	-0.005	-0.035	0.040	-0.029	-0.037
EA27	-0.014	-0.001	-0.013	-0.015	-0.007	0.041	-0.012	-0.009
EA28	-0.000	-0.000	0.001	-0.001	-0.017	0.010	-0.023	-0.018
EA29	0.008	0.001	0.006	0.006	-0.034	0.047	-0.042	-0.036
EA30	-0.002	-0.001	-0.000	-0.003	-0.012	0.052	-0.021	-0.014
MAE	0.005	0.002	0.005	0.005	0.018	0.028	0.018	0.019
RMSE	0.006	0.004	0.006	0.007	0.028	0.040	0.030	0.029
MAX	-0.016	-0.020	-0.014	-0.017	0.119	0.168	0.130	0.117

Table B.55: Errors of EAs (in eV) obtained with sd-LUCCSD(T) and ab-LUCCSD(T) with respect to the ones obtained with UCCSD(T).

	sd-LUCCSD(T)				ab-LUCCSD(T)			
	default	nomp2	keepcls	igskip	default	nomp2	keepcls	igskip
EA01	-0.000	-0.000	-0.000	-0.002	0.006	0.006	0.006	0.005
EA02	-0.001	-0.000	-0.001	-0.002	0.010	0.012	0.008	0.010
EA03	-0.000	-0.000	-0.000	-0.001	0.013	0.013	0.013	0.012
EA04	0.005	0.001	0.006	0.003	0.022	0.034	0.032	0.020
EA05	-0.006	0.001	-0.002	-0.007	0.002	0.014	0.003	0.001
EA06	-0.001	-0.000	-0.000	-0.002	0.048	0.030	0.044	0.047
EA07	0.003	-0.001	0.003	0.001	-0.008	0.015	-0.003	-0.009
EA08	-0.007	0.003	-0.007	-0.011	0.011	0.022	0.013	0.008
EA09	0.001	0.005	0.002	-0.002	0.118	0.180	0.130	0.116
EA10	0.001	0.003	0.002	-0.001	0.041	0.046	0.035	0.040
EA11	-0.021	-0.006	-0.019	-0.022	0.005	0.024	-0.010	0.004
EA12	-0.010	-0.003	-0.008	-0.012	0.011	0.030	0.006	0.008
EA13	-0.005	-0.001	-0.005	-0.007	0.016	0.028	0.007	0.013
EA14	-0.012	-0.003	-0.012	-0.015	-0.010	0.017	-0.010	-0.013
EA15	-0.000	-0.000	0.001	-0.002	-0.016	0.012	0.001	-0.017
EA16	-0.005	0.004	-0.004	-0.007	-0.008	0.017	-0.009	-0.009
EA17	-0.012	0.003	-0.012	-0.014	-0.003	0.007	-0.005	-0.005
EA18	0.005	0.001	0.005	0.003	0.003	0.023	-0.001	0.002
EA19	-0.007	-0.002	-0.008	-0.009	0.035	0.047	0.017	0.033
EA20	0.004	0.003	0.004	0.002	-0.010	0.043	-0.006	-0.014
EA21	-0.004	-0.000	0.005	0.003	0.032	0.002	0.047	0.035
EA22	-0.017	-0.001	-0.016	-0.019	-0.016	0.011	-0.012	-0.018
EA23	-0.049	-0.025	-0.053	-0.051	-0.064	-0.036	-0.062	-0.066
EA24	0.001	-0.001	0.002	-0.001	-0.022	0.019	-0.018	-0.024
EA25	-0.008	-0.002	-0.005	-0.009	-0.006	0.039	0.004	-0.009
EA26	-0.009	-0.001	-0.009	-0.012	-0.026	0.042	-0.018	-0.029
EA27	-0.022	-0.003	-0.022	-0.024	0.001	0.045	-0.002	-0.001
EA28	-0.002	-0.001	-0.001	-0.004	-0.020	0.013	-0.026	-0.021
EA29	0.006	-0.000	0.004	0.004	-0.022	0.055	-0.031	-0.025
EA30	-0.005	-0.002	-0.003	-0.007	-0.010	0.060	-0.019	-0.012
MAE	0.008	0.003	0.007	0.009	0.021	0.030	0.020	0.021
RMSE	0.012	0.005	0.012	0.013	0.031	0.043	0.032	0.031
MAX	-0.049	-0.025	-0.053	-0.051	0.118	0.180	0.130	0.116

Table B.56: Errors of EAs (in eV) obtained with UCCSD, RMP2, sd-LRMP2, and ab-LRMP2 with respect to the ones obtained with UCCSD(T).

	UCCSD	RMP2	sd-LRMP2			ab-LRMP2		
			default	domsel	cpldel	default	domsel	cpldel
EA01	-0.023	-0.033	-0.032	-0.032	-0.032	-0.016	-0.016	-0.029
EA02	-0.010	-0.025	-0.025	-0.025	-0.025	-0.015	-0.009	-0.015
EA03	-0.017	-0.031	-0.030	-0.030	-0.030	-0.019	-0.019	-0.019
EA04	-0.032	-0.039	-0.039	-0.039	-0.039	-0.003	-0.003	-0.003
EA05	-0.024	-0.038	-0.039	-0.038	-0.039	-0.029	-0.007	-0.028
EA06	-0.019	-0.031	-0.032	-0.032	-0.032	0.008	0.008	-0.004
EA07	-0.023	-0.038	-0.037	-0.037	-0.038	-0.033	-0.023	-0.022
EA08	-0.027	-0.049	-0.049	-0.049	-0.049	-0.014	-0.000	-0.022
EA09	-0.048	-0.059	-0.057	-0.059	-0.057	0.126	-0.015	0.103
EA10	-0.024	-0.038	-0.039	-0.039	-0.039	0.003	0.014	0.004
EA11	-0.025	-0.044	-0.046	-0.045	-0.046	-0.019	0.001	-0.018
EA12	-0.029	-0.037	-0.039	-0.037	-0.039	0.004	0.032	0.001
EA13	-0.026	-0.022	-0.024	-0.023	-0.024	0.025	0.049	0.004
EA14	-0.034	-0.047	-0.050	-0.047	-0.049	0.016	0.018	-0.018
EA15	-0.030	-0.030	-0.031	-0.031	-0.031	-0.014	0.016	-0.018
EA16	-0.035	-0.056	-0.056	-0.056	-0.056	-0.016	0.034	-0.032
EA17	-0.028	-0.051	-0.053	-0.053	-0.053	-0.023	0.033	-0.040
EA18	-0.027	-0.044	-0.044	-0.044	-0.044	-0.020	-0.017	-0.020
EA19	-0.033	-0.051	-0.052	-0.052	-0.051	-0.001	0.035	-0.001
EA20	-0.043	-0.023	-0.023	-0.023	-0.023	0.027	0.027	0.027
EA21	-0.065	0.259	0.263	0.260	0.262	0.271	0.265	0.266
EA22	-0.036	-0.062	-0.063	-0.062	-0.063	0.001	0.057	-0.040
EA23	-0.044	-0.067	-0.087	-0.069	-0.086	-0.015	0.047	-0.065
EA24	-0.029	-0.047	-0.047	-0.047	-0.047	-0.023	-0.004	-0.025
EA25	-0.037	-0.035	-0.037	-0.036	-0.037	0.005	0.051	0.009
EA26	-0.037	-0.041	-0.043	-0.043	-0.042	0.030	0.075	0.010
EA27	-0.035	-0.044	-0.144	-0.040	-0.046	0.031	0.042	0.011
EA28	-0.031	-0.049	-0.050	-0.050	-0.050	-0.008	0.025	-0.030
EA29	-0.037	-0.050	-0.050	-0.050	-0.050	0.018	0.077	0.016
EA30	-0.033	-0.052	-0.053	-0.052	-0.053	0.018	0.070	0.014
MAE	0.031	0.050	0.054	0.050	0.051	0.028	0.036	0.030
RMSE	0.033	0.064	0.070	0.064	0.066	0.058	0.060	0.057
MAX	-0.065	0.259	0.263	0.260	0.262	0.271	0.265	0.266

Table B.57: Errors of EAs (in eV) obtained with sd-LUCCSD and ab-LUCCSD with respect to the ones obtained with UCCSD(T).

	sd-LUCCSD				ab-LUCCSD			
	default	nomp2	keepcls	igskip	default	nomp2	keepcls	igskip
EA01	-0.023	-0.023	-0.023	-0.024	-0.020	-0.020	-0.020	-0.021
EA02	-0.011	-0.010	-0.011	-0.012	-0.003	-0.001	-0.005	-0.003
EA03	-0.017	-0.017	-0.017	-0.019	-0.007	-0.007	-0.007	-0.008
EA04	-0.026	-0.030	-0.025	-0.028	-0.010	-0.001	-0.003	-0.012
EA05	-0.027	-0.022	-0.024	-0.029	-0.023	-0.012	-0.022	-0.024
EA06	-0.020	-0.019	-0.019	-0.021	0.020	0.005	0.016	0.019
EA07	-0.021	-0.023	-0.021	-0.022	-0.033	-0.012	-0.029	-0.034
EA08	-0.031	-0.024	-0.030	-0.034	-0.014	-0.006	-0.012	-0.016
EA09	-0.045	-0.042	-0.044	-0.048	0.071	0.119	0.081	0.069
EA10	-0.022	-0.021	-0.021	-0.023	0.010	0.016	0.004	0.009
EA11	-0.041	-0.029	-0.039	-0.042	-0.021	-0.005	-0.036	-0.022
EA12	-0.035	-0.030	-0.034	-0.037	-0.029	-0.002	-0.034	-0.032
EA13	-0.029	-0.026	-0.028	-0.030	-0.021	-0.004	-0.029	-0.023
EA14	-0.042	-0.036	-0.041	-0.044	-0.052	-0.020	-0.052	-0.055
EA15	-0.029	-0.030	-0.028	-0.031	-0.048	-0.020	-0.036	-0.049
EA16	-0.036	-0.029	-0.035	-0.038	-0.039	-0.018	-0.040	-0.040
EA17	-0.035	-0.025	-0.035	-0.037	-0.030	-0.022	-0.031	-0.031
EA18	-0.022	-0.026	-0.022	-0.024	-0.029	-0.010	-0.034	-0.031
EA19	-0.037	-0.034	-0.038	-0.038	-0.011	0.006	-0.029	-0.013
EA20	-0.037	-0.039	-0.037	-0.039	-0.060	-0.001	-0.057	-0.063
EA21	-0.061	-0.064	-0.054	-0.056	-0.028	-0.057	-0.016	-0.025
EA22	-0.047	-0.036	-0.047	-0.049	-0.049	-0.025	-0.046	-0.050
EA23	-0.030	-0.064	-0.033	-0.031	-0.048	-0.072	-0.046	-0.049
EA24	-0.027	-0.029	-0.027	-0.029	-0.052	-0.015	-0.049	-0.053
EA25	-0.041	-0.038	-0.039	-0.042	-0.048	-0.000	-0.042	-0.051
EA26	-0.040	-0.035	-0.040	-0.042	-0.071	0.003	-0.065	-0.074
EA27	-0.049	-0.037	-0.049	-0.051	-0.043	0.006	-0.047	-0.045
EA28	-0.031	-0.031	-0.030	-0.033	-0.048	-0.022	-0.054	-0.049
EA29	-0.028	-0.036	-0.030	-0.030	-0.070	0.010	-0.079	-0.073
EA30	-0.035	-0.034	-0.033	-0.036	-0.045	0.018	-0.055	-0.047
MAE	0.033	0.031	0.032	0.034	0.035	0.018	0.036	0.036
RMSE	0.034	0.033	0.033	0.035	0.040	0.030	0.041	0.041
MAX	-0.061	-0.064	-0.054	-0.056	-0.071	0.119	0.081	-0.074

Table B.58: Formation energies (FE, in kcal/mol) of copper-oxygen complexes (high-spin open-shell triplet state) obtained with HF and RMP2 methods. The energies (in Hartree) of related molecules are also given.

	HF			RMP2		
	$(CuL)^+$	$(CuLO_2)^+$	FE	$(CuL)^+$	$(CuLO_2)^+$	FE
O_2	-149.652 757			-150.139 258		
L0	-420.957 270	-570.564 880	28.33	-422.428 752	-572.543 053	15.66
L1	-1106.251 895	-1255.878 601	23.41	-1110.485 667	-1260.609 831	9.47
L2	-1184.355 485	-1333.975 430	20.59	-1188.940 140	-1339.056 441	14.42
L3	-1375.306 303	-1524.926 095	20.69	-1379.263 681	-1529.377 352	16.06
L4	-1453.409 502	-1603.022 906	24.69	-1457.718 981	-1607.822 551	22.39

Table B.59: Formation energies (FE, in kcal/mol) of copper-oxygen complexes (high-spin open-shell triplet state) obtained with sd-LRMP2 and ab-LRMP2 methods. The energies (in Hartree) of related molecules are also given.

	sd-LRMP2			ab-LRMP2		
	$(CuL)^+$	$(CuLO_2)^+$	FE	$(CuL)^+$	$(CuLO_2)^+$	FE
O_2	-150.138 878			-150.138 103		
L0	-422.416 756	-572.530 051	16.05	-422.416 756	-572.529 258	16.06
L1	-1110.422 053	-1260.545 734	9.54	-1110.422 054	-1260.543 906	10.20
L2	-1188.867 589	-1338.983 101	14.66	-1188.867 589	-1338.981 357	15.27
L3	-1379.201 460	-1529.314 068	16.48	-1379.201 460	-1529.312 311	17.10
L4	-1457.647 748	-1607.750 915	22.41	-1457.647 749	-1607.749 074	23.08

Table B.60: Formation energies (FE, in kcal/mol) of copper-oxygen complexes (high-spin open-shell triplet state) obtained with sd-LUCCSD and sd-LUCCSD(T) methods. The energies (in Hartree) of related molecules are also given.

	sd-LUCCSD			sd-LUCCSD(T)		
	$(CuL)^+$	$(CuLO_2)^+$	FE	$(CuL)^+$	$(CuLO_2)^+$	FE
O_2	-150.119 571			-150.135 130		
L0	-422.398 439	-572.502 136	9.96	-422.444 663	-572.568 961	6.80
L1	-1110.448 874	-1260.565 672	1.74	-1110.653 747	-1260.789 490	-0.38
L2	-1188.921 570	-1339.033 320	4.91	-1189.139 967	-1339.269 339	3.61
L3	-1379.263 264	-1529.374 696	5.11	-1379.443 104	-1529.566 398	7.43
L4	-1457.736 340	-1607.842 548	8.38	-1457.930 864	-1608.047 531	11.59

Table B.61: Energies of glutamate (denoted as M1), 3-methylaspartate (denoted as M5), and 4 transition states (denoted as TS1, TS2, TS3, and TS4), 3 intermediates (denoted as M2, M3, and M4) in the transition states and intermediates of the inter-conversion from (S)-glutamate to (2S,3S)-3-methylaspartate obtained with HF, RMP2, sd-LRMP2, and ab-LRMP2 methods.

	HF	RMP2	sd-LRMP2	ab-LRMP2
M1	-1658.566 227	-1664.785 952	-1664.699 964	-1664.698 418
TS1	-1658.498 972	-1664.751 692	-1664.668 745	-1664.669 071
M2	-1658.560 855	-1664.782 366	-1664.699 807	-1664.698 787
TS2	-1658.516 866	-1664.752 793	-1664.672 910	-1664.671 997
M3	-1658.556 828	-1664.772 412	-1664.691 955	-1664.691 399
TS3	-1658.513 653	-1664.757 154	-1664.675 660	-1664.676 238
M4	-1658.557 219	-1664.777 370	-1664.695 708	-1664.694 848
TS4	-1658.489 852	-1664.746 450	-1664.664 639	-1664.665 728
M5	-1658.561 745	-1664.780 545	-1664.696 483	-1664.695 331

Table B.62: Energies of glutamate (denoted as M1), 3-methylaspartate (denoted as M5), and 4 transition states (denoted as TS1, TS2, TS3, and TS4), 3 intermediates (denoted as M2, M3, and M4) in the transition states and intermediates of the inter-conversion from (S)-glutamate to 3-methylaspartate obtained with sd-LUCCSD, sd-LUCCSD(T), and DFT-B3LYP methods.

	sd-LUCCSD	sd-LUCCSD(T)	DFT-B3LYP
M1	-1664.815 011	-1665.085 892	-1667.298 206
TS1	-1664.777 756	-1665.051 856	-1667.266 113
M2	-1664.812 624	-1665.085 320	-1667.298 125
TS2	-1664.779 946	-1665.054 678	-1667.279 823
M3	-1664.804 061	-1665.077 464	-1667.300 146
TS3	-1664.782 876	-1665.058 209	-1667.280 015
M4	-1664.807 925	-1665.080 733	-1667.289 614
TS4	-1664.767 900	-1665.044 305	-1667.258 498
M5	-1664.809 844	-1665.082 050	-1667.294 362

Bibliography

[1] M. W. Wong and L. Radom, J. Phys. Chem. **99**, 8582 (1995).

[2] C. J. Parkinson, P. M. Mayer, and L. Radom, Theor. Chim. Acta **102**, 92 (1999).

[3] R. H. Nobes, J. A. Pople, L. Radom, N. C. Handy, and P. J. Knowles, Chem. Phys. Lett. **138**, 481 (1987).

[4] C. W. Murray and N. C. Handy, J. Chem. Phys. **97**, 6509 (1992).

[5] P. J. Knowles, J. S. Andrews, R. D. Amos, N. C. Handy, and J. Pople, Chem. Phys. Lett. **186**, 130 (1991).

[6] H. B. Schlegel, J. Phys. Chem. **92**, 3075 (1988).

[7] J. Čížek, J. Chem. Phys. **45**, 4256 (1966).

[8] J. Čížek, Adv. Chem. Phys. **14**, 35 (1969).

[9] J. Čížek, and J. Paldus, Int. J. Quantum Chem. **5**, 359 (1971).

[10] C. Møller and M. S. Plesset, Phys. Rev. **46**, 618 (1934).

[11] R. Krishnan, M. J. Frisch, and J. A. Pople, J. Chem. Phys. **72**, 4244 (1980).

[12] P. J. Knowles, J. S. Andrews, R. D. Amos, N. C. Handy, and J. A. Pople, Chem. Phys. Letters **186**, 130 (1991).

[13] W. J. Lauderdale, J. F. Stanton, J. Gauss, J. D. Watts, and R. J. Bartlett, J. Chem. Phys. **97**, 6606 (1992).

[14] W. J. Lauderdale, J. F. Stanton, J. Gauss, J. D. Watts, and R. J. Bartlett, Chem. Phys. Lett. **187**, 21 (1991).

[15] J. Gauss, J. F. Stanton, and R. J. Bartlett, J. Chem. Phys. **97**, 7825 (1992).

[16] T. D. Crawford, H. F. Schaefer III, and T. J. Lee, J. Chem. Phys. **105**, 1060 (1996).

[17] G. Knizia and H.-J. Werner, J. Chem. Phys. **128**, 154103 (2008).

[18] M. Urban, J. Noga, S. J. Cole, and R. J. Bartlett, J. Chem. Phys. **83**, 4041 (1985).

[19] J. A. Pople, M. Head-Gordon, and K. Raghavachari, J. Chem. Phys. **87**, 5968 (1987).

[20] K. Raghavachari, G.W. Trucks, J.A. Pople, and M. Head-Gordon, Chem. Phys. Lett. **157**, 479 (1989).

[21] Z. He, and D. Cremer, Theor. Chim. Acta **85**, 305 (1993).

[22] M. J. O. Deegan, and P. J. Knowles, Chem. Phys. Lett. **227**, 321 (1994).

[23] J. D. Watts, J. Gauss, and R. J. Bartlett, J. Chem. Phys. **98**, 8718 (1993).

[24] O. Sinanoglu, Adv. Chem. Phys. **6**, 315 (1964).

[25] R. K. Nesbet, Adv. Chem. Phys. **9**, 321 (1965).

[26] S. Diner, J. P. Malrieu, and P. Claverie, Theor. Chim. Acta **13**, 18 (1969).

[27] J. M. Cullen and M. C. Zerner, Int. J. Quantum Chem. Symp. **9**, 343 (1975).

[28] G. Stollhoff and P. Fulde, J. Chem. Phys. **73**, 4548 (1980).

[29] B. Kirtman and C. deMeilo, J. Chem. Phys. **75**, 4592 (1981).

[30] J. M. Cullen and M. C. Zerner, Theor. Chim. Acta **61**, 203 (1982).

[31] J. M. Cullen and M. C. Zerner, J. Chem. Phys. **77**, 4088 (1982).

[32] B. Kirtman, J. Chem. Phys. **86**, 1059 (1982).

[33] P. Otto and J. Ladik, Int. J. Quantum Chem. **22**, 169 (1982).

[34] B. Kiel, G. Stollhoff, C. Weigel, P. Fulde, and H. Stoll, Z. Phys. B **46**, 1 (1982).

[35] W. D. Laidig, G. D. Purvis III, and R. J. Bartlett, Int. J. Quantum Chem. Symp. **6**, 561 (1982).

[36] W. D. Laidig, G. D. Purvis III, and R. J. Bartlett, Chem. Phys. Lett. **97**, 209 (1983).

[37] E. Kapuy, Z. Csepes, and C. Kozmutza, Int. J. Quantum Chem. **23**, 981 (1983).

[38] M. Takahashi and J. Paldus, Phys. Rev. B **31**, 5121 (1985).

[39] M. Takahashi and J. Paldus, Int. J. Quantum Chem. **28**, 459 (1985).

[40] W. D. Laidig, G. D. Purvis III, and R. J. Bartlett, J. Chem. Phys. **89**, 2161 (1985).

[41] W. Förner, J. Ladik, P. Otto, and J. Čížek, Chem. Phys. **97**, 251 (1985).

[42] J. Pipek and J. Ladik, Chem. Phys. **102**, 445 (1986).

[43] W. Meyer and L. Frommhold, Phys. Rev. A **33**, 3807 (1986).

[44] B. Kirtman and C. E. Dykstra, J. Chem. Phys. **85**, 2791 (1986).

[45] G. Stollhoff and P. Vasilopoulos, J. Chem. Phys. **84**, 2744 (1986).

[46] E. Kapuy, F. Bartha, F. Bogar, and C. Kozmutza, Theor. Chim. Acta **72**, 337 (1987).

[47] E. Kapuy, F. Bartha, C. Kozmutza, and F. Bogar, J. Mol. Struc. **47**, 59 (1988).

[48] G. Stollhoff and K. P. Bohnen, Phys. Rev. B **37**, 4678 (1988).

[49] J. Pipek and P. G. Mezey, J. Chem. Phys. **90**, 4916 (1989).

[50] M. V. Ganduglia-Pirovano, G. Stollhoff, P. Fulde, and K. P. Bohnen, Phys. Rev. B **39**, 5156 (1989).

[51] E. Kapuy, F. Bartha, F. Bogar, F. Csepes, and C. Kozmutza, Int. J. Quantum Chem. **38**, 139 (1990).

[52] G. Konig and G. Stollhoff, J. Phys. Chem. **91**, 2993 (1990).

[53] G. Konig and G. Stollhoff, Phys. Rev. Lett. **65**, 1239 (1990).

[54] C. Kozmutza and E. Kapuy, Int. J. Quantum Chem. **38**, 665 (1990).

[55] E. Kapuy, F. Bogar, F. Bartha, and C. Kozmutza, J. Mol. Struc. **79**, 61 (1991).

[56] E. Kapuy and C. Kozmutza, J. Chem. Phys. **94**, 5565 (1991).

[57] C. Kozmutza and E. Kapuy, J. Comput. Chem. **12**, 953 (1991).

[58] P. Pulay, Chem. Phys. Lett. **100**, 151 (1983).

[59] S. Saebø and P. Pulay, Chem. Phys. Lett. **113**, 13 (1985).

[60] P. Pulay and S. Saebø, Theor. Chim. Acta **69**, 357 (1986).

[61] S. Saebø and P. Pulay, J. Chem. Phys. **86**, 914 (1987).

[62] S. Saebø and P. Pulay, J. Chem. Phys. **88**, 1884 (1988).

[63] S. Saebø and P. Pulay, Annu. Rev. Phys. Chem. **44**, 213 (1993).

[64] M. Schütz, G. Hetzer, and H.-J. Werner, J. Chem. Phys. **111**, 5691 (1999).

[65] C. Hampel and H.-J. Werner, J. Chem. Phys. **104**, 6286 (1996).

[66] M. Schütz and H.-J. Werner, J. Chem. Phys. **114**, 661 (2001).

[67] M. Schütz, J. Chem. Phys. **116**, 8772 (2002).

[68] M. Schütz and H.-J. Werner, Chem. Phys. Lett. **318**, 370 (2000).

[69] M. Schütz, J. Chem. Phys. **113**, 9986 (2000).

[70] M. Schütz, Phys. Chem. Chem. Phys. **4**, 3941 (2002).

[71] H.-J. Werner, F. R. Manby, and P. J. Knowles, J. Chem. Phys. **118**, 8149 (2003).

[72] M. Schütz and F. R. Manby, Phys. Chem. Chem. Phys. **5**, 3349 (2003).

[73] P. E. Maslen and M. Head-Gordon, Chem. Phys. Lett. **283**, 102 (1998).

[74] G. E. Scuseria and P. Y. Ayala, J. Chem. Phys. **111**, 8330 (1999).

[75] A. A. Auer, and M. Nooijen, J. Chem. Phys. **125**, 024104 (2006).

[76] P. E. Maslen and M. Head-Gordon, J. Chem. Phys. **109**, 7093 (1998).

[77] M. S. Lee, P. E. Maslen, and M. Head-Gordon, J. Chem. Phys. **112**, 3592 (2000).

[78] P. E. Maslen, A. D. Dutoi, M. S. Lee, Y. H. Shao, and M. Head-Gordon, Mol. Phys. **103**, 425 (2005).

[79] J. Subotnik and M. Head-Gordon, J. Chem. Phys. **123**, 064108 (2005).

[80] J. E. Subotnik, A. Sodt, and M. Head-Gordon, J. Chem. Phys. **125**, 074116 (2006).

[81] A. Sodt, J. E. Subotnik, and M. Head-Gordon, J. Chem. Phys. **125**, 194109 (2006).

[82] J. E. Subotnik, A. Sodt, and M. Head-Gordon, J. Chem. Phys. **128**, 034103 (2008).

[83] J. E. Subotnik, and M. Head-Gordon, J. Phys-Condens. Mat. **20**, 294211 (2008).

[84] T. S. Chwee, A. B. Szilva, R. Lindh, and E. A. Carter, J. Chem. Phys. **128**, 224106 (2008).

[85] F. Neese, A. Hansen, and D. G. Liakos, J. Chem. Phys. **131**, 064103 (2009).

[86] F. Neese, F. Wennmohs, and A. Hansen, J. Chem. Phys. **130**, 114108 (2009).

[87] S. Li, J. Ma, and Y. Jiang, J. Comput. Chem. **23**, 237 (2002).

[88] W. Li, P. Piecuch, J. R. Gour, and S. Li, J. Chem. Phys. **131**, 114109 (2009).

[89] N. Flocke and R. J. Bartlett, J. Chem. Phys. **121**, 10935 (2004).

[90] T. F. Hughes, N. Flocke, and R. J. Bartlett, J. Phys. Chem. A **112**, 5994 (2008).

[91] H. Stoll, J. Chem. Phys. **97**, 8449 (1992).

[92] J. Friedrich, M. Hanrath, and M. Dolg, J. Chem. Phys. **126**, 154110 (2007).

[93] J. Friedrich, M. Hanrath, and M. Dolg, Chem. Phys. **346**, 266 (2008).

[94] J. Friedrich, and M. Dolg, J. Chem. Phys. **129**, 244105 (2008).

[95] J. Friedrich, and M. Dolg, **5**, 287 (2009).

[96] J. Friedrich, S. Coriani, T. Helgaker, and M. Dolg, J. Chem. Phys. **131**, 154102 (2009).

[97] S. F. Boys, Localized orbitals and localized adjustment functions, in Quantum Theory of Atoms, Molecules, and the Solid State, edited by P. O. Löwdin, pages 253–262, Academic Press, New York, 1966.

[98] C. Edmiston, K. Ruedenberg, J. Chem. Phys. **43**, S97 (1965).

[99] R. Mata and H.-J. Werner, Mol. Phys. **105**, 2753 (2007).

[100] J. W. Boughton and P. Pulay, J. Comput. Chem. **14**, 736 (1993).

[101] H. J. Werner, and K. Pflüger, Ann. Rev. Comp. Chem **2**, 53 (2006).

[102] D. M. Schrader and S. Prager, J. Chem. Phys. **37**, 3927 (1962).

[103] J. L. Whitten, J. Chem. Phys. **58**, 4496 (1973).

[104] E. J. Baerends, D. E. Ellis, and P. Ros, Chem. Phys. **2**, 41 (1973).

[105] B. I. Dunlap, J. W. D. Connolly, and J. R. Sabin, J. Chem. Phys. **71**, 3396 (1979).

[106] O. Vahtras, J. Almlöf, and M. W. Feyereisen, Chem. Phys. Lett. **213**, 514 (1993).

[107] S. Ten-no and S. Iwata, Chem. Phys. Lett. **240**, 578 (1995).

[108] F. Weigend, Phys. Chem. Chem. Phys. **4**, 4285 (2002).

[109] R. Polly, H.-J. Werner, F. R. Manby, and P. J. Knowles, Mol. Phys. **102**, 2311 (2004).

[110] M. W. Feyereisen, G. Fitzgerald, and A. Komornicki, Chem. Phys. Lett. **208**, 359 (1993).

[111] D. E. Bernholdt and R. J. Harrison, Chem. Phys. Lett. **250**, 477 (1996).

[112] F. Weigend and M. Häser, Theor. Chim. Acta **97**, 331 (1997).

[113] C. Hättig and F. Weigend, J. Chem. Phys. **5154**, 2000 (113).

[114] A. J. May, and F. R. Manby, J. Chem. Phys. **121**, 4479 (2004).

[115] H. J. Werner, T. B. Adler, and F. R. Manby, J. Chem. Phys. **126**, 164102 (2007).

[116] G. Knizia, and H. J. Werner, J. Chem. Phys. **128**, 154103 (2008).

[117] F. R. Manby, J. Chem. Phys. **119**, 4607 (2003).

[118] A. P. Rendell and T. J. Lee, J. Chem. Phys. **101**, 400 (1994).

[119] A. Heßelmann, G. Jansen, and M. Schütz, J. Chem. Phys. **122**, 014103 (2005).

[120] R. Bukowski, R. Podeszwa, and K. Szalewicz, Chem. Phys. Lett. **414**, 111 (2005).

[121] T. Korona, and B. Jeziorski, J. Chem. Phys. **128**, 144107 (2008).

[122] T. Korona, **5**, 2663 (2009).

[123] H.-J. Werner, F. R. Manby, and P. Knowles, J. Chem. Phys. **118**, 8149 (2003).

[124] B. I. Dunlap, Phys. Chem. Chem. Phys. **2**, 2113 (2000).

[125] T. B. Adler, H.-J. Werner, and F. R. Manby, J. Chem. Phys. **130**, 054106 (2009).

[126] T. B. Adler, and H.-J. Werner, J. Chem. Phys. **130**, 241101 (2009).

[127] M. Dolg, U. Wedig, H. Stoll, and H. Preuss, J. Chem. Phys. **86**, 866 (1987).

[128] H. Stoll, B. Metz, and M. Dolg, J. Comput. Chem. **23**, 767 (2002).

[129] W. Buckel, Appl. Microbiol. Biotechnol **57(3)**, 263 (2001).

[130] N. Marsh, Bioorganic Chemistry **28**, 176 (2000).

[131] A. D. MacKerell Jr., D. Bashford, R. L. Bellott, R. L. Dunbrack Jr., J. D. Evanseck, M. J. Field, S. Fischer, J. Gao, H. Guo, S. Ha, D. Joseph-McCarthy, L. Kuch- nir, K. Kuczera, F. T. K. Lau, C. Mattos, S. Mich- nick, T. Ngo, D. T. Nguyen, B. Prodhom, W. E. Rei- her III, B. Roux, M. Schlenkrich, J. C. Smith, R. Stote, J. Straub, M. Watanabe, J. Wiorkiewicz-Kuczera, D. Yin, and M. Karplus, J. Phys. Chem. B **102**, 3586 (1998).

[132] W. Smith, C. Yong, and P. Rodger, Bioorganic Chemistry **28**, 176 (2000).

[133] T. B. Adler, F. R. Manby, and H.-J. Werner, J. Chem. Phys. **130**, 054106 (2009).